

REPUBLIC OF CAMEROON

Peace –Work- Fatherland

.....  
THE UNIVERSITY OF YAOUNDE I

.....  
POSTGRADUATE SCHOOL OF  
SCIENCES, TECHNOLOGY AND  
GEOSCIENCES

.....  
RESEARCH AND POSTGRADUATE  
TRAINING UNIT FOR CHEMISTRY  
AND APPLICATIONS



REPUBLIQUE DU CAMEROUN

Paix-Travail-Patrie

.....  
UNIVERSITÉ DE YAOUNDÉ I

.....  
CENTRE DE RECHERCHE ET DE  
FORMATION DOCTORALE EN  
SCIENCES, TECHNOLOGIES ET  
GÉOSCIENCES

.....  
UNITÉ DE RECHERCHE ET DE  
FORMATION DOCTORALE EN  
CHIMIE ET APPLICATIONS

ENDOPHYTE AND PLANT NATURAL PRODUCTS LABORATORY

LABORATOIRE DES SUBSTANCES NATURELLES D'ORIGINE FUNGIQUE ET  
VÉGÉTALE

CHEMICAL CONSTITUENTS OF THREE ENDOPHYTIC FUNGI: *SIMPLICILLIUM SUBTROPICUM* HARBOURED IN *DUGUETIA STAUDTHI* (ANNONACEAE) AND TWO NEW *DIAPORTHE* SP. ISOLATED FROM *TREMA GUINEENSIS* (ULMACEAE); ANTIBACTERIAL ACTIVITY AND CYTOTOXICITY OF SELECTED COMPOUNDS

## THESIS

Defended publicly in Partial Fulfilment of the Requirements for the Award of a Doctorate/PhD degree in  
Organic Chemistry

By:

**Anoumedem Mouafo Elodie Gisèle**

Registration number: 09T0014

*MSc in Organic Chemistry*

Under the supervision of:

**Kouam Fogue Siméon**  
*Professor*



June 2023

REPUBLIQUE DU CAMEROUN  
Paix-Travail-Patrie  
\*\*\*\*\*  
UNIVERSITÉ DE YAOUNDÉ I  
\*\*\*\*\*  
FACULTÉ DES SCIENCES  
\*\*\*\*\*



REPUBLIC OF CAMEROON  
Peace-Work-Fatherland  
\*\*\*\*\*  
THE UNIVERSITY OF YAOUNDE I  
\*\*\*\*\*  
FACULTY OF SCIENCE  
\*\*\*\*\*

DEPARTEMENT DE CHIMIE ORGANIQUE  
DEPARTMENT OF ORGANIC CHEMISTRY

ATTESTATION DE CORRECTION DE MEMOIRE DE THESE DE DOCTORAT/Ph.D

DE Madame Anoumedem Mouafo Elodie Gisèle

**Sujet de la thèse:** Chemical constituents of three endophytic fungi: *Simplicillium subtropicum* harboured in *Duguetia staudtii* (Annonaceae) and two new *Diaporthe* sp. isolated from *Trema guineensis* (Ulmaceae); antibacterial activity and cytotoxicity of selected compounds.

Nous soussignés, enseignants ci-dessous nommés, membres du jury de soutenance de thèse de Doctorat/Ph.D de Madame Anoumedem Mouafo Elodie Gisèle, Matricule 09T0014, attestons que cette candidate a bel et bien pris en compte dans la mouture finale de sa thèse, toutes corrections et recommandations qui lui ont été faites au cours de sa soutenance en date du 11 Mai 2023.

En foi de quoi, la présente attestation de correction lui est délivrée pour servir et valoir ce que de droit.

Fait à Yaoundé, le 04/06/2023

**Le Jury :**

**Président**

Dieudonné E. Pegnyemb  
Pr, UYI

**Rapporteur**

Siméon F. Kouam  
Pr, UYI

**Membres**

Céline N. Nkenfou  
Pr, UYI

Bruno N. Lenta  
Pr, UYI

Joseph Thierry Ndongo  
MC. UYI

Jean Duplex Wansi  
Pr, UD

UNIVERSITÉ DE YAOUNDÉ I

Faculté des Sciences

Division de la Programmation et du  
Suivi des Activités Académiques

THE UNIVERSITY OF YAOUNDE I

Faculty of Science

Division of Programming and Follow-up  
of Academic Affairs

## LIST OF PERMANENT TEACHING STAFF OF THE FACULTY OF SCIENCE

ANNÉE ACADEMIQUE 2022/2023

(Par Département et par Grade)

DATE D'ACTUALISATION : 22 Juin 2022

**ADMINISTRATION****DOYEN** : TCHOUANKEU Jean- Claude, *Maître de Conférences***VICE-DOYEN / DPSAA** : ATCHADE Alex de Théodore, *Professeur***VICE-DOYEN / DSSE** : NYEGUE Maximilienne Ascension, *Professeur***VICE-DOYEN / DRC** : ABOSSOLO ANGUE Monique, *Maître de Conférences***Chef Division Administrative et Financière** : NDOYE FOE Florentine Marie Chantal,  
*Maître de Conférences***Chef Division des Affaires Académiques, de la Scolarité et de la Recherche DAASR** :  
AJEAGAH Gideon AGHAINDUM, *Professeur***1- DÉPARTEMENT DE BIOCHIMIE (BC) (39)**

N°	NOMS ET PRÉNOMS	GRADE	OBSERVATIONS
1	BIGOGA DAIGA Jude	Professeur	En poste
2	BOUDJEKO Thaddée	Professeur	En poste
3	FEKAM BOYOM Fabrice	Professeur	En poste
4	FOKOU Elie	Professeur	En poste
5	KANSCI Germain	Professeur	En poste
6	MBACHAM FON Wilfried	Professeur	En poste
7	MOUNDIPA FEWOU Paul	Professeur	Chef de Département
8	OBEN Julius ENYONG	Professeur	En poste
9	ACHU Merci BIH	Maître de Conférences	En poste

10	ATOGHO Barbara Mma	Maître de Conférences	En poste
11	AZANTSA KINGUE GABIN BORIS	Maître de Conférences	En poste
12	BELINGA née NDOYE FOE F. M. C.	Maître de Conférences	Chef DAF / FS
13	DJUIDJE NGOUNOUE Marcelline	Maître de Conférences	En poste
14	EFFA ONOMO Pierre	Maître de Conférences	En poste
15	EWANE Cécile Anne	Maître de Conférences	En poste
16	KOTUE TAPTUE Charles	Maître de Conférences	En poste
17	MOFOR née TEUGWA Clotilde	Maître de Conférences	Doyen FS/UDs
18	NANA Louise épouse WAKAM	Maître de Conférences	En poste
19	NGONDI Judith Laure	Maître de Conférences	En poste
20	NGUEFACK Julienne	Maître de Conférences	En poste
21	NJAYOU Frédéric Nico	Maître de Conférences	En poste
22	TCHANA KOUATCHOUA Angèle	Maître de Conférences	En poste
23	AKINDEH MBUH NJI	Chargé de Cours	En poste
24	BEBEE Fadimatou	Chargée de Cours	En poste
25	BEBOY EDJENGUELE Sara Nathalie	Chargé de Cours	En poste
26	DAKOLE DABOY Charles	Chargé de Cours	En poste
27	DJUIKWO NKONGA Ruth Viviane	Chargée de Cours	En poste
28	DONGMO LEKAGNE Joseph Blaise	Chargé de Cours	En poste
29	FONKOUA Martin	Chargé de Cours	En poste
30	KOUOH ELOMBO Ferdinand	Chargé de Cours	En poste
31	LUNGA Paul KEILAH	Chargé de Cours	En poste
32	MANANGA Marlyse Joséphine	Chargée de Cours	En poste
33	MBONG ANGIE M. Mary Anne	Chargée de Cours	En poste
34	OWONA AYISSI Vincent Brice	Chargée de Cours	En poste
35	Palmer MASUMBE NETONGO	Chargé de Cours	En poste
36	PECHANGOU NSANGOU Sylvain	Chargé de Cours	En poste
37	WILFRIED ANGIE Abia	Chargé de Cours	En poste
38	MBOUCHE FANMOE Marceline Joëlle	Chargé de Cours	En poste
39	FOUPOUAPOUOGNIGNI Yacouba	Assistant	En poste

## 2- DÉPARTEMENT DE BIOLOGIE ET PHYSIOLOGIE ANIMALES (BPA) (51)

1	AJEAGAH Gideon AGHAINDUM	Professeur	DAARS/FS
2	BILONG BILONG Charles-Félix	Professeur	Chef de Département
3	DIMO Théophile	Professeur	En Poste
4	DJIETO LORDON Champlain	Professeur	En Poste
5	DZEUFIET DJOMENI Paul Désiré	Professeur	En Poste
6	ESSOMBA née NTSAMA MBALA	Professeur	Vice Doyen/FMSB/UIYI
7	FOMENA Abraham	Professeur	En Poste
8	KEKEUNOU Sévilor	Professeur	En poste
9	NJAMEN Dieudonné	Professeur	En poste

10	NJIOKOU Flobert	Professeur	En Poste
11	NOLA Moïse	Professeur	En poste
12	TAN Paul VERNYUY	Professeur	En poste
13	TCHUEM TCHUENTE Louis Albert	Professeur	<i>Inspecteur de service Coord.Progr./MINS ANTE</i>
14	ZEBAZE TOGOUET Serge Hubert	Professeur	En poste
15	ALENE Désirée Chantal	Maître de Conférences	En poste
15	BILANDA Danielle Claude	Maître de Conférences	En poste
17	DJIOGUE Séfirin	Maître de Conférences	En poste
18	JATSA BOUKENG Hermine épouse MEGAPTCHE	Maître de Conférences	En Poste
19	LEKEUFACK FOLEFACK Guy B.	Maître de Conférences	En poste
20	MBENOUN MASSE Paul Serge	Maître de Conférences	En poste
21	MEGNEKOU Rosette	Maître de Conférences	En poste
22	MONY Ruth épouse NTONE	Maître de Conférences	En Poste
23	NGUEGUIM TSOFAK Florence	Maître de Conférences	En poste
24	NGUEMBOCK	Maître de Conférences	En poste
25	TOMBI Jeannette	Maître de Conférences	En poste
26	ATSAMO Albert Donatien	Chargé de Cours	En poste
27	BASSOCK BAYIHA Etienne Didier	Chargé de Cours	En poste
28	DONFACK Mireille	Chargée de Cours	En poste
29	ESSAMA MBIDA Désirée Sandrine	Chargée de Cours	En poste
30	ETEME ENAMA Serge	Chargé de Cours	En poste
31	FEUGANG YOUMSSI François	Chargé de Cours	En poste
32	GONWOUO NONO Legrand	Chargé de Cours	En poste
33	GOUNOUE KAMKUMO Raceline	Chargée de Cours	En poste
34	KANDEDA KAVAYE Antoine	Chargé de Cours	En poste
35	KOGA MANG DOBARA	Chargé de Cours	En poste
36	LEME BANOCK Lucie	Chargé de Cours	En poste
37	MAHOB Raymond Joseph	Chargé de Cours	En poste
38	METCHI DONFACK MIREILLE FLAURE EPSE GHOUMO	Chargé de Cours	En poste
39	MOUNGANG Luciane Marlyse	Chargée de Cours	En poste
40	MVEYO NDANKEU Yves Patrick	Chargé de Cours	En poste
41	NGOUATEU KENFACK Omer Bébé	Chargé de Cours	En poste
42	NJUA Clarisse Yafi	Chargée de Cours	Chef Div. UBA
43	NOAH EWOTI Olive Vivien	Chargée de Cours	En poste

44	TADU Zephyrin	Chargé de Cours	En poste
45	TAMSA ARFAO Antoine	Chargé de Cours	En poste
46	YEDE	Chargé de Cours	En poste
47	YOUNOUSSA LAME	Chargé de Cours	En poste
48	AMBADA NDZENGUE GEORGIA ELNA	Assistante	En poste
49	FOKAM Alvine Christelle Epse KEGNE	Assistante	En poste
50	MAPON NSANGO Indou	Assistant	En poste
51	NWANE Philippe Bienvenu	Assistant	En poste

<b>3- DÉPARTEMENT DE BIOLOGIE ET PHYSIOLOGIE VÉGÉTALES (BPV) (33)</b>			
1	AMBANG Zachée	Professeur	Chef Division/UYII
2	DJOCGOUE Pierre François	Professeur	En poste
3	MBOLO Marie	Professeur	En poste
4	MOSSEBO Dominique Claude	Professeur	En poste
5	YOUMBI Emmanuel	Professeur	Chef de Département
6	ZAPFACK Louis	Professeur	En poste
7	ANGONI Hyacinthe	Maître de Conférences	En poste
8	BIYE Elvire Hortense	Maître de Conférences	En poste
9	MALA Armand William	Maître de Conférences	En poste
10	MBARGA BINDZI Marie Alain	Maître de Conférences	CT/ MINESUP
11	NDONGO BEKOLO	Maître de Conférences	En poste
12	NGODO MELINGUI Jean Baptiste	Maître de Conférences	En poste
13	NGONKEU MAGAPTCHE Eddy L.	Maître de Conférences	En poste
14	TONFACK Libert Brice	Maître de Conférences	En poste
15	TSOATA Esaïe	Maître de Conférences	En poste
16	ONANA JEAN MICHEL	Maître de Conférences	En poste
17	DJEUANI Astride Carole	Chargé de Cours	En poste
18	GOMANDJE Christelle	Chargée de Cours	En poste
19	GONMADGE CHRISTELLE	Chargée de Cours	En poste
20	MAFFO MAFFO Nicole Liliane	Chargé de Cours	En poste
21	MAHBOU SOMO TOUKAM. Gabriel	Chargé de Cours	En poste
22	NGALLE Hermine BILLE	Chargée de Cours	En poste
23	NNANGA MEBENGA Ruth Laure	Chargé de Cours	En poste
24	NOUKEU KOUAKAM Armelle	Chargé de Cours	En poste
24	ONANA JEAN MICHEL	Chargé de Cours	En poste
25	NSOM ZAMBO EPSE PIAL ANNIE CLAUDE	Chargé de Cours	<i>En détachement/UNESCO MALI</i>

26	GODSWILL NTSOMBOH NTSEFONG	Chargé de Cours	En poste
27	KABELONG BANAHO Louis- Paul-Roger	Chargé de Cours	En poste
28	KONO Léon Dieudonné	Chargé de Cours	En poste
29	LIBALAH Moses BAKONCK	Chargé de Cours	En poste
30	LIKENG-LI-NGUE Benoit C	Chargé de Cours	En poste
31	TAEDOUNG Evariste Hermann	Chargé de Cours	En poste
32	TEMEGNE NONO Carine	Chargé de Cours	En poste
33	MANGA NDJAGA JUDE	Assistant	En poste

**4- DÉPARTEMENT DE CHIMIE INORGANIQUE (CI) (31)**

1	AGWARA ONDOH Moïse	Professeur	<i>Chef de Département</i>
2	Florence UFI CHINJE épouse MELO	Professeur	<i>Recteur Univ. Ngaoundéré</i>
3	GHOGOMU Paul MINGO	Professeur	<i>Ministre Chargé de Miss.PR</i>
4	NANSEU Njiki Charles Péguy	Professeur	En poste
5	NDIFON Peter TEKE	Professeur	<i>CT MINRESI</i>
6	NDIKONTAR Maurice KOR	Professeur	<i>Vice-Doyen Univ. Bamenda</i>
7	NENWA Justin	Professeur	En poste
8	NGAMENI Emmanuel	Professeur	<i>DOYEN FS Univ. Ngaoundéré</i>
9	NGOMO Horace MANGA	Professeur	<i>Vice Chancellor/UB</i>
10	ACAYANKA Elie	Maître de Conférences	En poste
11	EMADACK Alphonse	Maître de Conférences	En poste
12	KAMGANG YOUBI Georges	Maître de Conférences	En poste
13	KEMMEGNE MBOUGUEM Jean C.	Maître de Conférences	En poste
14	KENNE DEDZO Gustave	Maître de Conférences	En poste
15	KONG SAKEO	Maître de Conférences	En poste
16	MBEY Jean Aime	Maître de Conférences	En poste
17	NDI NSAMI Julius	Maître de Conférences	En poste
18	NEBAH Née NDOSIRI Bridget NDOYE	Maître de Conférences	<i>CT/ MINPROFF</i>
19	NJIOMOU C. épouse DJANGANG	Maître de Conférences	En poste
20	NJOYA Dayirou	Maître de Conférences	En poste
21	NYAMEN Linda Dyorisse	Maître de Conférences	En poste
22	PABOUDAM GBAMBIE AWAWOU	Maître de Conférences	En poste
23	TCHAKOUTE KOUAMO Hervé	Maître de Conférences	En poste
24	BELIBI BELIBI Placide Désiré	Chargé de Cours	CS/ ENS Bertoua

25	CHEUMANI YONA Arnaud M.	Chargé de Cours	En poste
26	KOUOTOU DAOUDA	Chargé de Cours	En poste
27	MAKON Thomas Beauregard	Chargé de Cours	En poste
28	NCHIMI NONO KATIA	Chargé de Cours	En poste
29	NJANKWA NJABONG N. Eric	Chargé de Cours	En poste
30	PATOUOSSA ISSOFA	Chargé de Cours	En poste
33	SIEWE Jean Mermoz	Chargé de Cours	En Poste

**5- DÉPARTEMENT DE CHIMIE ORGANIQUE (CO) (38)**

1	DONGO Etienne	Professeur	Vice-Doyen/FSE/UUI
2	NGOUELA Silvère Augustin	Professeur	Chef de Département UDS
3	NYASSE Barthélemy	Professeur	En poste
4	PEGNYEMB Dieudonné Emmanuel	Professeur	<i>Directeur/ MINESUP/</i> Chef de Département
5	WANDJI Jean	Professeur	En poste
6	MBAZOA née DJAMA Céline	Professeur	En poste
7	Alex de Théodore ATCHADE	Maître de Conférences	Vice-Doyen / DPSAA
8	AMBASSA Pantaléon	Maître de Conférences	En poste
9	EYONG Kenneth OBEN	Maître de Conférences	En poste
10	FOLEFOC Gabriel NGOSONG	Maître de Conférences	En poste
11	FOTSO WABO Ghislain	Maître de Conférences	En poste
12	KAMTO Eutrophe Le Doux	Maître de Conférences	En poste
13	KENMOGNE Marguerite	Maître de Conférences	En poste
14	KEUMEDJIO Félix	Maître de Conférences	En poste
15	KOUAM Jacques	Maître de Conférences	En poste
16	MKOUNGA Pierre	Maître de Conférences	En poste
17	MVOT AKAK CARINE	Maître de Conférences	En poste
18	NGO MBING Joséphine	Maître de Conférences	<i>Chef de Cellule</i> <i>MINRESI</i>
19	NGONO BIKOBO Dominique Serge	Maître de Conférences	C.E.A/ MINESUP
20	NOTE LOUGBOT Olivier Placide	Maître de Conférences	<i>DAAC/Uté Bertoua</i>
21	NOUNGOUE TCHAMO Diderot	Maître de Conférences	En poste
22	TABOPDA KUATE Turibio	Maître de Conférences	En poste
23	TAGATSING FOTSING Maurice	Maître de Conférences	En poste
24	TCHOUANKEU Jean-Claude	Maître de Conférences	<i>Doyen /FS/ UUI</i>
25	YANKEP Emmanuel	Maître de Conférences	En poste
26	ZONDEGOUMBA Ernestine	Maître de Conférences	En poste
27	NGNINTEDO Dominique	Chargé de Cours	En poste
28	NGOMO Orléans	Chargée de Cours	En poste
29	OUAHOUE WACHE Blandine M.	Chargée de Cours	En poste
30	SIELINOU TEDJON Valérie	Chargé de Cours	En poste

31	MESSI Angélique Nicolas	Chargé de Cours	En poste
32	TCHAMGOUE Joseph	Chargé de Cours	En poste
33	TSAMO TONTSA Armelle	Chargé de Cours	En poste
34	TSEMEUGNE Joseph	Chargé de Cours	En poste
35	MUNVERA MFIFEN Aristide	Assistant	En poste
36	NONO NONO Éric Carly	Assistant	En poste
37	OUETE NANTCHOUANG Judith	Assistante	En poste
38	TSAFFACK Maurice	Assistant	En poste

**6- DÉPARTEMENT D'INFORMATIQUE (IN) (22)**

1	ATSA ETOUNDI Roger	Professeur	<i>Chef Div.MINESUP</i>
2	FOUDA NDJODO Marcel Laurent	Professeur	<i>Chef Dpt ENS/Chef IGA.MINESUP</i>
3	NDOUNDAM René	Maître de Conférences	En poste
4	TSOPZE Norbert	Maître de Conférences	En poste
5	ABESSOLO ALO'O Gislain	Chargé de Cours	Sous-Directeur/MINFOPRA
6	AMINOUE Halidou	Chargé de Cours	<i>Chef de Département</i>
7	DJAM Xaviera YOUH - KIMBI	Chargé de Cours	En Poste
8	DOMGA KOMGUEM Rodrigue	Chargé de Cours	En poste
9	EBELE Serge Alain	Chargé de Cours	En poste
10	HAMZA Adamou	Chargé de Cours	En poste
11	JIOMEKONG AZANZI Fidel	Chargé de Cours	En poste
12	KOUOKAM KOUOKAM E. A.	Chargé de Cours	En poste
13	MELATAGIA YONTA Paulin	Chargé de Cours	En poste
14	MONTHE DJIADEU Valery M.	Chargé de Cours	En poste
15	OLLE OLLE Daniel Claude Delort	Chargé de Cours	Directeur adjoint ENSET. Ebolowa
16	TAPAMO Hyppolite	Chargé de Cours	En poste
17	BAYEM Jacques Narcisse	Assistant	En poste
18	EKODECK Stéphane Gaël Raymond	Assistant	En poste
19	MAKEMBE. S. Oswald	Assistant	En poste
20	MESSI NGUELE Thomas	Assistant	En poste
21	NKONDOCK. MI. BAHANACK.N.	Assistant	En poste
22	NZEKON NZEKO'O ARMEL JACQUES	Assistant	En poste

<b>7- DÉPARTEMENT DE MATHÉMATIQUES (MA) (31)</b>			
1	AYISSI Raoult Domingo	Professeur	Chef de Département
2	EMVUDU WONO Yves S.	Professeur	<i>Inspecteur MINESUP</i>
3	KIANPI Maurice	Maître de Conférences	En poste
4	MBANG Joseph	Maître de Conférences	En poste
5	MBEHOU Mohamed	Maître de Conférences	En poste
6	MBELE BIDIMA Martin Ledoux	Maître de Conférences	En poste
7	NOUNDJEU Pierre	Maître de Conférences	<i>Chef service des programmes &amp; Diplômes/FS/UJI</i>
8	TAKAM SOH Patrice	Maître de Conférences	En poste
9	TCHAPNDA NJABO Sophonie B.	Maître de Conférences	Directeur/AIMS Rwanda
10	TCHOUNDJA Edgar Landry	Maître de Conférences	En poste
11	AGHOUKENG JIOFACK Jean Gérard	Chargé de Cours	Chef Cellule MINPLAMAT
12	BOGSO ANTOINE MARIE	Chargé de Cours	En poste
13	CHENDJOU Gilbert	Chargé de Cours	En poste
14	DJIADEU NGAHA Michel	Chargé de Cours	En poste
15	DOUANLA YONTA Herman	Chargé de Cours	En poste
16	KIKI Maxime Armand	Chargé de Cours	En poste
17	MBAKOP Guy Merlin	Chargé de Cours	En poste
18	MENGUE MENGUE David Joe	Chargé de Cours	En poste
19	NGUEFACK Bernard	Chargé de Cours	En poste
20	NIMPA PEFOUKEU Romain	Chargée de Cours	En poste
21	OGADOA AMASSAYOGA	Chargée de Cours	En poste
22	POLA DOUNDOU Emmanuel	Chargé de Cours	En poste
23	TCHEUTIA Daniel Duviol	Chargé de Cours	En poste
24	TETSADJIO TCHILEPECK M. E.	Chargé de Cours	En poste
25	BITYE MVONDO Esther Claudine	Assistante	En poste
26	FOKAM Jean Marcel	Assistant	En poste
27	LOUMNGAM KAMGA Victor	Assistant	En poste
28	MBATAKOU Salomon Joseph	Assistant	En poste
29	MBIAKOP Hilaire George	Assistant	En poste
30	MEFENZA NOUNTU Thiery	Assistant	En poste
31	TENKEU JEUFACK Yannick Léa	Assistant	En poste

<b>8- DÉPARTEMENT DE MICROBIOLOGIE (MIB) (22)</b>			
1	ESSIA NGANG Jean Justin	Professeur	<i>Chef de Département</i>
2	NYEGUE Maximilienne Ascension	Professeur	<i>VICE-DOYEN / DSSE</i>
3	NWAGA Dieudonné M.	Professeur	En poste

4	ASSAM ASSAM Jean Paul	Maître de Conférences	En poste
5	BOUGNOM Blaise Pascal	Maître de Conférences	En poste
6	BOYOMO ONANA	Maître de Conférences	En poste
7	KOUITCHEU MABEKU Epse KOUAM Laure Brigitte	Maître de Conférences	En poste
8	RIWOM Sara Honorine	Maître de Conférences	En poste
9	SADO KAMDEM Sylvain Leroy	Maître de Conférences	En poste
10	BODA Maurice	Chargé de Cours	En position d'absence irrégulière
11	ESSONO OBOUGOU Germain G.	Chargé de Cours	En poste
12	NJIKI BIKOÏ Jacky	Chargée de Cours	En poste
13	TCHIKOUA Roger	Chargé de Cours	En poste
14	ESSONO Damien Marie	Chargé de Cours	En poste
15	LAMYE Glory MOH	Chargé de Cours	En poste
16	MEYIN A EBONG Solange	Chargé de Cours	En poste
17	NKOUDOU ZE Nardis	Chargé de Cours	En poste
18	TAMATCHO KWEYANG Blandine Pulchérie	Chargé de Cours	En poste
19	TOBOLBAÏ Richard	Chargé de Cours	En poste
20	MONI NDEDI Esther Del Florence	Assistante	En poste
21	NKOUÉ TONG ABRAHAM	Assistant	En poste
22	SAKE NGANE Carole Stéphanie	Assistante	En poste

**9. DEPARTEMENT DE PYSIQUE(PHY) (43)**

1	BEN- BOLIE Germain Hubert	Professeur	En poste
2	DJUIDJE KENMOE épouse ALOYEM	Professeur	En poste
3	EKOBENA FOU DA Henri Paul	Professeur	<i>Vice-Recteur. UN</i>
4	ESSIMBI ZOBO Bernard	Professeur	En poste
5	NANA ENGO Serge Guy	Professeur	En poste
6	NANA NBENDJO Blaise	Professeur	En poste
7	NDJAKA Jean Marie Bienvenu	Professeur	Chef de Département
8	NJANDJOCK NOUCK Philippe	Professeur	En poste
9	NOUAYOU Robert	Professeur	En poste
10	PEMHA Elkana	Professeur	En poste

11	SAIDOU	Professeur	<i>Chef de centre/IRGM/MINRESI</i>
12	TABOD Charles TABOD	Professeur	Doyen FS Univ/Bda
13	TCHAWOUA Clément	Professeur	En poste
14	WOAFO Paul	Professeur	En poste
15	ZEKENG Serge Sylvain	Professeur	En poste
16	BIYA MOTTO Frédéric	Maître de Conférences	DG/HYDRO Mekin
17	BODO Bertrand	Maître de Conférences	En poste
18	ENYEGUE A NYAM épouse BELINGA	Maître de Conférences	En poste
19	EYEBE FOUA Jean sire	Maître de Conférences	En poste
20	FEWO Serge Ibraïd	Maître de Conférences	En poste
21	HONA Jacques	Maître de Conférences	En poste
22	MBINACK Clément	Maître de Conférences	En poste
23	MBONO SAMBA Yves Christian U.	Maître de Conférences	En poste
24	NDOP Joseph	Maître de Conférences	En poste
25	SIEWE SIEWE Martin	Maître de Conférences	En poste
26	SIMO Elie	Maître de Conférences	En poste
27	VONDOU Derbetini Appolinaire	Maître de Conférences	En poste
28	WAKATA née BEYA Annie	Maître de Conférences	<i>Directeur/ENS/UYI</i>
29	ABDOURAHIMI	Chargé de Cours	En poste
30	CHAMANI Roméo	Chargé de Cours	En poste
31	EDONGUE HERVAIS	Chargé de Cours	En poste
32	FOUEDJIO David	Chargé de Cours	Chef Cell. MINADER
33	MELI'I Joelle Larissa	Chargée de Cours	En poste
34	MVOGO ALAIN	Chargé de Cours	En poste
35	WOULACHE Rosalie Laure	Chargée de Cours	Absente depuis Janvier 2022
36	AYISSI EYEBE Guy François Valérie	Chargé de Cours	En poste
37	DJIOTANG TCHOTCHOU Lucie Angennes	Chargée de Cours	En poste
38	OTTOU ABE Martin Thierry	Chargée de Cours	En poste
39	TEYOU NGOUPOU Ariel	Chargée de Cours	En poste
40	KAMENI NEMATCHOUA Modeste	Assistant	En poste
41	LAMARA Maurice	Assistant	En poste
42	NGA ONGODO Dieudonné	Assistant	En poste
43	WANDJI NYAMSI William	Assistant	En poste

<b>10- DÉPARTEMENT DE SCIENCES DE LA TERRE (ST) (42)</b>			
1	BITOM Dieudonné	Professeur	<i>Doyen / FASA / Uds</i>
2	FOUATEU Rose épouse YONGUE	Professeur	En poste
3	NDAM NGOUPAYOU Jules-Remy	Professeur	En poste
4	NDJIGUI Paul Désiré	Professeur	Chef de Département
5	NGOS III Simon	Professeur	En poste
6	NKOUMBOU Charles	Professeur	En poste
7	NZENTI Jean-Paul	Professeur	En poste
8	ABOSSOLO née ANGUE Monique	Maître de Conférences	<i>Vice-Doyen / DRC</i>
9	BISSO Dieudonné	Maître de Conférences	<i>Directeur/Projet Barrage Memve'ele</i>
10	EKOMANE Emile	Maître de Conférences	En poste
11	FUH Calistus Gentry	Maître de Conférences	<i>Sec. D'Etat/MINMIDT</i>
12	GANNO Sylvestre	Maître de Conférences	En poste
13	GHOGOMU Richard TANWI	Maître de Conférences	CD/Uma
14	MOUNDI Amidou	Maître de Conférences	<i>CT/ MINIMDT</i>
15	NGO BIDJECK Louise Marie	Maître de Conférences	En poste
16	NGUEUTCHOUA Gabriel	Maître de Conférences	CEA/MINRESI
17	NJILAH Isaac KONFOR	Maître de Conférences	En poste
18	NYECK Bruno	Maître de Conférences	En poste
19	ONANA Vincent Laurent	Maître de Conférences	<i>Chef service Maintenance &amp; du Matériel/UYII</i>
20	TCHAKOUNTE J. épouse NUMBEM	Maître de Conférences	<i>Chef.cell / MINRESI</i>
21	TCHOUANKOUE Jean-Pierre	Maître de Conférences	En poste
22	TEMGA Jean Pierre	Maître de Conférences	En poste
23	YENE ATANGANA Joseph Q.	Maître de Conférences	<i>Chef Div. /MINTP</i>
24	ZO'O ZAME Philémon	Maître de Conférences	<i>DG/ART</i>
25	ANABA ONANA Achille Basile	Chargé de Cours	En poste
26	BEKOA Etienne	Chargé de Cours	En poste
27	ELISE SABABA	Chargé de Cours	En poste
28	ESSONO Jean	Chargé de Cours	En poste
29	EYONG JOHN TAKEM	Chargé de Cours	En poste
30	MAMDEM TAMTO LIONELLE ESTELLE	Chargé de Cours	En poste
31	MBESSE CECILE OLIVE	Chargée de Cours	En poste
32	MBIDA YEM	Chargé de Cours	En poste
33	METANG Victor	Chargé de Cours	En poste
34	MINYEM Dieudonné-Lucien	Chargé de Cours	<i>CD/Uma</i>
34	NGO BELNOUN Rose Noël	Chargée de Cours	En poste
36	NOMO NEGUE Emmanuel	Chargé de Cours	En poste
37	NTSAMA ATANGANA Jacqueline	Chargé de Cours	En poste

38	TCHAPTCHET TCHATO De P.	Chargé de Cours	En poste
39	TEHNA Nathanaël	Chargé de Cours	En poste
40	FEUMBA Roger	Assistant	En poste
41	MBANGA NYOBE Jules	Assistant	En poste
42	NGO'O ZE ARNAUD	Assistant	En poste

**Répartition chiffrée des Enseignants de la Faculté des Sciences de l'Université de Yaoundé I**

NOMBRE D'ENSEIGNANTS					
DÉPARTEMENT	Professeurs	Maîtres de Conférences	Chargés de Cours	Assistants	Total
BCH	8 (00)	14 (10)	15 (05)	02 (01)	<b>39 (16)</b>
BPA	14 (01)	11 (07)	22 (07)	04 (02)	<b>51 (17)</b>
BPV	06 (01)	10(01)	16 (09)	01 (00)	<b>33 (11)</b>
CI	09(01)	14(04)	08 (01)	00 (00)	<b>31 (06)</b>
CO	06 (01)	20 (04)	08 (03)	04 (01)	<b>38(09)</b>
IN	02 (00)	02 (00)	12 (01)	06 (00)	<b>22 (01)</b>
MAT	02 (00)	08 (00)	14 (01)	07 (01)	<b>31 (02)</b>
MIB	03 (01)	06 (02)	10 (03)	03 (02)	<b>22 (08)</b>
PHY	15 (01)	13 (02)	11 (03)	04 (00)	<b>43 (06)</b>
ST	07 (01)	16 (03)	18 (04)	01 (00)	<b>42(08)</b>
<b>Total</b>	<b>72 (07)</b>	<b>114 (33)</b>	<b>134 (37)</b>	<b>32 (07)</b>	<b>352 (84)</b>

Soit un total de **352 (84)** dont :

- Professeurs **72 (07)**
- Maîtres de Conférences **114 (33)**
- Chargés de Cours **134 (37)**
- Assistants **32 (07)**

( ) = Nombre de Femmes **84**

## TABLE OF CONTENTS

LIST OF PERMANENT TEACHING STAFF OF THE FACULTY OF SCIENCE .....	i
TABLE OF CONTENTS.....	xiii
Thesis declaration .....	xvii
Dedication.....	xviii
Acknowledgements.....	xix
Glossary .....	xxii
LIST OF TABLES.....	xxiv
LIST OF FIGURES .....	xxv
LIST OF SCHEMES.....	xxix
ABSTRACT.....	xxx
RÉSUMÉ .....	xxxii
GENERAL INTRODUCTION.....	34
GENERAL INTRODUCTION.....	1
CHAPTER I: LITERATURE REVIEW.....	5
I. Endophytes from medicinal plants .....	5
I.1. Fungi and bacteria natural products in drug discovery.....	5
I.2. Endophytes: a rich source of bioactive compounds.....	6
I.2.1. Definition and classification.....	6
I.2.2. Endophyte-host plant interactions.....	7
I.2.3. Endophytes and epiphytes.....	7
I.3. Endophytic fungi.....	8
I.3.1. Definition and classification.....	8
I.3.2. Importance/functional significance of endophytic fungi .....	9
I.4. Endophytic fungi as a rich source of pharmaceutical agents.....	9

---

I.4.1. Anti-infective agents .....	9
I.4.2. Anticancer agents .....	10
I.4.3. Immunosuppressive agents .....	11
I.4.4. Cholesterol lowering agents .....	12
I.5. Previous investigation of endophytic fungi harboured in <i>Duguetia</i> genus.....	13
I.6. Previous chemical investigation of endophytic fungi harboured in <i>Trema</i> genus.....	13
I.7. Overview of the endophytic fungi of the genus <i>Simplicillium</i> and <i>Diaporthe</i> .....	13
I.7.1. Endophytic fungi of the genus <i>Simplicillium</i> .....	13
I.7.2. Overview of endophytic fungi of the genus <i>Diaporthe</i> .....	20
I.8. Mining silent gene clusters in endophytic fungi .....	40
I.9. Structure modification using endophytic fungi: biotransformation .....	41
I.10. Some techniques for structure determination and stereochemistry .....	41
I.10.1. The Mosher's method.....	41
I.10.2. Electronic circular dichroism (ECD, CD) .....	42
I.10.3. Single –crystal X-Ray diffraction .....	42
I.11. Literature overview about bacterial infectious diseases .....	43
I.11.1 Definition and classification of bacteria.....	43
I.11.2. Bacterial diseases .....	43
I.11.3. Treatment of bacterial infections.....	44
CHAPITRE II: RESULTATS ET DISCUSSION .....	46
II.1. Plant materials .....	46
II.2. Selection of fungal material.....	46
II.3. Morphological and molecular characterization of selected endophytic fungi.....	48
II.3.1. <i>Simplicillium subtropicum</i> .....	48
II.3.2. <i>Diaporthe</i> sp.1.nov.....	48

---

---

II.3.3. <i>Diaporthe</i> sp. 2.nov.....	48
II.4. Characterisation of isolated compounds.....	48
II.4.1. Secondary metabolites from <i>Simplicillium subtropicum</i> SPC3 .....	49
II.4.2. Secondary metabolites from <i>Diaporthe</i> sp. 2.nov .....	71
II.4.3. Secondary metabolites from <i>Diaporthe</i> sp.1.nov .....	120
II.5. Biogenesis relationship of isolated compounds.....	130
II.5.1. The hypothesis of the biogenetic relationship between the isolated compounds from <i>Simplicillium subtropicum</i> .....	130
II.5.2. The hypothesis of the biogenesis of the isolated compounds from <i>Diaporthe</i> sp.2.nov .....	131
II.5.3. The hypothesis of the biogenetic relationship between the isolated compounds from <i>Diaporthe</i> sp.1.nov .....	133
II.6. Biological activity of isolated compounds .....	133
II.6.1. Antimicrobial activities of selected isolated compounds.....	133
II.6.2. Cytotoxicity activity.....	135
GENERAL CONCLUSION AND OUTLOOK.....	137
CHAPTER III: EXPERIMENTAL PART .....	140
III. 1. General experimental procedures.....	140
III.1.1. Plant material.....	141
III.1.2. Fungal material .....	141
III.1.4. Isolation and purification of secondary metabolites.....	147
III.1.5. Determination of absolute stereochemistry by Mosher reaction .....	151
III.2. Physico-Chemical properties of isolated compounds .....	152
III.2.1. Compounds isolated from <i>Simplicillium subtropicum</i> . SPC3 .....	152
III.2.2. Compounds isolated from <i>Diaporthe</i> sp.2.nov.....	153
III.2.3. Compounds isolated from <i>Diaporthe</i> sp. 1.nov.....	157

---

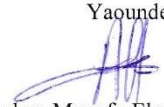
III.3. Biological materials and methods .....	157
III.3.1. Antimicrobial assays.....	157
III.3.3. Cytotoxicity assays .....	158
REFERENCES .....	172
Appendix.....	178
Appendix.....	179
Publications related to the thesis.....	179

### Thesis declaration

I, Anoumedem M.E. Gisèle, declare that the work described in this thesis, submitted in fulfilment of the requirements for the award of Doctorate/PhD in Organic Chemistry, at the Department of Organic Chemistry of the University of Yaoundé I, is wholly my own work. However, all efforts have been made to acknowledge or reference all contributions from other authors.

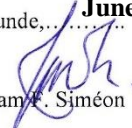
This work was done under the Supervision of Prof. Kouam F. Siméon, at the Laboratory of Fungi and Plant Natural Products of the Higher Teacher Training College (HTTC), University of Yaoundé 1 (Cameroon) in collaboration with Helmholtz Centre for Infection Research (HZI), Technical University of Braunschweig, Germany. I confirm that this work is original and has not been submitted for qualifications in any other academic institution.

Yaounde, **June 2, 2022**

  
Ms Anoumedem Mouafo Elodie Gisèle

In my capacity of the Supervisor of this thesis, and to the best of my knowledge, I declare that the above mention statement is true.

Yaounde, **June 2, 2022**

  
Prof. Kouam F. Siméon

## **Dedication**

**This thesis is dedicated to my mother, brothers and sisters, and my  
late father.**

## **Acknowledgements**

It is a pleasure to have the opportunity to thank all people that were involved directly or indirectly to the success of this doctoral thesis.

First of all, I thank God for making all this possible, for all his blessings and guidance in my life.

I would like to express my heartfelt gratitude to my supervisor Prof. Kouam F. Siméon, for offering me a great opportunity to join his research group since I was enrolled in my Master studies.

I wish to thank Prof. Nkengfack A. Ephrem for his numerous advice and support of various natures which contributed to the achievement of this work.

I wish to express my deepest gratitude to the Dean of the Faculty of Science Prof. Tchouankeu Jean Claude for his simple management of the administration.

Prof. Pegnyemb D. Emmanuel, the Head of Department of Organic Chemistry and all the teachers are acknowledged for initiating me to laboratory research and encouragements during my undergraduate and postgraduate studies.

I would like to express my deepest thanks and gratitude to all the teachers of the Department of Chemistry of the Higher Teacher Training College (HTTC) for their continuous encouragements.

Particularly, I express many cheers to the following Jury board that accepted to take part to the doctoral oral defence: Pegnyemb D. Emmanuel, Lenta N. Bruno , Nkenfou N. Céline, Professors and Ndongo J. Thierry, associated professor at the University of Yaoundé 1 and Wansi Jean Duplex, Professor at the University of Douala.

I would also like to express my special thanks and gratitude to Prof. Stadler Marc, Head of the Department of Microbial Drugs (MWIS) at the Helmholtz Centre for Infection Research (HZI) in Germany, who has always believed to my passion in the domain of bioactive natural products from fungi since my first steps in this research field in 2016 and for giving me the opportunity to achieve a part of this work at his institute, under the auspices of a scientific exchange project granted by the Alexander-von-Humboldt-Foundation (AvH).

I express my gratitude to the International Foundation for Sciences (IFS) for the grant they offered to me to support this work. The additional support of the German Academic Exchange Service

(DAAD), the AvH foundation and the World Academy of Sciences (TWAS) to Prof. Kouam F. Siméon is also appreciated.

I also express my cordial gratitude to my lab supervisors at HZI, Dr Thongbai Benjarong and Dr Yasmina Marin-Felix for their kind guidance and their instructive training, valuable suggestions, fruitful discussion in the area of fungi culture and their identification.

I also thank Dr. Surup Frank for his valuable contribution to the elucidations of some compounds reported in this thesis.

I deeply appreciate my former colleagues at HZI, namely Dr Wittstein Kathrin, Dr Schrey Hedda, Dr Hüttel Stephan, Dr Cheng Tian, Dr Becker Kevin, Ms. Hassan Khadija, Mr. Pfütze Sebastian, Mr. Pathompong P. Paomephan, Ms. Skiba Anke, Ms. Harms Karen, for sharing happiness during my research stay in Germany.

I am indebted to Dr Talontsi M. Ferdinand who gave me the strength to continue in the domain of fungi natural products research, as well as his valuable discussion and encouragements during my first step in the research area.

I sincerely thank all my colleagues and lab mates at HTTC of Yaoundé for their camaraderie and constant support. I express my deep appreciation and gratitude to my senior colleagues namely Dr Tatuedom K. Ostend, Dr Nguonpe W. Alain, Dr. Chenda N.L. Brancine, Dr Happy M. Gervais, Dr Tchamgoue Joseph, Dr Mountessou G.B. Yousouf, Dr Ngandjui T. Yvan, Dr Gathuissy Eliette, and Dr Ebessa Virginie for their good sense of teamwork and support. My profound gratitude to my lab mates Mbobda W.A. Sylvain, Dr Wouamba N. Steven, Dr Mouafon L. Iliassou, Kemgni F. Mireille, and Dr Kemayou M.G. Paulin for their fraternity spirit.

All that I have in my life is a result of huge sacrifices made by my parents. Really, I have no words to express my heartfelt gratitude and respect towards my parents and for their blessings, endless love and constant motivation throughout my studies, and for teaching me the spirit of education and integrity. My mother Zemkou Madeleine has always supported my ideas and directed me in my way. Mum, you are the best one can wish to have. To my late father, only God knows why he left me on the way and did not have the opportunity to be alive at the end of this work and I wish him to rest in peace.

I express many thanks to my lovely sister Ms Ngougni M.M. Noel and her husband Mr. Boulemo André, the best adoptive parents I have had since my first year at the University of Yaoundé I, for their constant encouragement and support during my studies.

To all my brothers and sisters Tsomo M.J.P. Bertrand, Mouafo T.A. Robinson, Kenfack M. Kevin, Atiofack M. H. Sylvie, Mejiokeng M.R. Armelle, and Nguimadjou M.A. Charlotte, I express my sincere gratitude for their permanent support and love during my education.

---

## Glossary

ATCC	American Type Culture Collection
brd	Broad doublet
brs	Broad singlet
CD	Circular Dichroism
COSY	Correlation spectroscopy
<i>d</i>	Doublet (in NMR)
DCM	Dichloromethane
<i>dd</i>	Doublet of doublet (in NMR)
DNA	Deoxyribonucleic acid
<i>D</i>	<i>Duguetia</i>
EC <sub>50</sub>	Effective concentration
ESI	Electrospray ionization
HMBC	Heteronuclear Multiple bond connectivity
HNC	Herbier National du Cameroun
HPLC	High performance liquid chromatography
HR-MS	High resolution mass spectrometry
HRESIMS	High Resolution electron spray ionisation mass spectrometry
IC <sub>50</sub>	Half maximal inhibitory concentration
IR	Infra-red
<i>J</i>	Coupling constant
LC	Liquid Chromatography
LC-MS	Liquid chromatography-mass spectrometry
<i>m</i>	Multiplet signal
MBC	Minimal bactericidal concentration
MIC	Minimum inhibitory concentration
MS	Mass spectrometry
MTPA	$\alpha$ -methoxy- $\alpha$ -trifluoromethylphenylacetic acid
mp	Melting point
<i>m/z</i>	Mass per charge
NMR	Nuclear magnetic resonance
PCR	Polymerase chain reaction

PDA	Potato destroxe Agar
PDB	Potato destroxe broth
ppm	Part per million
ROESY	Rotating frame overhauser enhancement spectroscopy
RP-18	Reversed phase C 18
rRNA	Ribosomal Ribonucleic Acid
RT	Retention time
<i>s</i>	Singlet signal
S.	Simplicillium
sp	Species
<i>t</i>	Triplet
TFA	Trifluoroacetic acid
TLC	Thin Layer chromatography
RT	Retention time
UV	Ultra-violet
WHO	Wold Health Organization

---

**LIST OF TABLES**

Table 1. Biological activities of some compounds from <i>Simplicillium</i> genus. ....	19
Table 2. Biological activity of some isolated compounds from <i>Diaporthe</i> . ....	36
Table 3. <sup>1</sup> H and <sup>13</sup> C NMR data (CDCl <sub>3</sub> ) of compound SPC-G1. ....	58
Table 4. <sup>1</sup> H and <sup>13</sup> C NMR data (CDCl <sub>3</sub> ) of compound SPC-G2. ....	65
Table 5. <sup>1</sup> H and <sup>13</sup> C NMR data (CDCl <sub>3</sub> ) of compound SPC-G3. ....	68
Table 6. <sup>1</sup> H NMR and <sup>13</sup> C NMR data (CDCl <sub>3</sub> ) of characteristic signals for compound SPC-G4 vs. ergosterol. ....	71
Table 7. <sup>1</sup> H and <sup>13</sup> C NMR data (DMSO- <i>d</i> <sub>6</sub> ) of compound DRT-G1. ....	73
Table 8. <sup>1</sup> H and <sup>13</sup> C NMR data (DMSO- <i>d</i> <sub>6</sub> ) of compound DRT-G2. ....	76
Table 9. <sup>1</sup> H and <sup>13</sup> C NMR data (DMSO- <i>d</i> <sub>6</sub> ) of compound DRT-G3. ....	82
Table 10. <sup>1</sup> H and <sup>13</sup> C NMR data (DMSO- <i>d</i> <sub>6</sub> ) of compound DRT-G4. ....	88
Table 11. <sup>1</sup> H and <sup>13</sup> C NMR data (CD <sub>3</sub> OD) of compound DRT-G5. ....	91
Table 12. <sup>1</sup> H and <sup>13</sup> C NMR data (CD <sub>3</sub> OD) of compound DRT-G6. ....	94
Table 13. <sup>1</sup> H and <sup>13</sup> C NMR data (CD <sub>3</sub> OD) of compound DRT-G7. ....	97
Table 14. <sup>1</sup> H and <sup>13</sup> C NMR data (CD <sub>3</sub> OD) of compound DRT-G8. ....	100
Table 15. <sup>1</sup> H and <sup>13</sup> C NMR data (CD <sub>3</sub> OD) of compound DRT-G9. ....	103
Table 16. <sup>1</sup> H and <sup>13</sup> C NMR data (CD <sub>3</sub> OD) of compound DRT-G10. ....	106
Table 17. <sup>1</sup> H and <sup>13</sup> C NMR data (CD <sub>3</sub> OD) of compound DRT-G11. ....	109
Table 18. <sup>1</sup> H and <sup>13</sup> C NMR data (DMSO- <i>d</i> <sub>6</sub> ) of compound DRT-G12. ....	112
Table 19. <sup>1</sup> H and <sup>13</sup> C NMR data (CD <sub>3</sub> OD) of compound DRT-G13. ....	114
Table 20. <sup>1</sup> H and <sup>13</sup> C NMR data (CD <sub>3</sub> OD) of compound DRT-G14. ....	117
Table 21. <sup>1</sup> H and <sup>13</sup> C NMR data (CD <sub>3</sub> OD) of compound DRT-G15. ....	120
Table 22. <sup>1</sup> H and <sup>13</sup> C NMR data (DMSO- <i>d</i> <sub>6</sub> ) of compound DLT-G1. ....	123
Table 23. <sup>1</sup> H and <sup>13</sup> C-NMR (DMSO- <i>d</i> <sub>6</sub> ).data of compound DLT-G2. ....	127
Table 24. <sup>1</sup> H and <sup>13</sup> C NMR (CD <sub>3</sub> OD).data of compound DLT-G3. ....	130
Table 25. Antibacterial activities of extracts and selected isolated compounds. ....	135
Table 26. Cytotoxic activities of 186 and 187 (IC <sub>50</sub> in µg/mL). ....	136

---

**LIST OF FIGURES**

Figure 1. Structures of some drugs from microorganisms. ....	6
Figure 2. Structures of some anti-infective agents from endophytes fungi. ....	10
Figure 3. Structures of some anticancer agents from endophytes fungi. ....	11
Figure 4. Structures of some immunosuppressive agents from endophytes fungi. ....	12
Figure 5. Structures of some cholesterol lowering agents from endophytic fungi. ....	12
Figure 6. <i>Simplicillium</i> strain a = Photography; b= Hyphae associated with the strain. ....	14
Figure 7. General biosynthesis of peptide bond. ....	15
Figure 8. Structures of some peptides isolated from <i>Simplicillium</i> . ....	17
Figure 9. Structures of some lipids isolated from <i>Simplicillium</i> . ....	17
Figure 10. Structures of some alkaloids isolated from <i>Simplicillium</i> . ....	18
Figure 11. Steroids of some terpenoids isolated from <i>Simplicillium</i> . ....	18
Figure 12. Structures of other classes of compounds isolated from <i>Simplicillium</i> . ....	19
Figure 13. <i>Diaporthe</i> strain; (a) = Photography; (b) and (c) = Hyphae associated with the strain .....	20
Figure 14. Structures of some xanthenes isolated from <i>Diaporthe</i> . ....	24
Figure 15. Structures of some chromones isolated from <i>Diaporthe</i> . ....	25
Figure 16. Structures of some chromanones isolated from <i>Diaporthe</i> . ....	26
Figure 17. Structures of some Furanones isolated from <i>Diaporthe</i> . ....	26
Figure 18. Structures of some pyrones isolated from <i>Diaporthe</i> . ....	27
Figure 19. Structures of some quinones isolated from <i>Diaporthe</i> . ....	28
Figure 20. Structures of some phenols isolated from <i>Diaporthe</i> . ....	29
Figure 21. Structures of some oblongolides isolated from <i>Diaporthe</i> . ....	30
Figure 22. Structures of some unclassified polyketides isolated from <i>Diaporthe</i> . ....	30
Figure 23. Structures of some terpenoids isolated from <i>Diaporthe</i> . ....	31
Figure 24. Structures of steroids isolated from <i>Diaporthe</i> . ....	31
Figure 25. Structures of some ten-membered lactones isolated from <i>Diaporthe</i> . ....	32
Figure 26. Structures of some alkaloids isolated from <i>Diaporthe</i> . ....	35
Figure 27. Structures of fatty acids isolated from <i>Diaporthe</i> . ....	35
Figure 28. Structure of some antibiotics. ....	44
Figure 29. LC-MS profile of the selected endophytic fungi. ....	47
Figure 30. Positive ion mode HR-ESI-MS of compound SPC-G1. ....	50
Figure 31. <sup>1</sup> H NMR spectrum (CDCl <sub>3</sub> , 500 MHz) of compound SPC-G1. ....	51

---

Figure 32. $^{13}\text{C}$ NMR spectrum ( $\text{CDCl}_3$ , 125 MHz) of compound SPC-G1.....	52
Figure 33. HSQC spectrum of compound SPC-G1.....	53
Figure 34. HMBC spectrum of compound SPC-G1 .....	54
Figure 35. COSY spectrum of compound SPC-G1.....	55
Figure 36. ROESY spectrum of compound SPC-G1 .....	55
Figure 37. $\Delta\delta^{\text{SR}}$ values (ppm) for the C-5' $\alpha$ -methoxy- $\alpha$ -trifluoromethylphenylacetyl (MTPA) esters for SPC-G1.....	57
Figure 38. J-based analysis of 4'-H/5'-H bond. Arrows indicate observed ROESY correlations. ....	57
Figure 39. (+)-HR-ESI-MS of compound SPC-G2.....	59
Figure 40. $^1\text{H}$ NMR spectrum ( $\text{CDCl}_3$ , 500 MHz) of compound SPC-G2.....	60
Figure 41. $^{13}\text{C}$ NMR ( $\text{CDCl}_3$ , 125 MHz) spectrum of compound SPC-G2. ....	61
Figure 42. COSY spectrum of compound SPC-G2.....	62
Figure 43. HSQC spectrum of compound SPC-G2.....	63
Figure 44. HMBC spectrum of compound SPC-G2 .....	63
Figure 45. ROESY spectrum of compound SPC-G2. ....	64
Figure 46. Negative ion mode (-)-ESI-MS of compound SPC-G3. ....	66
Figure 47. $^1\text{H}$ NMR ( $\text{CDCl}_3$ , 500 MHz,) spectrum of compound SPC-G3.....	67
Figure 48. $^1\text{H}$ NMR ( $\text{CDCl}_3$ , 500 MHz) spectrum of compound SPC-G4. ....	69
Figure 49. $^{13}\text{C}$ NMR ( $\text{CDCl}_3$ , 125 MHz) spectrum of compound SPC-G4. ....	70
Figure 50. (+)-HR-ESI-MS of compound DRT-G1.....	72
Figure 51. $^1\text{H}$ NMR spectrum ( $\text{DMSO}-d_6$ , 500 MHz) of compound DRT-G1.....	72
Figure 52. (+)-HR-ESI-MS of compound DRT-G2.....	74
Figure 53. $^1\text{H}$ NMR spectrum ( $\text{DMSO}-d_6$ , 500 MHz) of compound DRT-G2.....	75
Figure 54. (+)-HR-ESI-MS of compound DRT-G3.....	77
Figure 55. $^1\text{H}$ NMR spectrum ( $\text{DMSO}-d_6$ , 500 MHz) of compound DRT-G3.....	78
Figure 56. $^{13}\text{C}$ spectrum ( $\text{DMSO}-d_6$ , 125 MHz) of compound DRT-G3 .....	79
Figure 57. HSQC spectrum of compound DRT-G3.....	79
Figure 58. HMBC spectrum of compound DRT-G3.....	80
Figure 59. COSY spectrum of compound DRT-G3.....	81
Figure 60. HPLC chromatogram (a) and positive ion mode HR-ESI-MS spectrum (b) of compound DRT-G4.....	83
Figure 61. $^1\text{H}$ NMR spectrum ( $\text{DMSO}-d_6$ , 500 MHz). of compound DRT-G4.....	84

---

---

Figure 62. $^{13}\text{C}$ NMR spectrum (DMSO- $d_6$ , 125 MHz). of compound DRT-G4.....	85
Figure 63. COSY spectrum of compound DRT-G4.....	86
Figure 64. HSQC-DEPT spectrum of compound DRT-G4 .....	86
Figure 65. HMBC spectrum of compound DRT-G4.....	87
Figure 66. (+)-HR-ESI-MS of compound DRT-G5.....	89
Figure 67. $^1\text{H}$ NMR spectrum (CD $_3$ OD, 500 MHz) of compound DRT-G5.....	90
Figure 68. (+)-HR-ESI-MS of compound DRT-G6.....	92
Figure 69. $^1\text{H}$ NMR spectrum (CD $_3$ OD, 500 MHz) of compound DRT-G6.....	93
Figure 70. (+)-HR-ESI-MS of compound DRT-G7.....	95
Figure 71. $^1\text{H}$ NMR spectrum (CD $_3$ OD, 500 MHz) of compound DRT-G7.....	96
Figure 72. (+)-HR-ESI-MS of compound DRT-G8.....	98
Figure 73. $^1\text{H}$ NMR Spectrum (CD $_3$ OD, 500MHz) of compound DRT-G8.....	99
Figure 74. (+)-HR-ESI-MS of compound DRT-G9.....	101
Figure 75. $^1\text{H}$ NMR spectrum (CD $_3$ OD, 500 MHz) of compound DRT-G9.....	102
Figure 76. (+)-HR-ESI-MS of compound DRT-G10.....	104
Figure 77. $^1\text{H}$ NMR spectrum (CD $_3$ OD, 500 MHz) of compound DRT-G10.....	105
Figure 78. (+)-HR-ESI-MS of compound DRT-G11 .....	107
Figure 79. $^1\text{H}$ NMR spectrum (CD $_3$ OD, 500 MHz) of compound DRT-G11.....	108
Figure 80. (+)-HR-ESI-MS of compound DRT-G12.....	110
Figure 81. $^1\text{H}$ NMR spectrum (DMSO- $d_6$ , 500 MHz) of compound DRT-G12.....	111
Figure 82. (+)-HR-ESI-MS of compound DRT-G13.....	113
Figure 83. $^1\text{H}$ NMR spectrum (CD $_3$ OD, 500 MHz) of compound DRT-G13.....	113
Figure 84. (+) -HR-ESI-MS of compound DRT-G14.....	115
Figure 85. $^1\text{H}$ NMR spectrum (CD $_3$ OD, 500 MHz) of compound DRT-G14.....	116
Figure 86. (+)-HR-ESI-MS of compound DRT-G15.....	118
Figure 87. $^1\text{H}$ NMR spectrum (CD $_3$ OD, 500 MHz) of compound DRT-G15.....	119
Figure 88 (+)-HR-ESI-MS of compound DLT-G1. ....	121
Figure 89. $^1\text{H}$ NMR Spectrum (DMSO- $d_6$ , 500 MHz) of compound DLT-G1. ....	122
Figure 90. $^{13}\text{C}$ NMR (DMSO- $d_6$ , 125 MHz) spectrum of compound DLT-G1. ....	122
Figure 91. (+)-HR-ESI-MS of compound DLT-G2.....	124
Figure 92. $^1\text{H}$ NMR spectrum (DMSO- $d_6$ , 500 MHz) of compound DLT-G2. ....	125
Figure 93. $^{13}\text{C}$ NMR spectrum (DMSO- $d_6$ , 125 MHz) of compound DLT-G2. ....	126
Figure 94. (+)-HR-ESI-MS of compound DLT-G3.....	128

---

Figure 95 $^1\text{H}$ NMR Spectrum ( $\text{CD}_3\text{OD}$ , 500 MHz) of compound DLT-G3. ....	129
Figure 96. General workflow used during this work.....	142
Figure 97. <i>Simplicillium subtropicum</i> . (SPC3= pure strain). ....	143
Figure 98. <i>Diaporthe</i> sp.1 nov (F18 = pure strain). ....	143
Figure 99. <i>Diaporthe</i> sp.2.nov (R38 = pure strain).....	144

---

**LIST OF SCHEMES**

Scheme 1. Biosynthesis of polyketides .....	22
Scheme 2. Biosynthesis of polyketide benzopyranones.....	23
Scheme 3. Biosynthesis of cytochalasins. ....	33
Scheme 4. <sup>1</sup> H- <sup>1</sup> H COSY and important HMBC correlations (a) and key ROESY correlations (b) for SPC-G1. ....	56
Scheme 5. ROESY correlations of compound SPC-G2.....	62
Scheme 6. Structure of compound SPC-G3. ....	67
Scheme 7. Structure, key COSY and HMBC correlations in compound DRT-G3. ....	82
Scheme 8. Structure, Key COSY (—) and HMBC (↗) correlations of compound DRT-G4 .	88
Scheme 9. Proposed biogenetic relationship of the isolated from <i>Simplicillium subtropicum</i> . .....	131
Scheme 10. Proposed biogenetic relationship of the isolated Compounds from <i>Diaporthe</i> sp.2.nov. ....	132
Scheme 11. Proposed biogenetic relationship of the isolated compounds from <i>Diaporthe</i> sp.1.nov. ....	133
Scheme 12. Secondary metabolites from fermentation of <i>Simplicillium subtropicum</i> SPC3.	148
Scheme 13. Secondary metabolites from solid medium of <i>Diaporthe</i> sp.1.nov. ....	149
Scheme 14. Secondary metabolites from solid medium of <i>Diaporthe</i> sp.2.nov. ....	151

---

## ABSTRACT

The present work deals with the isolation, structural elucidation, and evaluation of antimicrobial and cytotoxicity activities of secondary metabolites isolated from potential endophytic harboured in two Cameroonian medicinal plants *Duguetia staudtii* and *Trema guineensis* (Ulmaceae). Notably, *Simplicillium subtropicum* isolated from the stem bark of *D. staudtii* showed variety of chemical compounds and therefore was cultured in a liquid medium. While two new *Diaporthe* sp. (1 and 2) isolated from the leaves and roots of *Trema guineensis* also produced remarkable chemical compositions and were separately cultured in a solid medium. Each extract was subjected to a variety of chromatographic techniques viz., liquid chromatography-mass spectrometry (LC-MS), column chromatography (CC), thin layer chromatography (TLC), and preparative high performance liquid chromatography (HPLC) to produce a total of twenty-two (22) compounds. The structures of all compounds were fully characterized by usual spectroscopic (UV, IR, 1D and 2D NMR), mass spectrometry (HRESIMS) techniques and by comparison with relevant data reported in the literature. However, four (04) compounds were isolated from *S. subtropicum* among which two (02) new polyketides, named simplicilones A and B whose the configuration of asymmetric centers were completed using Mosher ester method, and one (01) known fatty acid (linoleic acid) and the ubiquitous fungal sterol (ergosterol). Eighteen (18) compounds were also isolated from the two new *Diaporthe* sp. and were sorted into several classes of secondary metabolites viz., four (04) benzopyrones (including one new derivative: 3,9- diacetylalternariol), one (01) new benzofuranone, diapobenzofuranone, together with three known (03) alternariol derivatives (including alternariol, 2-hydroxyalternariol and 4-hydroxyalternariol), seven (07) known cytochalasins (including cytochalasin H, cytochalasin N, epoxycytochalasin H, cytochalasin J, cytochalasin J2, cytochalasin J3 and cytochalasin RKS-1778), two (02) cytosporones (cytosporones C and E); one (01) macrolide (lasiodiplodin), (01) biphenyl (5'-methoxy-6-methyl-biphenyl-3,4,3'-triol), one (01) chromone (2,5-dimethyl-7-hydroxychromone), one (01) glycol (sorbitol).

Extracts from *Diaporthe* sp. strains as well as some of the isolated compounds were screened *in vitro* for their antibacterial and antifungal activities on a plethora of microorganisms, including clinical strains. Extract from *Diaporthe* sp.1 displayed good antibacterial activity against *E. coli* with an MIC value of 15.6 µg/mL compared to the standard ciprofloxacin (MIC = 0.078 µg/mL) and moderate antibacterial activity against *S. enterica muenchen* and *E. cloacae* with MIC values

of 125 and 250  $\mu\text{g/mL}$ , respectively. Moreover, 2-hydroxyalternariol, lasiodiplodin showed moderate antibacterial activity against *E. coli* with MIC 62.5 – 125  $\mu\text{g/mL}$ . Simplicilones A and B displayed moderate *in vitro* cytotoxicity with  $\text{IC}_{50}$  values of 25 and 29  $\mu\text{g/mL}$ , respectively, against the cervix carcinoma cancer cell line KB3.1. They were inactive against the murine fibroblast cancer cell line. However, both compounds did not show any activity against Gram-positive and Gram-negative bacteria nor the used fungi strains.

**Keywords:** *Duguetia staudtii*; *Trema guineensis*; Endophytic fungi; *Simplicillium subtropicum*, *Diaporthe* sp., Polyketide, Antibacterial.

## RÉSUMÉ

Le présent travail porte sur l'isolement, l'élucidation structurale et l'évaluation des activités antimicrobiennes et cytotoxiques de métabolites secondaires isolés des endophytes potentiels isolés de *Duguetia staudtii* et *Trema guineensis* (Ulmaceae). Notamment, *Simplicillium subtropicum* isolé de l'écorce de tige de *Duguetia staudtii* a montré un bon profil chimique dans le milieu liquide et a été cultivé à grande l'échelle dans ce même milieu à fin d'obtenir un extrait brut. Tandis que les deux nouveaux *Diaporthe* sp. (1 et 2) isolés des feuilles et des racines de *Trema guineensis* respectivement ont également produit des profils chimiques remarquables et leurs cultures à grande échelle sur milieu solide ont conduit à deux extraits respectifs. Chaque extrait a été soumis à une variété de techniques chromatographiques, à savoir la chromatographie liquide-spectrométrie couplé à la masse (LC-MS), la chromatographie sur colonne (CC), la chromatographie sur couche mince (CCM) et la chromatographie liquide à haute performance (HPLC) pour produire un total de 22 composés. Les structures de ces composés ont été entièrement caractérisées par des techniques usuelles de spectroscopie (UV, IR, RMN 1D et 2D), d'analyse par spectrométrie de masse (HRESIMS) et par comparaison avec des données de la littérature. Cependant, quatre (04) composés ont été isolés de *S. subtropicum* parmi lesquels deux (02) nouveaux polykétides nommés simplicilones A et B dont la configuration des centre asymétriques ont été complétées par la méthode des esters de Mosher, et un (01) acide gras connu (acide linoléique) et le stérol (ergostérol). Dix-huit (18) composés ont également été isolés des deux nouveaux *Diaporthe* sp. et ont été classé en plusieurs classes de métabolites secondaires à savoir, quatre (04) benzopyrones (dont un dérivé nouveau: 3, 9-diacetylalternariol), un (01) benzofuranone nouveau (diapobenzofuranone) ensemble avec alternariol, 2-hydroxyalternariol et 4- hydroxyalternriol connus, sept (07) cytochalasins connues (cytochalasin H, cytochalasin N, epoxytochalasin H, cytochalasin J, cytochalasin J2, cytochalasin J3 et cytochalasin RKS-1778), deux (02) cytosporones connues (cytosporones C et E), un (01) macrolide connu (lasiodiplodine) un (01) biphényle connu (5'-méthoxy-6-méthyl-biphényl-3,4,3'-triol ; une (01) chromone connue (2,5-diméthyl-7 hydroxychromone) ; un (01) glycol connu (sorbitol).

Les extraits obtenus des nouvelles souches de *Diaporthe* sp. ainsi que certains des composés isolés ont été criblés *in vitro* pour leurs activités antibactériennes et antifongiques sur une pléthore de micro-organismes, y compris des souches cliniques. L'extrait de *Diaporthe* sp.1 a

montré une bonne activité antibactérienne contre *E. coli* avec une CMI de 15,6 µg/mL par rapport à la ciprofloxacine standard (CMI = 0,078 µg/mL) et une activité antibactérienne modérée contre *S. enterica muenchen* et *E. cloacae* avec des valeurs de CMI de 125 et 250 µg/mL, respectivement. De plus, le 2-hydroxyalternariol, lasiodiplodine a montré une activité antibactérienne modérée contre *E. coli* avec une CMI de 62,5 à 125 µg/mL. Simplicilones A et B ont présenté une cytotoxicité modérée avec des valeurs de cytotoxicité *in vitro* (CI<sub>50</sub>) de 25 et 29 µg/mL, respectivement, contre la lignée cellulaire de carcinome du cancer du col de l'utérus KB3.1. Ils étaient inactifs contre la lignée cellulaire du cancer de fibroblastes murins. Cependant, les deux composés n'ont montré aucune activité contre les bactéries Gram-positives et Gram négatives ni les souches de champignons utilisées.

**Mots-clés** : *Duguetia staudtii*; *Trema guineensis*; Champignons endophytes; *Simplicillium subtropicum*, *Diaporthe* sp, Polykétide, Antibactérien.

# **GENERAL INTRODUCTION**

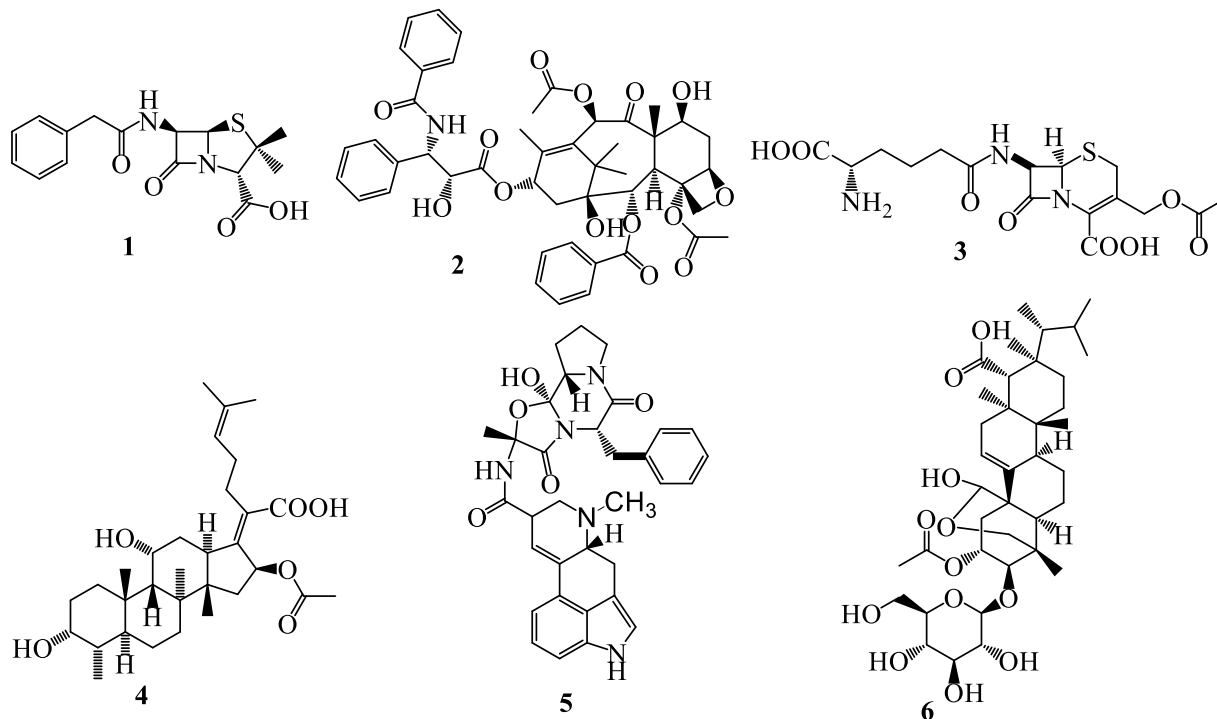


## GENERAL INTRODUCTION

Endophytes are microorganisms, which spend all or part of their lifecycle residing symbiotically within the healthy tissues of higher host plant. During their entire life, they mimic the chemistry of their respective host and therefore produce bioactive natural products, drops or derivatives as their hosts. Some tropical trees can increase their resistance by hosting endophytic microorganisms (Tiwari *et al.*, 2021; Rodriguez *et al.*, 2004). In exchange, plants provide up to the fifth of their carbohydrates from photosynthesis to their associated fungal partner (Wright *et al.*, 1998). Though the global diversity of endophytic fungi is far from being accessed, they are considered as potential metabolic factories capable of producing bioactive natural products with chemical, pharmacological, and toxicological profiles that can allow them to be considered as prototype molecules for the development of new bioactive agents. Metabolites so far isolated from endophytes have exhibited a plethora of biological activities including antimicrobial, antineoplastic, immunosuppressive and cytotoxic activities, with some already used as drugs (Schulz and Boyle, 2005). Some of these bioactive compounds have been commercialized as antibiotic drugs. Historically, the seminal discovery of penicillin (**1**) by Alexander Fleming from *penicillium rubens* (Fleming, 1929) resulted in an intense period of pursuit of fascinating chemically rich organisms as a reservoir of molecule templates for lead discovery. Since then, more than 23,000 bioactive metabolites of which 17,000 antibiotics (including e.g., cephalosporins, erythromycin, vancomycin, and daptomycin) have been discovered from microorganisms in the last 50 years (Janos Berdy, 2005; Arnold, 2013). Among these microorganisms, filamentous fungi represent an important group of eukaryotic organisms that are well known for producing many novel secondary metabolites directly used as drugs or lead compounds for synthetic analogs. For instance, the anticancer paclitaxel also known as taxol (**2**), is one of the promising medicines use to treat ovarian and breast cancers; the antibacterial cephalosporin (**3**), a second member of the beta-lactam antibiotic family was discovery from the endophytic fungus *cephalosporium acremonium* (Aoki and Okuhara, 1980); the steroidal clinical antibiotic produced by *Fusidium coccineum*, fusidic acid (**4**), is used for the treatment of Gram-positive bacterial infections (Adeleke and Babalola, 2021; Hamilton-Miller, 2008). Furthermore, ergotamine (**5**) is a vasoconstricting ergot alkaloid from *Claviceps purpurea* and used for the treatment of migraine type headaches, while an antifungal drug enfunmafungin (**6**) is a terpenoid

---

glycoside isolated from *Hormonema* sp demonstrated their ability to specifically inhibit glucan synthesis in fungi (Bills and Gloer, 2016).



Endophytic fungi include taxa with high metabolic activity, versatility, and an ability to produce different bioactive compounds. This chemical diversity is attractive for the discovery of new compounds with potential in the treatment or prevention of infective and neglected diseases. However, Alexander Fleming warned already in 1945 that frequent and irresponsible use of antibiotics triggered by public demand would lead to a loss of efficacy. His statement that “microbes are educated to resist penicillin” was an early warning that deserved much more attention than it actually received (Fleming, 1945) in strong contrast to the current situation, where antibiotic resistance is considered to be a health crisis by the World Health Organization. The six most problematic clinical pathogens were summarized by Louis Rice under the abbreviation “ESKAPE” bugs, namely *Enterococcus faecium*, *Staphylococcus aureus*, *Klebsiella pneumoniae*, *Acinetobacter baumannii*, *Pseudomonas aeruginosa*, and *Enterobacter* species. *Staphylococcus aureus*, for instance, gradually developed resistance to  $\beta$ -lactamases like penicillins and cephalosporins (Chambers *et al.*, 2001 ; Rice *et al.*, 2008).

Therefore, the need for new and efficient pharmaceutical compounds for the development of new antimicrobial drugs, especially those from natural origin and without toxic effects is felt

more than ever. In this regard, endophytic fungi in symptomless plants have been shown to be a promising source of antimicrobial and anticancer compounds.

Based on these observations the Department of Organic Chemistry of the University of Yaounde I, in collaboration with other universities and institutes around the world, focuses on Natural Product Chemistry as one of the main goals of its research program. In continuation of our ongoing search for bioactive metabolites from endophytic fungi harboured in Cameroonian medicinal plants ([Happi \*et al.\*, 2013](#), [Talontsi \*et al.\*, 2014](#)), we have investigated in this work, the chemical constituents of three endophytic fungi associated with *Duguetia staudtii* and *Trema guineensis* with the main objective to search for antibacterial and cytotoxic secondary metabolites from those selected endophytic fungi.

More specifically, we will have:

- To isolate and characterize endophytic fungi associated with *Duguetia staudtii* and *Trema guineensis*,
- To screen the obtained axenic cultures and select potent strains,
- To isolate and characterize secondary metabolites from selected strains,
- To evaluate antibacterial activity and cytotoxicity of crude extracts and isolated compounds.

Our work will be presented following three chapters. Chapter one is literature overview, the second chapter outlines the results obtained during the study, and finally the third chapter concerns the experimental part.

# **CHAPTER I: LITERATURE REVIEW**

## I. ENDOPHYTES FROM MEDICINAL PLANTS

### I.1. FUNGI AND BACTERIA NATURAL PRODUCTS IN DRUG DISCOVERY

Natural products generally originating from animal sources, insects, plants, and microbes are from prebiotic origin (Nakanishi, 1999). Moreover, many pharmaceutical records, such as Egyptian pharmaceutically recorded “Ebers Papyrus”; the Chinese Material medical, India Tibetan medicine found the necessity to describe the medical functions of plants, minerals and animals that were widely employed in traditional clinic (Borchardt, 2002). In effect, plants play an important role in humans for basic necessities like food clothing, residence as well as sources of medicines for the treatment of wide variety of diseases. In addition, medicinal substances from mushrooms often express promising curative effects which may include antitumor, immune modulating, cardiovascular, antiviral, antibacterial, and antiparasitic activities. Moreover, the investigation of microorganisms for bioactive metabolites was initiated by the discovery of penicillin G from *Penicillium notatum* by Alexander Fleming more than 80 years ago (1928). Since then, microorganisms as well as mushrooms became a hunting ground for novel drug leads (Rishton, 2008). Many scientists have contributed significantly to the rational development of drugs from Natural products. However, in 1947, chloramphenicol (**7**) has been isolated from soil actinomycete, *Streptomyces venezuelae* and used for the treatment of a wide range of gram-positive and gram-negative pathogens (Ehrlich *et al.*, 1947, Butler, 2004). Furthermore, erythromycin (**8**) has been discovered in 1952 from the actinomycete, *Saccharopolyspora etrthraea* (Butler, 2004). Strobilurins A (**9**) and B (**10**), were isolated from the mycelium of the basidiomycete, *Strobilurus tenacellus*, were developed as fungicides (Bartett *et al.*, 2001). echinocandin B (**11**) and Pneumocandin B (**12**), isolated from *Aspergillus rugulovalvus* and *Glarea lozoyensis*, respectively, were the lead compounds and templates for the semisynthetic antifungal drugs caspofungin and was developed as the antifungal drugs named caspofungin. (Morris and Villmann, 2006a).

Each of these discoveries contributed a milestone to Natural products development. Until now bioactive natural products are used in three categories: natural products with biological activities used directly as drugs, natural products as semi-synthetic templates and synthetically derived compounds inspired from nature (Newman *et al.*, 2003).

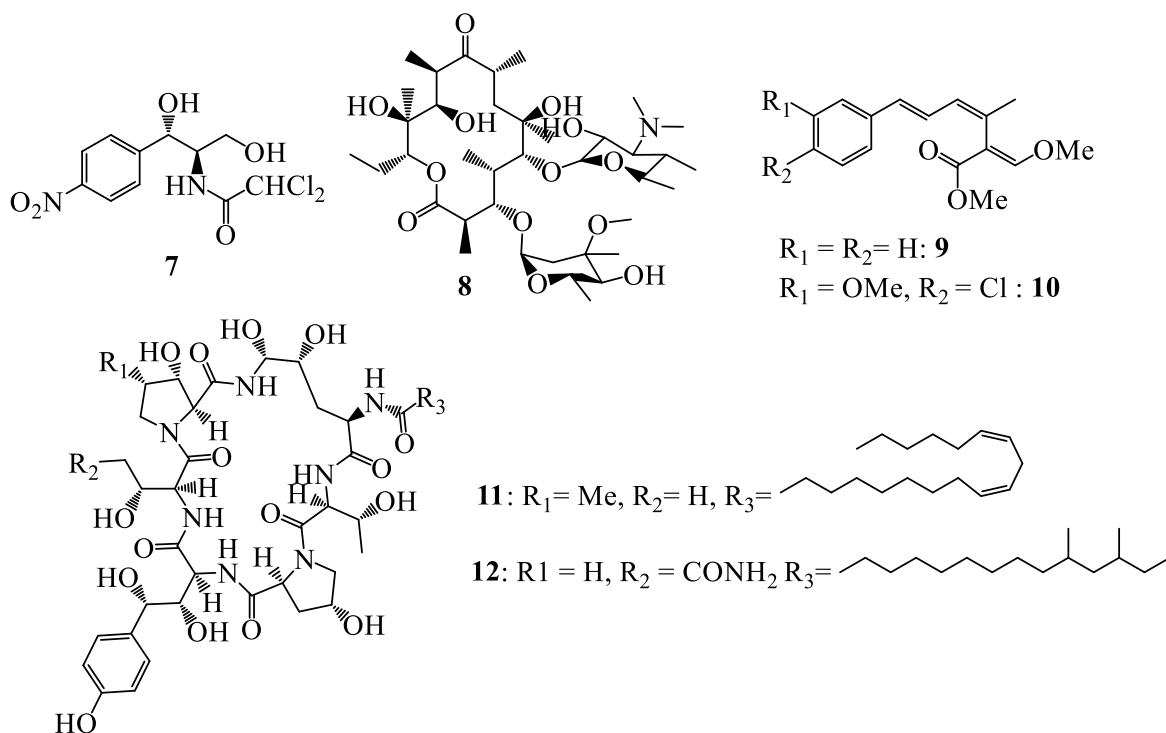


**Figure 1.** Structures of some drugs from microorganisms.

## I.2. ENDOPHYTES: A RICH SOURCE OF BIOACTIVE COMPOUNDS

### I.2.1. Definition and classification

Endophyte is the term used to characterize organisms found within tissues of living plants, including everything from virulent foliar pathogens to mycorrhizal roots symbionts. Firstly, introduced in 1866 by de Bary, mycologists generally agree today that, endophytes are organisms that colonize different parts of internal plant tissues without causing apparent harm to their host (Golinska *et al.*, 2015). These organisms are categorized into bacteria and fungi. More than 200 bacterial genera have been identified as endophytes distributed among the phyla Actinobacteria, Proteobacteria and Firmicutes (Golinska *et al.*, 2015). Endophytes are well known to produce a wide variety of bioactive compounds including antibiotics, antitumor and immunosuppressive agents, plant growth hormones, and biological substances like enzymes and vitamins which can play a vital role in pharmaceutical industry and agriculture (Uzma *et al.*, 2018; Mishra *et al.*, 2017a). They are also reported diactive compounds having the ability to inhibit bacterial and fungi pathogens and could help in protecting plants against phytopathogens (Rai *et al.*, 2016). In general, few endophytes share their compounds produced with plants as well (Kumara *et al.*, 2014; Shweta

*et al.*, 2014). These findings demonstrate that endophytes are present within plant tissues and are a reservoir of bioactive metabolites (Tan and Zou, 2001, Priti *et al.*, 2009).

### **I.2.2. Endophyte-host plant interactions**

Endophytes have been defined as microbes that invade almost all tissues of host plant. The relationship with the host plant lies on a symbiotic continuum, expressing itself as mutualism, commensalism and parasitism (Kogel *et al.*, 2006). Recently it has become clear that some of these interactions with endophytic bacteria and fungi can be latently pathogenic and/or mutualistic. In mutualistic interactions, the endophyte may improve growth of the host, convey stress tolerance, induce systemic resistance, or supply the host with nutrients. On the other hand, most endophytes are also able to grow saprotrophically, e.g., from surface-sterilized tissues on media containing dead organic substrates. Thus, it has become obvious that endophytes have multiple life history strategies. This intimate association and collaboration give rise to complex plant microbiome interactions, bringing forth an exciting explorable frontier (Yuan *et al.*, 2009). In addition, the co-evolution of endophytes and their particular host plants in adapting to environmental adversities and altered endophyte-host communication is believed to be linked to the biosynthesis of natural products (Aly *et al.*, 2011). Endophytic fungi have been documented to contribute to host plant defense in circumstances of biotic and abiotic stress (Rodriguez *et al.*, 2009). Endophytes have attracted increased attention since their first elaboration in 1904, following the discovery of paclitaxel a vital anticancer drug produced by endophytic fungus *Taxomyces andreanna*, which was harboured in the parent source plant, *Taxus brevifolia* (Stierle *et al.*, 1993). This evoked a shift toward endophytes as new sources of therapeutic agents and more comprehensive research pharmaceutically important fungal-endophyte derived natural products have been reported with unraveling bioactivity. However, research on the fungal biosynthesis of plants-associated metabolites in process and new approaches to improve the production of commercially essential plant-derivate compounds of endophytic fungi origin are still a challenge in the bioprospecting of endophytes (Aly *et al.*, 2010; Debbab *et al.*, 2012).

### **I.2.3. Endophytes and epiphytes**

Endophytes are sometimes contrasted to epiphytes which live on external tissue of plants surfaces (Santamaria and Bayman, 2005). In practice, the distinction is that epiphytes can be

washed of plant surfaces or be inactivated by surface disinfection, usually with sodium hypochlorite and ethanol to break surface tension, whereas endophytes cannot. Thus, epiphytes that survive surface disinfection and grows in culture might be confirmed to be an endophyte (Arnold and Lutzoni, 2007). Although, there are few studies comparing phylloplane and endophytic fungal communities of the same leaves, comparison within pin and coffee leaves indicates that endophytic communities are distinct from epiphytic ones, even though they may live less than a millimeter apart (Santamaria and Bayman, 2005). Temporally as well as practically, the distinction between endophytes and epiphytes is often arbitrary. Many horizontally transmitted endophytes presumably start growing on the surface of the leaf before penetration. Also, endophytes may become epiphytes when internal tissues are exposed, and may protect the exposed tissues to environmental attacks. In shoot tip derived tissues culture of *Pinus sylvestries*, calli were found to be covered by hyphae of the endophytes *Hormonema dematioides* and *Rhodotorula minuta* (Pirttilä *et al.*, 2002).

### **I.3. ENDOPHYTIC FUNGI**

#### **I.3.1. Definition and classification**

Endophytic fungi are microorganisms that live inside plants during a period of their life cycle or during their entire life, without causing visible disease to the host plant. They are present in all plants over the world and in every organ of angiosperms, gymnosperms, ferns, mosses, hepatics and algae. Fungi can also grow inside fruiting bodies of others fungi and in lichen thalli, mostly when they are located close to be photobiont (Krings *et al.*, 2007).

Endophytic fungi living inside the plants without causing symptoms are mostly species of Ascomycota and often belong to the Diaporthales, Helotiales, Hypocreales, Pleosporales or Xylariales (Piepenbring, 2015). They have been classified into two major groups based in difference in taxonomy, host range, colonization transmission patterns, tissue specificity and ecological function. The first group is the Clavicipitaceous endophytes (C-endophytes) which infect some grasses in cool regions. This group of fungi (Hypocreales, Ascomycota) includes free living and symbiotic species associated with insects, other fungi or grass rushes and edges (Bacon and White, 2000). The second one is non-Clavicipitaceous endophytes (NC-endophytes) which can be isolated from healthy tissues of non-vascular plants like ferns and their allies, conifers and angiosperms. It was classified into three functional groups based on host colonization and

---

transmission in plant biodiversity and fitness benefits conferred to hosts. Most of them belong to the Ascomycota family with a minority of basidiomycetes and protect hosts against fungal pathogens (Shweta *et al.*, 2014).

### **I.3.2. Importance/functional significance of endophytic fungi**

Fungi have important and complex role in the ecosystem. They contribute to the cycle of nutrients through ecosystem by the decomposition of dead organic material, and provide nutrients to plants. All plants in natural ecosystem appear to be symbiotic with their associated endophytic fungi (Rodriguez *et al.*, 2009). The highly diverse groups of endophytic fungi may offer significant benefits to their host by producing secondary metabolites that provide protection for survival, such as conferring abiotic and biotic stress tolerance, increasing biomass and decreasing water consumption, enhancing insect and disease resistance, and a source for the secretion of bioactive compounds.

## **I.4. ENDOPHYTIC FUNGI AS A RICH SOURCE OF PHARMACEUTICAL AGENTS**

### **I.4.1. Anti-infective agents**

The first group of antibiotics discovered in 1928 was penicillin (Fleming, 1929). This Penicillin family includes penicillin G (**13**), penicillin V (**14**) and benzathine penicillin which are all  $\beta$ -lactams (Shi *et al.*, 2011). Penicillin G shows its antimicrobial activity against Gram positive and only few Gram-negative bacteria such as *Neisseria gonorrhoeae* and *N. meningitidis*. The four membered  $\beta$ -lactam ring was found to be the activity center in the structure of penicillin. Fungi have initially been and still are used to produce medicines to treat infectious diseases (Shi *et al.*, 2011). Another  $\beta$ -lactam group was isolated in 1948 named cephalosporin. Moreover, cephalosporin C (**15**) was isolated from *Acremonium chrysogenum* (Sweet and Dahl, 1970). A novel antibacterial agent, guignardic acid (**16**), was isolated from the endophytic fungus *Guignardia bidwellii*. (Rodriguez *et al.*, 2009). The antifungal agent griseofulvin (**17**) has been isolated from the endophytic fungus *Penicillium griseofulvum* in 1939 and been used as an antifungal drug for treatment of ringworm in skin and nail in humans and animals (Petersen *et al.*, 2014).

---

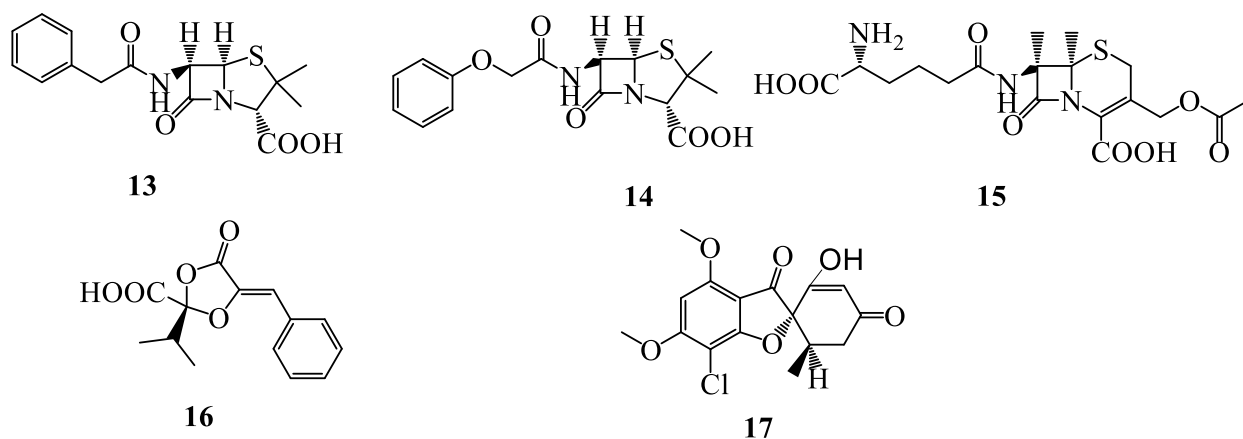


**Figure 2.** Structures of some anti-infective agents from endophytes fungi.

#### I.4.2. Anticancer agents

Paclitaxel (taxol) (**2**), the world wide famous anticancer drug is a densely function-groups substituted diterpene derivative that was firstly reported from endophytic fungi in 1993 from *Taxomyces andreanae* isolated from the yew *Taxus brevifolia* (Stierle *et al.*, 1993). This drug is used to treat ovarian cancer, breast cancer and lung cancer (Wood *et al.*, 1995). Initially isolated from the plant *Taxus brevifolia*, it was later isolated from the endophytic fungi *Pestalotiopsis* sp (Vennila and Muthumary, 2011). More anticancer compounds were isolated later such as vinblastine (**18**) from *Alternaria* sp and *Fusarium oxysporum* (Cragg and Newman, 2003; Kumar *et al.*, 2013). Another anticancer drug, which has been used in chemotherapy for some types of cancers including leukemia, lymphoma, breast and lung cancer for many years, is the indole derivative vincristine (**19**). This drug, available under the trade names Oncovin®, Vincasar®, and Vincrex®, was originally obtained from *Catharanthus roseus*. Very recently, a Chinese group reported preliminary evidence that vincristine might be produced by *Fusarium oxysporum* endophytic isolated from the same plant (Zhang *et al.*, 2006). In addition, topotecan (**20**) and irinotecan (**21**), two derivatives of camptothecin (**22**) were previously isolated from the stem and bark of the plant *Camptotheca acuminata* and were later isolated from endophytic fungi (*Entrophospora infrequens*, *Neurosporas* sp and *Fusarium Solani*). These compounds showed cytotoxicity against several cell lines such as lung cancer, liver cancer and ovarian cancer (Kharwar *et al.*, 2011).

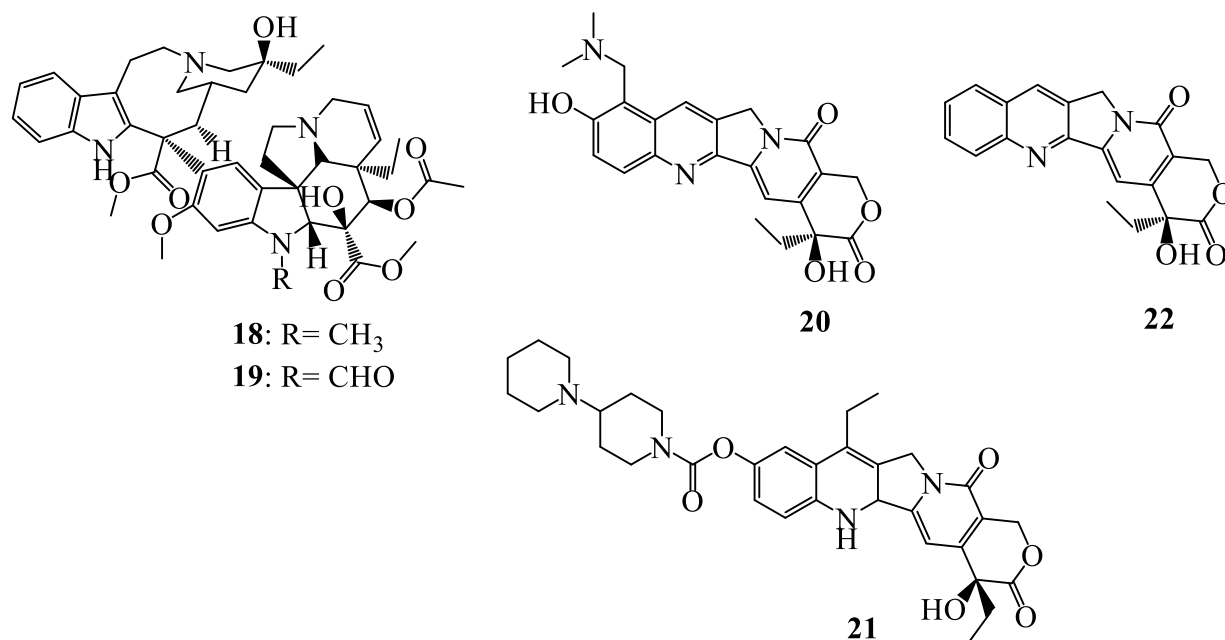


**Figure 3.** Structures of some anticancer agents from endophytes fungi.

#### I.4.3. Immunosuppressive agents

Mizoribine (**23**), an immunosuppressive agent was first isolated from the endophytic fungus *Penicillium* sp and later from *Eupenicillium brefeldianum* and Mycophenolic that is used as a prodrug of mycophenolate mofetil. It is used to inhibit the proliferation of lymphocytes selectively via inhibition of inosin monophosphate-dehydrogenase (IMPDH) (Ishikawa, 1999). Further, mycophenolic acid (**24**) is used as a non-competitive reversible inhibitor of IMPDH and then as the rate-limiting enzyme in the novo pathway of guanosine nucleotide synthesis (Chin *et al.*, 2006). In addition, cyclosporine A (**25**) produced by the endophytic fungus *Tolypocladium inflatum*; played an important role as immunosuppressive drug used to prevent rejection of organ and tissue transplantation (Cantrell and Smith, 1984). subglutinols A (**26**) and B (**27**), are noncytotoxic diterpene pyrones produced by *Fusarium subglutinans*, an endophyte of *Tripterigium wilfordii*. In the mixed lymphocyte reaction assay the subglutinols were roughly as potent as cyclosporine (Lee *et al.*, 1995; Tan and Zou, 2001).

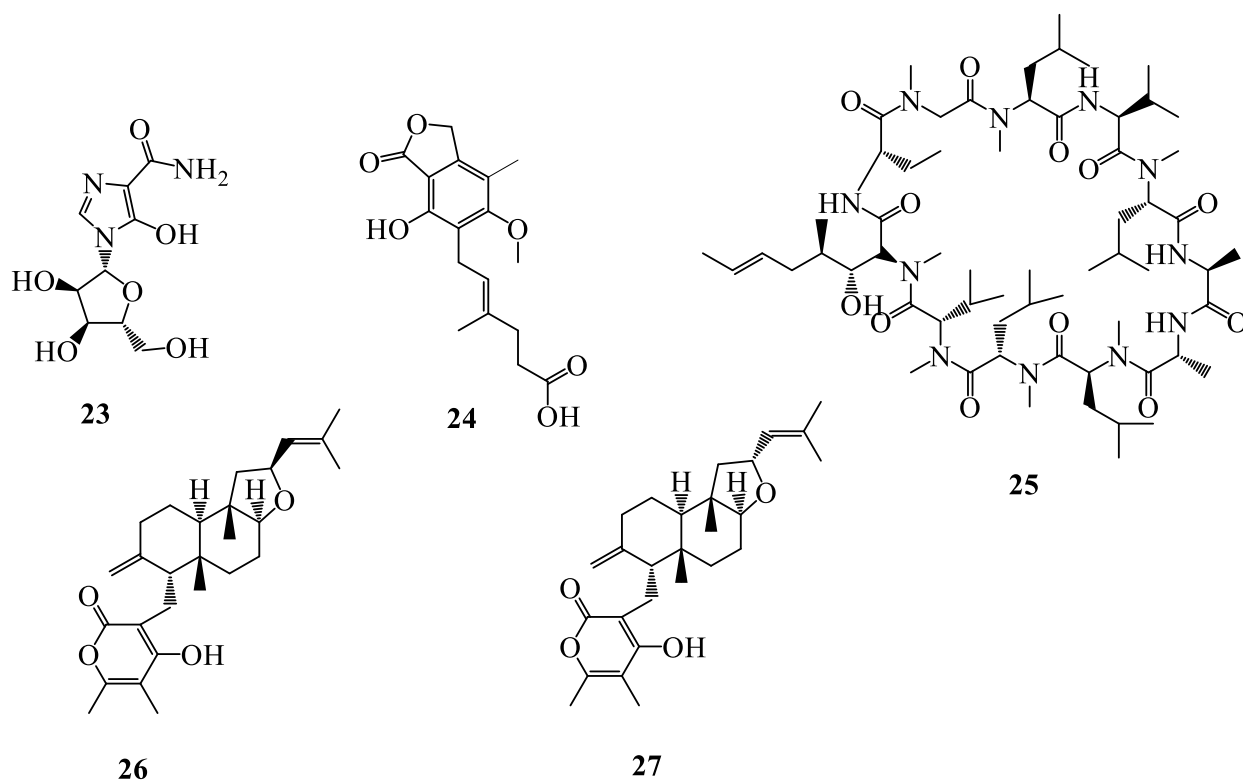


**Figure 4.** Structures of some immunosuppressive agents from endophytes fungi.

#### I.4.4. Cholesterol lowering agents

Lovastatin (**28**) isolated from an endophytic fungi *Aspergillus luchuensis*, LERV10 was the first commercialized hydroxymethylglutaryl coenzyme A reductase inhibitor among cholesterol lowering agents and was approved in 1987 (Lin *et al.*, 2014). Another fungal derived statin, mevastatin (**29**) was isolated from *Penicillium brevicompactum* (Endo, 1985). However, derivatives rosuvastatin calcium (**30**) and pitavastatin (**31**) were approved to be lipid-lowering agents and for the treatment of dyslipidemia respectively (Chin *et al.*, 2006).

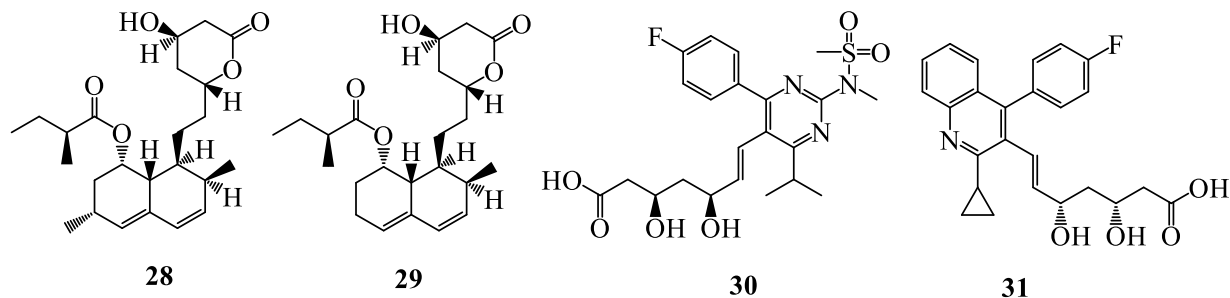
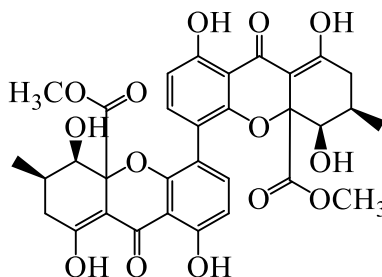


**Figure 5.** Structures of some cholesterol lowering agents from endophytic fungi.

## I.5. PREVIOUS INVESTIGATION OF ENDOPHYTIC FUNGI HARBOURED IN *DUGUETIA* GENUS

*Duguetia* is a largely common plant in sub-tropical regions and have limited information regarding study of their associated endophytic fungi.

However, [Koolen et al., 2013](#) have reported a novel xanthone dimer, talaroxanthone (**32**) isolated from the endophytic fungus *Talaromyces* sp. DgCr22.1b associated with *Duguetia stelechantha* (Diels) R. E. Fries.



32

## I.6. PREVIOUS CHEMICAL INVESTIGATION OF ENDOPHYTIC FUNGI HARBOURED IN *TREMA* GENUS

This is first reported research on the endophytic fungi from a medicinal plant in the genus *Trema*.

## I.7. OVERVIEW OF THE ENDOPHYTIC FUNGI OF THE GENUS *SIMPLICILLIUM* AND *DIAPORTHE*

### I.7.1. Endophytic fungi of the genus *Simplicillium*

#### I.7.1.1. General characteristics

The genus *Simplicillium* was first introduced in 2001 by Zare and Gams to accommodate four taxa including *Simplicillium lanosoniveum* and three other species *Simplicillium lamellicola*; *Simplicillium obclavatum* and *simplicillium wallacei*. *Simplicillium* was previously described as *Verticillium* sect., whereas *Simplicillium* species consistently formed a monophyletic group apart from the other described taxa in this family ([Zare et al., 2000](#); [Sung et al., 2001](#)). Recently, Clavicipitaceae was divided into three families, based on multi-gene phylogenetic analyses and *Simplicillium* was assigned to Cordycipitaceae ([Zare and Gams 2001](#); [Guo et al., 2012](#)).

Fungi species of the genus *Simplicillium* has a wide distribution and are considered as mammal and plant-parasitic, symbiotic, entomopathogenic, fungicolous and nematophagous fungi, as they have a broad spectrum of hosts and substrates, such as insects, plants, nematodes, human nails, canine tissues and mushrooms, *Chroococcus* sp., soil, freshwater, marine and terrene environments (Liu and Cai 2012; Dong *et al.*, 2018; Liang *et al.*, 2016; Sun *et al.*, 2019).

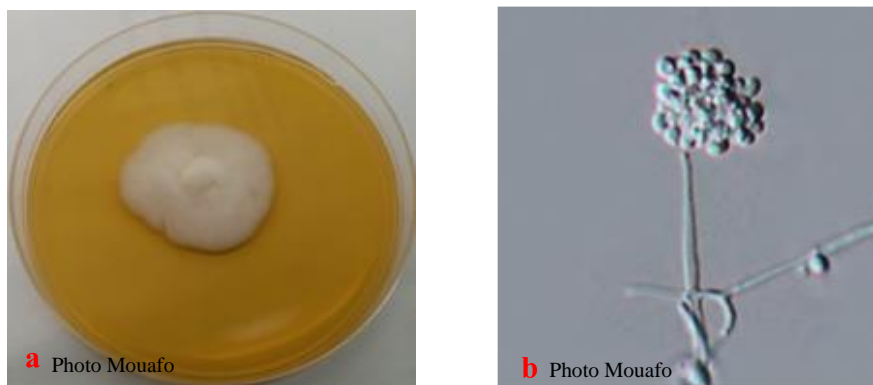


**Figure 6.** *Simplicillium* strain a = Photography; b= Hyphae associated with the strain

#### I.7.1.2. Importance and uses

*Simplicillium* species are microorganisms with considerably high ecological and economical value for biocontrol and bioactive compounds (Takata *et al.*, 2013; Yan *et al.*, 2015; Hyde *et al.*, 2019). For example, *Simplicillium chinense* can be a biological control agent against plant parasitic nematodes (Zhao *et al.*, 2013; Luyen 2017). *Simplicillium lamellicola* can suppress plant bacterial diseases and grey mould diseases of *Solanum lycopersicum* and *Panax ginseng* (Dang *et al.*, 2014; Shin *et al.*, 2017). *Simplicillium obclavatum* has the ability to produce multiple xylanases and endoglucanases that have the potential to be used in biofuels, animal feed and food industry applications (Roy *et al.*, 2013).

#### I.7.1.3. Previous chemical works on the genus *Simplicillium*

In recent decades, many chemical investigations carried out on the genus *Simplicillium* showed that fungi of this genus are capable of producing a wide variety of polyketides with new or novel structures and important biological activities (Liang *et al.*, 2017). Herein, previous isolated compounds can be classified into xanthenes, chromones, chromanones, benzofuranones, pyrones, quinones, phenols, oblongolides, and unclassified polyketides. The most frequent classes of compounds in *Simplicillium* genus are notably the Pyrolidine alkaloid, linear peptides and cyclic peptides, lipids, cyclohexane lactone.

### I.7.1.3.1. Peptides

#### I.7.1.3.1.1. Generalities about peptides and classification

Peptides are short strings of amino acids, typically comprising 2-50 amino acids. They have different properties and origin. They can be produced from different organisms. Biological peptides can also be synthesized chemically and characterized. Peptides also have many properties, including antihypertensive, antioxidant, antimicrobials, and anticoagulant and chelating effects. The formation of the covalent peptide bond is a condensation reaction between amino acids (Fig: 8). Their structure can be cyclic or not and each peptide has its own unique structure and biochemical characteristics.

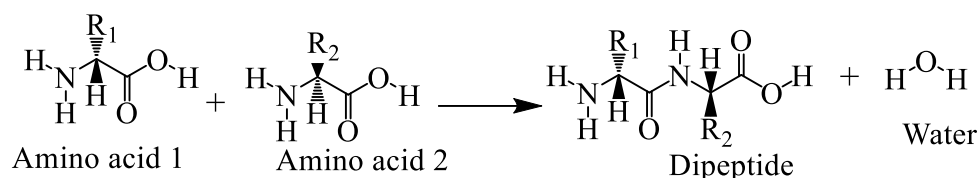
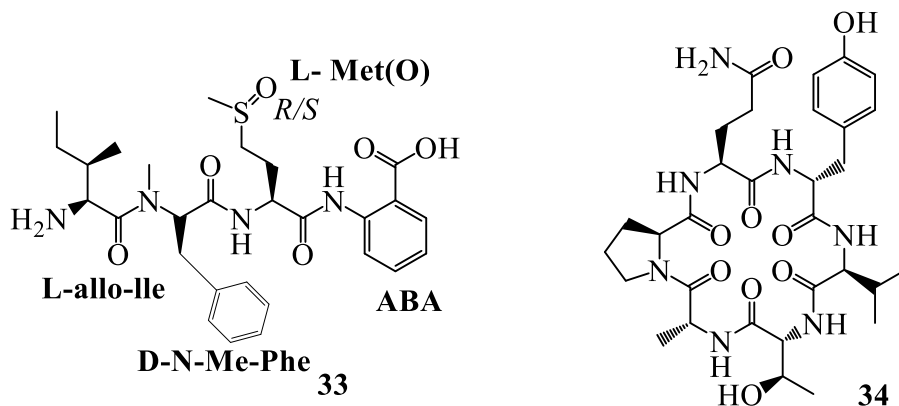


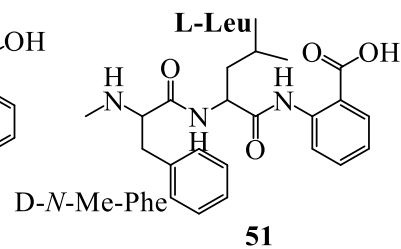
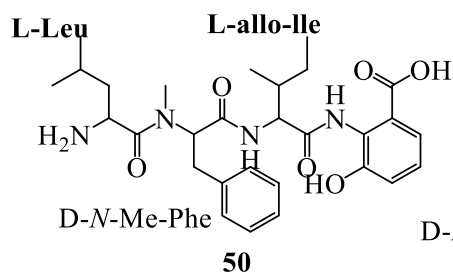
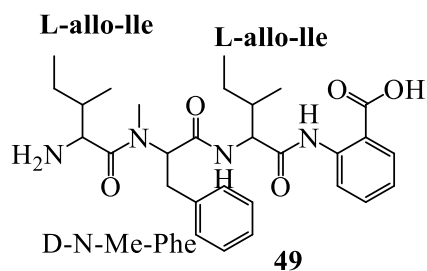
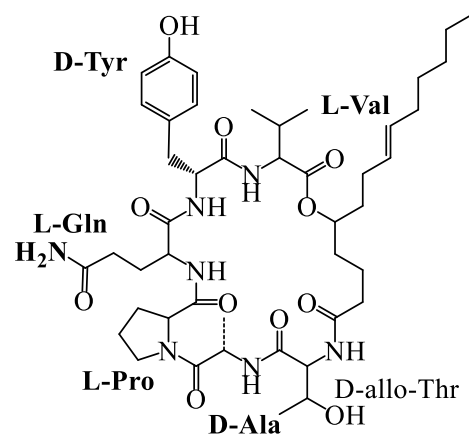
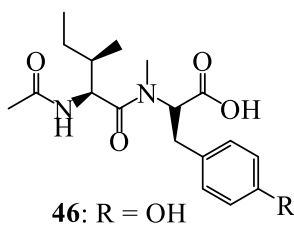
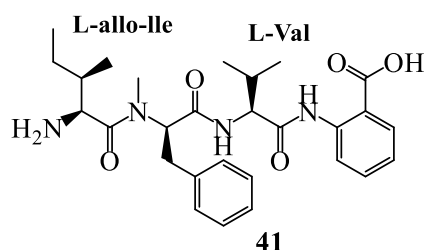
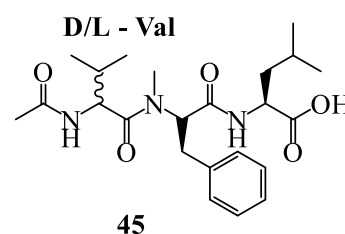
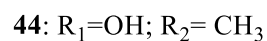
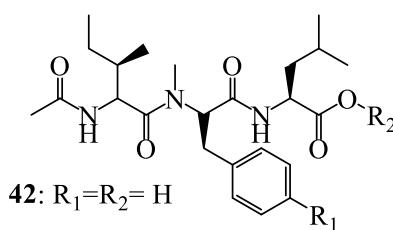
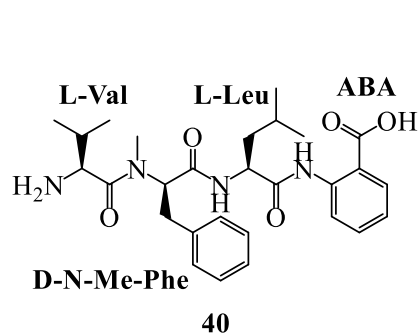
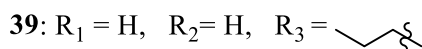
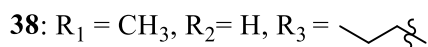
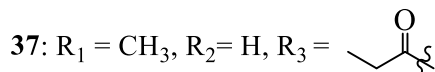
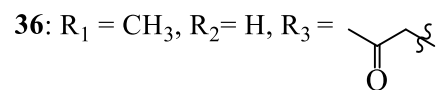
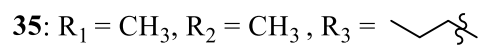
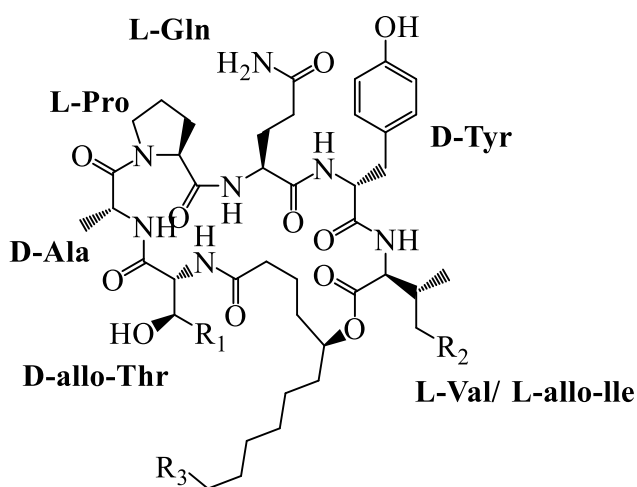
**Figure 7.** General biosynthesis of peptide bond

#### I.7.1.3.1.2. Peptides isolated from *Simplicillium* genus

Chemical work on *Simplicillium* species led to isolation and characterization of several cyclic and linear peptides. The linear peptide simplicilliumtide I (**33**) together with cyclic peptides simplicilliumtides J-M (**34-37**) and their analogues verlamelins A (**38**) and B (**39**) have been isolated from the deep-sea-derived fungal strain *Simplicillium obclavatum* EIODSF 020 (Liang *et al.*, 2017). From the same strain, eight peptides, simplicilliumtides A-H (**40-47**) have been isolated from the endophytic fungus *Simplicillium abclavatum* ELODSF 020 (Liang *et al.*, 2016).

Dai *et al.*, 2018 isolated five peptides, sinulariapeptides A-E (**48-52**) together with verlamilins A-B (**53-54**) and hirsutellic acid A (**55**) from *Simplicillium* sp. SCSIO 41209.





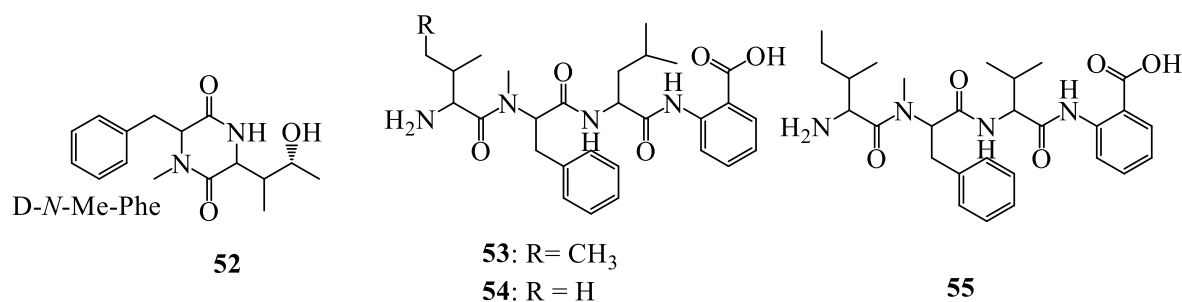


**Figure 8.** Structures of some peptides isolated from *Simplicillium*

#### I.7.1.3.1.3. Lipids isolated from the genus *Simplicillium*

Previous chemical investigation of *Simplicillium lamellicola* BCP led to the isolation of three manosyl lipids named halymecins F (**56**) and G (**58**) together with (3R,5R)-3-O-β-D-mannosyl 3,5-dihydrodecanoic acid (**59**) (Dang *et al.*, 2014).

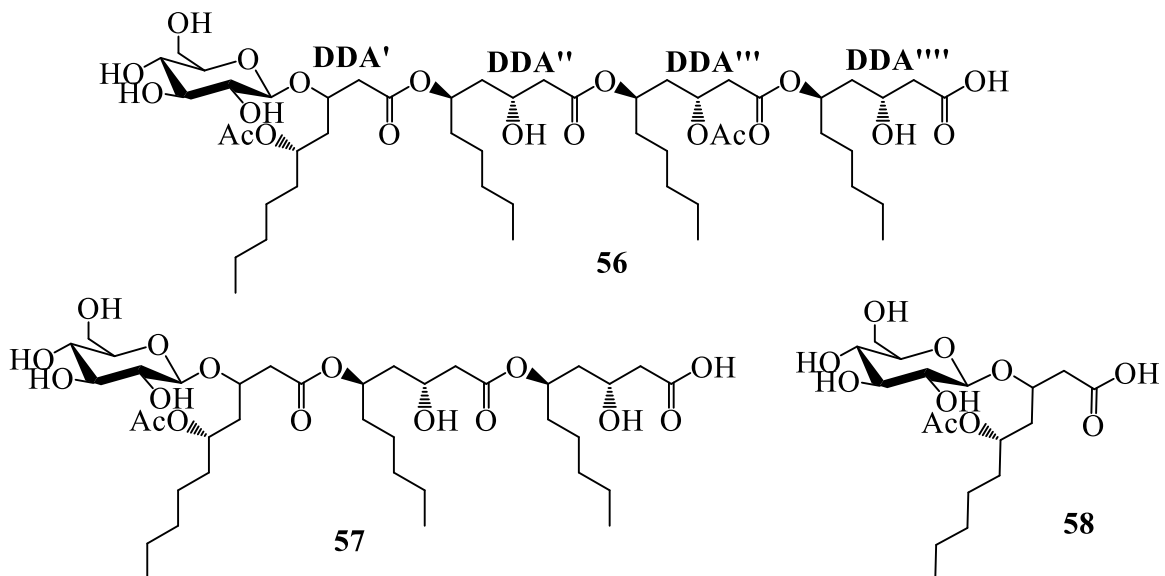


**Figure 9.** Structures of some lipids isolated from *Simplicillium*

#### I.7.1.3.1.4. Alkaloids isolated from genus *Simplicillium*

Previous chemical investigation led to the isolation and characterization of two pyrrolidine alkaloids, Preussin B (**58**) and Preussin (**59**) (Fukuda *et al.*, 2014). In addition, diketopiperazine alkaloid cyclo-(2-hydroxy-Pro-Gly) (**60**) has been isolated from the cultures of a sponge-derived fungus *Simplicillium* sp. YZ-11 (Yan *et al.*, 2015).

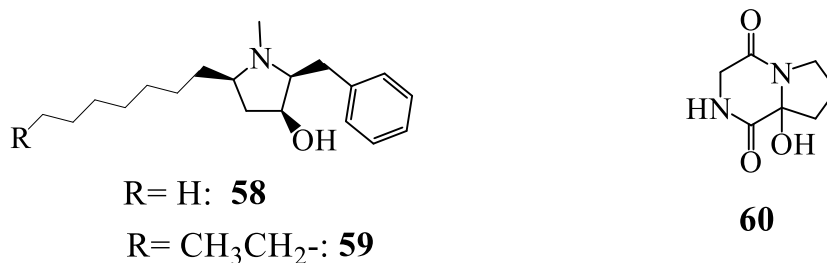


**Figure 10.** Structures of some alkaloids isolated from *Simplicillium*

#### I.7.1.3.1.5. Steroids isolated from the genus *Simplicillium*

Chemical investigation of the cultures of a sponge-derived fungus *Simplicillium* sp. YZ-11 led to the isolation of five ergostane-type sterols (22E,24R)-5 $\alpha$ ,6 $\alpha$ -epoxy-ergosta-8,22-dien-3 $\beta$ ,7 $\alpha$ -diol (**61**), (22E,24R)-5 $\alpha$ ,6 $\alpha$ -epoxy-ergosta-8,22-dien-3 $\beta$ ,7 $\alpha$ -diol (**62**), (22E,24R) 5 $\alpha$ ,8 $\alpha$ -epidioxy-ergosta-6,22-dien-3 $\beta$ -ol (**63**), (22E,24R)-5 $\alpha$ ,8 $\alpha$ -epidioxy-ergosta 6,9(11),22 trien-3 $\beta$ -ol (**64**), and (22E,24R)-6 $\beta$  methoxyergosta-7,22-dien-3 $\beta$ ,5 $\alpha$ -diol (**65**) (Yan *et al.*, 2015).

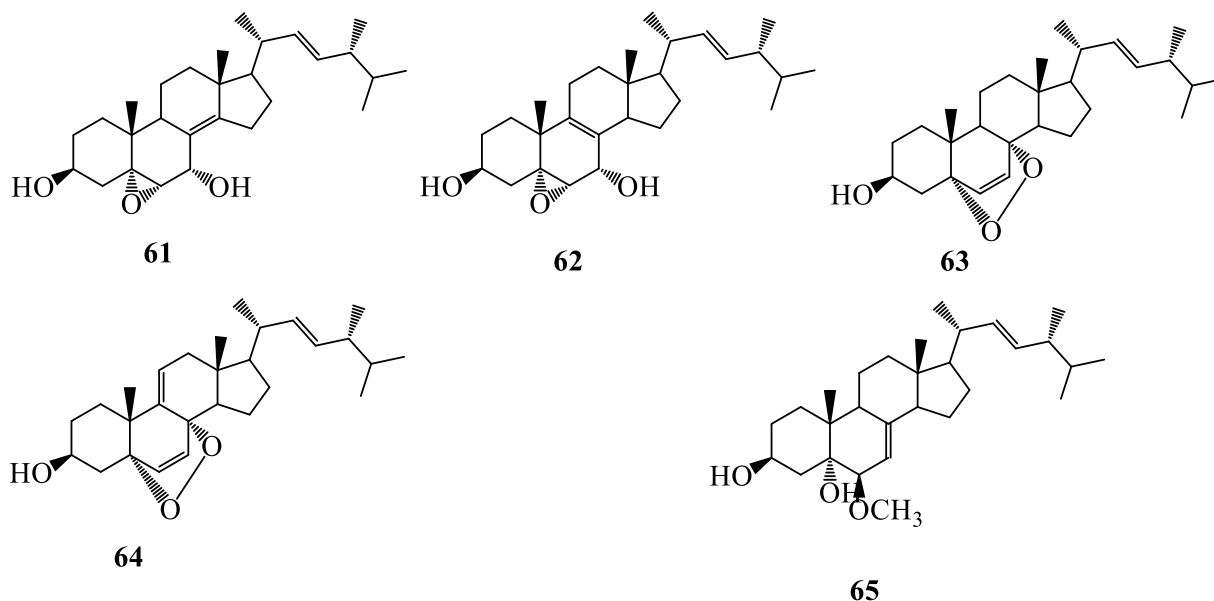


**Figure 11.** Steroids of some terpenoids isolated from *Simplicillium*

#### I.7.1.3.1.6. Other secondary metabolites isolated from *Simplicillium*

Massoia lactone (-)-massoia lactone; DDA, 3, 5-dihydroxydecanoic acid (**66**) and (+) (3R, 5R)-3-hydroxydecan-5-olide (**67**) have been isolated from *Simplicillium lamellicola* BCP (Dang *et al.*, 2014). aogacillins A (**68**) and B (**69**); with  $\beta$ -keto- $\gamma$ -methyliden- $\delta$ -lactone ring connected to a 2-ethyl-6-methylcyclohexane ring by *spiro* conjugation have been isolated from a culture broth

of *Simplicillium* sp. FKI-5985 (Takata *et al.*, 2013). simplifungin (**70**) has been isolated from the fungus *Simplicillium minatense* FKI-4981 (Ishijima *et al.*, 2016). Moreover, a natural lactone (S)-dihydro-5-[(S)-hydroxyphenylmethyl]-2(3H)-furanone (**71**) has been isolated from the cultures of a sponge-derived fungus *Simplicillium* sp. YZ-11 (Yan *et al.*, 2015).

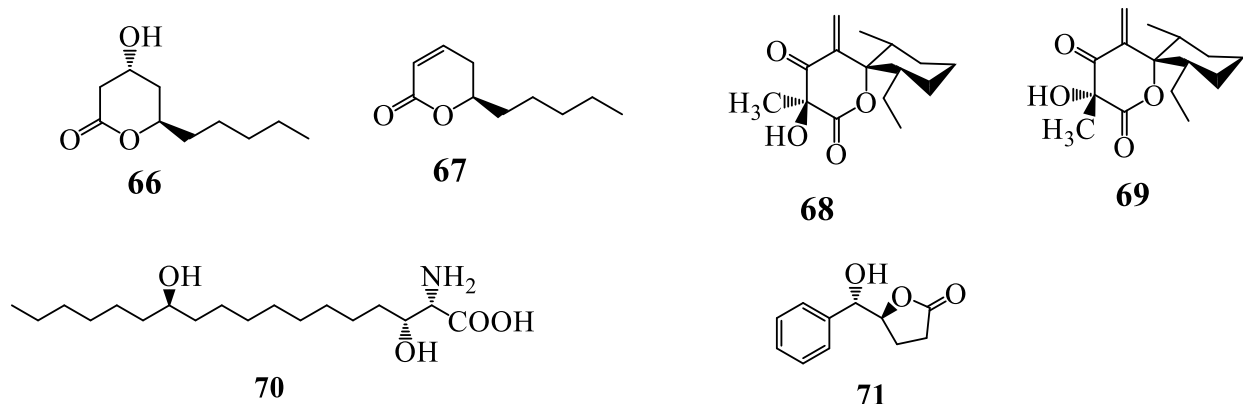


**Figure 12.** Structures of other classes of compounds isolated from *Simplicillium*

#### I.7.1.4. Biological activity of some isolated compounds from *Simplicillium*

The isolated compounds from the genus *Simplicillium* revealed several biological activities and the most important are attributed to peptides. Some reported compounds with their bioactivities are presented in Table 1.

**Table 1.** Biological activities of some compounds from *Simplicillium* genus.

Compounds	References	Compounds	References
<b>Antifungal activity</b>		<b>Antifouling activity</b>	
Simplicilliumtide J ( <b>34</b> )	Liang <i>et al.</i> , 2017	Simplicilliumtide D ( <b>43</b> )	Liang <i>et al.</i> , 2017
Verlamelin A & B ( <b>38-39</b> )	Liang <i>et al.</i> , 2017	<b>Cytotoxicity activity</b>	
Verlamelin A & B ( <b>53-54</b> )	Dai <i>et al.</i> , 2018	Simplicilliumtide A ( <b>40</b> )	
Simplifungin ( <b>70</b> )	Ishijima <i>et al.</i> , 2016.	Simplicilliumtide E ( <b>44</b> )	
<b>Antibacterial activity</b>		Simplicilliumtide G ( <b>46</b> )	Liang <i>et al.</i> , 2016
Halymecin F ( <b>56</b> )	Dang <i>et al.</i> , 2014	Simplicilliumtide H ( <b>47</b> )	
<b>Activiral activity</b>			
Verlamelin A ( <b>38</b> ) & B ( <b>39</b> )	Liang <i>et al.</i> , 2017		
Simplicilliumtide J ( <b>34</b> )	Liang <i>et al.</i> , 2017		

## I.7.2. Overview of endophytic fungi of the genus *Diaporthe*

### I.7.2.1. General characteristics

The genus *Diaporthe* was introduced in 1870 by Nitschke and their asexual states *Phomopsis* (Sacc.) in 1905 by Bubák. It comprises several hundreds of species and belongs to the family Diaporthaceae, order Diaporthales, class Dothideomycetes (Rossman *et al.*, 2015). In Index Fungorum (2020), more than 1120 records of *Diaporthe* and 986 of *Phomopsis* are listed (<http://www.indexfungorum.org/>, accessed December 2020). The *Phomopsis*-like asexual states of *Diaporthe* have been reported as one of the most frequently encountered genera of endophytic fungi in several plant hosts (Murali *et al.*, 2006; Botella and Diez, 2011). After implementation of a “One Fungus–One Name” concept in fungal nomenclature, the name *Diaporthe* now takes preference over *Phomopsis* according to a recommendation by a specialist committee (Rossman *et al.*, 2015). Therefore, the name *Phomopsis* should no longer be used to describe novel taxa, even if they are only known from their conidial state. The genus *Diaporthe* has pathogenic, endophytic and saprobic species with both temperate and tropical distributions. Although species of *Diaporthe* have been distinguished based on host association, studies have also confirmed several taxa to have wide host ranges, suggesting that they move freely between hosts, frequently co-colonizing diseased or dead tissue, while some species are known to be host-specific (Gomes *et al.*, 2013). They are also very frequently isolated as endophytes of seed, leaves or stem in plants. Due to their importance as plant pathogens, the genus has been chemically investigated for the discovery of novel bioactive natural products (Rossman *et al.*, 2015, Gomes *et al.*, 2013). Previous chemical work of the genus *Diaporthe* led to the isolation and characterization of several classes of polyketides, but also cytochalasins and other types of commonly encountered fungal secondary metabolites such as chromones and alkaloids. Meanwhile, their bioactivities mainly involve cytotoxic, antifungal, antibacterial, antiviral, antioxidant, anti-inflammatory, anti-algae, phytotoxic, and enzyme inhibitory activities (Gomes *et al.*, 2013).

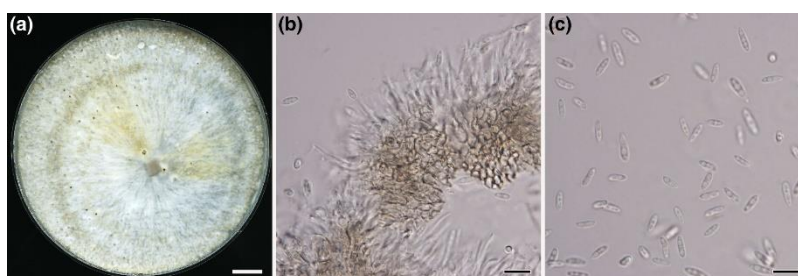


**Figure 13.** *Diaporthe* strain; (a) = Photography; (b) and (c) = Hyphae associated with the strain

### I.7.2.2. Importance and uses

The genus *Diaporthe* has been demonstrated to contribute to plant natural defenses by preventing herbivory and invasion from superficial pathogens. Some species have been used in biotechnology for the production of bioherbicide (Souza *et al.*, 2015; Pes *et al.*, 2016).

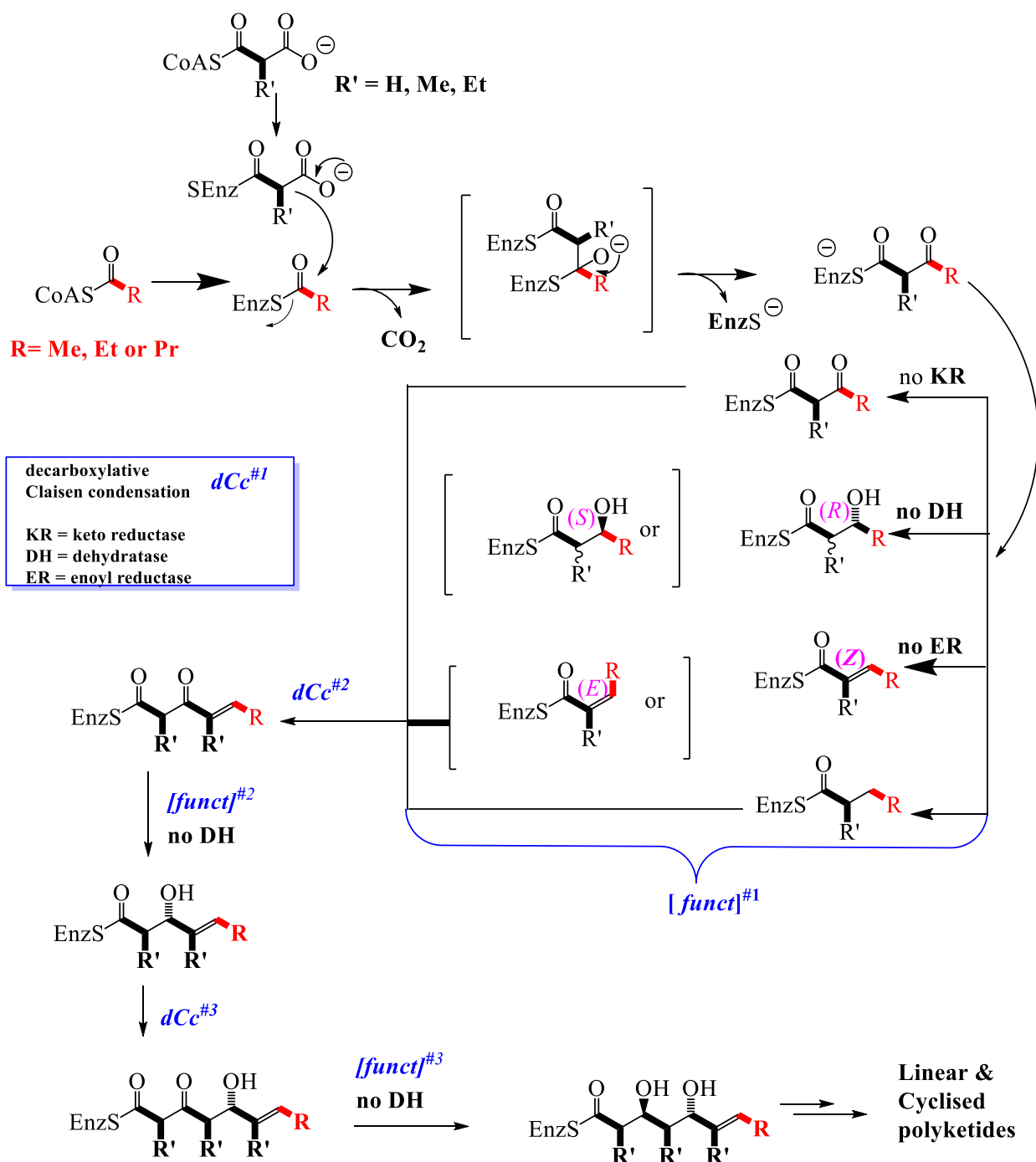
### I.7.2.3. Previous chemical work on the *Diaporthe* genus

In recent decades, many chemical investigations carried out on the genus *Diaporthe* showed that fungi of this genus are capable to produce a wide variety of secondary metabolites with new or novel structures and important biological activities (Chepkirui and Stadler, 2017). The most encountered classes of compounds are classified into polyketides, terpenoids, steroids, macrolides, ten-membered lactones, alkaloids, flavonoids, and fatty acids. Polyketides constitute the main chemical population, accounting for 64% (Xu *et al.*, 2021).

#### I.7.2.3.1. Polyketides

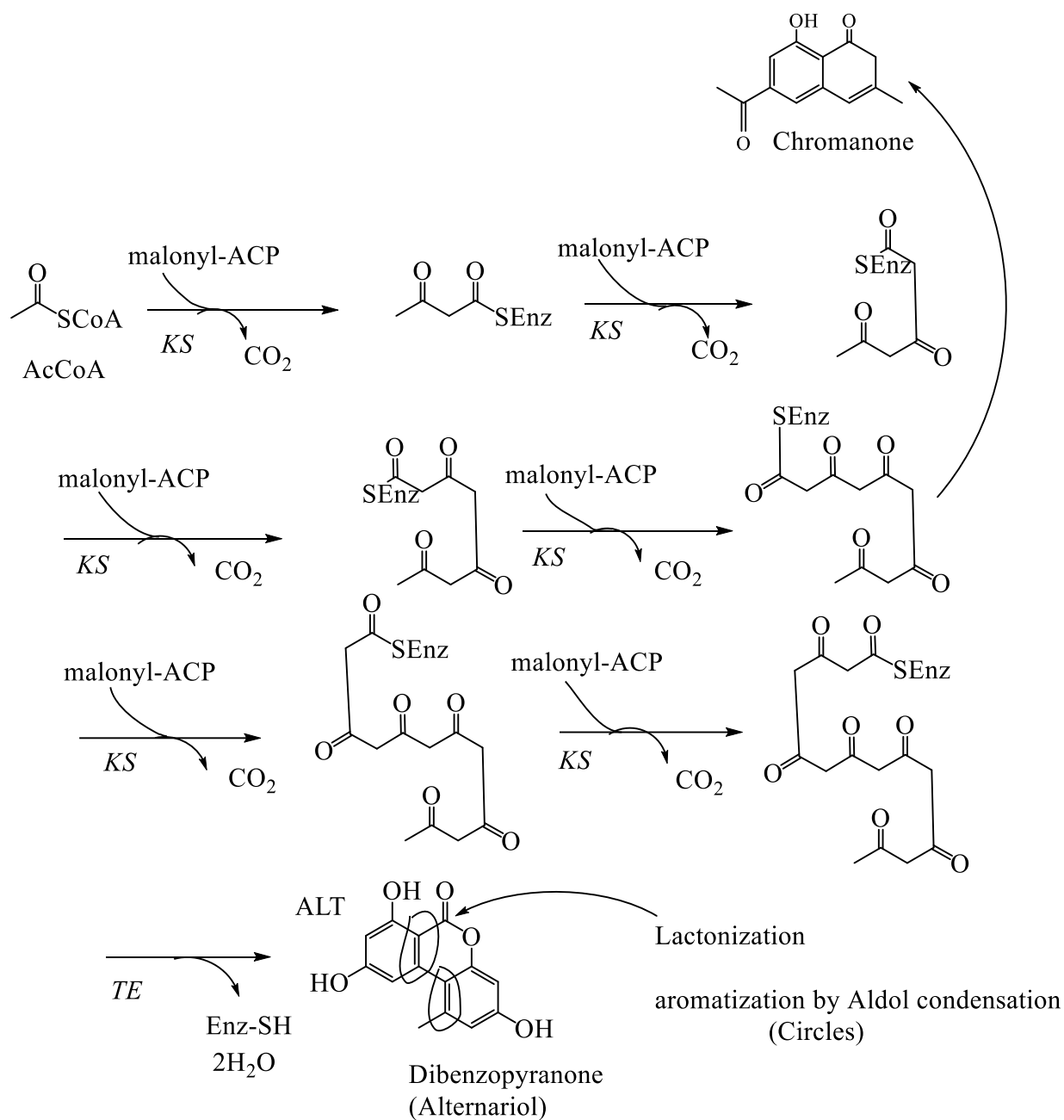
Polyketides, sometimes known as acetogenins or polyketones are group of secondary metabolites known to possess remarkable variety, not only in their structure, but also in their functions. They are produced by some organisms such as bacteria (e.g., tetracycline from *Streptomyces aureofaciens*) (Zhang *et al.*, 2015); fungi (e.g., lovastatin from *Phomopsis vexans*) (Piel, 2015); plants (e.g., emodin from *Rheum palmatum*); protists (e.g., maitotoxin-1 from *Gambierdiscus australes*) insects (e.g., stegobinone from *Stegobium paniceum*); and mollusks (e.g., elysione from *Elysia viridis*) (Keatingeclay., 2012). These organisms could use the polyketides they produce as protective compounds and for pheromonal communication in the case for insects. Polyketides exhibit a wide range of bioactivities such as antibacterial (e.g., tetracycline), antifungal (e.g., amphotericin B), anticancer (e.g., doxorubicin), antiviral (e.g., balticolid), immune-suppressing (e.g., rapamycin), anti-cholesterol (e.g., lovastatin), and anti-inflammatory activity (e.g., flavonoids) (Yu *et al.*, 2012).

Their chemical structure contains the alternation of ketone group and methylene acetyl group in their carbon chain. Acetyl-CoA constitutes the starting point for the biosynthesis of polyketide secondary metabolites (**scheme 1**). These metabolites are topologically very different to fatty acid metabolites but are in fact synthesized in a very similar fashion. The significant difference is that during the iterative cycle of chain extension, the  $\beta$ -keto group is generally not completely reduced out (Yu *et al.*, 2012).



**Scheme 1. Biosynthesis of polyketides**

This gives rise to huge structural diversity based around a 1,3-oxygenation pattern & cyclisation to give aromatic compounds. Below the biosynthesis of some polyketides benzopyranones compounds classes found in *Diaporthe* genus and its asexual state *Phomopsis*.



**Scheme 2.** Biosynthesis of polyketide benzopyranones

In general polyketides are structurally diverse and are used in a vast array of biological and pharmacological activities, including anticancer, antifungal, antibacterial, anti-parasitic, and immunosuppressive applications. Their structure includes pyrones, naphthopyrones, macrolides and polyketone. Most polyketides isolated from the genus *Diaporthe* and its asexual state *Phomopsis* showed cytotoxic, antibacterial and antifungal bioactivities. Herein, these polyketides

are classified into xanthenes, chromones, chromanones, benzofuranones, pyrones, quinones, phenols, oblongolides, and unclassified ones.

### I.7.2.3.1.1. Xanthenes

Xanthenes are class of compounds with the framework of 9H-xanthen-9-one. These compounds exhibit various bioactivities, such as cytotoxic, antifungal, antibacterial, antiviral, antioxidant, anti-inflammatory, phytotoxic, antitubercular, antifibrotic, antidiabetic, antimigratory, antiangiogenic, antihyperlipidemic, inhibiting leishmanial growth, activating the NF-kB pathway, enzyme inhibition, inhibitory effects on osteoclastogenesis, antifeedant, contact toxicity, and oviposition deterrent activities (Le Pogam *et al.*, 2016). Previous Chemical investigation of *Diaporthe* sp. SCSIO 41011 derived from mangrove plant *R. stylosa* led to the isolation of 3,8-dihydroxy-6-methyl-9-oxo-9H-xanthene-1-carboxylate (**72**). phomoxanthone A (**73**) with a novel carbon skeleton was isolated from the fungus *Diaporthe* sp. GZU-1021 derived from a red-clawed crab *Chiromantes haematocheir* and *D. phaseolorum* FS431 of deep-sea sediment from the Indian Ocean (Niu *et al.*, 2019).

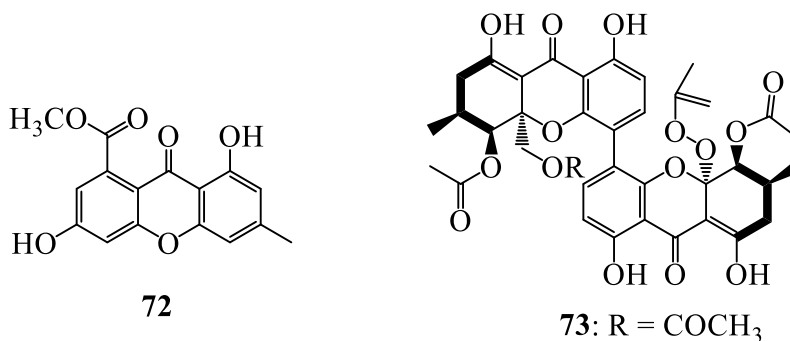


**Figure 14.** Structures of some xanthenes isolated from *Diaporthe*

### I.7.2.3.1.2. Chromones

Chromones are a class of bioactive compounds with a benzo- $\gamma$ -pyrone skeleton, which have been reported to have various activities, such as anti-tumor, anti-viral, antimicrobial, anti-inflammatory, and antioxidant (Duan *et al.*, 2019). From the fermentation of *Diaporthe* sp. GZU-1021 associated with *Chiromantes haematocheir*, penialidin A (**74**) and (-)-phomopsichin B (**75**) have been isolated (Liu *et al.*, 2019). The chemical investigation of *D. phaseolorum* SKS019 derived from mangrove plant *A. ilicifolius* led to the isolation of (-)-phomopsichin A (**76**), (+)-phomopsichin B (**77**), diaporchromanones C (**78**) and D (**79**), along with, (+)-phomopsichin A (**80**) and (-)-phomopsichin (Cui *et al.*, 2017). Futhemore, pestalotiopsones F (**81**) and B (**82**) were

isolated from *Diaporthe* sp. SCSIO 41011 (Luo *et al.*, 2018). Two benzopyranones, diaportheones A (**83**) and B (**84**), were isolated from *Diaporthe* sp. P133 derived from *Pandanus amaryllifolius* (Bungihan *et al.*, 2011).

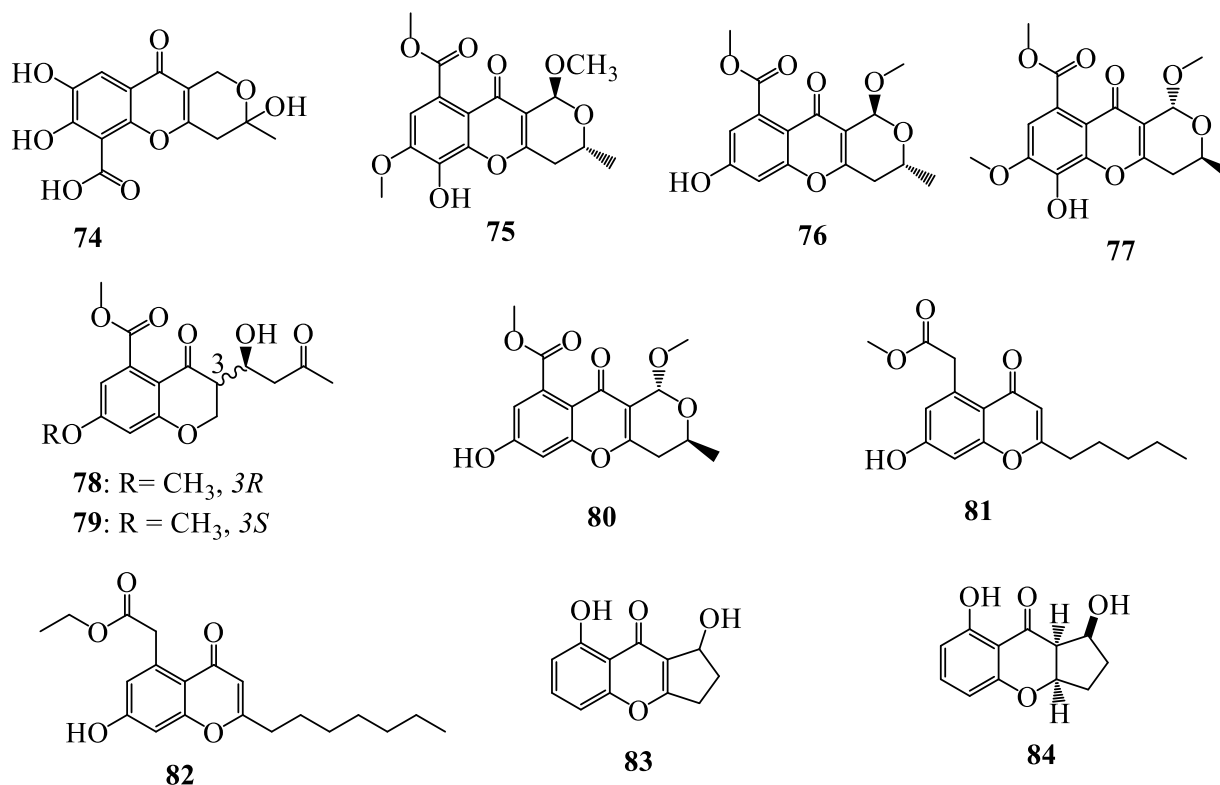


**Figure 15.** Structures of some chromones isolated from *Diaporthe*

#### I.7.2.3.1.3. Chromanones

Two isocoumarins, (10*S*)-diaporthin (**85**) and orthosporin (**86**), have been reported during the chemical investigation of *D. terebinthifolii* LGMF907 isolated from *Schinus terebinthifolius* (Medeiros *et al.*, 2018). Also, cytosporone D (**87**) and mucorisocoumarin A (**88**) were isolated from the endophytic fungus *D. pseudomangiferaea* associated with *Tylophora ouata* (Liu *et al.*, 2018). The fungus *D. eres* derived from pathogen-infected leaf of *Hedera helix* produced an isocoumarin, 3,4-dihydro-8-hydroxy-3,5-dimethylisocoumarin (**89**) (Meepagala, *et al.*, 2018). diportharine A (**90**), was obtained from the culture of *Diaporthe* sp. isolated from *Datura inoxia* (Sharm *et al.*, 2018).

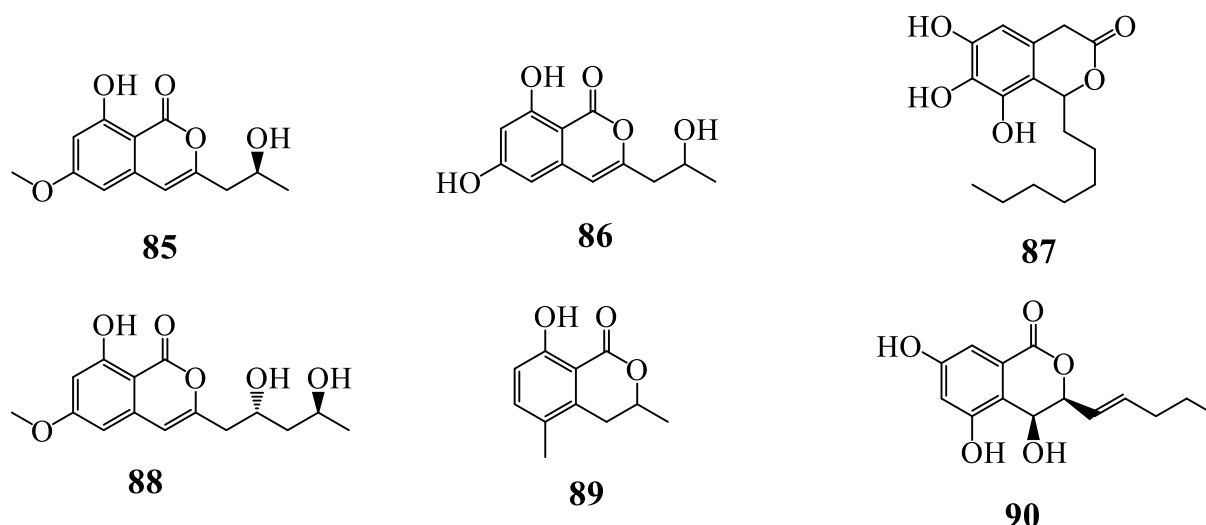


**Figure 16.** Structures of some chromanones isolated from *Diaporthe*

#### I.7.2.3.1.4. Furanones

Four bioactive furanones were derived from *Diaporthe* sp. SXZ-19 associated with *C. acuminata*, including the (1*R*,2*E*,4*S*,5*R*)-1-[(2*R*)-5-oxotetrahydrofuran-2-yl]-4,5-dihydroxy-hex-2-en-1-yl(2*E*)-2-methylbut-2-enoate (**91**) and three linear furanopolyketides (**92–94**) (Liu *et al.*, 2013). Moreover, the 3-substituted-5-diazenylcyclopentendione, named kongiidiazadione (**95**), has been isolated from *D. kongii* haboured in *C. lanatus* (Evidente *et al.*, 2015).

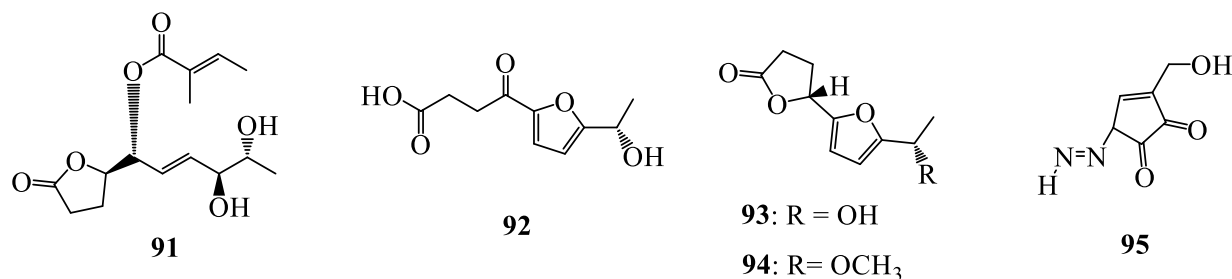


**Figure 17.** Structures of some Furanones isolated from *Diaporthe*

#### I.7.2.3.1.5. Pyrones

The chemical study of *D. maritima* associated with *Picea mariana* and *Picea rubens* needles led to the isolation and characterization of three dihydropyrones named phomopsolides A (**96**), B (**97**), and C (**98**), together with a stable  $\alpha$ -pyrone, (*S,E*)-6-(4-hydroxy-3-oxopent-1-en-1-yl)-2H-pyran-2-one (**99**) (Tanney *et al.*, 2016). Two known metabolites, 7-hydroxy-6-methoxycoumarin (**100**) and coumarin (**101**), were isolated from the endophytic fungus *D. lithocarpus* obtained from *Artocarpus heterophyllus* (Riga *et al.*, 2019).

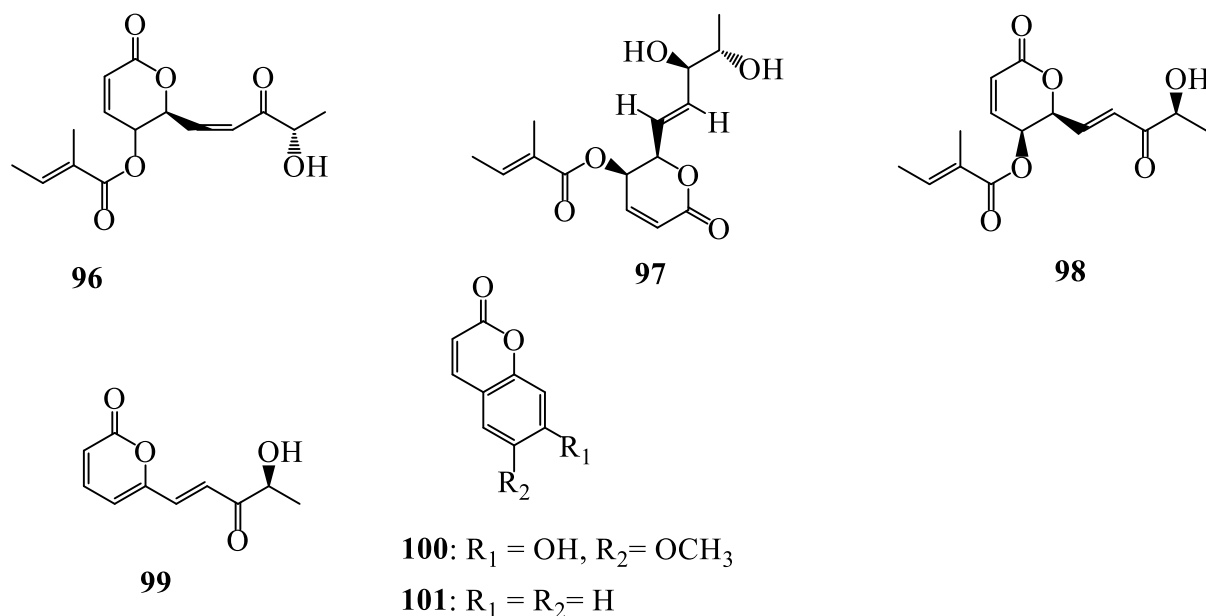


**Figure 18.** Structures of some pyrones isolated from *Diaporthe*

#### I.7.2.3.1.6. Quinones

Two cyclohexeneoxidedione derivatives, phyllostine acetate (**102**) and (-)-Phyllostine (**103**), have been isolated from *Cyperus iria* associated endophytic fungus of the plant *D. miriciae* (Ratnaweera *et al.*, 2020). biatriosporin N (**104**) was isolated from the marine-derived fungus *Diaporthe* sp. GZU-1021 (Liu *et al.*, 2019). Two anthraquinone derivatives, emodin (**105**) and 1,2,8-trihydroxyanthraquinone (**106**), were isolated from an endophytic fungus *D. lithocarpus* (Riga *et al.*, 2019). A bis-anthraquinone derivative, named (+)-2,2'-epicytoskyrin A (**107**), was isolated from *Diaporthe* sp. GNBP-10 of *Uncaria gambir* Roxb (Wulansari *et al.*, 2016). Two cytoskyrin type bisanthraquinones, cytoskyrin C (**108**) and (+)-epicytoskyrin (**109**), were isolated from *Diaporthe* sp., an endophytic fungus obtained from *Anoectochilus roxburghii* (Tian *et al.*, 2018).

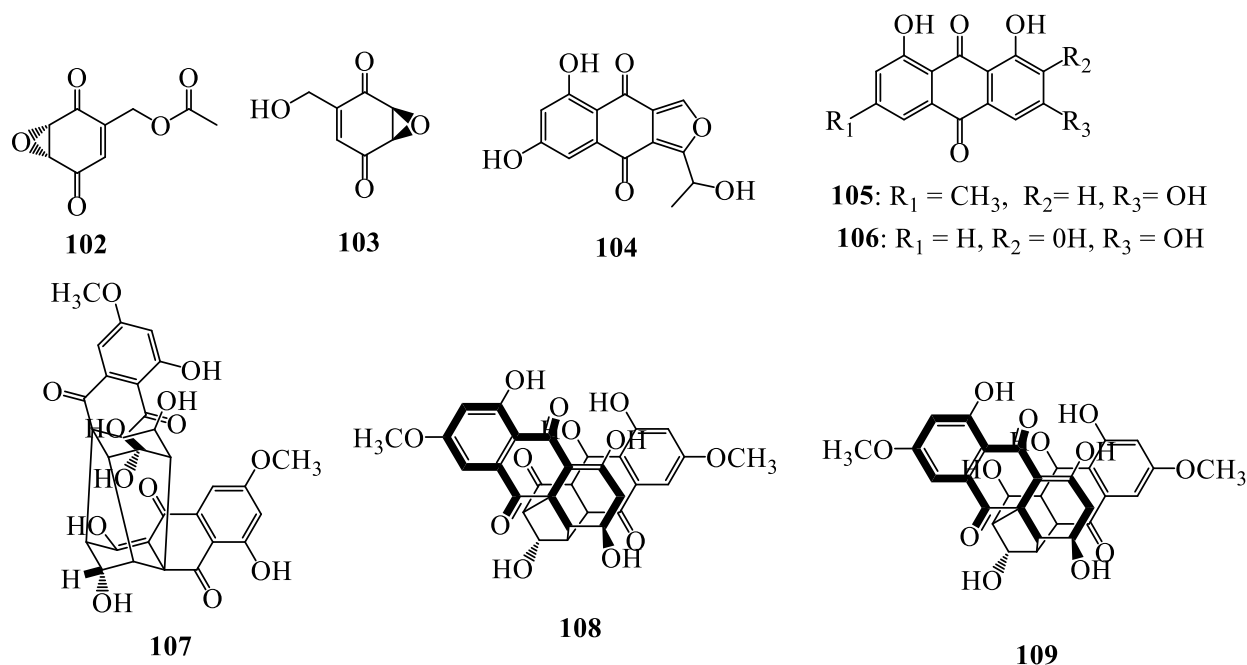


**Figure 19.** Structures of some quinones isolated from *Diaporthe*

#### I.7.2.3.1.7. Phenols

The phenolic metabolite, tyrosol (**110**) has been extracted from *D. helianthi* isolated from *Luehea divaricate* (Specian *et al.*, 2012). 2,5-Dihydroxybenzyl alcohol (**111**) was derived from *D. vochysiae* LGMF1583 of the medicinal plant *Vochysia divergens* (Noriler *et al.*, 2019). In addition, four phytotoxic compounds, 4-hydroxybenzaldehyde (**112**), *p*-cresol (**113**), 4-hydroxybenzoic acid (**114**), and tyrosol, were isolated from *D. eres* of grapevine (*V. vinifera*) wood. arbutin (**115**), obtained from an endophytic fungus *D. lithocarpus* (Tanney *et al.*, 2016). Phomosines A (**116**) and C (**117**), were extracted from *Diaporthe* sp. F2934 haboured in *Siparuna gesnerioides* (Sousa *et al.*, 2016). Flavomannin-6,6'-di-*O*-methyl ether (**118**) was extracted from an endophytic strain of *D. melonis* from *Annona squamosal* (Ola *et al.*, 2014). Acetoxidothiorelone B (**119**), and dothiorelones B (**120**), L (**121**) and G (**122**), have been isolated from *D. pseudomangiferaea* (Liu *et al.*, 2018). Futhermore, diaporthols A (**123**) and B (**124**), were extracted from *Diaporthe* sp. ECN-137 isolated from the leaves of *Phellodendron amurense* (Nakashima *et al.*, 2018). Tenellone C (**125**) was obtained from *Diaporthe* sp. SYSU-HQ3 of mangrove plant *E. agallocha* (Cui *et al.*, 2017).

Six compounds have been isolated from endophytic fungus *Diaporthe* sp. SYSU-HQ3 derived from the branches of *E. agallocha*, including a new benzophenone derivative, tenellone D (**126**),

four unusual 2,3-dihydro-1*H*-indene isomers, diaporindenes A-D (**127- 130**), and isoprenylisobenzofuran A (**131**) (Cui *et al.*, 2018).

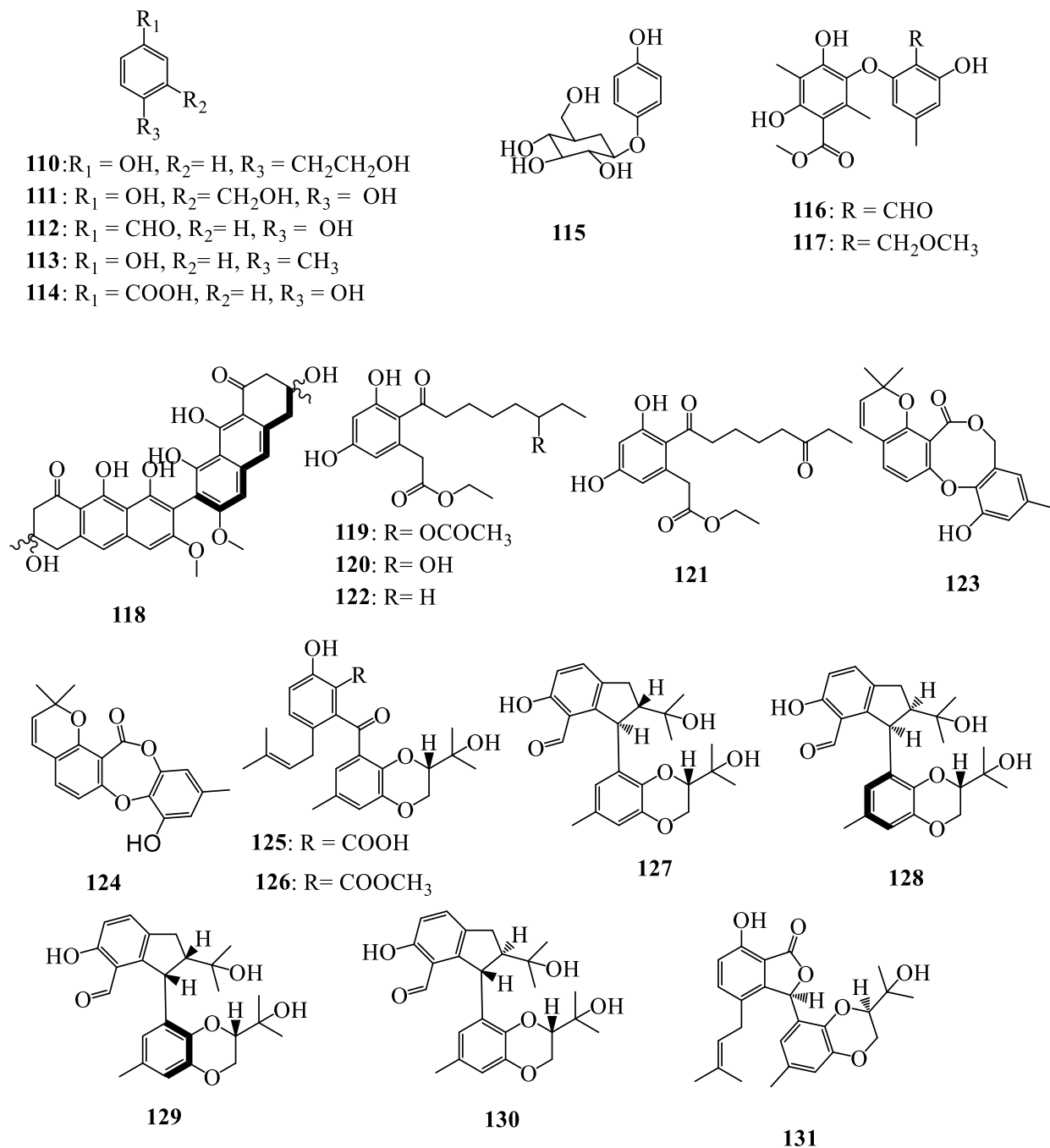


**Figure 20.** Structures of some phenols isolated from *Diaporthe*

#### I.7.2.3.1.8. Oblongolides

Four lovastatin analogues, oblongolides D (**132**), H (**133**), P (**134**) and V (**135**), were obtained from the endophytic fungus *Diaporthe* sp. SXZ-19 (Liu *et al.*, 2013).

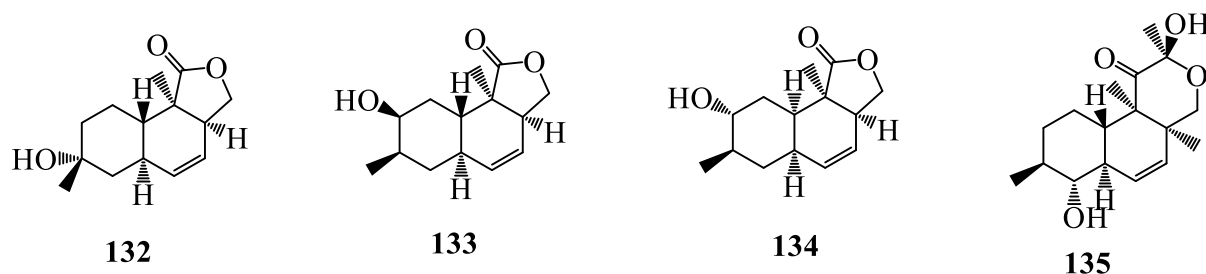


**Figure 21.** Structures of some oblongolides isolated from *Diaporthe*

#### I.7.2.3.1.9. Unclassified Polyketides

Phomentrioloxin B (**136**) was obtained from a strain of *D. gulyae* isolated from *C. lanatus* (Andolfi *et al.*, 2015). The fungus *Diaporthe* sp. SCSIO 41011 derived from mangrove plant *R. stylosa*, afforded two metabolites, *epi*-isochromophilone II (**137**) and isochromophilone D (**138**) (Luo *et al.*, 2018).

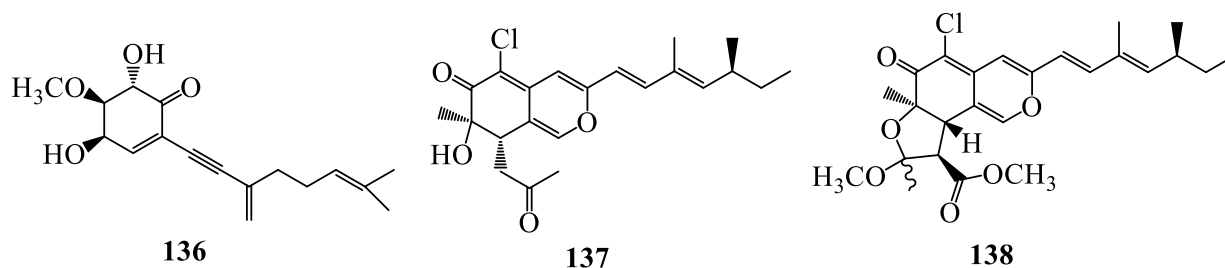


**Figure 22.** Structures of some unclassified polyketides isolated from *Diaporthe*

#### I.7.2.3.2. Terpenoids

(1*R*,2*R*,4*R*)-Trihydroxy-*p*-menthane (**139**) was isolated from *Diaporthe* sp. SXZ-19 (Liu *et al.*, 2013). Two  $\alpha$ -pyrones, gulypyrones A (**140**) and B (**141**), were extracted from *D. gulyae*. (Andolfi *et al.*, 2015). A pentaketide monoterpene, nectriapyrone (**142**), was isolated from the culture of *D. Kongii* (Evidente *et al.*, 2015). A brasilane-type sesquiterpenoid, diaporol R (**143**) was produced by an endophytic fungus *Diaporthe* sp. isolated from leaves of *Rhizophorastylusa* (Chen *et al.*, 2015). In addition, eremofortin F (**144**) was obtained from endophytic fungus *Diaporthe* sp. SNB-GSS10 of *Sabicea cinerea* (Mandavid *et al.*, 2015). Two eremophilanes, lithocarins B (**145**) and C (**146**), were extracted from *D. lithocarpus* A740, an endophytic fungus isolated from *Morinda officinalis* (Liu *et al.*, 2019). A triterpenoid, 19-nor-lanosta-5(10),6,8,24-tetraene-1 $\alpha$ ,3 $\beta$ ,12 $\beta$ ,22*S*-tetraol (**147**), was isolated from *Diaporthe* sp. LG23 of the Chinese medicinal plant *Mahonia fortune* (Li *et al.*, 2015).

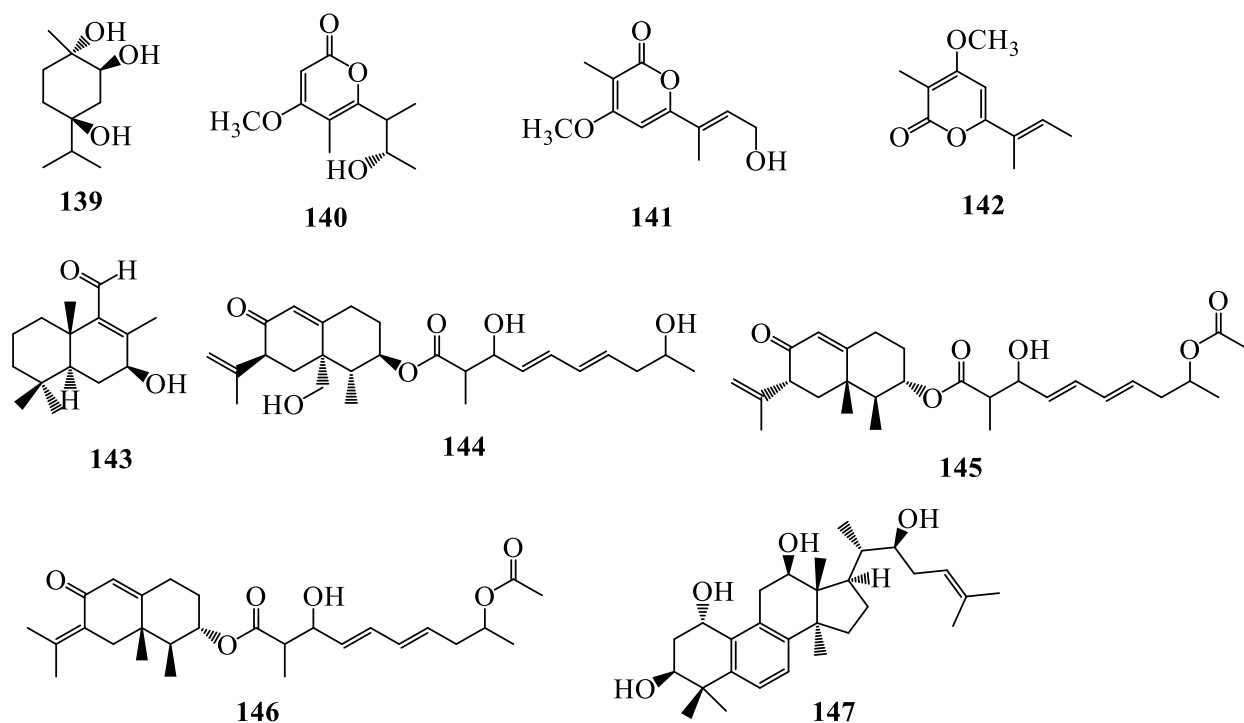


**Figure 23.** Structures of some terpenoids isolated from *Diaporthe*

#### I.7.2.3.3. Steroids

Only two steroids,  $3\beta,5\alpha,9\alpha$ -trihydroxy-( $22E,24R$ )-ergosta-7,22-dien-6-one (**148**) and chaxine C (**149**), have been already isolated from *Diaporthe* sp. LG23 (Li *et al.*, 2015).

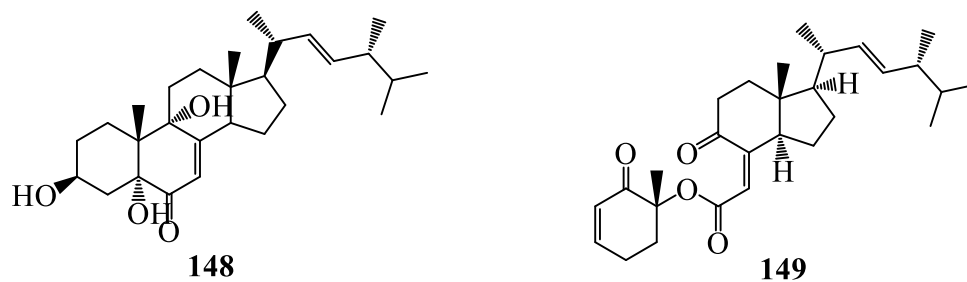


**Figure 24.** Structures of steroids isolated from *Diaporthe*.

#### I.7.2.3.4. Ten-Membered lactones

Ten-membered lactones always have anti-tumor, anti-inflammatory, anti-viral, antibacterial and other pharmacological activities, exhibiting important medical value in clinical practice (Zheng *et al.*, 2015), like phomolide C (**150**) from *Diaporthe* sp. of *Aucuba japonica* var. (Ito *et al.*, 2015). The endophytic fungus *D. terebinthifolii* GG3F6 derived from medicinal plant *Glycyrrhiza glabra*, afforded two known compounds, xylarolide (**151**) and phomolide G (**152**)

(Yedukondalu *et al.*, 2017). The novel metabolites, named xylarolide A (**153**) & B (**154**), were isolated from the fungus *Diaporthe* sp. of *D. inoxia*. (Sharma *et al.*, 2018).

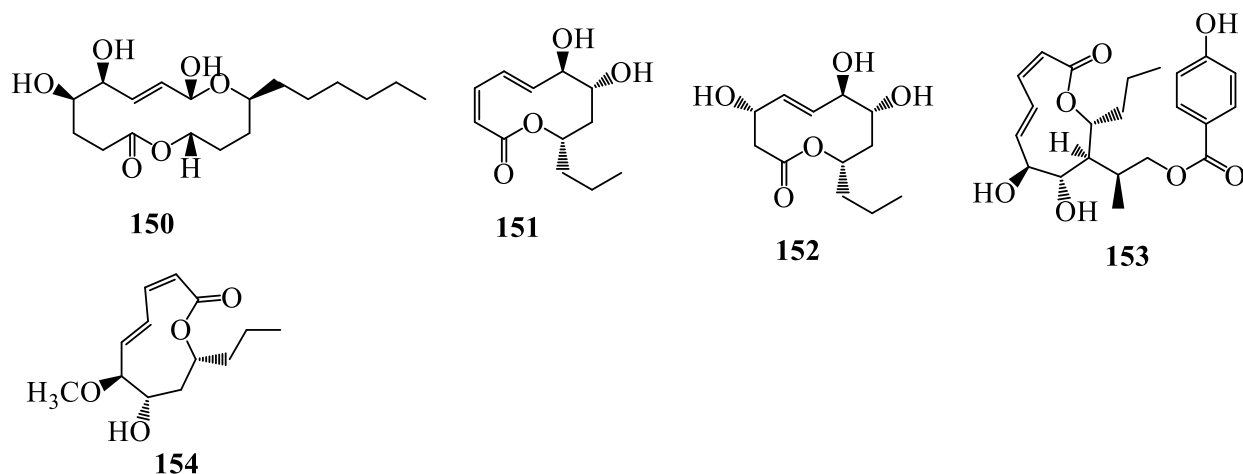
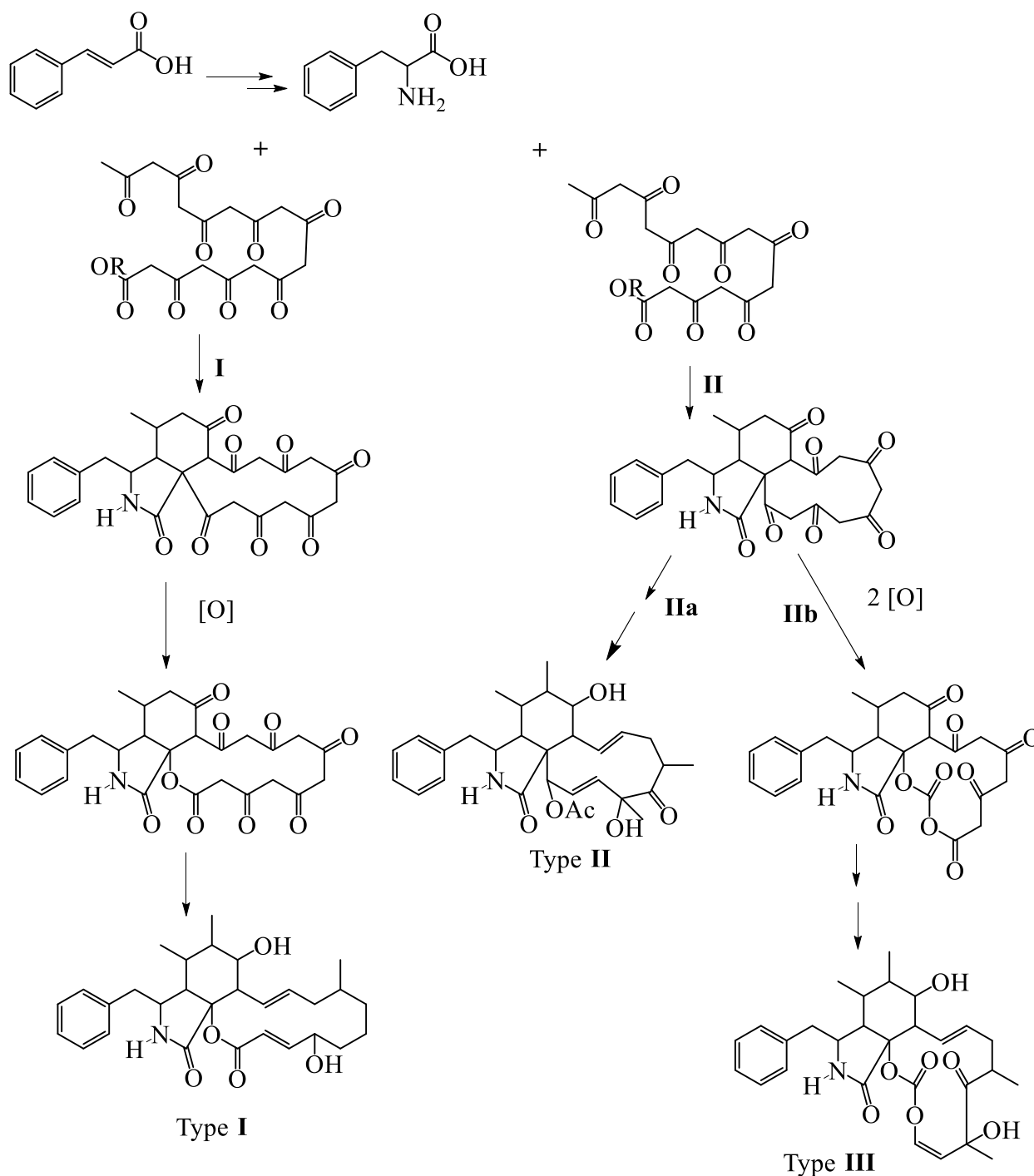


**Figure 25.** Structures of some ten-membered lactones isolated from *Diaporthe*

#### I.7.2.3.3.5. Alkaloids

The major class of alkaloids found in *Diaporthe* genus and his asexual state *Phomopsis* are cytochalasins.

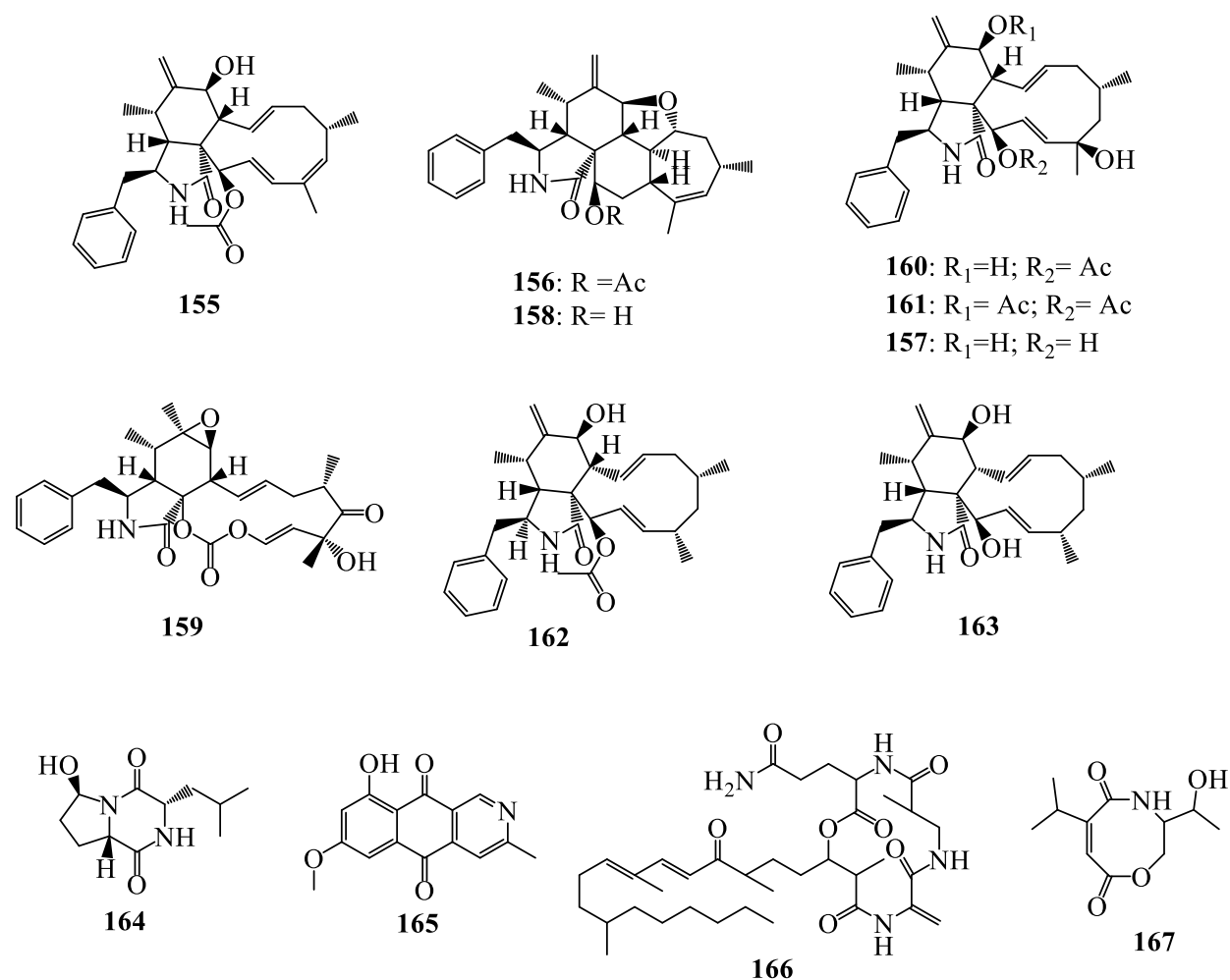
The fundamental units of the biogenesis of the cytochalasins are the primary metabolites phenylalanine and a nonaketide or octaketide or their biogenetic equivalents. Phenylalanine is formed from shikimic acid (Scheme 3), and is thus derived ultimately from sugars; the nonaketide or octaketide is formed from acetate units by a process similar to the synthesis of fatty acids, but without the reduction steps (Huang *et al.*, 2019). The linkage of phenylalanine to the nonaketide leads by path I to the 24-oxa-cytochalasins, while linkage to the octaketide leads by path II to the cytochalasins and to the 21,23-dioxa-cytochalasins. At some point, the oxidative insertion of oxygen atoms could occur in path I and path IIb, with formation of the lactone group on the one hand and the carbonic diester group on the other. After the further steps mentioned, this would lead us to the three basic type of cytochalasins (type I, type II and type III) (Michael Binder and Christoph Tamm, 1973).



**Scheme 3.** Biosynthesis of cytochalasins.

Huang *et al.*, 2019 isolated a series of cytochalasin named 21-acetoxycytochalasins J<sub>2</sub>–J<sub>3</sub> (**155**–**156**) together with cytochalasin J (**157**), cytochalasin J<sub>3</sub> (**158**), cytochalasin E (**159**), cytochalasin H (**160**) and 7-acetoxycytochalasin H (**161**) from *Diaporthe* sp. GDG-118 associated with *Sophora tonkinensis*. Moreover, 18-Des-hydroxy cytochalasin H (**162**) was obtained from the

endophytic fungus *D. phaseolorum*-92C associated with *Combretum lanceolatum*. The fungus *Diaporthe* sp. GZU-1021 yielded cytochalasin H and 21-*O*-deacetyl-L-696,474 (**163**) (Liu *et al.*, 2019). Cordysin A (**164**) was derived from endophytic fungus *D. arecae* associated with *Kandelia obovate*. Further research led to the isolation and characterization of 5-deoxybostrycoidin (**165**) and fusaristatin A (**166**) from *D. phaseolorum* SKS019 of mangrove plant *A. ilicifolius* (Cui *et al.*, 2017). A new carboxamide, vochysiamide B (**167**), was extracted from new species *D. vochysiae* LGMF1583. Four compounds, diaporisoindoles A (**168**), B (**169**), D (**170**), and E (**171**), have been obtained from an endophytic fungus *Diaporthe* sp. SYSU-HQ3 (Cui *et al.*, 2018). Phomopsin F (**172**) was isolated from *D. toxica* (Schloss *et al.*, 2017).



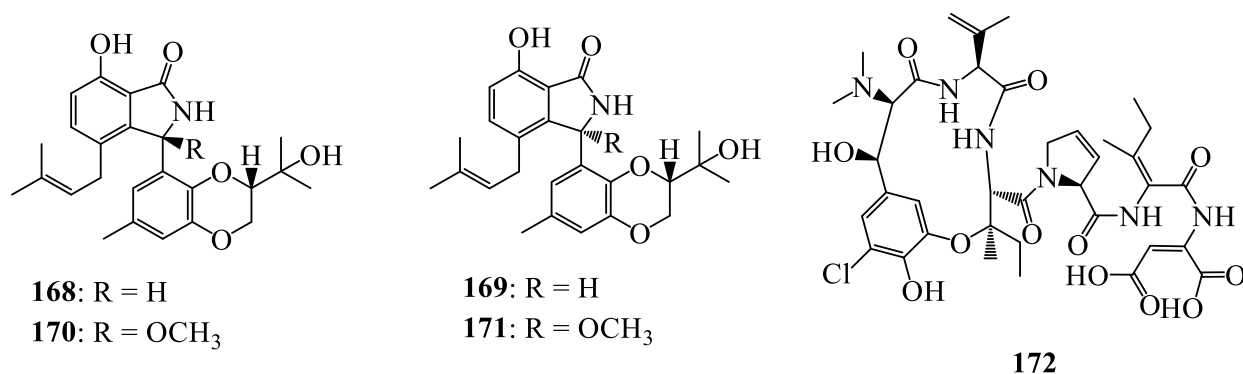


**Figure 26.** Structures of some alkaloids isolated from *Diaporthe*

#### I.7.2.3.3.6. Fatty acids

Fatty acids are simple linear compounds that play an important role in the synthesis and catabolism of organisms (Jozwiak *et al.*, 2020). Up to date, six fatty acids are reported from *Diaporthe* genus. The fungus *D. phaseolorum* derived from *Laguncularia racemose*, afforded 3-hydroxypropionic acid (**173**) (Sebastianes *et al.*, 2012). Phytotoxic metabolite, 3-nitropropionic acid (**174**), was isolated from *D. gulyae* (Andolfi *et al.*, 2015). Two fatty acids, diapolic acids A and B (**175** and **176**), were isolated from endophytic fungus *D. terebinthifolii* (Yedukondalu *et al.*, 2017). Studies of the strain *Diaporthe* sp. J CJ7 from stems of *Dendrobium nobile* led to the isolation of diaporthsin E (**177**) (Hu *et al.*, 2018). Moreover, 3-hydroxy-5-methoxyhex-5-ene-2,4-dione (**178**), was derived from *Diaporthe* sp. ED2 associated with medicinal herb *Orthosiphon stamieus* Benth (Yenn *et al.*, 2017).

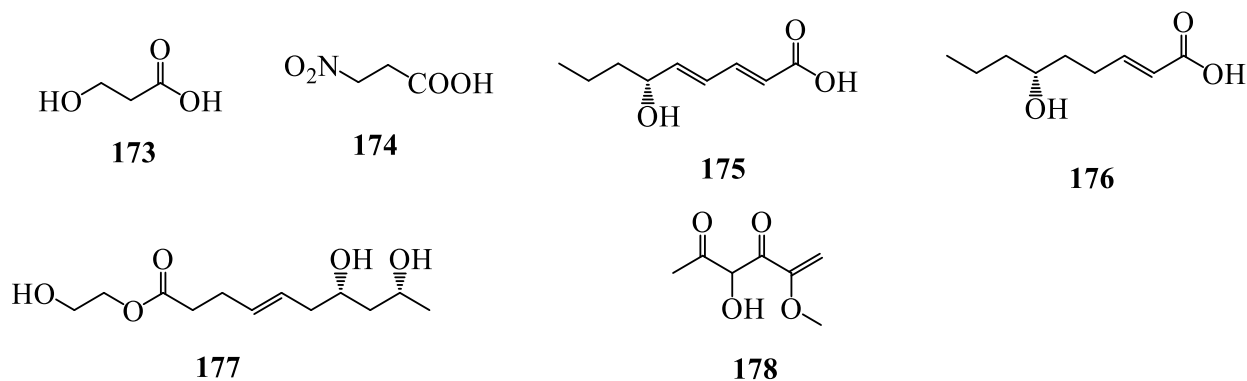


**Figure 27.** Structures of fatty acids isolated from *Diaporthe*.

#### I.7.2.4. Biological activities of some isolated compounds from *Diaporthe* genus

Endophytes fungi belonging to the genus *Diaporthe* represent a chemical reservoir with antihyperlipidemic, antifibrotic, antidiabetic, antitubercular, antifeedant, antioxydant, phytotoxic, anti-angiogenic, inhibitory effects, contact toxicity, antiviral, cytotoxicity activities etc. The most important activities are summary in the table 2 below.

**Table 2.** Biological activity of some isolated compounds from *Diaporthe*.

Compounds	References	Compounds	References
<b>Antihyperlipidemic</b>		<b>Antifibrotic activity</b>	
Diaporthsin E ( <b>177</b> ) Antagonistic	Hu <i>et al.</i> , 2018	Mucorisocoumarin A ( <b>88</b> )	Liu <i>et al.</i> , 2018
Tyrosol ( <b>110</b> )	Specian <i>et al.</i> , 2012	Pestalotiopson B ( <b>82</b> )	Liu <i>et al.</i> , 2018
<b>Anti-migration</b>		Acetoxydothirelone B ( <b>119</b> )	Liu <i>et al.</i> , 2018
Diaporthol A ( <b>123</b> )	Nakashima <i>et al.</i> , 2018	Dothiorelone B ( <b>120</b> )	Liu <i>et al.</i> , 2018
Diaporthol B ( <b>124</b> )	Nakashima <i>et al.</i> , 2018	Dothiorelone L ( <b>113</b> )	Liu <i>et al.</i> , 2018
<b>Antidiabetic activity</b>		Dothiorelone G ( <b>121</b> )	Liu <i>et al.</i> , 2018
Cytosporone D ( <b>87</b> )	Liu <i>et al.</i> , 2018	Diaporthol A ( <b>123</b> )	Liu <i>et al.</i> , 2018
<b>Antifeedant activity</b>		<b>Antitubercular activity</b>	
3,8-Dihydroxy-6-methyl-9-oxo-9H-Xanthene-1-carboxylate ( <b>72</b> )	Luo <i>et al.</i> , 2018	Diaportheone A ( <b>183</b> )	Bungihan <i>et al.</i> , 2011
Pestalotiopson F ( <b>81</b> )	Luo <i>et al.</i> , 2018	Diaportheone B ( <b>84</b> )	
Pestalotiopson B ( <b>82</b> )	Luo <i>et al.</i> , 2018	<b>Antioxydant activity</b>	
<b>Anti-angiogenic</b>		Cytosporone D ( <b>87</b> )	Liu <i>et al.</i> , 2018
Cordysin A ( <b>164</b> )	Chang <i>et al.</i> , 2019	Diportharine A ( <b>90</b> )	Sharma <i>et al.</i> , 2018
<b>Phytotoxic activity</b>		Xylarolide A ( <b>153</b> )	Sharma <i>et al.</i> , 2018
<i>p</i> -Cresol ( <b>113</b> )	Reveglia <i>et al.</i> , 2019	18-Des-hydroxy cytochalasin H ( <b>162</b> )	Brissow <i>et al.</i> , 2017
		<b>Inhibitory effects</b>	
		(+) -Phomopsichin A ( <b>80</b> )	
		(-) -Phomopsichin A ( <b>76</b> )	Cui <i>et al.</i> , 2017

4-Hydroxybenzoic acid (114)	Reveglia <i>et al.</i> , 2019	(+) -Phomopsichin B (77)
Phomentrioloxin B (136)	Andolfi <i>et al.</i> , 2015	(-) -Phomopsichin B (75)

Table 2. Biological activity of some isolated compounds from *Diaporthe* (continued).

Compounds	References	Compounds	References
Gulypyrone A-B (140-141)	Andolfi <i>et al.</i> , 2015	Diaporchromanone C (78) Diaporchromanone D (79)	Cui <i>et al.</i> , 2017
Nectriapyrone (142)	Evidente <i>et al.</i> , 2015	Pestalotiopsone B (82)	Luo <i>et al.</i> , 2018
3, 4-Dihydro-8-hydroxy-3,5-dime-thyl-isocoumarin (89)	Meepagala <i>et al.</i> , 2018	Tenellone C (125)	Cui <i>et al.</i> , 2017
Tyrosol (110)	Specian <i>et al.</i> , 2012	Phomolide C (150)	Ito <i>et al.</i> , 2015
3-Nitropropionic acid (174)	Andolfi <i>et al.</i> , 2015	Diaporisoindole D (170)	Cui <i>et al.</i> , 2017
Kongiidiadzadione (95)	Evidente <i>et al.</i> , 2015	<b>Anti-IAV</b>	
<b>Contact toxicity</b>		3,8-Dihydroxy-6-methyl 9-oxo-9H-Xanthene-1- carboxylate (72)	Luo <i>et al.</i> , 2018
Phyllostine acetate (102)	Ratnaweera <i>et al.</i> , 2020	Pestalotiopsone F (81)	
(-)-Phyllostine (103)	Ratnaweera <i>et al.</i> , 2020	Pestalotiopsone B (82)	
<b>Antiviral activity</b>			
3,8-dihydroxy-6-methyl-9-oxo-9H-xanthene-1-carboxylate (72)	(Niu <i>et al.</i> , 2019).		

**Table 2.** Biological activity of some isolated compounds from *Diaporthe* (continued).

Compounds	References
<b>Cytotoxicity activity</b>	
Phomoxanthone A ( <b>73</b> )	Niu <i>et al.</i> , 2019
5-Deoxybostrycoidin	Cui <i>et al.</i> , 2017
Fusaristatin A ( <b>166</b> )	Cui <i>et al.</i> , 2017
Vochysiamide B ( <b>167</b> )	Noriler <i>et al.</i> , 2019
Emodin ( <b>105</b> )	Riga <i>et al.</i> , 2019
2,5-Dihydroxybenzyl alcohol ( <b>111</b> )	Noriler <i>et al.</i> , 2019
4-Hydroxybenzaldehyde ( <b>112</b> )	Noriler <i>et al.</i> , 2019
Arbutin ( <b>115</b> )	Riga <i>et al.</i> , 2019
Oblongolide D ( <b>132</b> )	Liu <i>et al.</i> , 2013
Oblongolide H ( <b>133</b> )	Liu <i>et al.</i> , 2013
Oblongolide P ( <b>134</b> )	Liu <i>et al.</i> , 2013
Isochromophilone D ( <b>138</b> )	Luo <i>et al.</i> , 2018
(1 <i>R</i> ,2 <i>R</i> ,4 <i>R</i> )-Trihydroxy- <i>p</i> -menthane ( <b>139</b> )	Liu <i>et al.</i> , 2013
Diaporol R ( <b>143</b> )	Chen <i>et al.</i> , 2015
Eremofortin F ( <b>144</b> )	Mandavid <i>et al.</i> , 2015
Lithocarin B-C ( <b>145-146</b> )	Liu <i>et al.</i> , 2019
Phomolide C ( <b>150</b> )	Ito <i>et al.</i> , 2015
Xylarolide ( <b>151</b> )	Yedukondalu <i>et al.</i> , 2017
Phomopsin F ( <b>172</b> )	Schloss <i>et al.</i> , 2017
Cytosporone D ( <b>87</b> )	Liu <i>et al.</i> , 2018
3,4-Dihydro-5'-[(1 <i>R</i> )-1-hydroxymethylethyl]bifuran]-5(2 <i>H</i> )-one	[2,2'-Liu <i>et al.</i> , 2013
<i>Epi</i> -Isochromophilone II ( <b>137</b> )	Luo <i>et al.</i> , 2018
1 <i>R</i> ,2 <i>E</i> ,4 <i>S</i> ,5 <i>R</i> ) -1-[(2 <i>R</i> ) -5-Oxotetrahydrofuran-2-yl] -4,5-dihydroxy-hex-2-en-1-yl(2 <i>E</i> ) enoate ( <b>91</b> )	-2-methylbut-2-Liu <i>et al.</i> , 2013
Xylarolide A ( <b>153</b> )	Sharma <i>et al.</i> , 2018

**Table 2.** Biological activity of some isolated compounds from *Diaporthe* (continued).

Compounds	References
18-Des-hydroxy cytochalasin H (162)	Brissow <i>et al.</i> , 2017
<b>Antifungal activity</b>	
Phomopsolide A (96)	Evidente <i>et al.</i> , 2015
21-Acetoxyctochalasin J2 (155)	Huang <i>et al.</i> , 2019
21-Acetoxyctochalasin J3 (156)	Huang <i>et al.</i> , 2019
Cytochalasin J3 (158)	Huang <i>et al.</i> , 2019
Cytochalasin H (160)	Huang <i>et al.</i> , 2019
Phomopsolide B (97)	Tanney <i>et al.</i> , 2016
Phomopsolide C (98)	Tanney <i>et al.</i> , 2016
( <i>S</i> , <i>E</i> )-6-(4-Hydroxy-3-oxopent-1-en-1-yl)-2 <i>H</i> -pyran-2-one (99)	Tanney <i>et al.</i> , 2016
7-Hydroxy-6-metoxycoumarin (100)	Riga <i>et al.</i> , 2019
Coumarin (101)	Riga <i>et al.</i> , 2019
(+) -2,2'-Epicytoskyrin A (107)	Wulansari <i>et al.</i> , 2016
7-Acetoxyctochalasin H (161)	Huang <i>et al.</i> , 2019
Cytochalasin E (159)	Huang <i>et al.</i> , 2019
3-hydroxy-5-methoxyhex-5-ene-2,4-dione (178)	Yenn <i>et al.</i> , 2017
<b>Antibacterial activity</b>	
10S – Diaporthin (85)	De Medeiros <i>et al.</i> , 2018)
Orthosporin (86)	
Kongiiazadione (95)	Evidente <i>et al.</i> , 2015
Emodin (105)	Riga <i>et al.</i> , 2019
1,2,8-Trihydroxyanthraquinone (106)	Riga <i>et al.</i> , 2019
Phomosine A (116)	Sousa <i>et al.</i> , 2016
Phomosine C (117)	Sousa <i>et al.</i> , 2016
19-Nor-lanosta-5(10),6,8,24-tetraene-1 $\alpha$ ,3 $\beta$ ,12 $\beta$ ,22 <i>S</i> -tetraol (147)	Li <i>et al.</i> , 2015
3 $\beta$ ,5 $\alpha$ ,9 $\alpha$ -Trihydroxy-(22 <i>E</i> ,24 <i>R</i> ) -ergosta-7,22-dien-6-one (148)	Li <i>et al.</i> , 2015
Chaxine C (149)	Li <i>et al.</i> , 2015
Phomolide G (152)	Yedukondalu <i>et al.</i> , 2017
21-Acetoxyctochalasin J3 (156)	Huang <i>et al.</i> , 2019

**Table 2.** Biological activity of some isolated compounds from *Diaporthe* (continued).

Compounds	References
<b>Antibacterial activity</b>	
Cytochalasin J3 (158)	Huang <i>et al.</i> , 2019
7-Acetoxyoctochalasin H (161)	Huang <i>et al.</i> , 2019
Cytochalasin J (157)	Huang <i>et al.</i> , 2019
Cytochalasin E (159)	Huang <i>et al.</i> , 2019
Vochysiamide B (167)	Noriler <i>et al.</i> , 2019
3-Hydroxypropionic acid (173)	Sebastianes <i>et al.</i> , 2012
Diapolic acid A (175)	Yedukondalu <i>et al.</i> , 2017
<b>Anti-inflammatory activity</b>	
Compounds	References
Phomoxanthone A (73)	Liu <i>et al.</i> , 2019
Penialidin A (74)	Liu <i>et al.</i> , 2019
(-) -Phomopsichin B (75)	Liu <i>et al.</i> , 2019
Tenellone D (126)	Cui <i>et al.</i> , 2018
Diaporindene A –D (127-130)	Cui <i>et al.</i> , 2018
Isoprenylisobenzofuran A (131)	Cui <i>et al.</i> , 2018
Diaporisoindole A (168)	Cui <i>et al.</i> , 2018
Diaporisoindole B (169)	Cui <i>et al.</i> , 2018
Diaporisoindole D (170)	Cui <i>et al.</i> , 2018
Diaporisoindole E (171)	Cui <i>et al.</i> , 2018
Phomoxanthone A (73)	Liu <i>et al.</i> , 2019
Penialidin A (74)	Liu <i>et al.</i> , 2019
Biatriosporin N (104)	Liu <i>et al.</i> , 2019
Cytochalasin H (160)	Liu <i>et al.</i> , 2019
21- <i>O</i> -Deacetyl-L-696,474 (163)	Liu <i>et al.</i> , 2019

## 1.8. MINING SILENT GENE CLUSTERS IN ENDOPHYTIC FUNGI

Different strategies have been developed to induce the production of new endophytic fungi compounds, via the activation of silent genes. Such methods include the addition of epigenetic modifier or a modification of nutrients into the culture medium, and the co-cultivation of endophytes. Moreover, sequencing data of the fungal genomes indicated that a large part of secondary metabolic gene clusters are silent under standard laboratory culture conditions (Rutledge and Challis, 2015). The strategies for triggering silent gene clusters were applied, using the OSMAC (One Strain MANY Compounds) approach, co-cultivation, chemical epigenetic modulation and genetic modification (Wiemann and Keller, 2014). Variated culture conditions

approach is frequently used for the optimization of compounds production and therefore encourages the production of a wider range of natural products from a microorganism.

## **1.9. STRUCTURE MODIFICATION USING ENDOPHYTIC FUNGI: BIOTRANSFORMATION**

Endophytic fungi used to induce selective conversions of natural and /or synthetic substances into useful products using whole cells and/or isolated enzymes or biocatalysts, have been gaining increased relevance recently ([Adelin et al, 2012](#)).

This technique called biotransformation is a different process, encompassing the biosynthesis of complex products such as carbon dioxide, ammonia or glucose. However, biotransformation has evolved from nineteenth century by the pioneer work of several researchers. Biotransformations are increasingly in use in biotechnological science with one of its most appreciated features being to catalyse regiospecific and stereospecific reactions under chemical (pH) and physical (Temperature, pressure) conditions close to ambient condition. Moreover, biotransformation allows for the production of new products as well as improves the production of already known molecules).

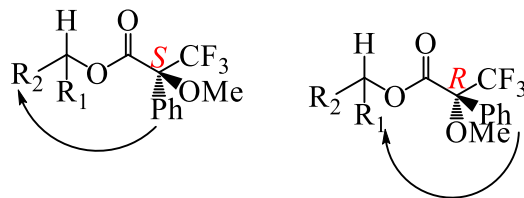
## **1.10. SOME TECHNIQUES FOR STRUCTURE DETERMINATION AND STEREOCHEMISTRY**

### **1.10.1. The Mosher's method**

Mosher reaction is an empirical method based on NMR spectroscopy to deduce the configuration of second alcohol centers or analogs, such as amines where the hydroxyl group is replaced by an amine. The principle for this method lies in the difference in anisotropic effects between two diastereomers which are prepared from the substrate with a pair of enantiomeric chiral derivatizing agents, respectively. In practical use, it is the differences in chemical shifts ( $\Delta\delta^{\text{RS}}$  or  $\Delta\delta^{\text{SR}}$ ) between the two derivatives of a substrate that are used to assign the absolute configuration ([Hoye, 2007](#)).

The *R*- (+)- $\alpha$ -Methoxy- $\alpha$ -trifluoromethylphenylacetic acid (*R*-(+)-MTPA-OH) or *R*- (+)-MTPA-Cl together with (*S*- (-)- $\alpha$ -Methoxy- $\alpha$ -trifluoromethylphenyl acetic acid (*S*-(-)-MTPA-OH) or *S*- (-)-MTPA-Cl are used as Mosher reagents. *R*-MTPA ester and *S*-MTPA ester are obtained after reaction of Mosher reagent with the compounds. The anisotropic, magnetic shielding effect on protons residing above (or below) the plane of the aryl ring on the MTPA esters results in a more

upfield chemical shift for the affected (especially proximal) protons in the NMR spectrum. The conversions of  $\Delta\delta^{\text{SR}}$  ( $\delta_{\text{S}} - \delta_{\text{R}}$ ) values are assigned to determine the absolute structures of the secondary alcohol stereocenters. Those protons that have positive  $\Delta\delta^{\text{SR}}$  values reside within  $\text{R}^1$ , whereas those with negative values belong to  $\text{R}^2$  as presented below (Hyde *et al.*, 2007).



## I.10.2. Electronic circular dichroism (ECD, CD)

### I.10.2.1. Definition and principles

Originally discovered by Arago and Biot in the early 19<sup>th</sup> century, it is used when the molecule contains one more chiral chromophore (Berova *et al.*, 2007). The absorption of left-handed circularly polarized light would be different, and thus, circular dichroism (CD) occurs.” CD signal present positive or negative depending on whether L-CPL is absorbed to greater extent than R-CPL (CD signal positive) or to the less extent (CD signal negative) under the same wavelength.

According to the different wavelengths used in the experiments, ECD (electronic circular dichroism) and VCD (vibrational circular dichroism) have been studied. For ECD, a chromophore is necessary in the structure, which is responsible for UV and Vis range absorption band of VCD spectra (Taniguchi *et al.*, 2008).

## I.10.3. Single –crystal X-Ray diffraction

Single crystal X-ray diffraction is a powerful non-destructive method which allows to unambiguously identify crystalline phases, determine a crystal structure and, if required, a phase composition. It is a direct and predominant method for molecules having anomalous scattering effects. It has been used for decades by chemists to determine the absolute configuration of natural products obtained in crystal form or crystallized, for their ability to “see” the arrangement of atoms in a single crystal.

---

## I.11. LITERATURE OVERVIEW ABOUT BACTERIAL INFECTIOUS DISEASES

### I.11.1 Definition and classification of bacteria

Bacteria are single-cells, nucleus-free microorganisms. They are the cause of infectious diseases such as cholera, syphilis, leprosy, gonorrhea, tuberculosis etc.

Bacteria can be classified into two large groups depending on the nature of their wall: Thin-walled bacteria known as Gram-positive (*Staphylococcus aureus*, *Staphylococcus saprophyticus*) and thick-walled bacteria known as Gram-negative (*Escherichia coli*, *Klebsiella pneumoniae*). These names attributed to bacteria derive from the reaction of cells to a so-called Gram stain. This is because Gram-positive bacteria retain the dark blue stain while Gram-negative bacteria do not retain stain when treated with Gram's liquor. Sometimes, they retain the color and, in some cases, do not retain it at all. They are therefore said to have variable Gram staining. Such a difference in affinity results not only from a difference in the structure but also in the chemical composition of the two types of walls (Hermann, 1985; Van, 2001).

Generally, these organisms are grouped into three types as beneficial, saprophyte and opportunistic pathogens when they can cause diseases (Madigan and Martinko, 2006). Their pathogenic power depends not only on their invasive power (ability to spread and disperse in the tissues with a view to establishing an infectious focus despite immune defenses), but also on their toxicogenic power (ability to produce toxins).

### I.11.2. Bacterial diseases

Bacterial diseases include all types of illnesses caused by bacteria. Bacteria are a type of microorganism, which are tiny forms of life that can only be seen with a microscope. Millions of bacteria normally live on the skin, in the intestines, and on the genitalia. The vast majority of bacteria do not cause disease, and many bacteria are actually helpful and even necessary for good health. These bacteria are sometimes referred to as “good bacteria” or “healthy bacteria.”

Harmful bacteria that cause bacterial infections and disease are called pathogenic bacteria. Bacterial diseases occur when pathogenic bacteria get into the body and begin to reproduce and crowd out healthy bacteria, or grow in tissues that are normally sterile (Walsh, 2003). Harmful bacteria may also emit toxins that damage the body. Common pathogenic bacteria and the types of bacterial diseases they cause include: *Escherichia coli and Salmonella*, *Helicobacter pylori*, *Neisseria gonorrhoeae*, *Neisseria meningitides*, *Staphylococcus aureus*, *Streptococcal bacteria* (Walsh, 2003)

---

### I.11.3. Treatment of bacterial infections

There are several classes of antibiotics namely, aminoglycosides,  $\beta$ -lactams, glycopeptides, macrolides, quinolones, sulfonamides, tetracyclines, peptide antibiotics, diketopiperazine derivatives, cyclic peptides, etc. Each of these antibiotics have a very specific mode of action on the bacterial cell wall or cytoplasm, among others. They are active either by bacteriostasis, (inhibition of bacterial growth and multiplication), or by bactericidal (destruction of the bacteria) (Chin *et al.*, 2006; Newman *et al.*, 2000). They can also be classified according to other criteria such as: their origin, their spectrum of action or their mechanism of action. Indeed, they can act by inhibiting one or more vital functions of the bacteria such as: inhibition of protein synthesis and that of DNA and its precursors, inhibition of synthesis of the cell wall bacteria and that of the cytoplasmic membrane (Walsh, 2003).

From the general point of view, the treatment of bacterial infections is done today using antibiotics including, amoxicillin (**179**), clindamycin (**180**), fosfomycin (**181**) nitrofurantoin (**182**), cefpodoxime (**183**), sulfamethoxazole (**184**), ceftriaxone (**185**) etc.

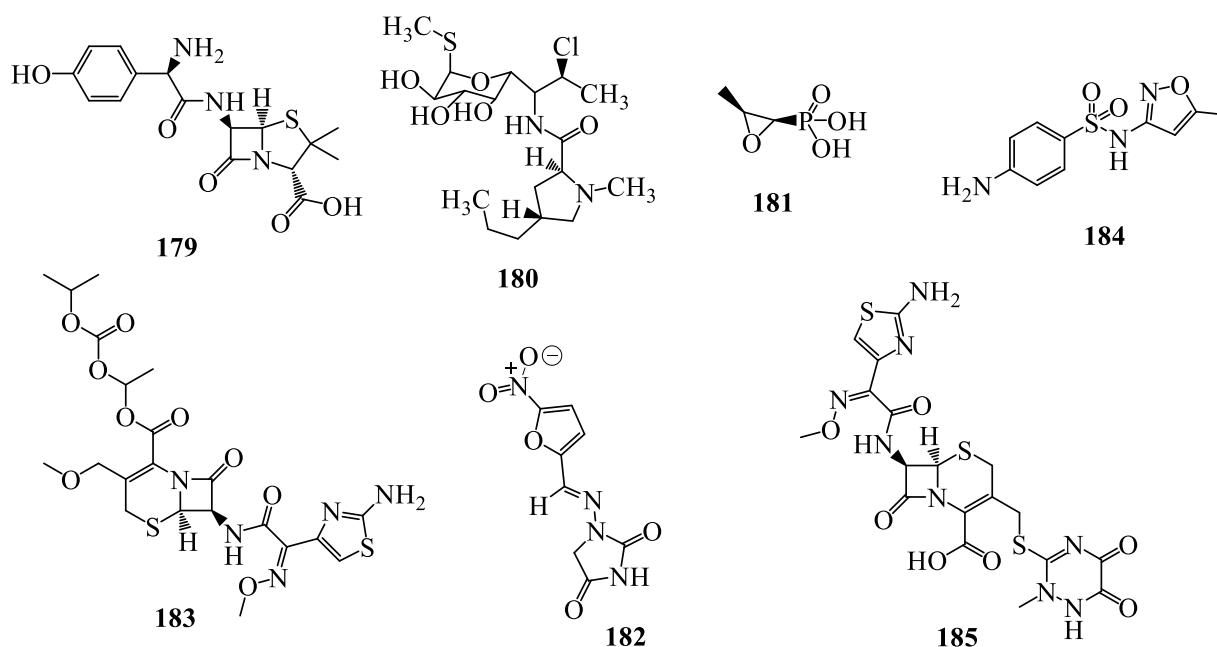


**Figure 28.** Structure of some antibiotics.

From endophytic fungi, several antibacterial secondary metabolites were previously isolated including polyketides, alkaloids and lactams and terpenoids (See Table 2. P 40).

---

# **CHAPTER II: RESULTS & DISCUSSION**

---

## II.1. PLANT MATERIALS

Different parts of *Duguetia staudtii* (Engl. and Diels) Chatrou were collected in July 2017, at the Dja rain forest (GPS coordinates provided by system WGS8: Altitude 665 m; Latitude N 4°34'38"; Longitude E 13°41'04"), in the locality of Lomié-Bertoua, East Region of Cameroon. The plant material was identified by Mr. Victor Nana, a botanist at the National Herbarium of Cameroon where a voucher specimen was deposited under the number 52711/HNC. A total 06 endophytic fungal strains were isolated from the stem bark following the protocol previously reported (Talontsi *et al*, 2014; Petrini *et al.*, 1984). The plant material of *T. guineensis* (Schumach & Thonn) (leaves, roots and stem bark and fruits) was collected in January 2019, at the mount Kala, the centre region of Cameroon and identified under voucher number 42166HNC. A total of 12 fungal strains were isolated from the leaves and 06 from the roots using the protocol mentioned above.

## II.2. SELECTION OF FUNGAL MATERIAL

All the obtained pure isolates were cultured in small scale in solid (rice, PDA and wheat) and liquid (PDB, YMG) media. The crude extracts were obtained and the prescreening were done using LC-MS analyzed, following by the bioassays The first selected strain, isolated from the stem bark of *D. staudtii* and identified as *Simplicillium subtropicum*, SPC3 was inoculated in ten 500 mL-Erlenmeyer flask containing 200 mL of Yeast Malt Glucose (YMG) medium for 6 days and extracted with acetone to yield 2.0 g of crude extract. The second and third selected strains characterized as *Diaporthe* sp. 1. nov. F<sub>18</sub> and *Diaporthe* sp. 2.nov.R<sub>38</sub>, isolated from the leaves and roots respectively of *T. guineensis* were cultured in rice (80g of rice + 100mL distilled water) for 30 days. Then, their ethyl acetate extraction yields 20.5 g crude extract for *Diaporthe* sp.1.nov and 12.0 g for *Diaporthe* sp.2.nov. The following LC-MS profiles results were obtained for selected strains (Fig 29). The crude extract obtained from each selected fungus was separated and the pure compounds were analyzed for their structure determination.

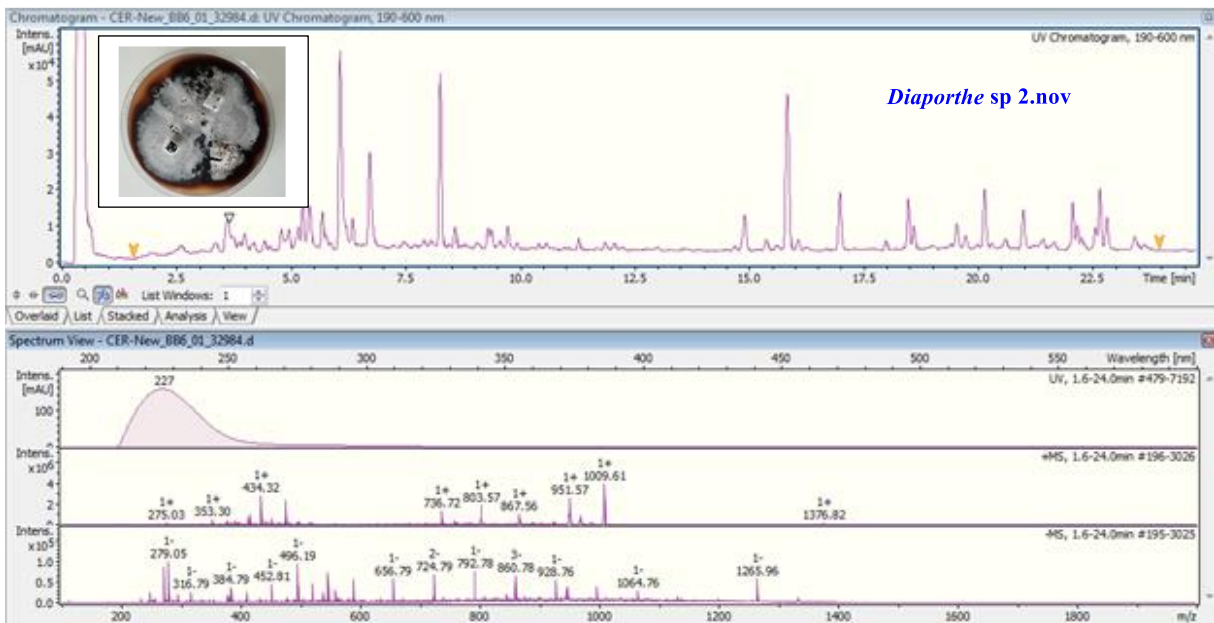
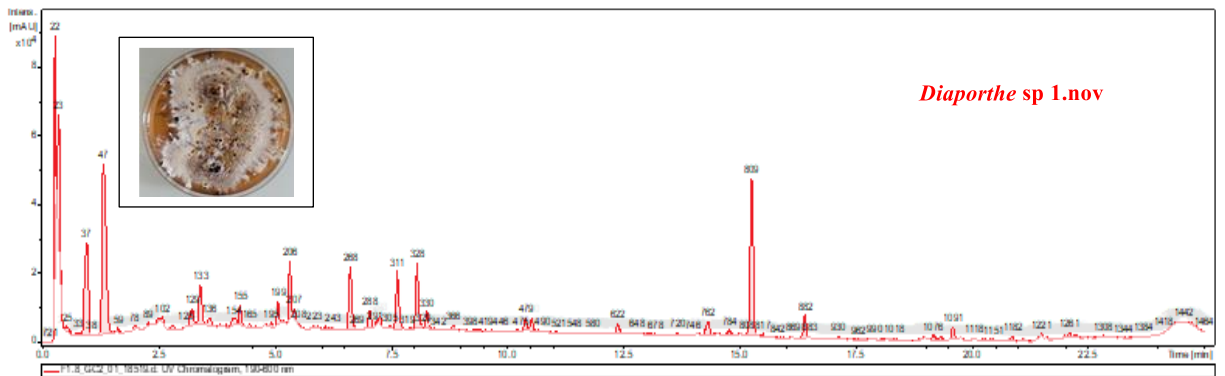
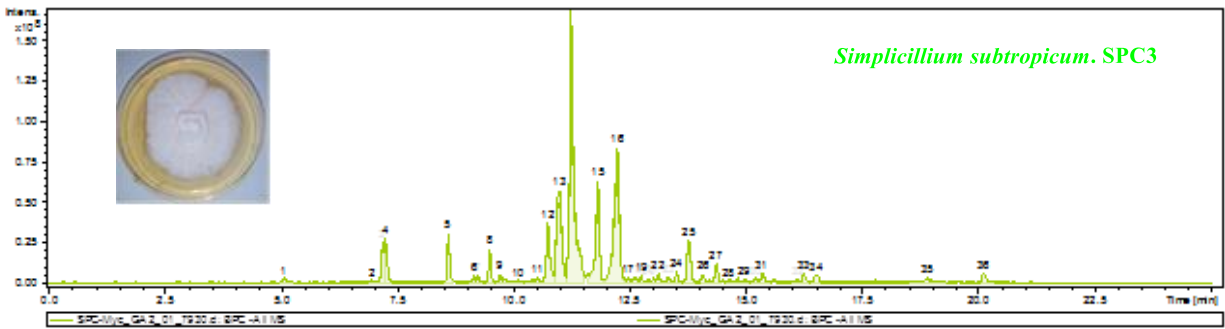


Figure 29. LC-MS profile of the selected endophytic fungi.

### II.3. MORPHOLOGICAL AND MOLECULAR CHARACTERIZATION OF SELECTED ENDOPHYTIC FUNGI

#### II.3.1. *Simplicillium subtropicum*

*Simplicillium subtropicum*, SPC3 was isolated from the stem bark of *Duguetia staudtii* and was identified by the combination of both morphological and molecular method (ITS locus). In addition, a BLAST search was used to search for closest matched sequences in the GenBank database (<http://www.ncbi.nlm.nih.gov/genbank/>). These morphological characteristics enabled the identification of the endophytic fungus as *S. subtropicum*, SPC3, which was reinforced by the sequence of its 18S rRNA that gave a 98% sequence similarity to those accessible by BLAST analyses of available *S. subtropicum* sequences.

#### II.3.2. *Diaporthe* sp.1.nov

*Diaporthe* sp.1.nov (F18) was isolated from the leaves of *T. guineensis* and its characterization was carried out by combination of morphological, phenotypic, and phylogenetic study. The phylogenetic analysis was carried out based on the combination of the five loci sequences (ITS, cal, *his3*, *tef1*, *tub2*) of our isolate and all *Diaporthe* sp. available to date to identify the closest species to our isolate. Our strain was located in an independent branch distant from other species of *Diaporthe*, demonstrating that this represented a new species and the named *Diaporthe* sp.1.nov was attributed. The establishment of his total named for their introduction in the GenBank is ongoing.

#### II.3.3. *Diaporthe* sp. 2.nov

*Diaporthe* sp.2.nov (R38) was isolated from the roots of *T. guineensis* and characterized following the same method as the one used for F18. The fungal R38 was also found to be another new species of *Diaporthe* and was named *Diaporthe* sp.2.nov. The establishment of his total named for their introduction in the GenBank is ongoing.

### II.4. CHARACTERISATION OF ISOLATED COMPOUNDS

Twenty-two (22) compounds were isolated from the acetone extract of *S. subtropicum* and ethyl acetate extracts of the two new *Diaporthe* sp. These compounds were sorted into four classes.

-04 dibenzopyrones including one new derivative (3, 9- diacetylalternariol) together with known alternariol, 2-hydroxyalternariol and 4-hydroxyalternriol,

---

- 01 new benzofuranone: diapobenzofuranone,
- 02 new polyketides: simplicilones A and B,
- 07 known cytochalasins: cytochalasin H, cytochalasin N, epoxycytochalasin H, cytochalasin J, cytochalasin J2, cytochalasin J3 and cytochalasin RKS-1778,
- 02 chromanones : cytosporone C and E,
- 01 known macrolide : lasiodiplodin,
- 01 biphenyl: 5'-methoxy-6-methyl-biphenyl-3,4,3'-triol,
- 01 known chromone : 2,5-dimethyl-7-hydroxychromone,
- 01 known glycol : sorbitol,
- 01 fatty acid : linoleic acid,
- 01 known sterol : ergosterol.

#### **II.4.1. Secondary metabolites from *Simplicillium subtropicum* SPC3**

With the aim of isolation and identification of new biologically active metabolites from the associated plant fungi, we have investigated the constituents of an endophytic fungus *Simplicillium subtropicum*. SP3, isolated from *Duguetia Staudtii*. Chromatographic separation of the crude extract obtained from this fungal strain, yielded two unknown polyketides, linoilic acid and ergosterol.

##### **II.4.1.1. Characterization of compound SPC-G1**

Compound **SPC-G1** was obtained as a colourless oil with the molecular formula  $C_{24}H_{35}NO_5$ , as deduced from its positive mode high resolution electrospray ionisation mass spectrometry, (+) HR-ESI-MS data (Fig. 30), which showed the protonated molecular ion peak  $m/z$  418.2589  $[M + H]^+$  (calcd. for  $C_{24}H_{35}NO_5$ : 418.2593).

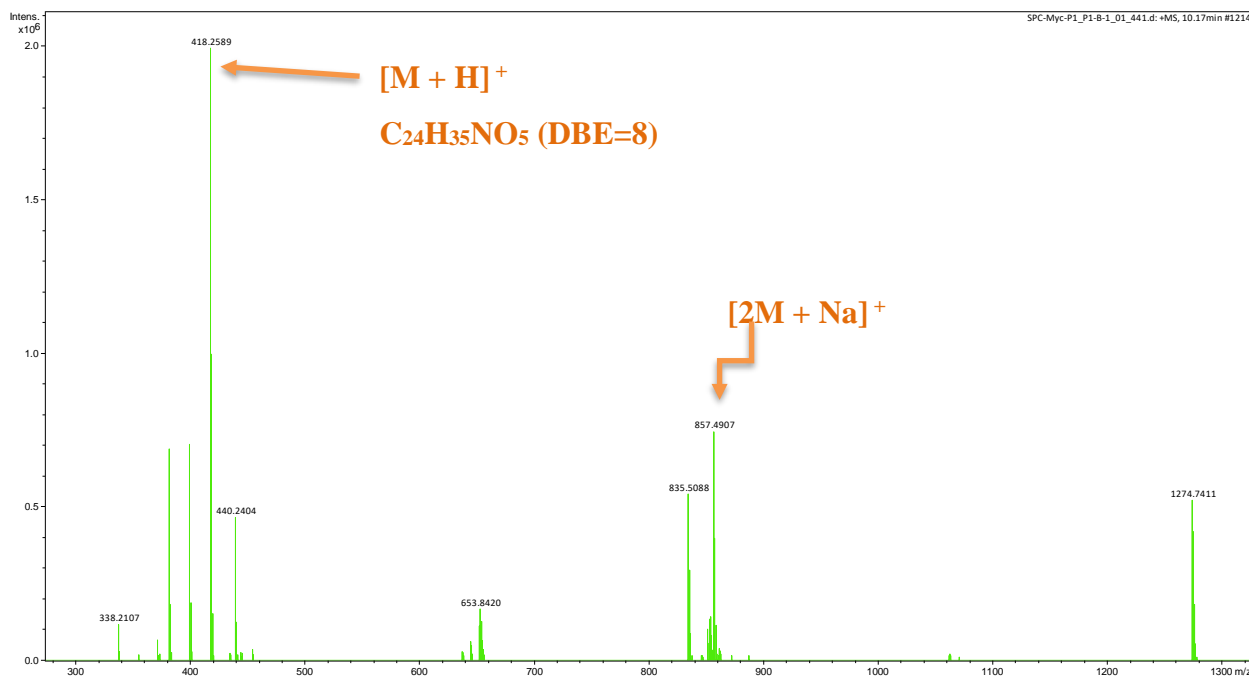


**Figure 30.** Positive ion mode HR-ESI-MS of compound **SPC-G1**.

The  $^1H$  NMR spectrum (Fig. 31) of SPC-G1 showed signals of an olefinic proton ( $\delta_H$  5.72), an oxymethine proton ( $\delta_H$  4.04) and five methyl protons including protons of a heteroatom-linked methyl ( $\delta_H$  3.19) which was further confirmed by the  $^{13}C$  NMR spectrum (Fig. 32) with resonances at 132.9, 69.8, 23.6, 25.5, 17.6, 11.4, 17.6 and 31.7.

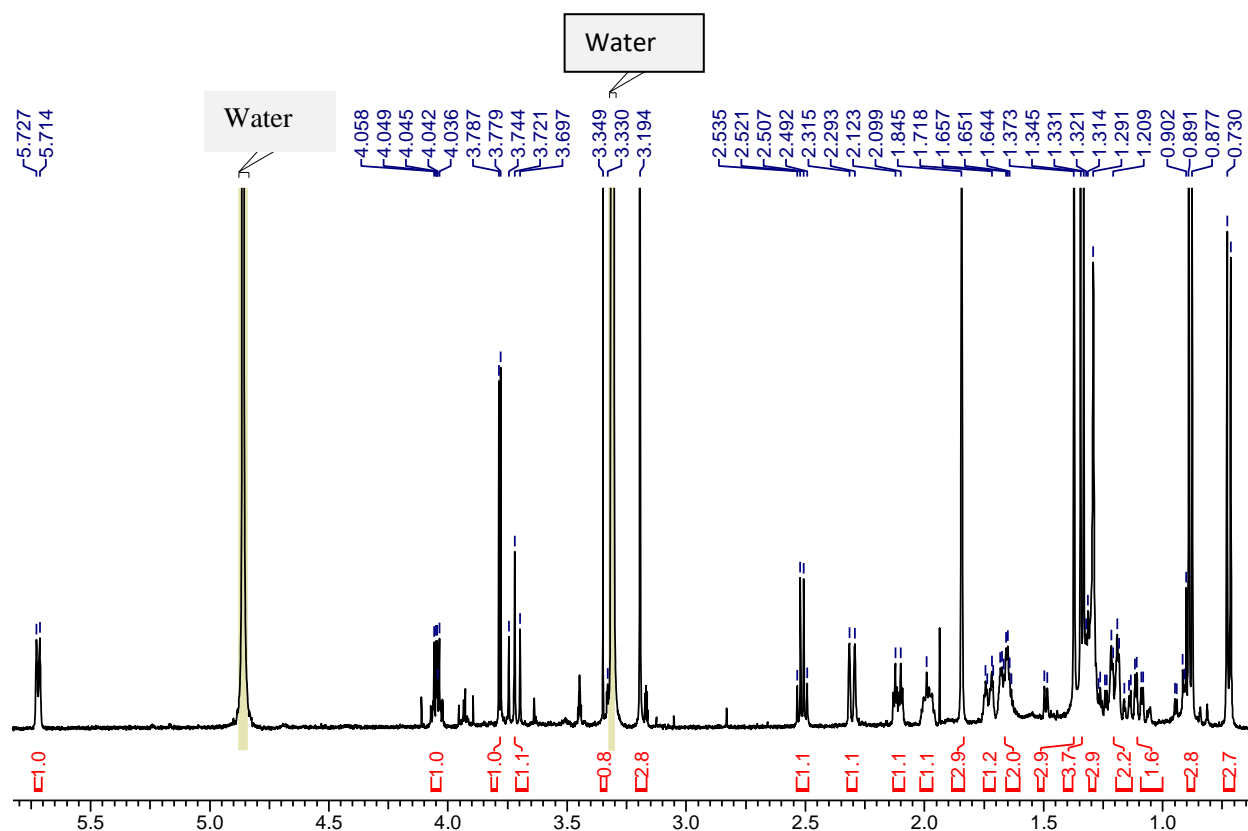


**Figure 31.**  $^1\text{H}$  NMR spectrum ( $\text{CDCl}_3$ , 500 MHz) of compound **SPC-G1**

Furthermore, its broad band (BB)  $^{13}\text{C}$  NMR spectrum (Fig. 32) displayed signals for twenty-four carbon atoms, which were sorted by the HSQC experiment (Fig. 33) into six methyls, three methylenes, nine methines and six quaternary carbons including three carbonyl signals at  $\delta_{\text{C}}$  205.8 (C-3'), 201.7 (C-1) and 172.8 (C-1'). The  $^{13}\text{C}$  NMR of compound **SPC-G1** also showed signals at  $\delta_{\text{C}}$  132.9 (C-10) and 134.0 ppm (C-9), which were assigned to the two olefinic carbons on the fused bicyclic unit. The first fused ring system (A-B), named 4,5-disubstituted-3,7-dimethylbicyclo [4.4.0] dec-2-ene, was clearly supported by the HMBC cross peaks observed between the olefinic proton signals at  $\delta_{\text{H}}$  5.72 (H-9) with the carbon signals at  $\delta_{\text{C}}$  59.2 (C-11), 37.9 (C-3) and 31.5 (C-7), and also between the methyl protons at  $\delta_{\text{H}}$  1.84 (H-15) with the carbon signals at  $\delta_{\text{C}}$  132.9 (C-9) and 134.0 (C-10) (Scheme 4).

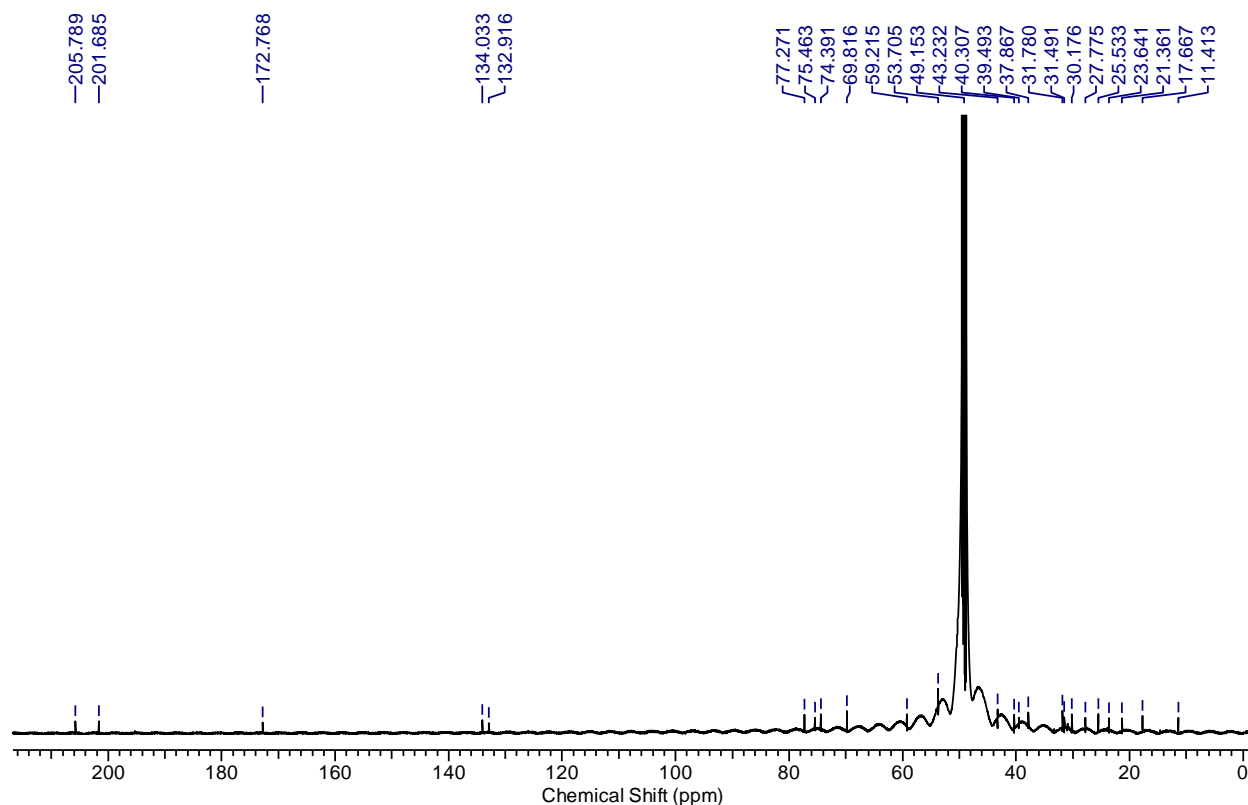


**Figure 32.**  $^{13}\text{C}$  NMR spectrum ( $\text{CDCl}_3$ , 125 MHz) of compound **SPC-G1**.

The later HMBC correlations gave clear evidence for the attachment of the methyl group H-15 at  $\delta_{\text{H}}$  1.84 at the C-10 position of the fused ring unit (A-B). This ring was also supported by multiple COSY correlations as shown in [Scheme 4](#). In addition, the methyl group (H-14) at  $\delta_{\text{H}}$  0.72 was located at C-4 of the (A-B) ring, as illustrated by cross peak correlations observed between the methyl proton signals at  $\delta_{\text{H}}$  0.72 with the carbon signals (C-4) at  $\delta_{\text{C}}$  39.5, (C-3) at 37.9 and (C-5) at  $\delta_{\text{C}}$  30.1. The five membered heterocyclic spiro ring unit (C-D), named 4,8,9-trisubstituted-3-methylazaspiro[4.5]deca-2,5,10-trione was deduced, and the chemical shift of C-2' ( $\delta_{\text{C}}$  75.5) in **SPC-G1** was comparable to that of a spiro quaternary carbon of spylidone ([Koyama et al., 2005](#)). This spiro ring formed a bridge junction via C-2 ( $\delta_{\text{C}}$  43.2) and C-11 ( $\delta_{\text{C}}$  59.2) of the fused ring (A-B) as a key  $^3J$  HMBC cross peak was observed between the proton signals (H-3) at  $\delta_{\text{H}}$  2.11 with the carbonyl carbon signal (C-1) at  $\delta_{\text{C}}$  201.7 and another one between the proton signals (H-3) at  $\delta_{\text{H}}$  2.11 with the spiro quaternary carbon signal (C-2'). Further HMBC cross peaks observed between the methyl proton signals (H-16) at  $\delta_{\text{H}}$  1.37 with the carbon signals (C-12) at  $\delta_{\text{C}}$  77.3 and (C-11) at  $\delta_{\text{C}}$  59.2 and also, between the methyl proton signals (H-17) at  $\delta_{\text{H}}$  0.88 with the carbon signals (C-13), at  $\delta_{\text{C}}$  53.7. C-12 and C-2' clearly indicated the points of attachment of these

two methyl groups (C-16 and C-17) at C-13 and C-12 positions, respectively (Fig.34). Moreover, the deshielded methyl protons (H-7') at  $\delta_{\text{H}}$  3.19 resided next to the nitrogen atom as they showed HMBC cross peak correlations with the carbonyl (C-1') at  $\delta_{\text{C}}$  172.8 and the carbon signal (C-4') at  $\delta_{\text{C}}$  74.3 ppm.

In addition, in the  $^1\text{H}$  NMR spectrum, the 1-hydroxyethyl moiety was deduced from the signals at  $\delta_{\text{H}}$  4.04 (1H, dq, 4.3, 7.0 Hz) and 1.34 (3H, s) which was further confirmed by the  $^{13}\text{C}$  NMR spectrum with resonances at  $\delta_{\text{C}}$  69.8 and 17.6, respectively. This moiety was attached at C-4' of the C-D ring of compound **SPC-G1** as illustrated by HMBC correlations (Scheme 4) observed between the methyl protons at  $\delta_{\text{H}}$  4.04 (H-5') with the carbon signals (C-4') at  $\delta_{\text{C}}$  74.3 and (C-5') at 69.8 and also, between the methine proton (H-4') at  $\delta_{\text{H}}$  3.78 with the carbon signals (C-3') at  $\delta_{\text{C}}$  205.8, (C-2') at  $\delta_{\text{C}}$  75.5, (C-5')  $\delta_{\text{C}}$  69.8 and (C-6') at  $\delta_{\text{C}}$  17.6 ppm.

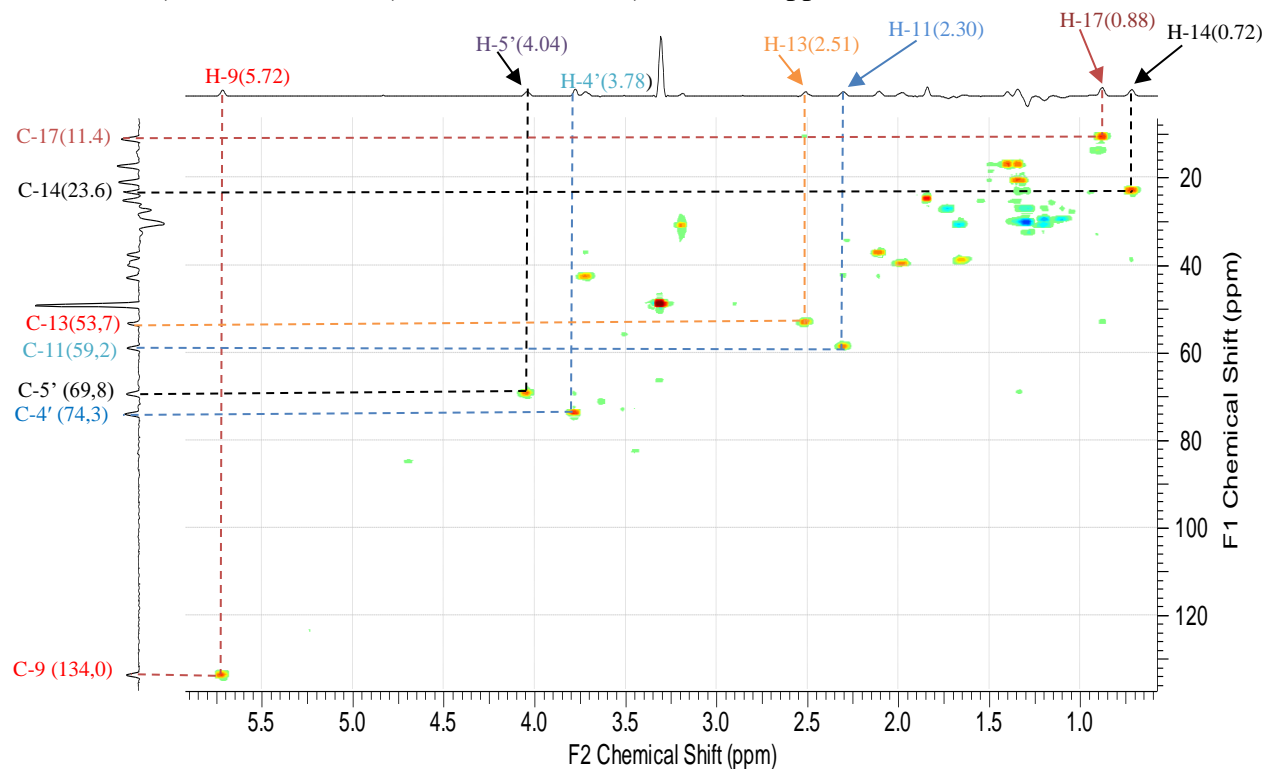


**Figure 33.** HSQC spectrum of compound **SPC-G1**

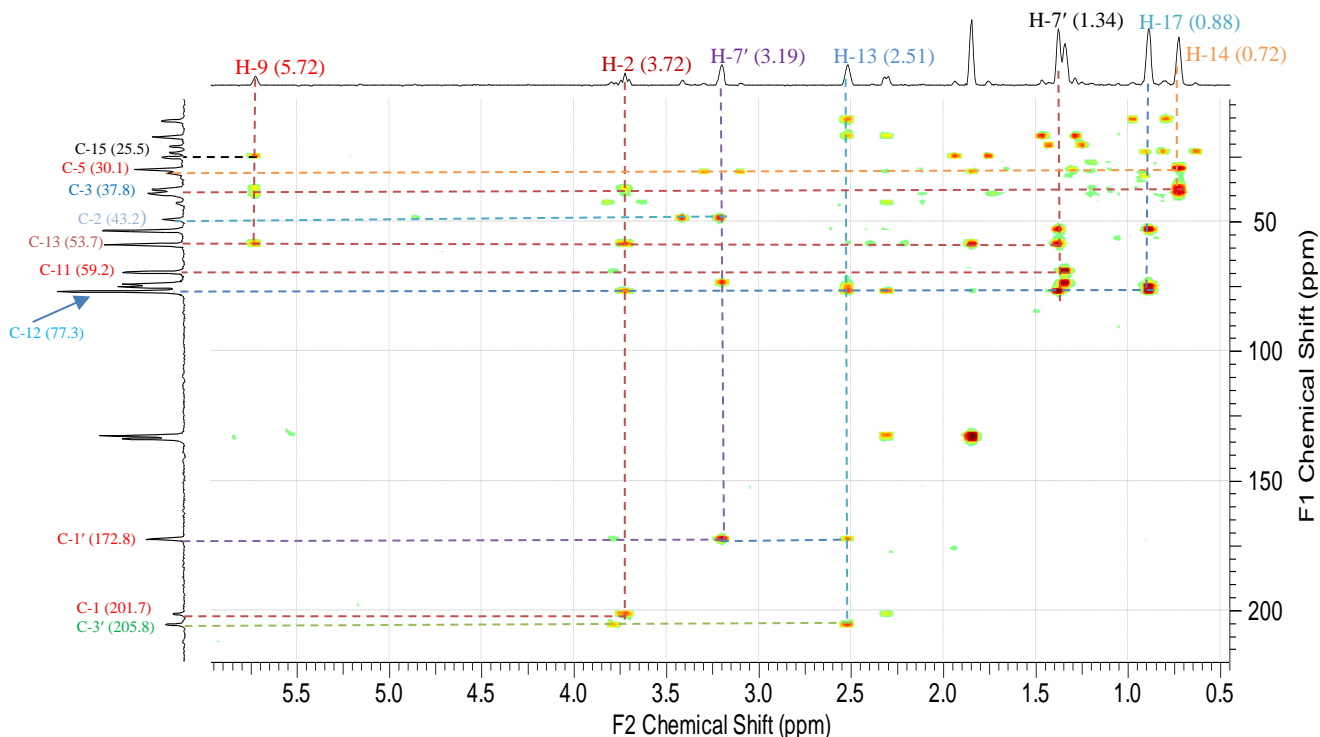


**Figure 34.** HMBC spectrum of compound **SPC-G1**

Furthermore, in the ROESY spectrum (Fig. 36), correlations observed between protons signal (H-2) at  $\delta_{\text{H}}$  3.72 with (H-16) at  $\delta_{\text{H}}$  1.37 gave an indication of their *cis*-orientation, whereas in the  $^1\text{H}$  NMR spectrum, the proton signals of H-2 which concurrently coupled ( $J = 11.7$  Hz) with both the methine proton signals (H-11) at  $\delta_{\text{H}}$  2.30 and (H-3) at  $\delta_{\text{H}}$  2.11 indicated *trans*-orientations of H-2 with respect to both H-3 and H-11. Additionally, in the  $^1\text{H}$  NMR spectrum, the small value of the coupling constant ( $J = 3.6$  Hz) observed between H-3 and H-8 ( $\delta_{\text{H}}$  1.99) also indicated a *cis*-juncture between the A and B rings. These results revealed that, in the tricyclic fused ring (A-B-C), the A ring formed a chair-conformation while the B and C rings formed boat-conformations as demonstrated by [Koyama et al.2005](#). It is noteworthy that the methine proton (H-4') showed a *cis*-orientation with its vicinal homologue (H-5') as evidenced of the small value of their coupling constant ( $J = 4.3$  Hz), whereas in the ROESY spectrum, its correlation with the methyl protons (H-17) at  $\delta_{\text{H}}$  0.88 gave an indication of their *cis*-spatial orientation.

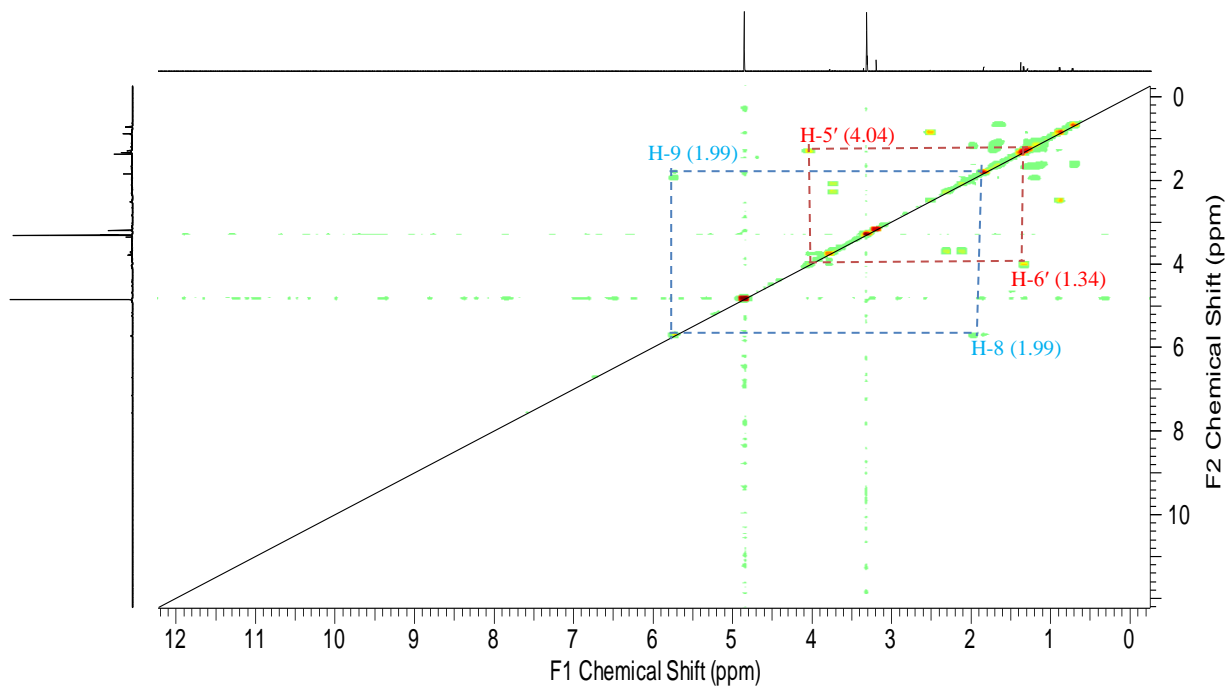


**Figure 35.** COSY spectrum of compound **SPC-G1**

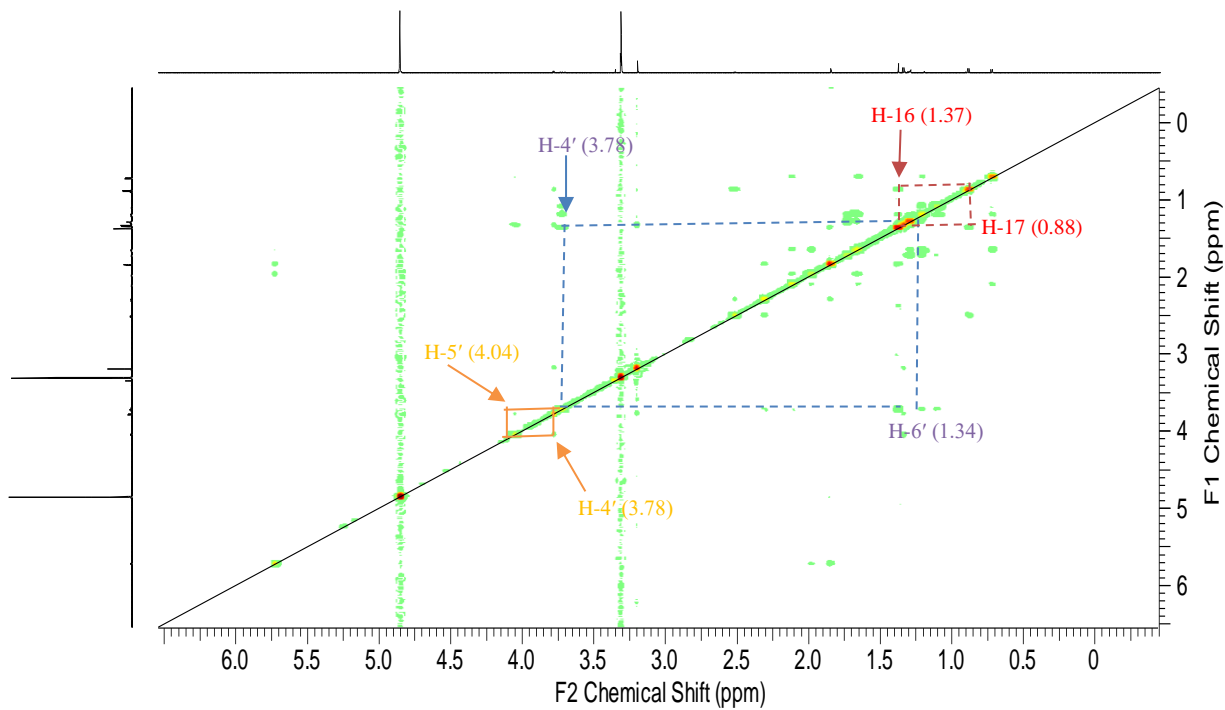
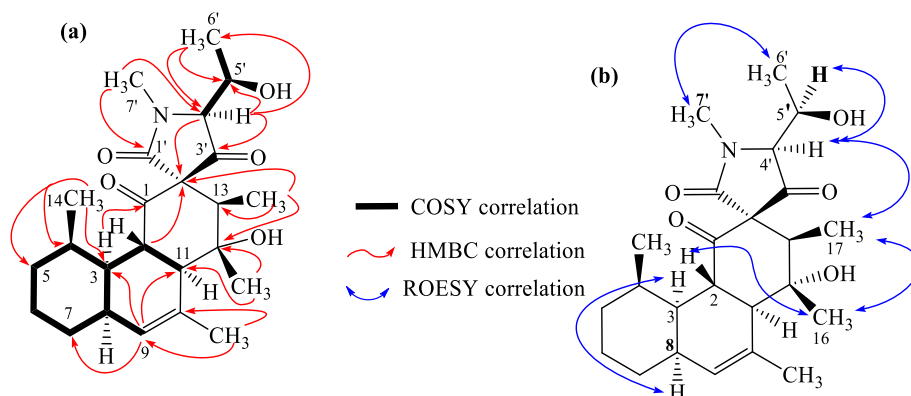


**Figure 36.** ROESY spectrum of compound **SPC-G1**



**Scheme 4.**  $^1\text{H}$ - $^1\text{H}$  COSY and important HMBC correlations (a) and key ROESY correlations (b) for SPC-G1.

The presence of a secondary alcohol at C-5' in compound **SPC-G1** was helpful in the determination of its absolute stereochemistry, by utilizing the modified Mosher's method (Hoye *et al.*, 2007). (*R*)- and (*S*)- $\alpha$ -methoxy- $\alpha$ -trifluoromethylphenylacetyl (MTPA) esters of **SPC-G1** were prepared in pyridine- $d_5$  in situ by the treatment of **SPC-G1** with (*S*)- and (*R*)- $\alpha$ -methoxy- $\alpha$ -trifluoromethylphenylacetyl (MTPA) chloride, respectively. Significant  $\Delta\delta$  values ( $\Delta\delta = \delta_{\text{S-MTPA-ester}} - \delta_{\text{R-MTPA-ester}}$ ) were observed for the protons near the chiral centre C-5' as shown in Fig. 38. Thus, the absolute configuration at C-5' was determined as (*R*). This configuration was used as a starting point and consequently, the other configurations of stereogenic centres in compound **SPC-G1** were determined (Scheme 4) by combination of coupling constants and significant ROESY correlations. Coupling constants of  $J_{\text{H}4',\text{H}5'} = 4.3$  Hz,  $J_{\text{H}4',\text{C}5'} = 2.5$  Hz,  $J_{\text{H}4',\text{C}6'} = 1.9$  Hz indicated a gauche conformation between 4'-H and 5'-H as well as  $\text{CH}_3$ -6' and an anti-periplanar conformation between 4'-H and 5'-OH (Fig. 38). The small coupling constants  $J_{\text{H}5',\text{C}4'} = 2.5$  Hz and  $J_{\text{H}5',\text{C}3'} = 2.2$  Hz indicate an anti-peri-planar conformation of 5'-H and the nitrogen atom, but a gauge conformation between 5'-H and C-3'. Taken together, this information supports a 4'*S*,5'*R* configuration. The coupling constants of  $J_{\text{H}13,\text{C}1'} = 3.3$  Hz and  $J_{\text{H}13,\text{C}3'} = 7.5$  Hz, together with the observed ROESY correlation between 17- $\text{H}_3$  and 4-H, allowed to span the stereochemical information via the spiro centre to the remaining stereocenters. Thus, the structure of compound **SPC-G1** was assigned and was named simplicilone A (**186**)

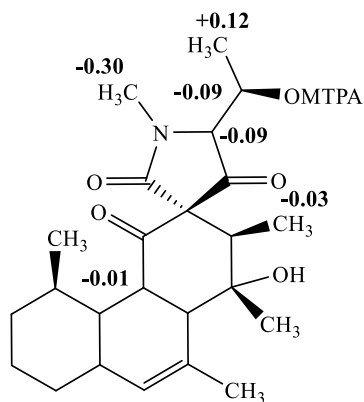


**Figure 37.**  $\Delta\delta^{\text{SR}}$  values (ppm) for the C-5'  $\alpha$ -methoxy- $\alpha$ -trifluoromethylphenylacetyl (MTPA) esters for SPC-G1.

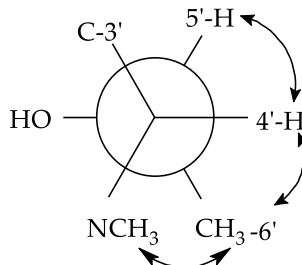
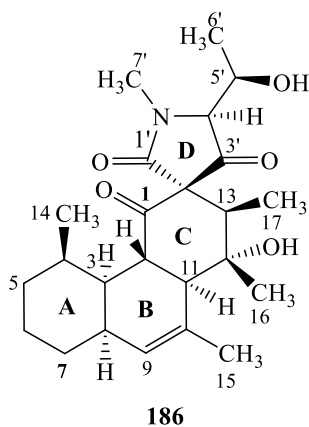


**Figure 38.** J-based analysis of 4'-H/5'-H bond. Arrows indicate observed ROESY correlations.



The complete assignments of  $^{13}\text{C}$  and  $^1\text{H}$  NMR for compound **SPC-G1** are given in Table 3

**Table 3.**  $^1\text{H}$  and  $^{13}\text{C}$  NMR data ( $\text{CDCl}_3$ ) of compound **SPC-G1**.

Position	Compound SPC-G1	
	$\delta_{\text{C}}$	$\delta_{\text{H}}$ (mult., $J$ in Hz)
1	201.7	–
2	43.2	3.72 (pseudo $t$ , 11.7)
3	37.9	2.11 ( $dt$ , 3.6, 11.6)
4	39.5	1.65 ( $m$ )
5	30.9	1.29 ( $m$ )
6	27.8	1.73 ( $m$ ), 1.30 ( $m$ )
7	31.5	1.66 ( $m$ ), 1.21( $m$ )
8	40.3	1.99 ( $m$ )
9	134.0	5.72 ( $d$ , 6.7)
10	132.9	–
11	59.2	2.30 ( $d$ , 11.6)
12	77.3	–
13	53.7	2.51 ( $q$ , 7.0)
14	23.6	0.72 ( $d$ , 7.3)
15	25.5	1.84 ( $s$ )
16	17.7	1.37 ( $s$ )
17	11.4	0.88 ( $d$ , 7.0)
1'	172.8	–
2'	75.5	–
3'	205.8	–
4'	74.3	3.78 ( $d$ , 4.3)
5'	69.8	4.04 ( $dq$ , 4.3, 7.0)
6'	17.6	1.34 ( $d$ , 7.0)
7'	31.7	3.19 ( $s$ )

#### II.4.1.2. Characterization of compound SPC-G2

Compound **SPC-G2** was obtained as a colourless oil. Its molecular formula was determined as,  $\text{C}_{24}\text{H}_{35}\text{NO}_6$  from the protonated molecular ion peak  $[\text{M}+\text{H}]^+$  at  $m/z$  434.2542 (calcd for  $\text{C}_{24}\text{H}_{35}\text{NO}_6$ : 434.2542), obtained by (+)-HR-ESI-MS (Fig 39) and is consistent with eight double bond equivalent.

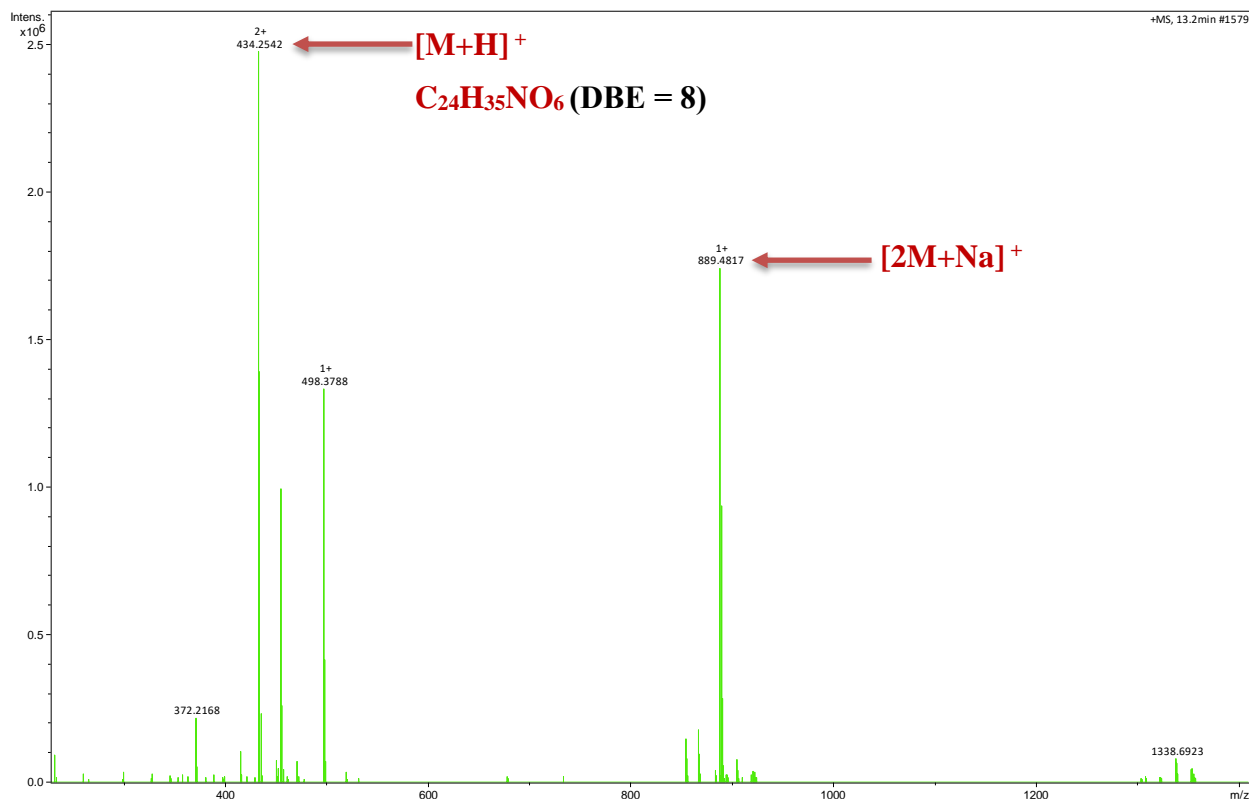


**Figure 39.** (+)-HR-ESI-MS of compound **SPC-G2**

Its  $^1\text{H}$ ,  $^{13}\text{C}$ , NMR spectra (Fig. 41 and 42) exhibited similarities to those of compound **SPC-G1**.

Thus, it was certain that the structure of compound **SPC-G2** could be deduced by careful comparison of its data to those of compound **SPC-G1**. Its molecular ion as shown by HR-ESI-MS differed by 16 amu from that of compound **SPC-G1**, suggesting compound **SPC-G2** to have an additional oxygen atom. This information was further supported by the  $^{13}\text{C}$  NMR spectrum which showed four carbonyl carbon signals (instead of three) at  $\delta_{\text{C}}$  211.5,  $\delta_{\text{C}}$  209.3 (C-1), 191.4 (C-3') and 163.8 (C-1'). Three of them were similar to those observed in the  $^{13}\text{C}$  NMR spectrum of compound **SPC-G1**.

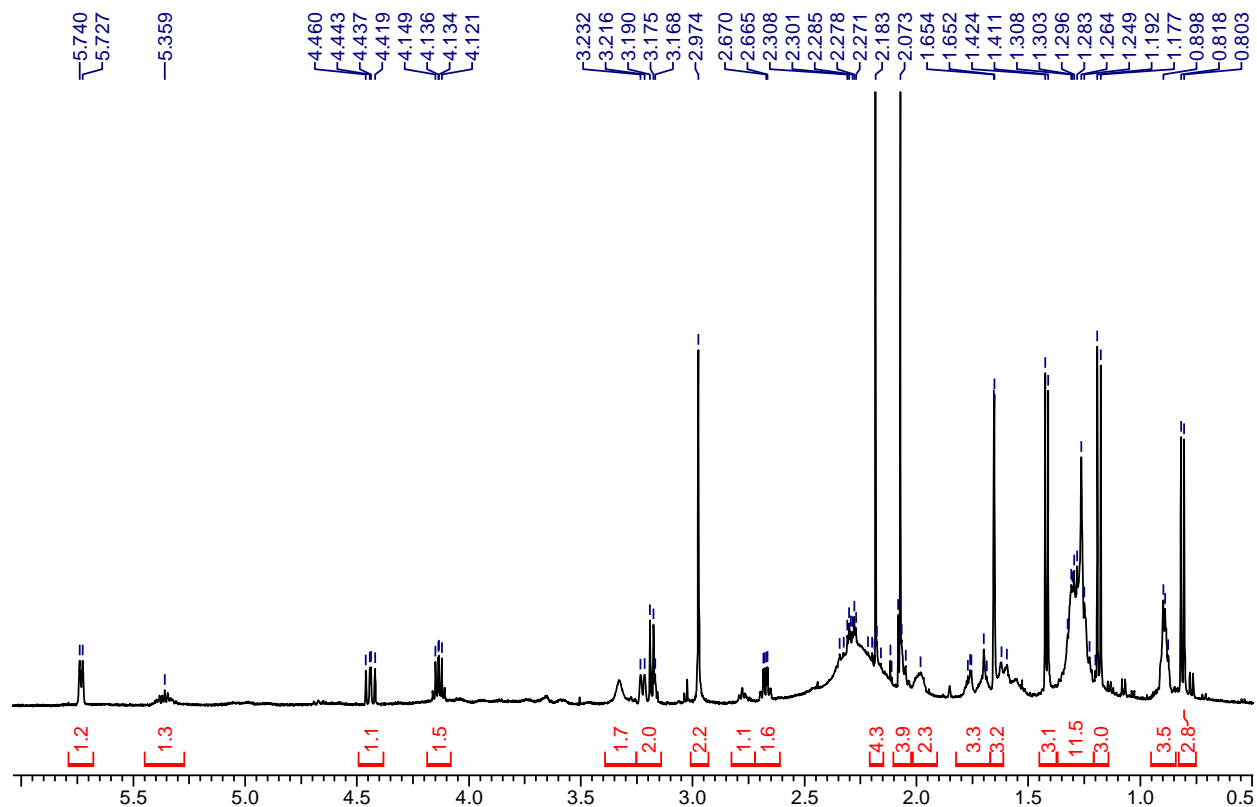


**Figure 40.**  $^1\text{H}$  NMR spectrum ( $\text{CDCl}_3$ , 500 MHz) of compound **SPC-G2**

Although characteristic signals due to the A-B fused ring were observed in both  $^1\text{H}$  and  $^{13}\text{C}$  NMR spectra, in the HMBC the two methyl signals (H-17) at  $\delta_{\text{H}}$  2.07 and (H-16) at  $\delta_{\text{H}}$  1.18 showed strong cross peaks to the additional carbonyl signal (C-13) at  $\delta_{\text{C}}$  211.5, indicating the loss of the spiro centre found in compound **SPC-G1**.

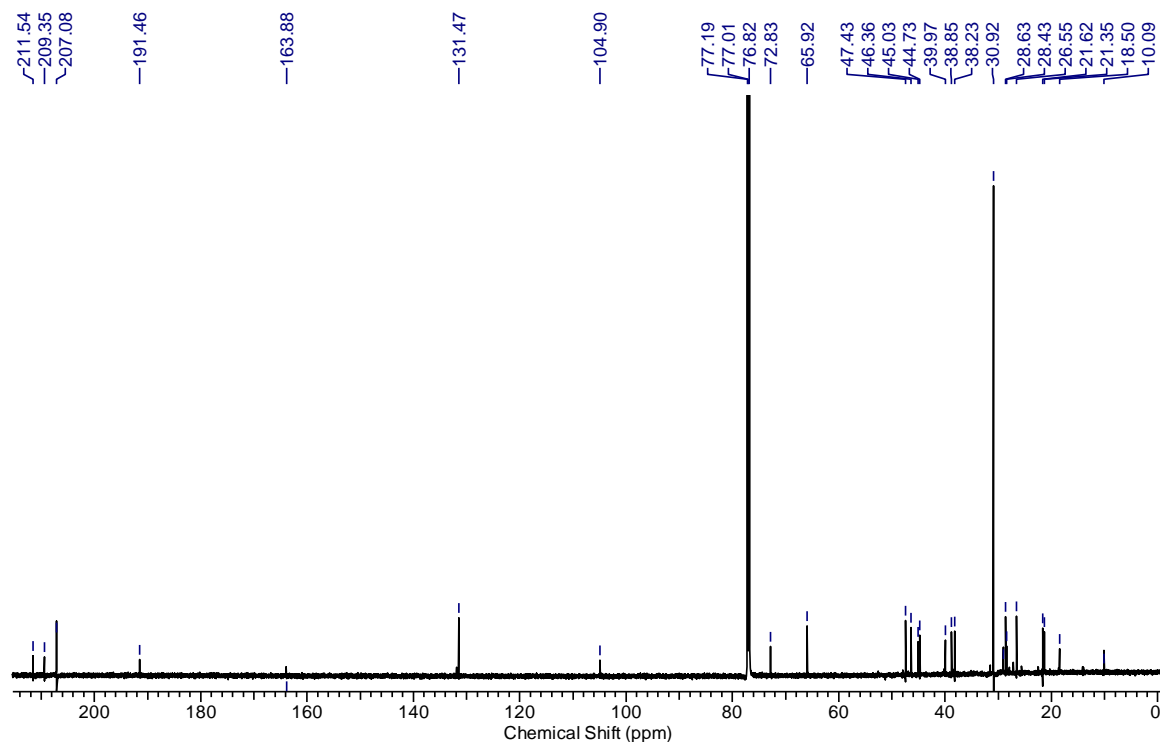
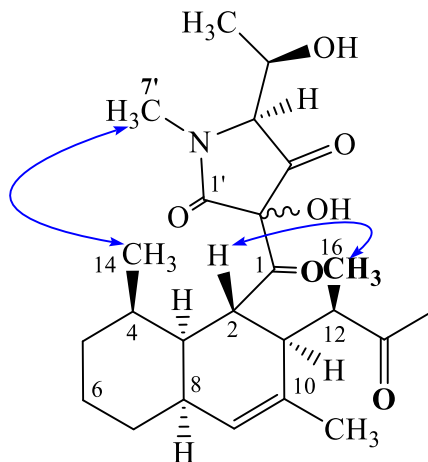


**Figure 41.**  $^{13}\text{C}$  NMR ( $\text{CDCl}_3$ , 125 MHz) spectrum of compound **SPC-G2**.

This was further confirmed in the HMBC spectrum where the methine proton signal of the heterocyclic ring (H-4') at  $\delta_{\text{H}}$  3.18 showed a cross peak with the deshielded  $\text{sp}^3$  oxygenated carbon at  $\delta_{\text{C}}$  104.9, instead of  $\delta_{\text{C}}$  75.5 for the spiro quaternary carbon (C-2') observed in compound **SPC-G1**. In the  $^1\text{H}$  NMR and HMBC spectra (Fig 40 and 44), signals for 2-keto-1-methylpropyl group were deduced from the signal of a three-proton singlet (H-17) at  $\delta_{\text{H}}$  2.07 which showed an HMBC correlation with the carbonyl signal (C-13); at  $\delta_{\text{C}}$  211.5, a methyl proton signal (C-16) at  $\delta_{\text{H}}$  1.18 displayed cross peaks correlations with the carbon signals (C-11) at  $\delta_{\text{C}}$  46.3, (C-12) at  $\delta_{\text{C}}$  47.4 and C-13; a methine proton doublet of quadruplet at  $\delta_{\text{H}}$  2.67 (2.5, 7.0 Hz, H-12) exhibited  $^3J$  HMBC cross peaks with the carbon signals (C-10) at  $\delta_{\text{C}}$  131.9 and (C-17) at  $\delta_{\text{C}}$  28.4 It is noteworthy that the same ROESY correlations (Scheme 5) were observed for both compounds **SPC-G1** and **SPC-G2**.



**Scheme 5.** ROESY correlations of compound SPC-G2

This information was expected, since the two compounds were isolated from the same organism. However, the stereochemistry at C-2' was not determined. Based on the above investigations, the structure of compound **SPC-G2** was determined compound as unknown derivative and the name **Simplicilone B (187)** was attributed.

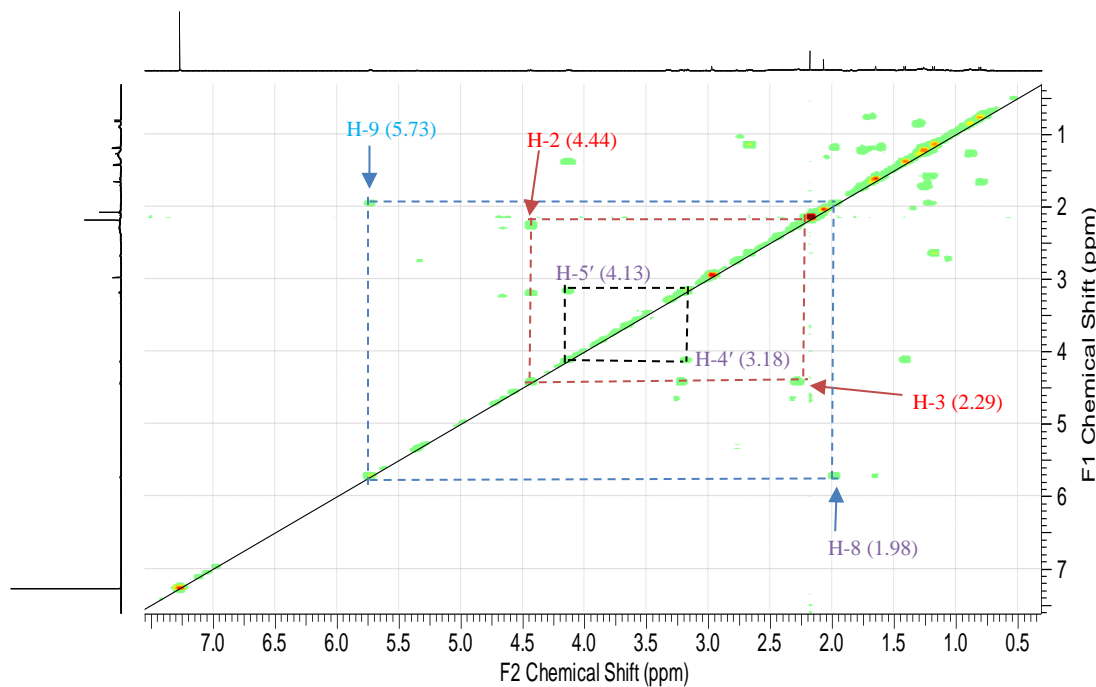


**Figure 42.** COSY spectrum of compound SPC-G2.

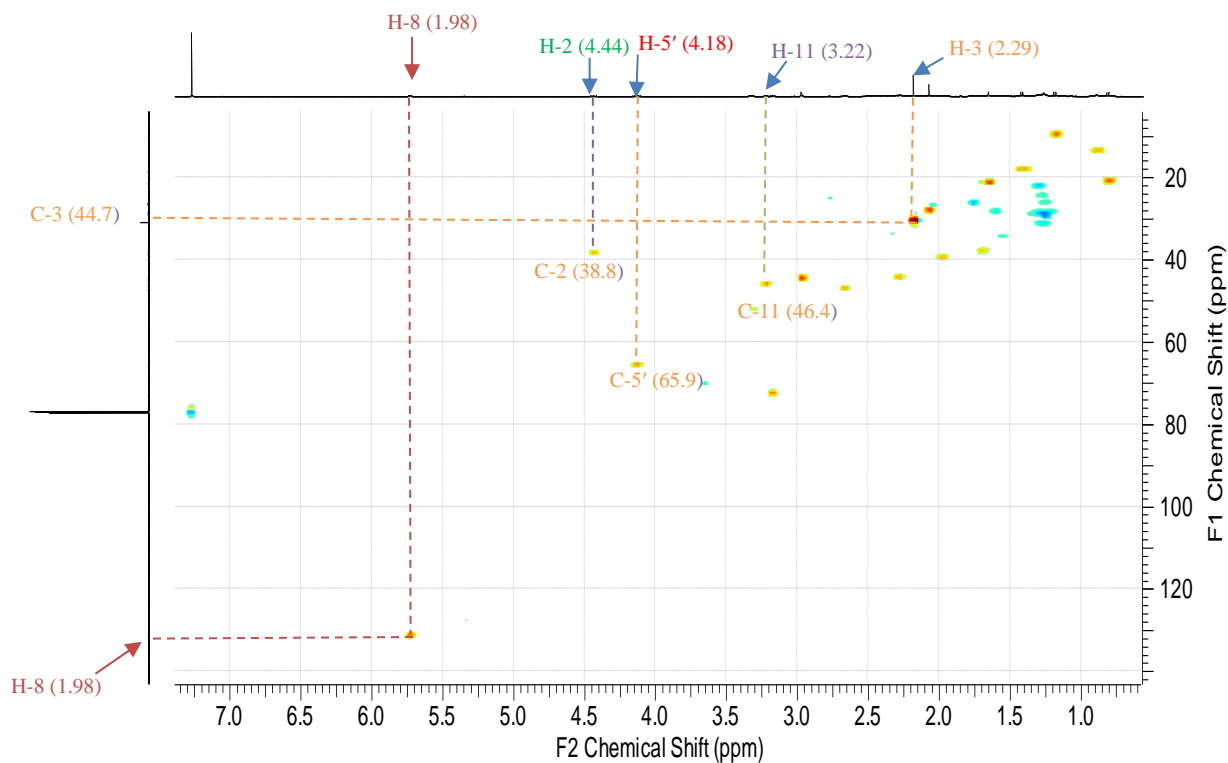


**Figure 43.** HSQC spectrum of compound **SPC-G2**

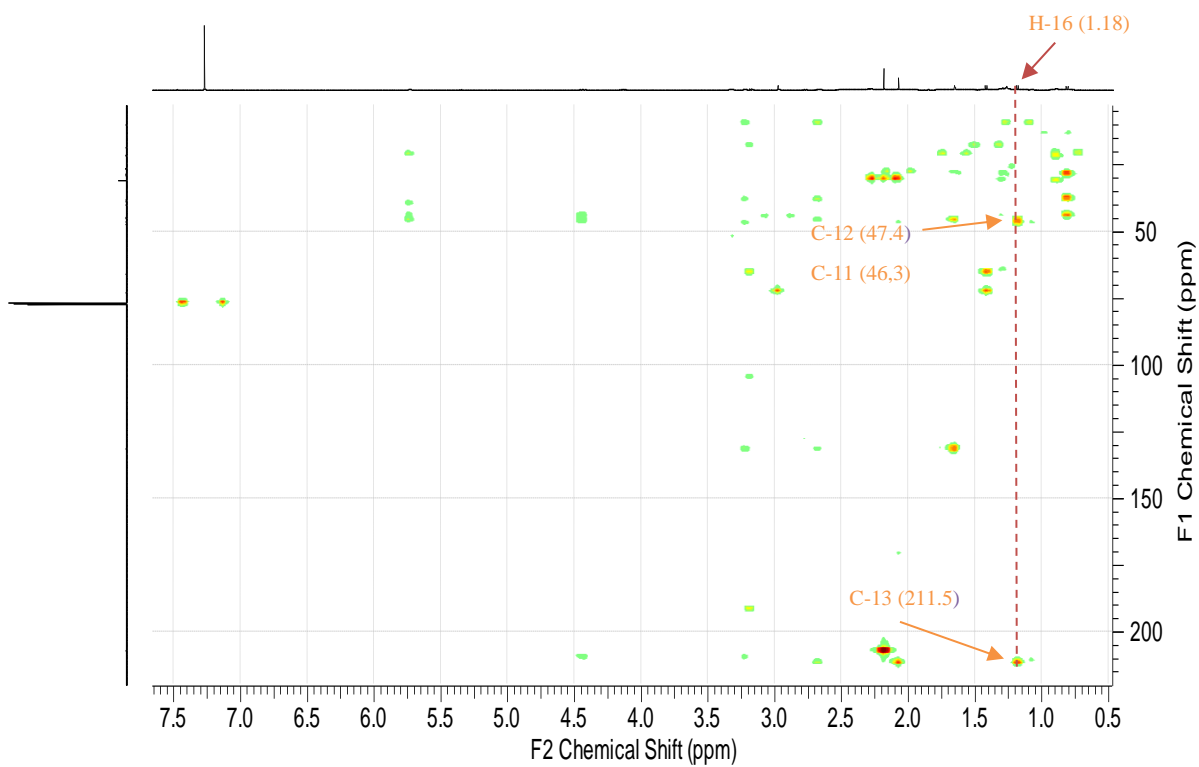


**Figure 44.** HMBC spectrum of compound **SPC-G2**

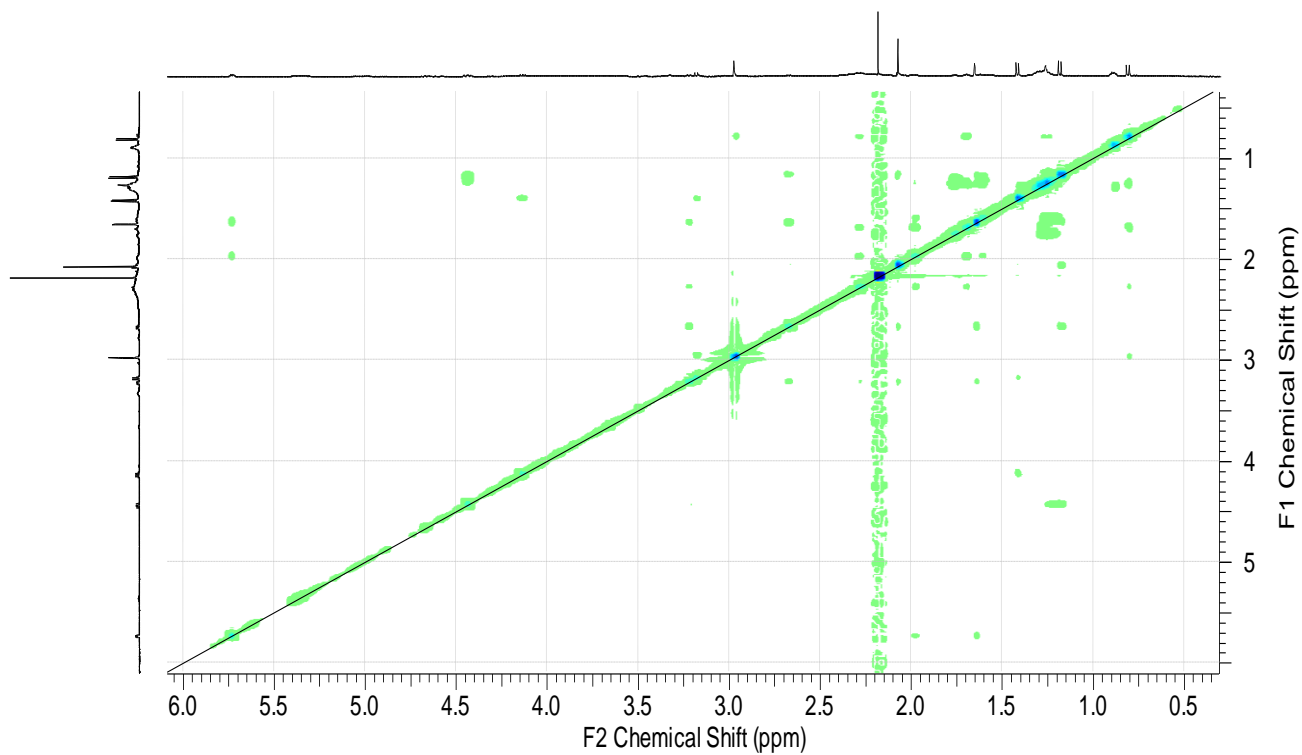
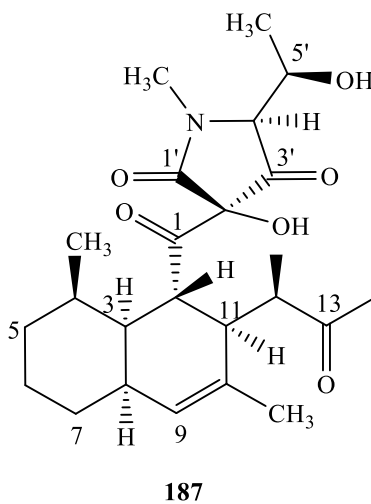


**Figure 45.** ROESY spectrum of compound **SPC-G2**.



The complete assignments of  $^{13}\text{C}$  and  $^1\text{H}$  NMR for compound **SPC-G2** are given in Table 4

**Table 4.**  $^1\text{H}$  and  $^{13}\text{C}$  NMR data ( $\text{CDCl}_3$ ) of compound **SPC-G2**.

Position	Compound SPC-G2	
	$\delta_{\text{C}}$	$\delta_{\text{H}}$ (mult., $J$ in Hz)
1	209.3	–
2	38.8	4.44 (1H, <i>dd</i> , 11.6, 8.8,)
3	44.7	2.29 ( <i>m</i> )
4	38.2	1.70 ( <i>m</i> )
5	29.0	1.25 ( <i>m</i> ), 1.20 ( <i>m</i> )
6	28.6	1.76 ( <i>m</i> ), 1.26 ( <i>m</i> )
7	31.4	1.28 ( <i>m</i> )
8	39.9	1.98 ( <i>m</i> )
9	131.5	5.73 ( <i>br d</i> , 6.7)
10	131.9	–
11	46.4	3.22 ( <i>dd</i> , 2.5, 11.6)
12	47.4	2.67 ( <i>dq</i> , 2.5, 7.0)
13	211.5	–
14	21.4	0.81 ( <i>d</i> , 7.6)
15	21.6	1.65 ( <i>s</i> )
16	10.1	1.18 ( <i>d</i> , 7.3)
17	28.4	2.07 ( <i>s</i> )
1'	163.8	–
2'	104.9	–
3'	191.4	–
4'	72.8	3.18 ( <i>d</i> , 7.6)
5'	65.9	4.13 ( <i>dq</i> , 6.4, 7.6)
6'	18.5	1.41 ( <i>d</i> , 6.4)
7'	45.0	2.97 ( <i>s</i> )

#### II.4.1.3. Identification of compound SPC-G3

Compound SPC-3 was isolated as white oil at the retention time at the retention time of 13.3 min. Its molecular formula was determined as  $\text{C}_{18}\text{H}_{32}\text{O}_2$  from the protonated molecular ion peak  $[\text{M}-\text{H}]^-$  at  $m/z$  279.12, obtained by (-)-ESI-MS and was consistent with three double bond equivalents. (Fig.46).

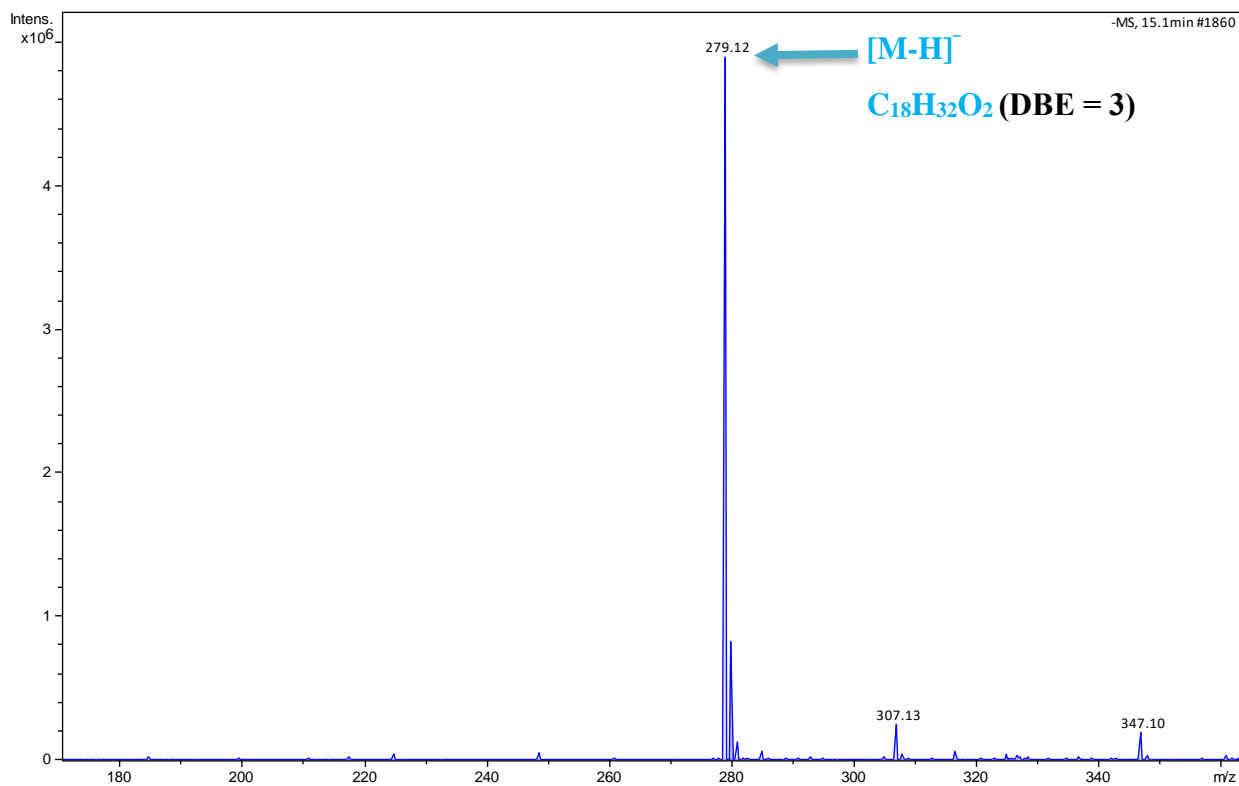


**Figure 46.** Negative ion mode (-)ESI-MS of compound **SPC-G3**.

Its <sup>1</sup>H NMR spectrum (Fig. 47) shows resonance peaks for the terminal methyl groups, allylic methylene and bis-allylic methylene at 0.88– 0.91, 2.04–2.08, and 2.36–2.80 ppm, respectively, and two olefinic protons at 5.37 ppm each.

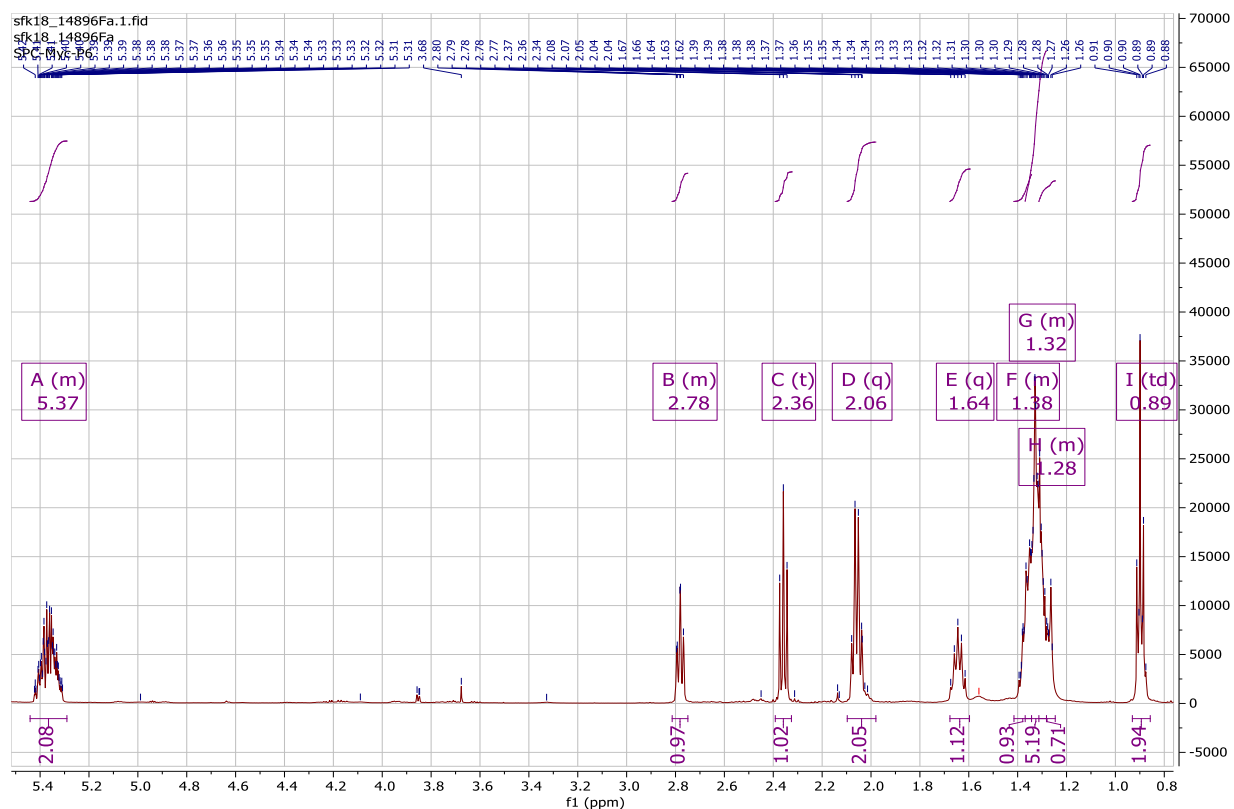
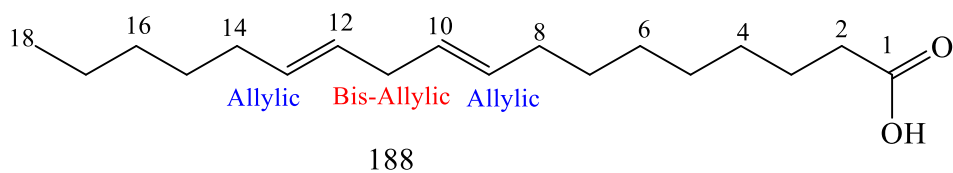


**Figure 47.**  $^1\text{H}$  NMR ( $\text{CDCl}_3$ , 500 MHz,) spectrum of compound **SPC-G3**.

The  $^{13}\text{C}$  NMR, HSQC and HMBC data displayed four olefinic carbons at  $\delta_{\text{C}}$  130.2, 130.0, 128.6 and 127.8 ppm, suggesting the presence of two double bonds in compound SPC-G3. In addition, the same data show the resonance peaks for carbonyl at  $\delta_{\text{C}}$  179.0 ppm, for twelve methylene carbons at  $\delta_{\text{C}}$  22.4 – 33.8 ppm and one terminal methylene carbon at  $\delta_{\text{C}}$  14.0 ppm. These data were characteristic of an unsaturated fatty acid in its free form. The correlations show in scheme 6 let to identify SPC-G3 as a C-18 fatty acid with two double bonds between C-9 and C-10 and between C-12 and C-13. Thus, compound **SPC-G3** was identified as linoleic acid (**188**) already reported from methanol extracts of ginseng (Kim *et al.*, 2021)



**Scheme 6.** Structure of compound SPC-G3.

The complete assignments of  $^{13}\text{C}$  and  $^1\text{H}$  NMR for compound SPC-G3 are given in Table 5.

**Table 5.**  $^1\text{H}$  and  $^{13}\text{C}$  NMR data ( $\text{CDCl}_3$ ) of compound **SPC-G3**.

Position	Compound SPC-G3	
	$\delta_{\text{C}}$	$\delta_{\text{H}}$ (mult., $J$ in Hz)
1	179.0	–
2	33.8	2.35 (2H, <i>t</i> , 7.5)
3	24.6	1.64 (1H, <i>q</i> , 6.5, 7.0)
4	29.0	1.36 (2H, <i>m</i> )
5	29.0	2.06 (2H, <i>q</i> , 6.5, 7.0)
6	29.0	2.06 (2H, <i>q</i> , 6.5, 7.0)
7	29.5	2.06 (2H, <i>q</i> , 6.5, 7.0)
8	27.1	2.06 (2H, <i>q</i> , 6.5, 7.0)
9	130.2	5.37 (1H, <i>m</i> )
10	127.8	5.37 (1H, <i>m</i> )
11	31.5	2.78 (2H, <i>m</i> )
12	130.0	5.37 (1H, <i>m</i> )
13	128.6	5.37 (1H, <i>m</i> )
14	33.8	2.06 (2H, <i>d</i> , 7.6)
<b>15</b>	22.4	1.32 (2H, <i>m</i> )
<b>16</b>	31.5	1.32 (2H, <i>m</i> )
<b>17</b>	24.4	1.28 (2H, <i>m</i> )
<b>18</b>	14.0	0.89 (3H, <i>dt</i> , 6.9, 4.7)

#### II. 4.1.4. Identification of compound SPC-G4

Compound **SPC-G4** was obtained as a colourless solid at the retention time 6.3 min. Its molecular formula was determined as  $\text{C}_{28}\text{H}_{44}\text{O}$  from the protonated molecular ion peak  $[\text{M}+\text{H}]^+$  at  $m/z$  397.2320 (calcd for  $\text{C}_{28}\text{H}_{45}\text{O}$ : 397.2325), obtained by (+)-HR-ESI-MS and was consistent with six double bond equivalents. It reacted positively to Liebermann-Burchard test; which therefore indicates its sterol property.

Its  $^1\text{H}$  NMR spectrum (Fig. 48) corroborated with sterol  $\Delta^{5,7}$  structures by signals at  $\delta_{\text{H}}$  5.54 (1H, *dd*, 6.7; 6.7) and 5.36 (1H, *m*) diagnostic for olefin hydrogens H-6 and H-7, besides multiplet at  $\delta_{\text{H}}$  3.55 (H-3) indicate the presence of oxymethine proton. double bonds were deduced from the signal at  $\delta_{\text{H}}$  5.19 (*m*) relative to H-22 and H-23. Moreover, the proton signals between  $\delta_{\text{H}}$  0.8 and 1.1 relative to methyl groups were identified as two singular protons at  $\delta_{\text{H}}$  0.92 ( $\text{CH}_3$ -C-18) and 0.64 ( $\text{CH}_3$ -C-19), and four doublets' protons at  $\delta_{\text{H}}$  0.83 ( $\text{CH}_3$ -27), 0.83 ( $\text{CH}_3$ -26); 0.92 ( $\text{CH}_3$ -28) and 1.04 ( $\text{CH}_3$ -21). The  $^{13}\text{C}$  NMR spectrum (Fig. 49) of compound **SPC-G4** reveals  $\text{C}_{28}$ -sterol

ergostane skeleton, including signals of six unsaturated carbons at  $\delta_c$  116.2–141.0 corresponding to C-5 ( $\delta_c$  139.9); C-6 ( $\delta_c$  119.4), C-7 ( $\delta_c$  116.2), C-8 ( $\delta_c$  141.0), C-22 ( $\delta_c$  135.5) and C-23 ( $\delta_c$  131.8). Methyl carbon signals were also observed and were assigned to C-18 ( $\delta_c$  11.6), C-19 ( $\delta_c$  15.8), C-21 ( $\delta_c$  20.9) C-26 ( $\delta_c$  19.2), C-27 ( $\delta_c$  19.6) and C-28 ( $\delta_c$  17.2), whereas hydroxyl group was observed at  $\delta_c$  70.5 (C-3). The  $^1\text{H}$  and  $^{13}\text{C}$ -NMR data of compound **SPC-G4** were in agreement with previously published data for Ergosterol (**189**) (Kang *et al.*, 2003).

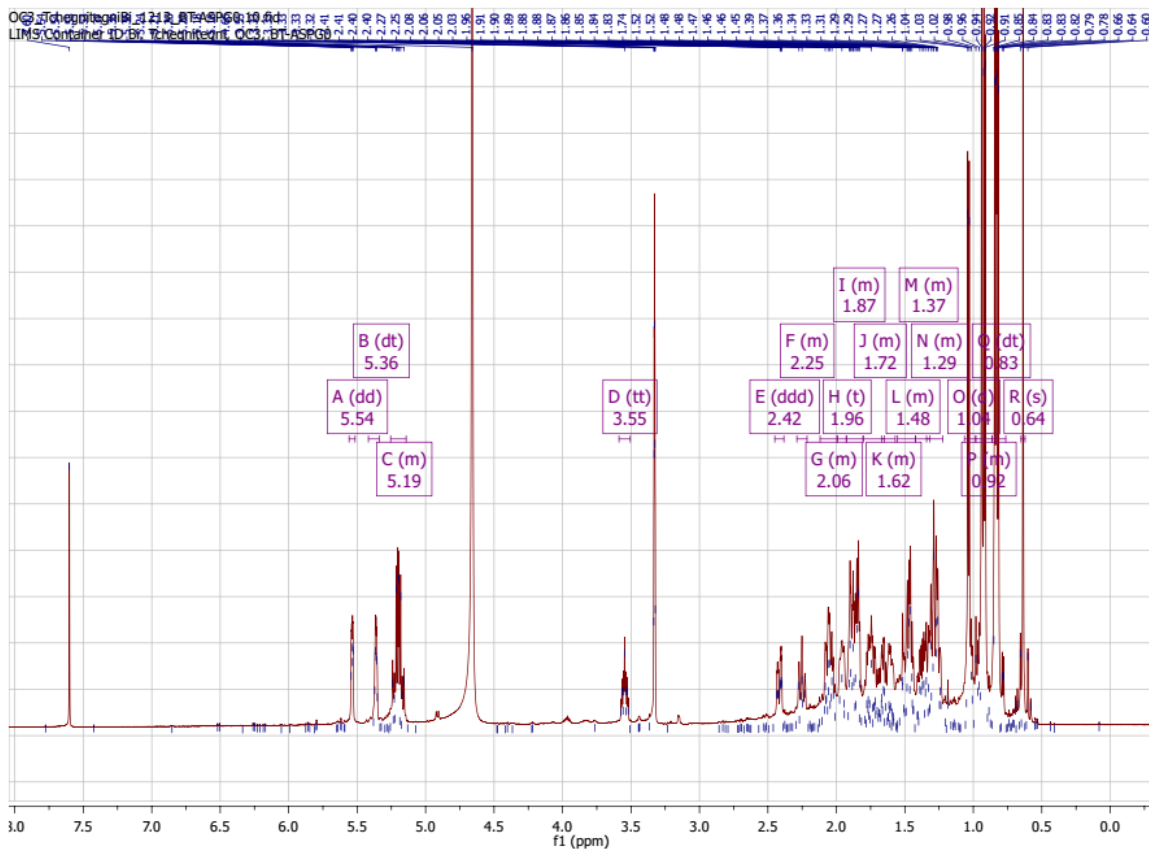


**Figure 48.**  $^1\text{H}$  NMR ( $\text{CDCl}_3$ , 500 MHz) spectrum of compound **SPC-G4**.

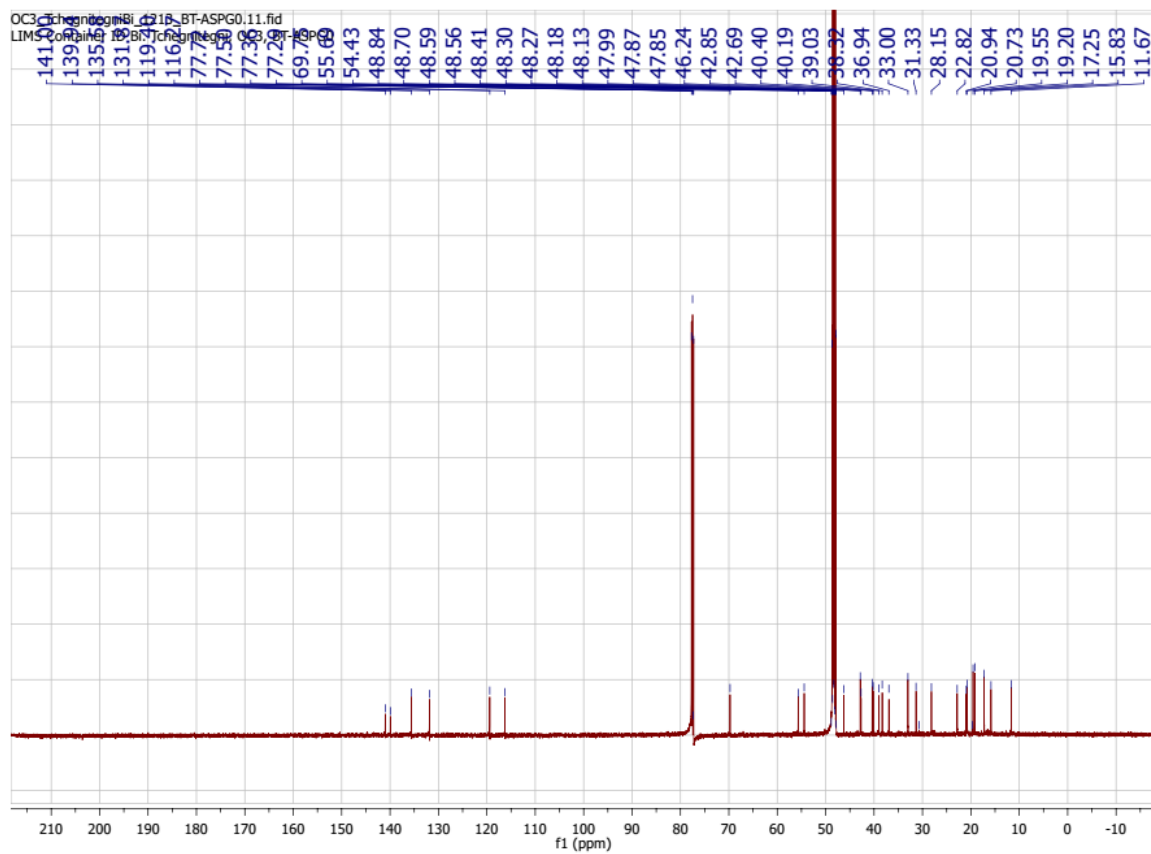


**Figure 49.**  $^{13}\text{C}$  NMR ( $\text{CDCl}_3$ , 125 MHz) spectrum of compound **SPC-G4**.

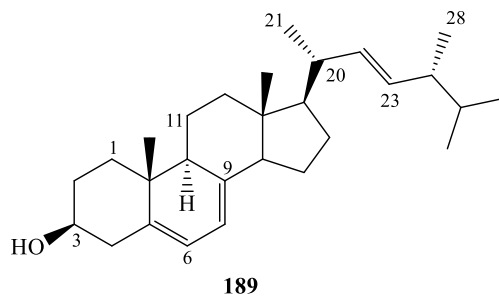


**Table 6.**  $^1\text{H}$  NMR and  $^{13}\text{C}$  NMR data ( $\text{CDCl}_3$ ) of characteristic signals for compound **SPC-G4** vs. ergosterol.

Position	ergosterol		Compound SPC-G4	
	$\delta_{\text{C}}$	$\delta_{\text{H}}$ (mult., J in Hz)	$\delta_{\text{C}}$	$\delta_{\text{H}}$ (mult., J in Hz)
3	70.5	3.63 (1H, <i>m</i> )	69.7	3.55 (1H, <i>m</i> )
6	119.6	5.60 (1H, <i>dd</i> , 6.6, 6.6)	119.4	5.54 (1H, <i>dd</i> , 6.7, 6.7)
7	116.3	5.40 (1H, <i>m</i> )	116.2	5.36 (1H, <i>m</i> )
18	12.1	0.62 (3H, <i>s</i> )	11.6	0.92 (3H, <i>s</i> )
19	16.3	0.96 (3H, <i>s</i> )	15.8	0.64 (3H, <i>s</i> )
21	21.3	1.04 (3H, <i>d</i> , 6.6)	20.9	1.04 (3H, <i>d</i> , 6.6)
22	135.5	5.18 (1H, <i>dd</i> , 15.6, 7.2)	135.5	5.19 (1H, <i>dd</i> , 15.6, 7.1)
23	132.3	5.22 (1H, <i>dd</i> , 15.7, 7.2)	131.8	5.19 (1H, <i>dd</i> , 15.6, 7.1)
26	19.7	0.85 (3H, <i>d</i> , 6.6)	19.2	0.83 (3H, <i>d</i> , 6.7)
27	20.0	0.85 (3H, <i>d</i> , 6.6)	19.6	0.83 (3H, <i>d</i> , 6.7)
28	17.6	0.92 (3H, <i>d</i> , 6.6)	17.2	0.92 (3H, <i>d</i> , 6.6)

#### II.4.2. Secondary metabolites from *Diaporthe* sp. 2.nov

At least fifteen compounds were isolated from the solid culture of *Diaporthe* sp R38 among which five (03) alternariol derivatives including one unknown compound, one new benzofuranone, seven (07) cytochalasins and five (04) others classes of compounds.

##### II.4.2.1. Alternariol derivatives

###### II.4.2.1.1. Structure identification of DRT-G1

Compound **DRT-G1** was isolated as a white amorphous powder at the retention time of 6.88 min. Its UV spectrum revealed three maxima absorption bands at  $\lambda_{\text{max}}$  222, 257 and 340 nm. While its molecular formula was established as  $\text{C}_{14}\text{H}_{10}\text{O}_5$  from the positive mode HRESI-MS which showed the protonated molecular ion peak  $[\text{M}+\text{H}]^+$  at  $m/z$  259.0598 (calcd for  $\text{C}_{14}\text{H}_{11}\text{O}_5$ : 259.0599) and consistent with ten double bond equivalents (Fig. 50).

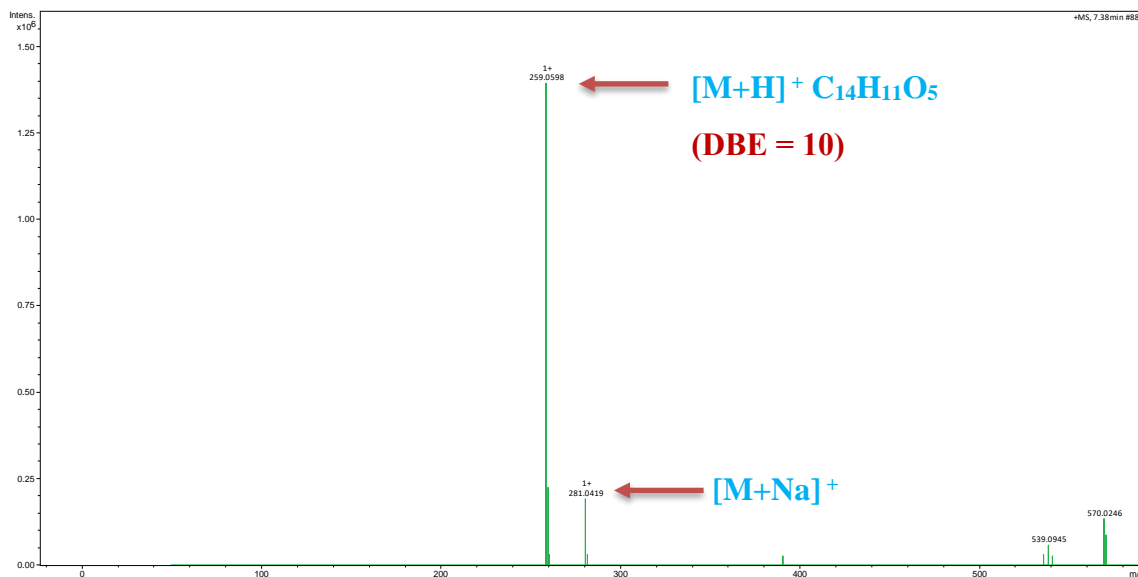


**Figure 50.** (+)-HR-ESI-MS of compound **DRT-G1**.

The  $^1\text{H}$  NMR spectrum (Fig. 51) revealed six peaks viz., one hydroxyl chelated proton at  $\delta_{\text{H}}$  11.77 ppm, one indicative of a methyl group proton at  $\delta_{\text{H}}$  2.70 ppm attached to an aromatic carbon and two pairs of meta-coupled aromatic protons.

DRT-G1.002.esp

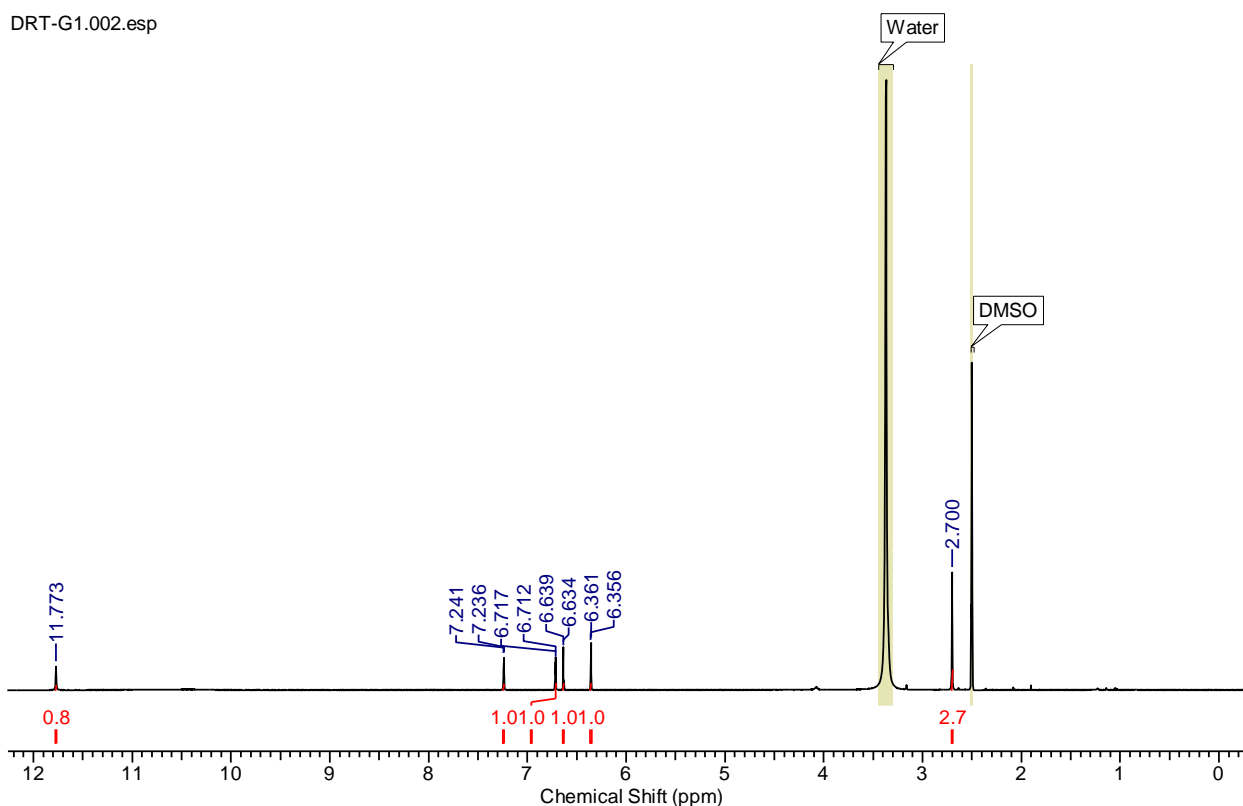
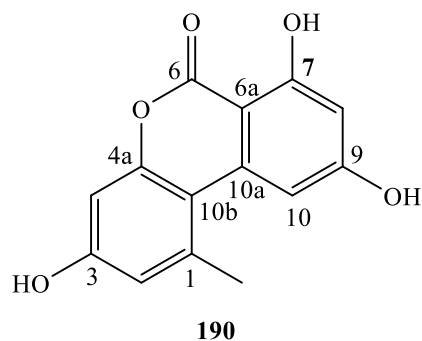


**Figure 51.**  $^1\text{H}$  NMR spectrum (DMSO- $d_6$ , 500 MHz) of compound **DRT-G1**.

The first pair showed resonances at  $\delta_{\text{H}}$  7.23 and 6.36 (1H each, *d*, 2.0 Hz), and the second pair was detected at  $\delta_{\text{H}}$  6.64 and 6.71 (1H each, *d*, 2.6). The molecular formula of compound **DRT-G1** and its NMR data correspond to those of alternariol (**190**), previously isolated from *Alternaria tenuis* (Raistrick *et al.*, 1953) and other *Alternaria* species).



The complete assignments of  $^{13}\text{C}$  and  $^1\text{H}$  NMR for compound **DRT-G1** are given in Table 7.

**Table 7.**  $^1\text{H}$  and  $^{13}\text{C}$  NMR data (DMSO- $d_6$ ) of compound **DRT-G1**.

Compound <b>DRT-G1</b>		
Position	$\delta_{\text{H}}$ (nH, <i>mult.</i> , <i>J</i> in Hz)	$\delta_{\text{C}}$
1	–	138.3
2	6.71 (1H, <i>d</i> , 2.5)	109.3
3	–	158.4
4	6.64 (1H, <i>d</i> , 2.5)	101.6
4a	-	152.6
6	-	165.7
6a	-	97.1
7	-	164.7
8	6.36 (1H, <i>d</i> , 2.5)	100.9
9	-	164.1
10	7.23 (1H, <i>d</i> , 2.5)	104.4
10a	-	138.1
10b	-	109.0
1-CH <sub>3</sub>	2.70 (3H, <i>s</i> )	24.9
7-OH	11.77 (1H, <i>s</i> )	-

#### II.4. 2.1.2. Structure identification of **DRT-G2**

Compound **DRT-G2** was obtained as a white amorphous powder at the retention time of 6.3 min. Its UV spectrum revealed three maxima absorption bands at  $\lambda_{\text{max}}$  218, 256 and 344 nm,

suggesting this compound to share the same core structure with compound **DRT-G1**. Its molecular formula was deduced from the (+) -HRESI-MS which showed the pseudo molecular ion peak  $[M+H]^+$  at  $m/z$  275.0547,  $[M+Na]^+$  at  $m/z$  295.0213 and  $[2M+Na]^+$  at  $m/z$  602.0144 attributed to the molecular formula  $C_{14}H_{10}O_5$  whose double bond equivalents corresponded to ten (Fig. 52).

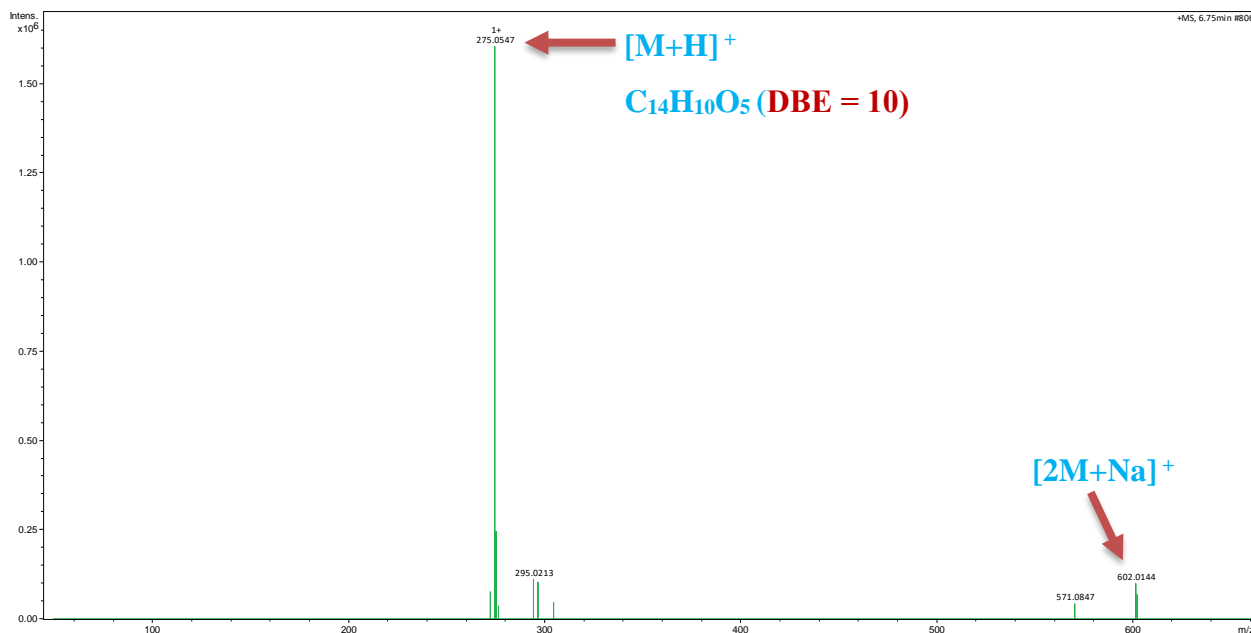
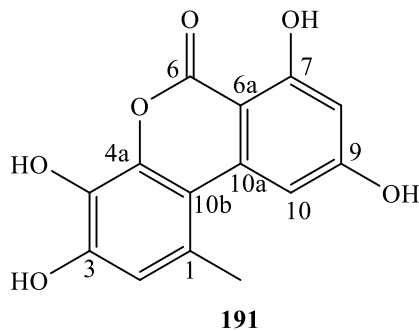


**Figure 52.** (+)-HR-ESI-MS of compound **DRT-G2**

The  $^1H$  NMR spectrum of compound **DRT-G2** (Fig. 53) revealed signals for a methyl proton singlet at  $\delta_H$  2.58 (*s*), three aromatic protons including a pair of meta-coupled protons at  $\delta_H$  7.27 and 6.35 (1H each, *d*, 1.5) and a singlet at  $\delta_H$  6.69 (1H, *s*) in addition to the signal of a phenolic hydroxyl group at  $\delta_H$  11.88 (1H, *s*).

The NMR data were similar to those of alternariol and compound **DRT-G2** was therefore identified as 4-Hydroxyalternariol (**191**) previously isolated from the lichen mycobiont of *Graphis scripa* var (Tanahashi *et al.*, 1997, 2003). However, to the best of our knowledge, this compound is reported here for the first time from the genus *Diaporthe*.



DRT-G2.001.esp

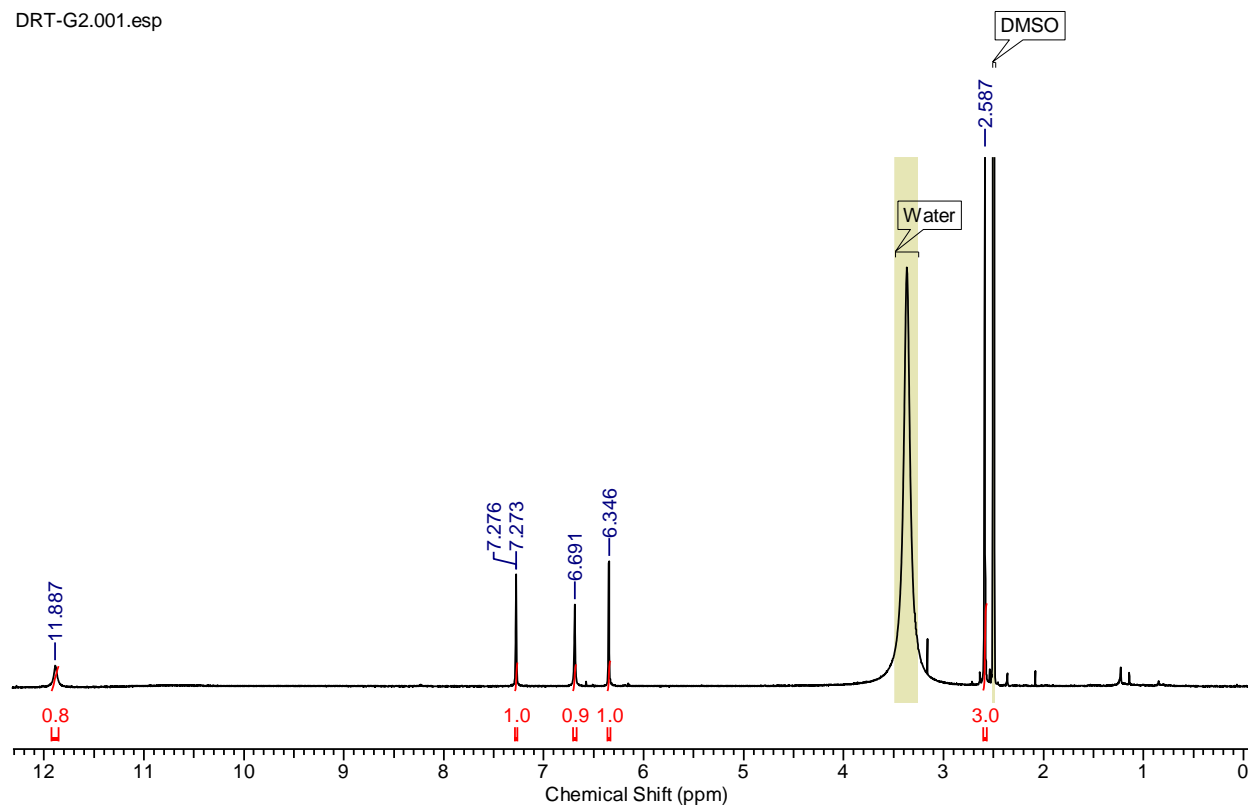


**Figure 53.**  $^1\text{H}$  NMR spectrum ( $\text{DMSO-}d_6$ , 500 MHz) of compound **DRT-G2**

The complete assignments of  $^{13}\text{C}$  and  $^1\text{H}$  NMR for compound **DRT-G2** are presented in [Table 8](#).

**Table 8.**  $^1\text{H}$  and  $^{13}\text{C}$  NMR data (DMSO- $d_6$ ) of compound **DRT-G2**.

Compound DRT-G2		
Position	$\delta_{\text{H}}$ (nH, <i>mult.</i> , <i>J</i> in Hz)	* $\delta_{\text{C}}$
1	–	122.9
2	6.69 (1H, <i>s</i> )	101.6
3	–	148.3
4	–	142.9
4a	–	146.8
6	–	167.6
6a	–	99.3
7	–	164.3
8	7.27 (1H, <i>d</i> , 1.5)	103.9
9	–	164.5
10	6.34 (1H, <i>d</i> , 1.5)	100.3
10a	–	140.5
10b	–	110.9
1-CH <sub>3</sub>	2.58 (3H, <i>s</i> )	15.5
7-OH	11.88 (1H, <i>s</i> )	–

\*The estimated chemical shifts for  $^{13}\text{C}$  were read in the HSQC-DEPT and HMBC spectrum as the  $^{13}\text{C}$  NMR spectrum of the compound was not recorded; *mult.* = multiplicity.

#### II.4.2.1.3. Structure elucidation of compound **DRT-G3**

(+)-HR-ESI-MS analysis of compound **DRT-G3** isolated as a white amorphous powder (RT = 46 min) afforded pseudo-molecular ion peaks  $[\text{M}+\text{H}]^+$  at  $m/z$  343.0810 (calcd for  $\text{C}_{18}\text{H}_{15}\text{O}_7$  343.0812) attributed to the molecular formula  $\text{C}_{18}\text{H}_{15}\text{O}_7$  (12 double bond equivalents). Its UV spectrum showed absorption bands at  $\lambda_{\text{max}}$  222, 257 and 330 nm indicated that **DRT-G3** might have the same nucleus as that of alternariol (**190**).

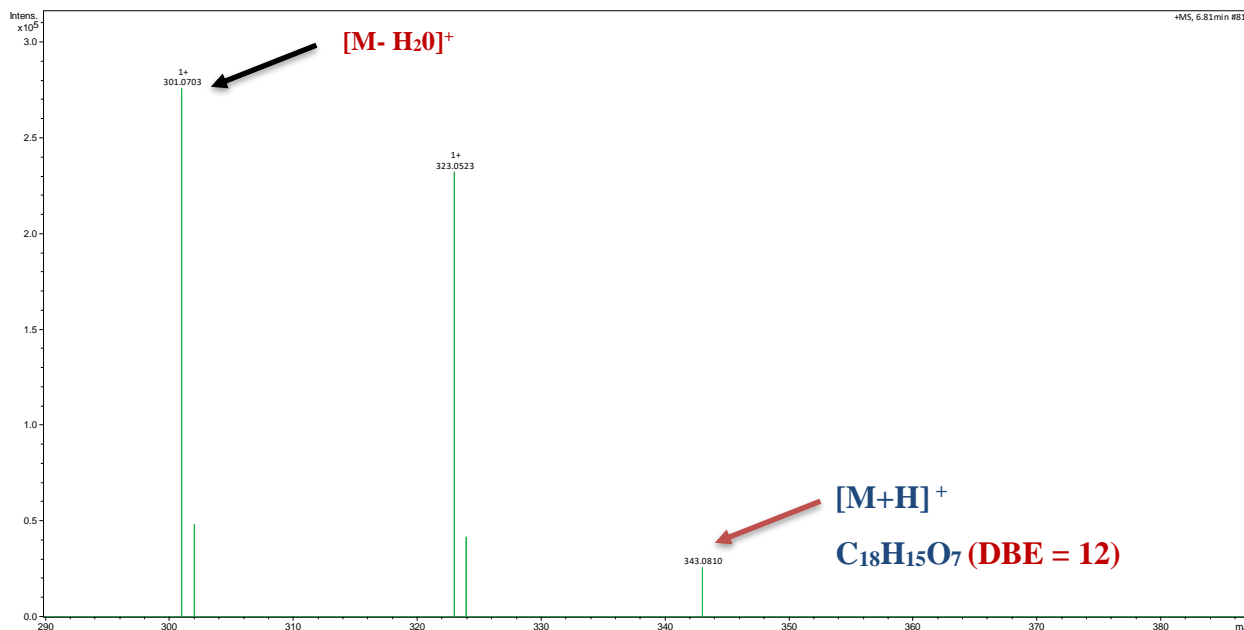


**Figure 54.** (+)-HR-ESI-MS of compound **DRT-G3**.

The  $^1\text{H}$  NMR spectrum (Fig. 56) showed signals of four aromatics protons at  $\delta_{\text{H}}$  7.57 (1H, brs), 6.68 (1H, *d*, 2.0), 6.62 (1H, brs) and 6.55 (1H, *d*, 2.0) assignable to two pairs of meta-coupled protons on two separate benzene rings. The  $^1\text{H}$  NMR spectrum also showed two alkyl protons at  $\delta_{\text{H}}$  2.71 (1H, *s*) and 2.29 (1H, *s*) assignable to one aromatic methyl and a pair of methyl signals of acetyl groups respectively. These  $^1\text{H}$  NMR data were close to that of compound **190** except for the methyl signal of an acetyl group at  $\delta_{\text{H}}$  2.29 ppm. This was further confirmed by the  $^{13}\text{C}$  NMR spectrum (Fig 57) with the resonances at  $\delta_{\text{C}}$  109.6, 117.0, 108.6, 101.1, 25.1 and 21.0 ppm.

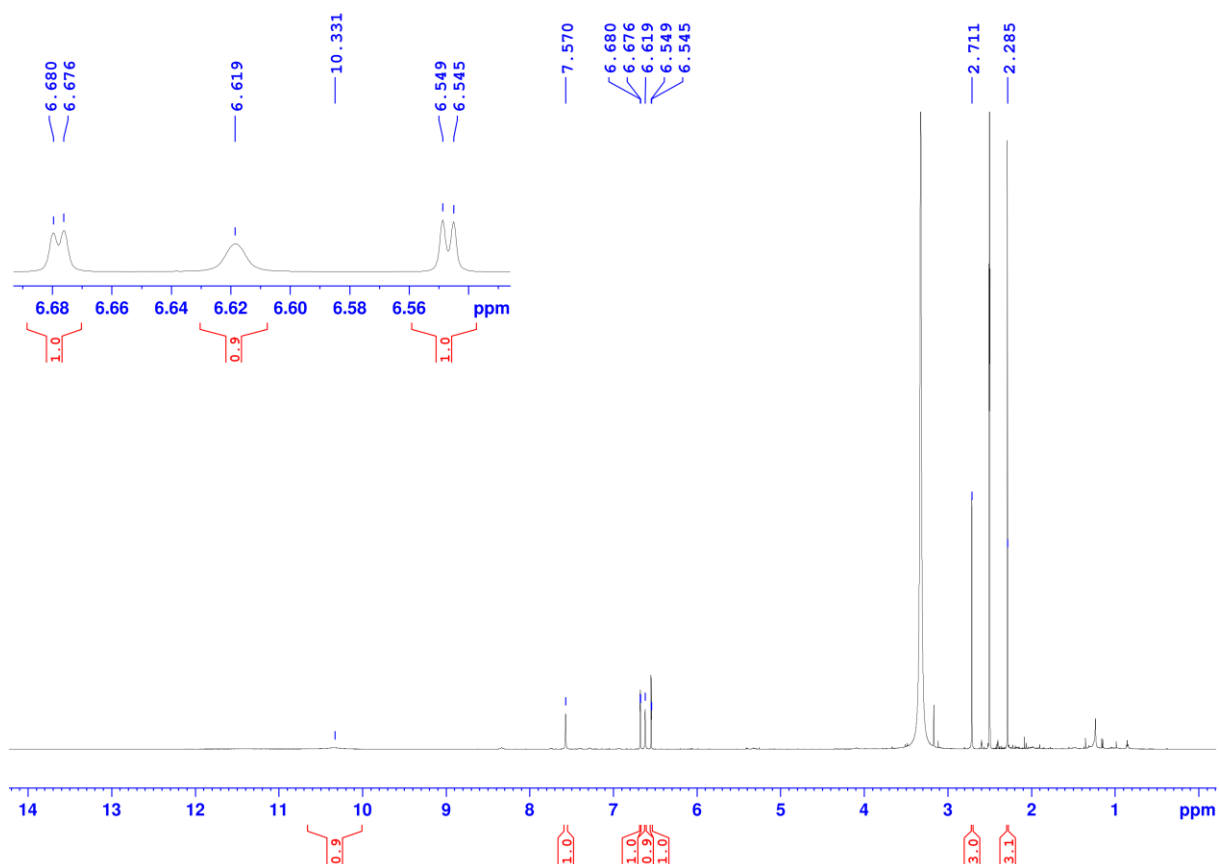


**Figure 55.**  $^1\text{H}$  NMR spectrum ( $\text{DMSO-}d_6$ , 500 MHz) of compound **DRT-G3**.

Its broad band (BB)  $^{13}\text{C}$  NMR spectrum (Fig. 56) displayed additional carbons signals, which were sorted by the HSQC experiment (Fig. 57) into two methyl at  $\delta_{\text{C}}$  21.0 (C-11) and 25.1 (CH<sub>3</sub>-1) ppm; four methine at  $\delta_{\text{C}}$  117.0 (C-2), 101.1 (C-4), 110.3 (C-8) and 109.6 (C-10). In addition, ten quaternary carbons were observed in the same spectrum including carbonyl signal at  $\delta_{\text{C}}$  169.0 and eight benzene ring carbons at  $\delta_{\text{C}}$  153.2 (C-3), 156.9 (C-7), 154.2 (C-9), 153.2 (C-4a), 139.3 (C-10a), 137.8 (C-1), 110.3 (C-6a), 108.6 (C-10b) (Table 9).

DRT 13C.esp

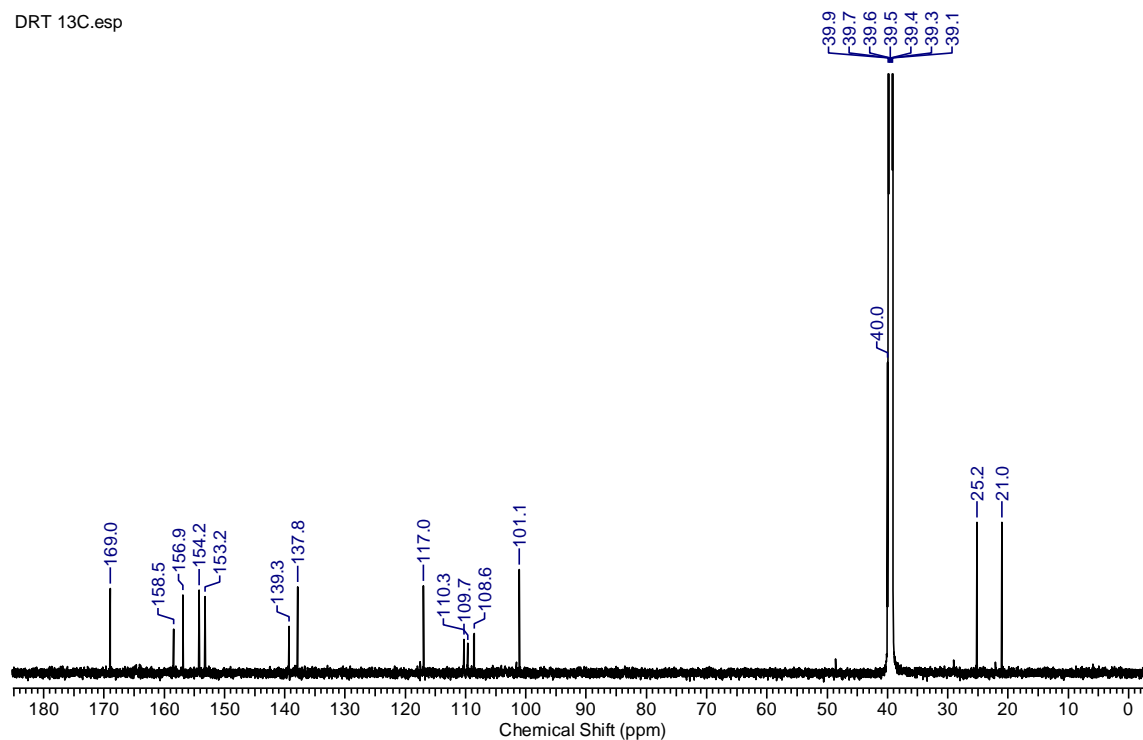


Figure 56.  $^{13}\text{C}$  spectrum (DMSO- $d_6$ , 125 MHz) of compound **DRT-G3**

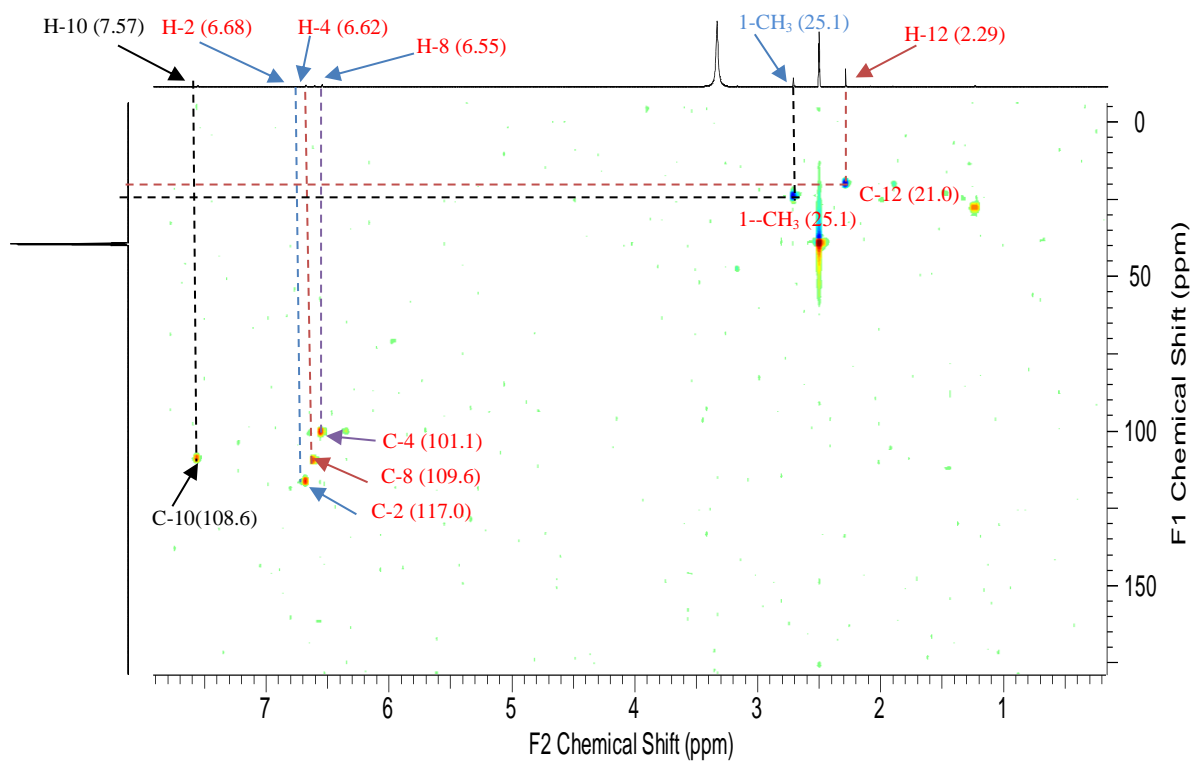
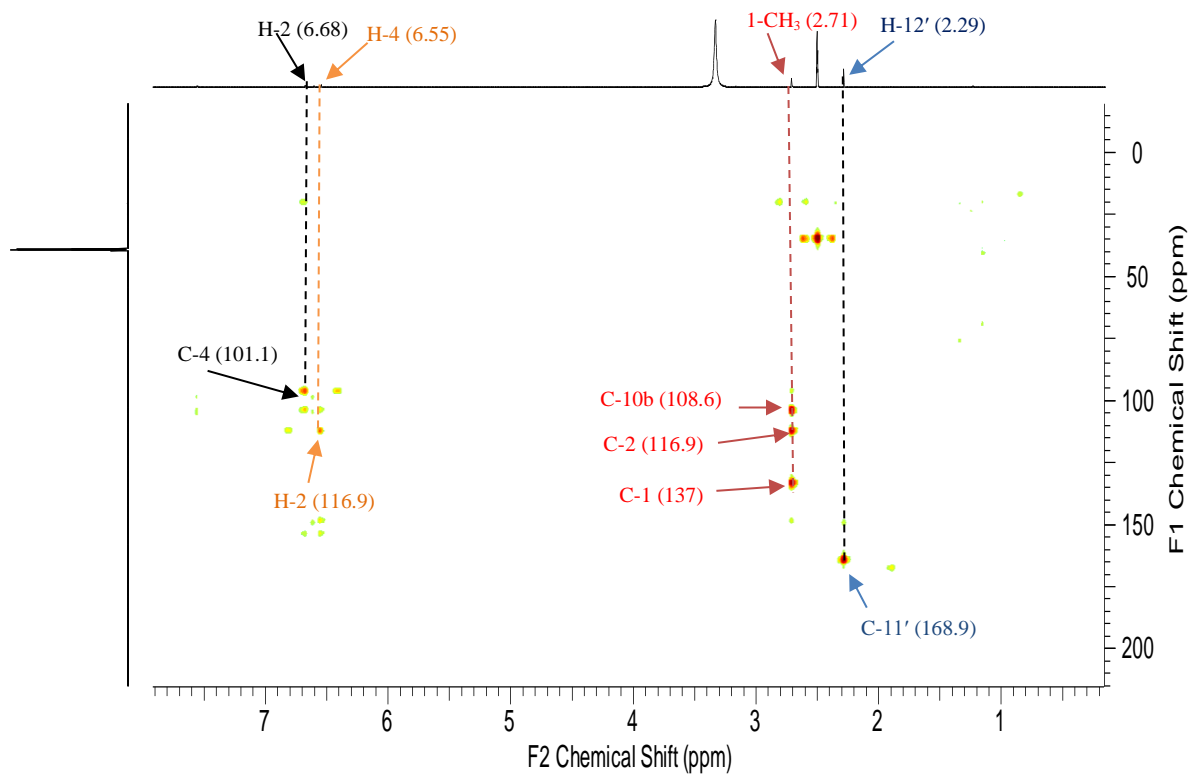
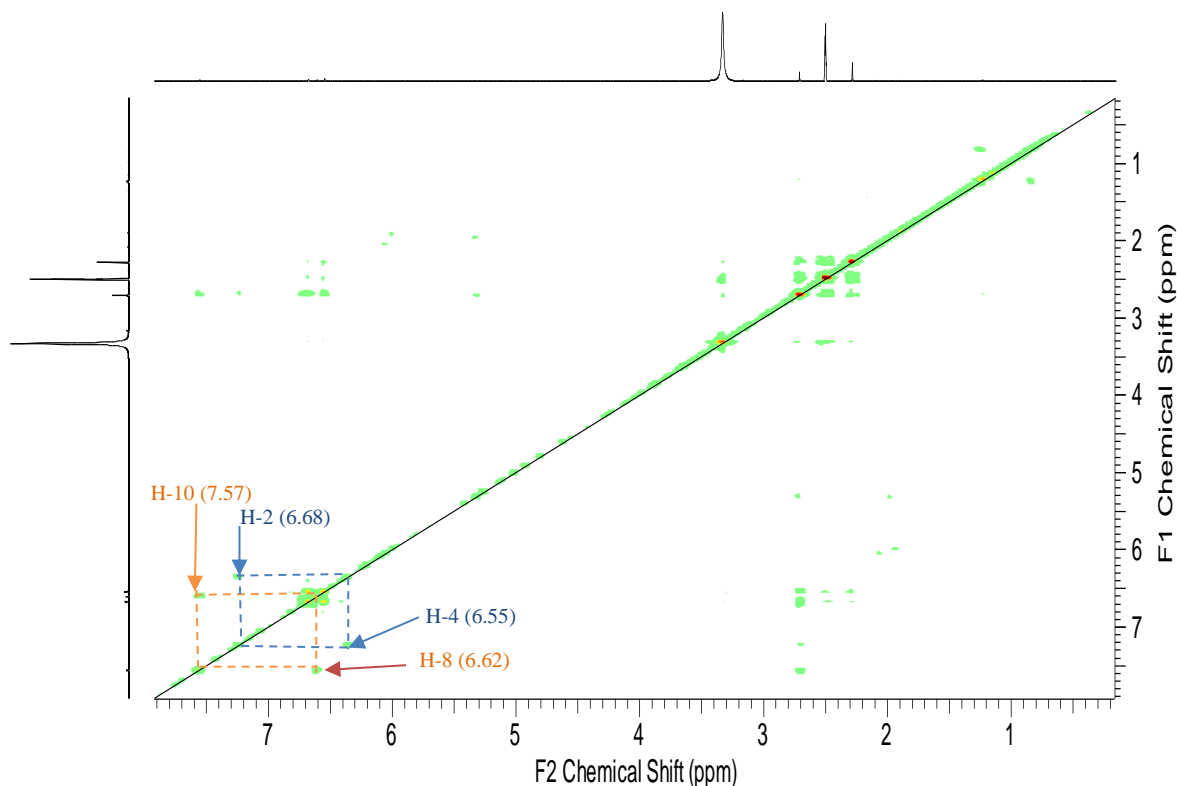


Figure 57. HSQC spectrum of compound **DRT-G3**.

The above informations were clearly supported by the HMBC cross peaks observed between the aromatic proton signals at  $\delta_{\text{H}}$  6.68 (H-2) and the carbon signals at  $\delta_{\text{C}}$  25.1 (CH<sub>3</sub>-1), 101.1 (C-4), 108.6 (C-10b) and 153.2 (C-3), and also between the proton at  $\delta_{\text{H}}$  6.55 (H-4) with the carbon signals at  $\delta_{\text{C}}$  108.6 (C-10b), 117.0 (C-2), 153.2 (C-4a) and 153.2 (C-3). The HMBC spectrum (Fig. 58) also showed the correlation between the proton signal at  $\delta_{\text{H}}$  2.71 (CH<sub>3</sub>-1) with the carbon signals at  $\delta_{\text{C}}$  108.6 (C-10b), 117.1 (C-2), 137.8 (C-1) and 153.2 (C-4a).



**Figure 58.** HMBC spectrum of compound **DRT-G3**

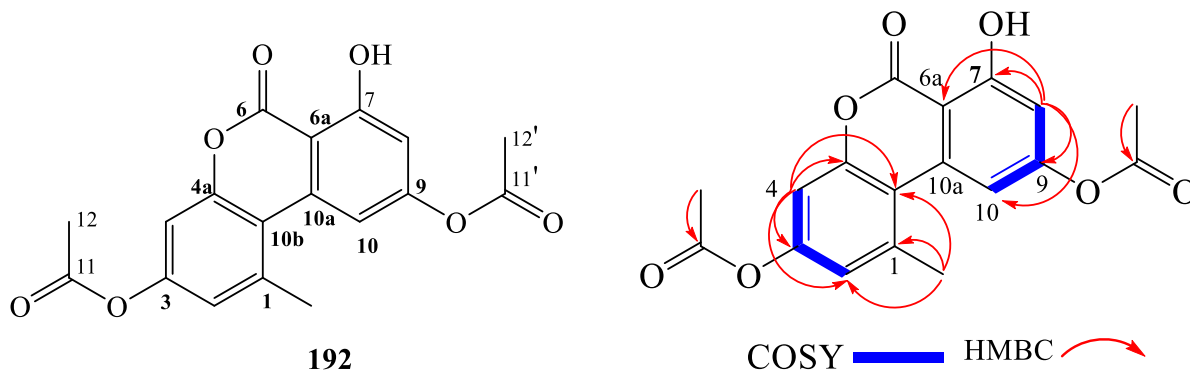


**Figure 59.** COSY spectrum of compound **DRT-G3**.

The NMR data of **DRT-G3** were similar to those of **190** except for the presence of an additional acetyl group in compound **DRT-G3**. Moreover, the carbons signals of C-3 ( $\delta_{\text{C}}$  158.5) and C-9 (154.2) observed in  $^{13}\text{C}$  NMR spectrum shift of compound **DRT-G3** in comparison to that of **190**, suggesting that the acetyl group was located at C-3 and C-9.

Furthermore, this was corroborated by the HMBC correlation seen from acetyl proton  $\delta_{\text{H}}$  2.29 (H-12') to the carbonyl at  $\delta_{\text{C}}$  169.0 of the acetyl group.

Based on  $^1\text{H}$ - $^1\text{H}$  COSY,  $^1\text{H}$ - $^{13}\text{C}$  HSQC and  $^1\text{H}$ - $^{13}\text{C}$  HMBC experiments, the signals of all protons and carbons in the molecule were unambiguously assigned and compound **DRT-G3** was identified as a new derivative of alternariol named 3, 9- diacetylalternariol (**192**).



**Scheme 7.** Structure, key COSY and HMBC correlations in compound **DRT-G3**.

Compound **DRT-G3** was completely assigned as shown in [Table 9](#).

**Table 9.**  $^1\text{H}$  and  $^{13}\text{C}$  NMR data (DMSO- $d_6$ ) of compound **DRT-G3**.

Compound <b>DRT-G3</b>		
Position	$\delta_{\text{H}}$ (nH, <i>mult.</i> , <i>J</i> in Hz)	$\delta_{\text{C}}$
1	-	137.8
2	6.68 (1H, <i>d</i> , 2.0)	117.0
3	-	153.2
4	6.55 (1H, <i>d</i> , 2.0)	101.1
4a	-	153.2
6	-	158.5
6a	-	110.3
7	-	156.9
8	6.62 (1H, <i>brs</i> )	109.6
9	-	154.2
10	7.57 (1H, <i>brs</i> )	108.6
10a	-	139.3
10b	-	108.6
11= 11'	-	169.0
12= 12'	2.29 (3H, <i>s</i> )	21.0
(1-CH <sub>3</sub> )	2.71 (3H, <i>s</i> )	25.1
7-OH	10.33 (1H, <i>s</i> )	

### II.4.2.2. Benzofuranone derivative

#### II.4. 2.2.1. Structure elucidation of compound DRT-G4

Compound **DRT-G4** was obtained as a yellow oil. Its molecular formula  $C_{12}H_{14}O_4$  that fit with six double bond equivalents, was established from the positive ion mode HR-ESI-MS (Fig. 60), showing the protonated molecular ion peak  $[M+H]^+$  at  $m/z$  223.0961 (calcd. for  $C_{12}H_{15}O_4$ , 223.0965).

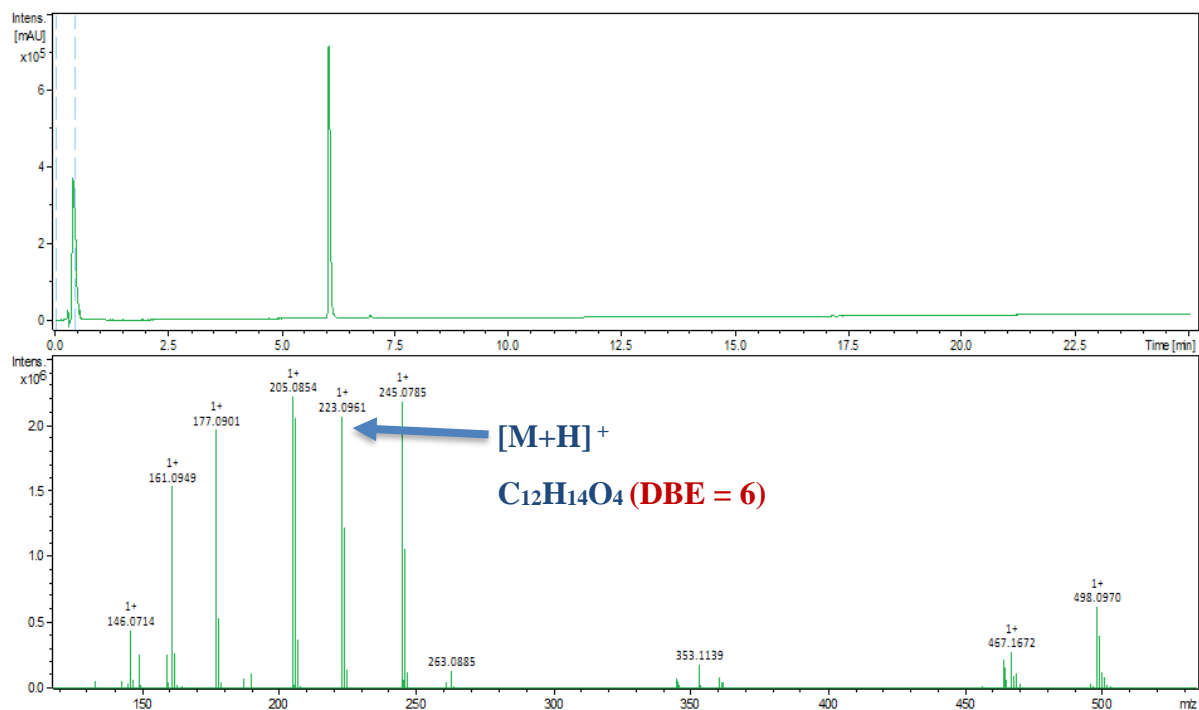


**Figure 60.** HPLC chromatogram (a) and positive ion mode HR-ESI-MS spectrum (b) of compound **DRT-G4**

Its  $^1H$  NMR spectrum (Fig. 61) displayed in the aromatic region, a singlet signal at  $\delta_H$  7.12 and in the shielded region, resonances for two aromatic methyl groups at  $\delta_H$  2.09 (s) and 2.02 (s). Characteristic signals at  $\delta_H$  1.75 (2H, q, 7.0 Hz) and 0.75 (3H, t, 7.0 Hz) indicated an ethyl group and were confirmed in the COSY spectrum (Fig. 63) with cross-peaks between the methylene and the methyl proton signals.

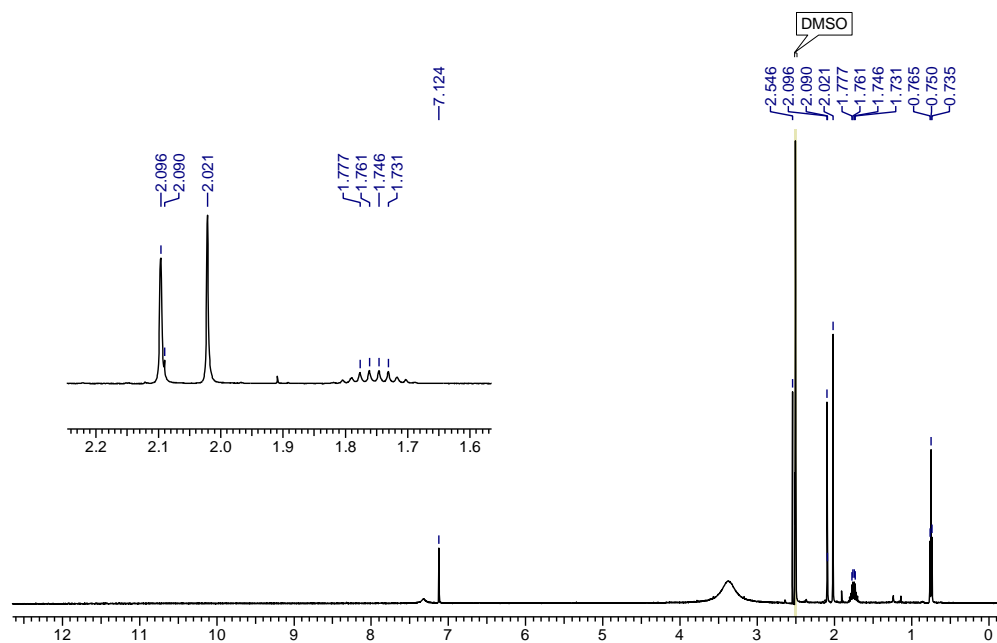


**Figure 61.**  $^1\text{H}$  NMR spectrum (DMSO- $d_6$ , 500 MHz). of compound **DRT-G4**

Its broad band (BB)  $^{13}\text{C}$  NMR spectrum (Fig. 62) displayed carbons signals, which were sorted by the HSQC experiment (Fig. 64) into three methyl at  $\delta_{\text{C}}$  7.1 (C-2');  $\delta_{\text{C}}$  8.1 (CH<sub>3</sub>-7) and  $\delta_{\text{C}}$  16.6 (CH<sub>3</sub>-5) ppm; one methylene signal at  $\delta_{\text{C}}$  28.8(C-1') and one methine carbon signal at  $\delta_{\text{C}}$  124.9 (C-4) ppm. In addition, seven quaternary carbons were observed in the same spectrum including carbonyl signal at  $\delta_{\text{C}}$  196.1 ppm and six benzene ring carbons at  $\delta_{\text{C}}$  169.2 (C-7a), 165.6 (C-6), 120.3 (C-5), 109.3 (C-3a), 106.3 (C-7), 106.2 (C-2) ppm.

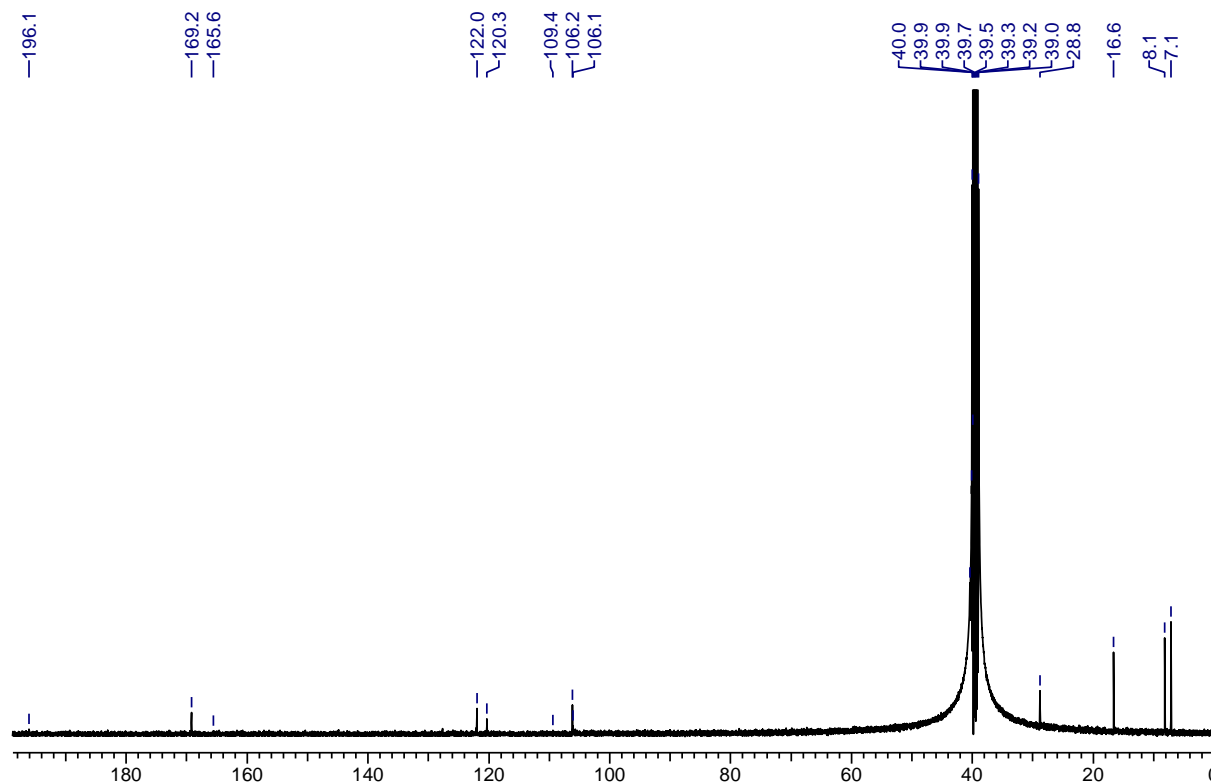


**Figure 62.**  $^{13}\text{C}$  NMR spectrum (DMSO- $d_6$ , 125 MHz). of compound **DRT-G4**

The five aforementioned protons showed HSQC cross peaks with their respective carbon signals at  $\delta_{\text{C}}$  121.9, 28.8, 16.6, 8.1, and 7.1, respectively. In the HMBC spectrum (Fig. 65), key correlations were observed between the olefinic proton signal ( $\delta_{\text{H}}$  7.12) and six carbon signals including three deshielded ones at  $\delta_{\text{C}}$  196.1 for a ketone group, 169.2 and 165.6 attributed to oxygenated aromatic carbons, and three other signals at  $\delta_{\text{C}}$ , 109.3, 106.3, and 16.6. On the other hand, each of the two aromatic methyl signals displayed a set of three cross peaks; the first one at  $\delta_{\text{H}}$  2.09 with the carbon signals at  $\delta_{\text{C}}$  165.6, 121.9 and 120.3, and the second one at  $\delta_{\text{H}}$  2.02 with the carbon signals at  $\delta_{\text{C}}$  169.2, 165.6 and 106.3. These findings clearly indicated the presence of the 1,3-dimethylbenzene moiety linked to a side chain containing an ethyl group and a ketone group. Furthermore, the ethyl group was attached to a hemiketal group ( $\delta_{\text{C}}$  106.2) as evidenced of the HMBC cross-peaks observed between the methylene proton signals at  $\delta_{\text{H}}$  1.75 with the carbon signals at  $\delta_{\text{C}}$  196.1, 106.2 and 7.1, and also between the methyl proton signals at  $\delta_{\text{H}}$  0.75 with the carbon signals at  $\delta_{\text{C}}$  106.2 and 28.8.

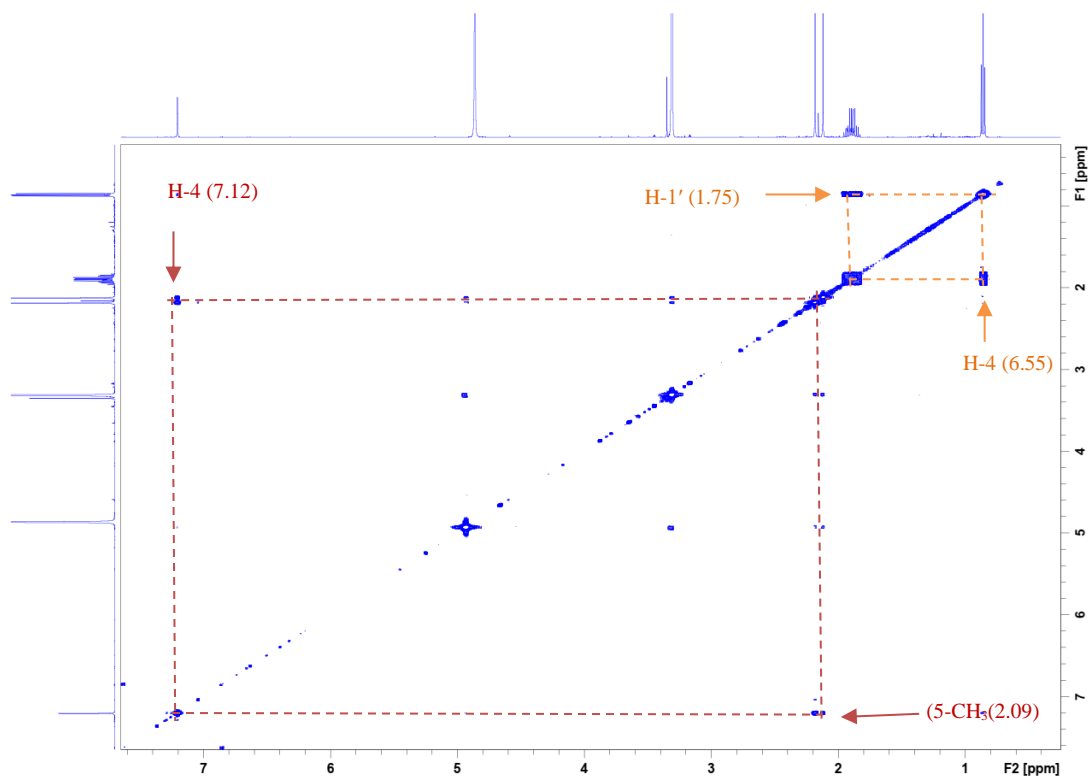


**Figure 63.** COSY spectrum of compound **DRT-G4**

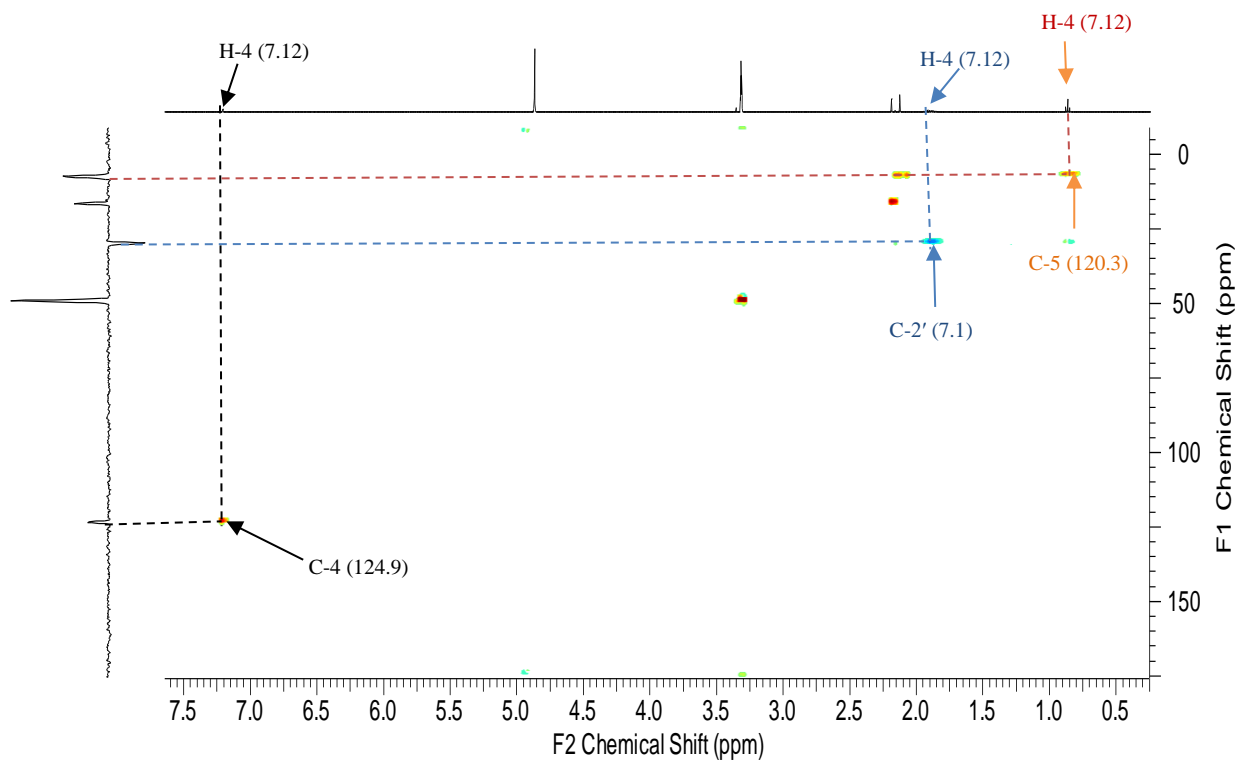


**Figure 64.** HSQC-DEPT spectrum of compound **DRT-G4**

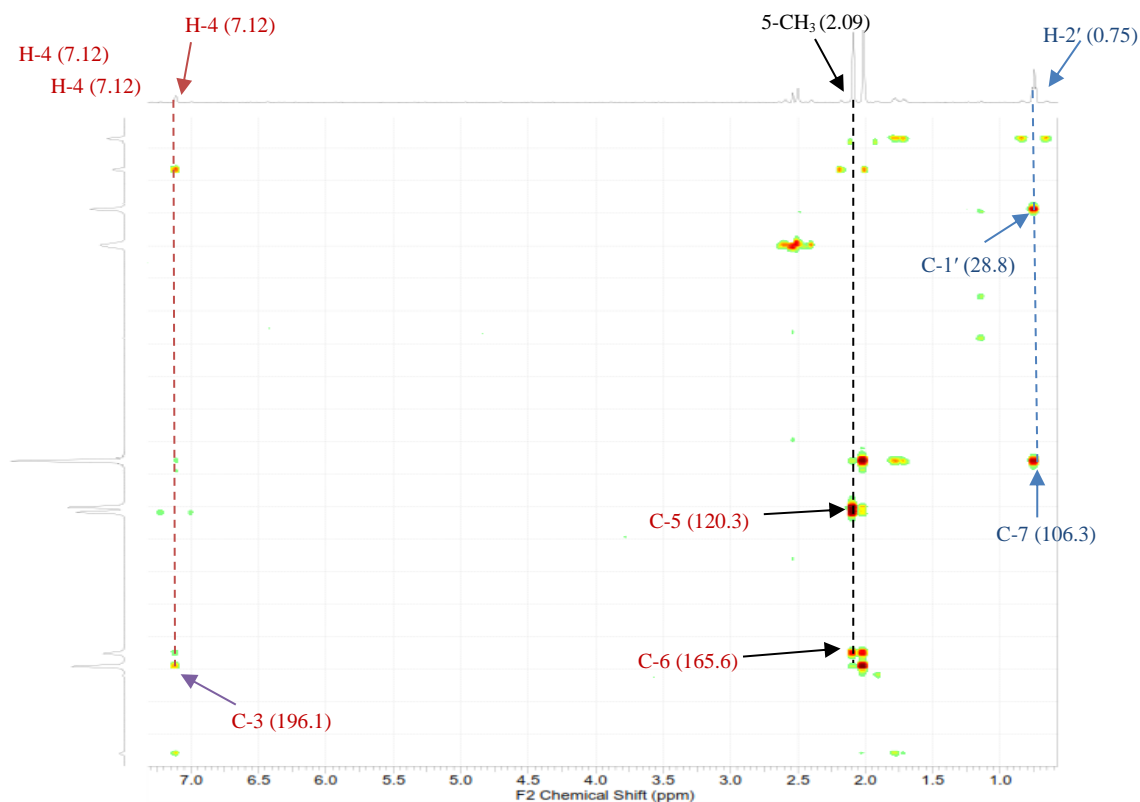
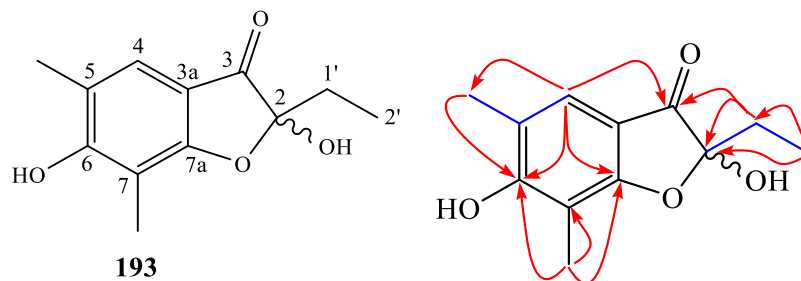


**Figure 65.** HMBC spectrum of compound **DRT-G4**.

Hence, these key correlations permitted to attachment of the hemiketal carbon ( $\delta C$  106.2) to the ketone group and the benzene ring. Key COSY and HMBC correlations of **DRT-G4** are illustrated in Scheme 9. This compound was found to be a racemate since no specific optical rotation was observed.

Based on the above evidence, the structure of compound DRT-G4 was assigned with a trivial name of diapobenzofuranone (**193**), a new benzofuranone derivative. The proposed structure was fully supported (Table 10) by HSQC-DEPT, HMBC, and COSY spectra.



**Scheme 8.** Structure, Key COSY (—) and HMBC (↷) correlations of compound **DRT-G4**

The complete assignments of  $^1\text{H}$  and  $^{13}\text{C}$  NMR for compound DRT-G4 are presented in Table 10

**Table 10.**  $^1\text{H}$  and  $^{13}\text{C}$  NMR data (DMSO- $d_6$ ) of compound **DRT-G4**

Compound DRT-G4		
Position	$\delta_{\text{H}}$ ( <i>mult.</i> , <i>J</i> in Hz)	$\delta_{\text{C}}$ ( <i>mult.</i> )
2	—	106.2
3	—	196.1
3a	—	109.3
4	7.12 ( <i>s</i> )	124.9
5	—	120.3
6	—	165.6
7	—	106.3
7a	—	169.2
1'	1.75 ( <i>m</i> )	28.8
2'	0.75 ( <i>t</i> , 7.3)	7.1
5-CH <sub>3</sub>	2.09 ( <i>s</i> )	16.6
7-CH <sub>3</sub>	2.02 ( <i>s</i> )	8.1

### II.4.2.3. Cytochalasin derivatives

#### II.4.2.3.1. Identification of compound DRT-G5

Compound **DRT-G5** to which the structure (194) was assigned, was isolated as a white crystal at the retention time of 8.31 min. Its UV spectrum revealed three maxima absorption bands  $\lambda_{\text{max}}$  at 201, 218 and 258 nm. While its molecular formula was established as  $\text{C}_{30}\text{H}_{39}\text{NO}_5$  by (+)-HR-ESI-MS at  $m/z$  494.2895,  $[\text{M}+\text{H}]^+$  (calcd for  $\text{C}_{30}\text{H}_{39}\text{NO}_5$ : 494.2897) and consistent with twelve double bond equivalent (Fig. 66).

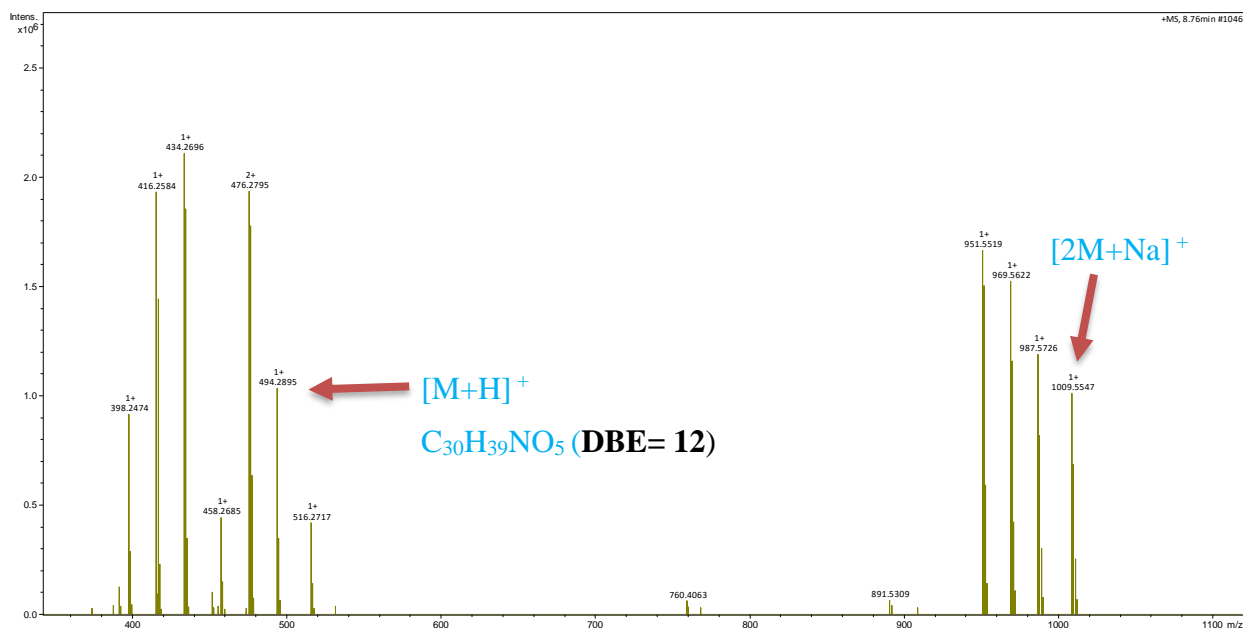


**Figure 66.** (+)-HR-ESI-MS of compound **DRT-G5**.

The  $^1\text{H}$  NMR spectrum of **DRT-G5** (Fig. 67) revealed signals of a mono-substituted benzene ring at  $\delta_{\text{H}}$  7.19 (2H, *brd*, 7.5, H-3', 5'), 7.23 (1H, *brd*, 2.5, H-4'), and 7.30 (2H, *t*, 8.0, H-2', 6'), three olefinic double bonds range of  $\delta_{\text{H}}$  5.76-4.98 ppm including signals of a terminal double bands for diastereotopic protons at  $\delta_{\text{H}}$  5.20 and 4.98 (1H each, *brs*, H-12a, H-12b). The  $^1\text{H}$  NMR spectrum also displayed signals of three hetroatom-linked methine protons at  $\delta_{\text{H}}$  5.63 (1H, *s*, H-21), 3.80 (1H, *brs*, H-7), 3.28 (1H, *m*, H-3). In addition, four methyl groups at  $\delta_{\text{H}}$  2.28 (3H, *s*, H-25), 1.28 (3H, *s*, H-23), 1.02 (3H, *d*, 6.5, H-22) and 0.57 (3H, *d*, 6.5, H-11); four methines signals at  $\delta_{\text{H}}$  5.29 (1H, *m*, H-8), 2.77 (1H, *m*, H-5), 2.16 (1H, *m*, H-4) and 1.72 (1H, *m*, H-16), three methylene signals at  $\delta_{\text{H}}$  2.65 (1H, *m*, H-10b) and 2.86 (1H, *m*, H-10a), 2.02 (1H, *dd*, 11.5, 4.7, H-15a) and 1.80 (1H, *m*, H-15b), 1.77 (1H, *dd*, 14.4, 3.3, H-17a) and 1.55 (1H, *dd*, 14.3, 3.1, H-17b) were observed in the same spectrum (Table 11).

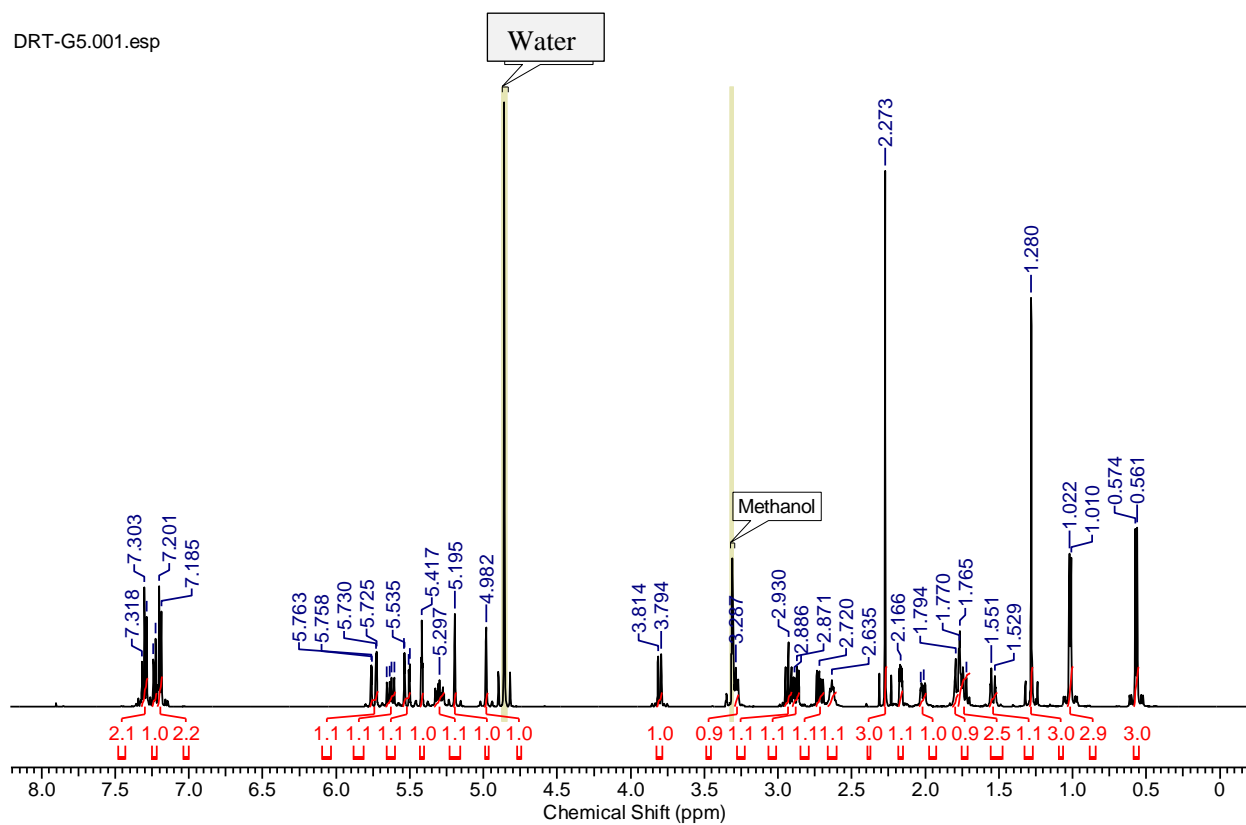


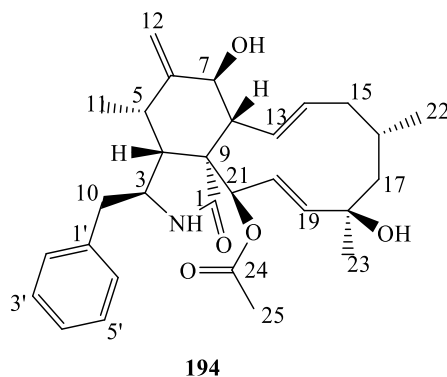
**Figure 67.**  $^1\text{H}$  NMR spectrum ( $\text{CD}_3\text{OD}$ , 500 MHz) of compound **DRT-G5**.

**Table 11.**  $^1\text{H}$  and  $^{13}\text{C}$  NMR data ( $\text{CD}_3\text{OD}$ ) of compound **DRT-G5**.

Compound DRT-G5		
Position	$\delta_{\text{H}}$ (nH, <i>mult.</i> , <i>J</i> in Hz)	* $\delta_{\text{C}}$
1	-	174.6
2	-	-
3	3.28 (1H, <i>m</i> ),	54.9
4	2.16 (1H, <i>m</i> )	49.6
5	2.77 (1H, <i>m</i> )	33.4
6	-	147.2
7	3.80 (1H, <i>brs</i> ),	72.5
8	2.93 (1H, <i>m</i> )	47.9
9	-	52.4
10a	2.86 (1H, <i>m</i> )	45.5
10b	2.65 (1H, <i>m</i> )	
11	0.57 (3H, <i>d</i> , 6.5).	13.4
12a	5.20 (1H, <i>brs</i> )	114.0
12b	4.98 (1H, <i>brs</i> )	
13	5.53 (1H, <i>m</i> )	127.4
14	5.29 (1H, <i>m</i> )	137.7
15a	2.02 (1H, <i>dd</i> , 11.5, 4.7)	44.5
15b	1.80 (1H, <i>m</i> )	
16	1.72 (1H, <i>m</i> )	29.1
17a	1.77 (1H, <i>dd</i> , 14.4, 3.3)	55.2
17b	1.55 (1H, <i>dd</i> , 14.3, 3.1)	
18	-	74.2
19	5.63 (1H, <i>m</i> )	138.3
20	5.76 (1H, <i>m</i> )	127.4
21	5.41 (1H, <i>s</i> )	78.6
22	1.02 (3H, <i>d</i> , 6.5)	26.3
23	1.28 (3H, <i>s</i> )	30.7
24	-	172.3
25	2.27 (3H, <i>s</i> )	20.5
1'		137.3
2'=6'	7.30 (2H, <i>t</i> , 8.0)	129.6
3'=5'	7.19 (2H, <i>brd</i> , 7.5)	129.5
4'	7.23 (1H, <i>brd</i> , 2.5)	127.7

\*The estimated chemical shifts for  $^{13}\text{C}$  were read in the HSQC-DEPT spectrum as the  $^{13}\text{C}$  NMR spectrum of the compound was not recorded; *mult* = multiplicity.

Based on the data mentioned above data as well as by comparison with the literature, compound **DRT-G5** was found to be identical to cytochalasin H (**194**), which was previously isolated from the endophytic fungus *Phomopsis* sp (Beno *et al.*, 1977; Izawa *et al.*, 1989) and from *Gleditsia sinensis* Thorns (Lee *et al.*, 2014).



#### II.4.2.3.2. Identification of compound DRT-G6

Compound **DRT-G6**, identified as cytochalasin N was obtained as fatty white oil at the retention time of 9.42 min. its UV spectrum revealed two maxima at 200 and 217 nm. Its UV spectrum revealed two maxima absorption bands at  $\lambda_{\max}$  200 and 217 nm. While, its molecular formula  $C_{30}H_{39}NO_5$  was established by the positive ion mode which showed ion clusters  $[M+H]^+$  at  $m/z$  494.2899, (calcd, for  $C_{30}H_{39}NO_5$  494.2897) and consistent with twelve double bond equivalents (**Fig 68**).

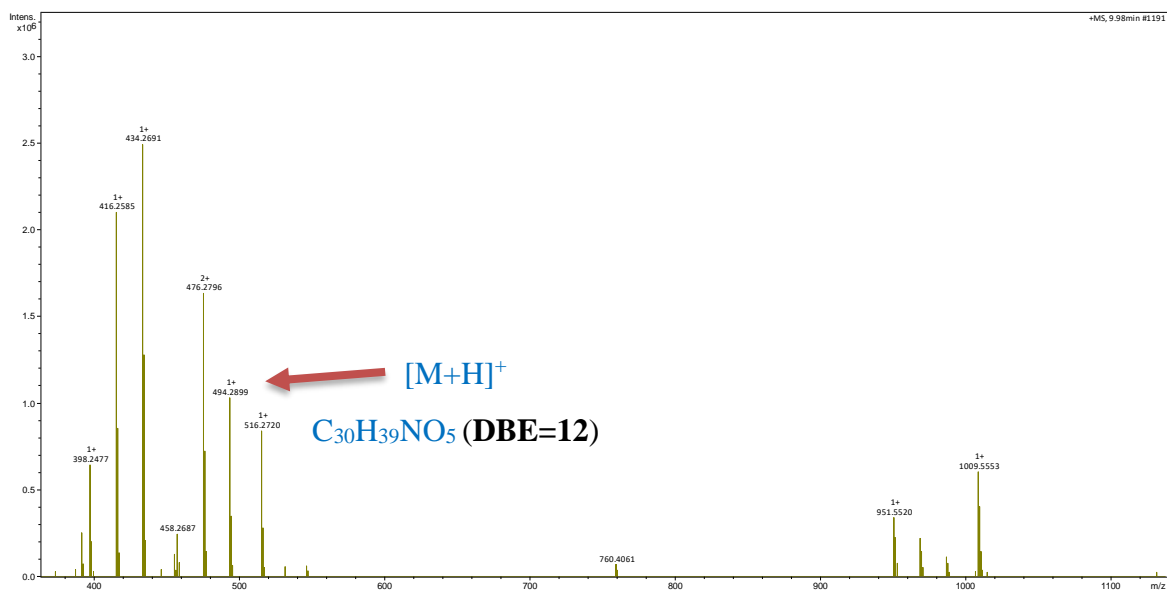


**Figure 68.** (+)-HR-ESI-MS of compound **DRT-G6**.

Compound **DRT-G6** had the same molecular formula as **DRT-G5** and its HRESI-MS (Fig.68) ions fragments were almost the same to those of compound **DRT-G5**, indicating that **DRT-G6** is an isomer of **DRT-G5**. However, its  $^1\text{H}$  NMR spectrum signals were similar to those of compound **DRT-G5**, except the signals at  $\delta_{\text{H}}$  5.20 and 4.98 (1H each, brs, H-12a, H-12b) characteristics of for the terminal double bond protons which were absent. Meanwhile, the analysis of the  $^1\text{H}$  NMR, spectrum (Fig.69) revealed the presence of two additional protons signals at  $\delta_{\text{H}}$  1.31 (3H, s) and 1.61 (3H, s), suggesting the reduction of the double bond between groups. This clearly established the position of the methyl groups as well as the double bond between C-5 and C-6.

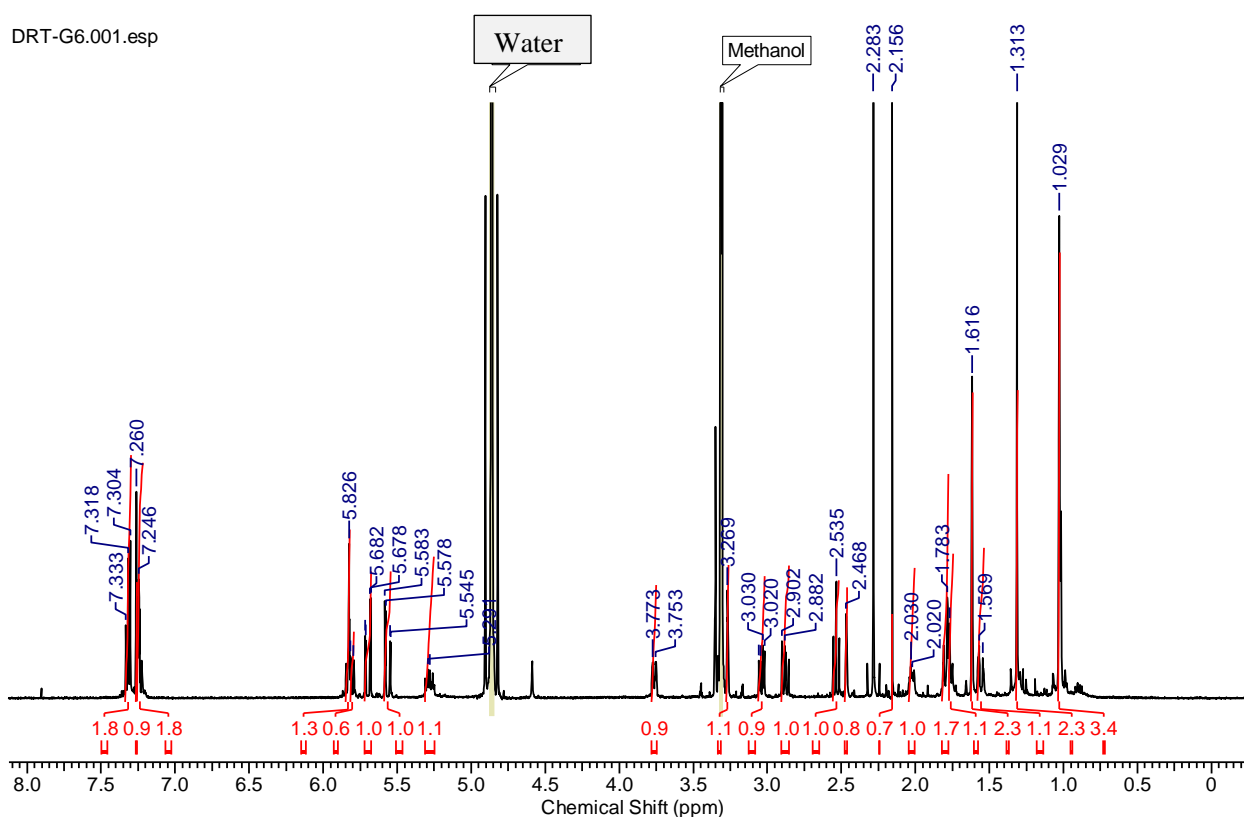


**Figure 69.**  $^1\text{H}$  NMR spectrum ( $\text{CD}_3\text{OD}$ , 500 MHz) of compound **DRT-G6**.

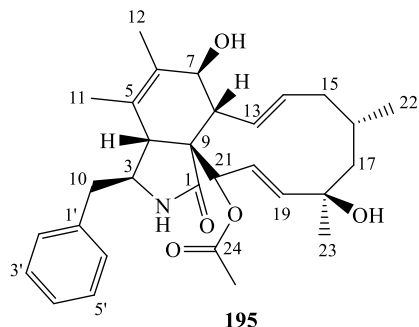
The complete assignments of all  $^{13}\text{C}$  and  $^1\text{H}$  NMR for compound **DRT-G6** are presented in [Table 12](#).

**Table 12.**  $^1\text{H}$  and  $^{13}\text{C}$  NMR data ( $\text{CD}_3\text{OD}$ ) of compound **DRT-G6**.

Position	Compound DRT-G6	
	$\delta_{\text{H}}$ (nH, <i>mult.</i> , <i>J</i> in Hz)	$\delta_{\text{C}}$
1	-	174.6
2	-	-
3	3.27 (1H, <i>m</i> )	62.1
4	2.46 (1H, <i>m</i> )	50.2
5	-	126.0
6	-	130.8
7	3.77 (1H, <i>d</i> , 9.2)	70.4
8	2.53 (1H, <i>t</i> , 10.0, 10.0)	50.5
9	-	51.0
10a	3.02 (1H, <i>m</i> )	44.6
10b	2.87 (1H, <i>m</i> )	
11	1.31 (3H, <i>s</i> )	18.5
12	1.61 (3H, <i>s</i> )	14.4
13	5.80 (1H, <i>m</i> )	129.8
14	5.28 (1H, <i>m</i> )	137.2
15a	2.03 (1H, <i>m</i> )	44.6
15b	1.74 (1H, <i>m</i> )	
16	1.77 (1H, <i>m</i> )	28.9
17a	1.80 (1H, <i>m</i> )	55.0
17b	1.56 (1H, <i>m</i> )	
18	-	74.2
19	5.55 (1H, <i>m</i> )	139.4
20	5.71 (1H, <i>m</i> )	126.3
21	5.83 (1H, <i>s</i> )	76.7
22	1.02 (3H, <i>d</i> , 6.5)	26.5
23	1.30 (3H, <i>s</i> )	30.9
24	-	172.3
25	2.28 (3H, <i>s</i> )	20.5
1'		137.3
2'= 6'	7.21 (2H, <i>t</i> , 8.0)	130.5
3'= 5'	7.32 (2H, <i>brd</i> , 7.5)	129.5
4'	7.25 (1H, <i>brd</i> , 2.5)	127.7

\*The estimated chemical shifts for  $^{13}\text{C}$  were read in the HSQC-DEPT spectrum, as the  $^{13}\text{C}$  NMR spectrum of the compound was not recorded; *mult.* = multiplicity.

Hence compound **DRT-G6** was confirmed as cytochalasin N (**195**), previously isolated from the endophytic fungi *Phomopsis* sp. 68-GO-164 and *Pestalotia* sp ([Izawa et al., 1989](#)).



#### II.4.2.3.3. Identification of compound DRT-G7

Compound **DRT-G7** was isolated as a white oil at the retention time 8.21 min. Its UV spectrum revealed two maxima at 195 and 217 nm. Its molecular formula was established as  $C_{30}H_{39}NO_5$  by (+)-HR-ESI-MS  $m/z$  494.2902,  $[M+H]^+$  (calcd, for  $C_{30}H_{39}NO_5$  494.2905) and consistent with twelve double bond equivalents (Fig. 70).

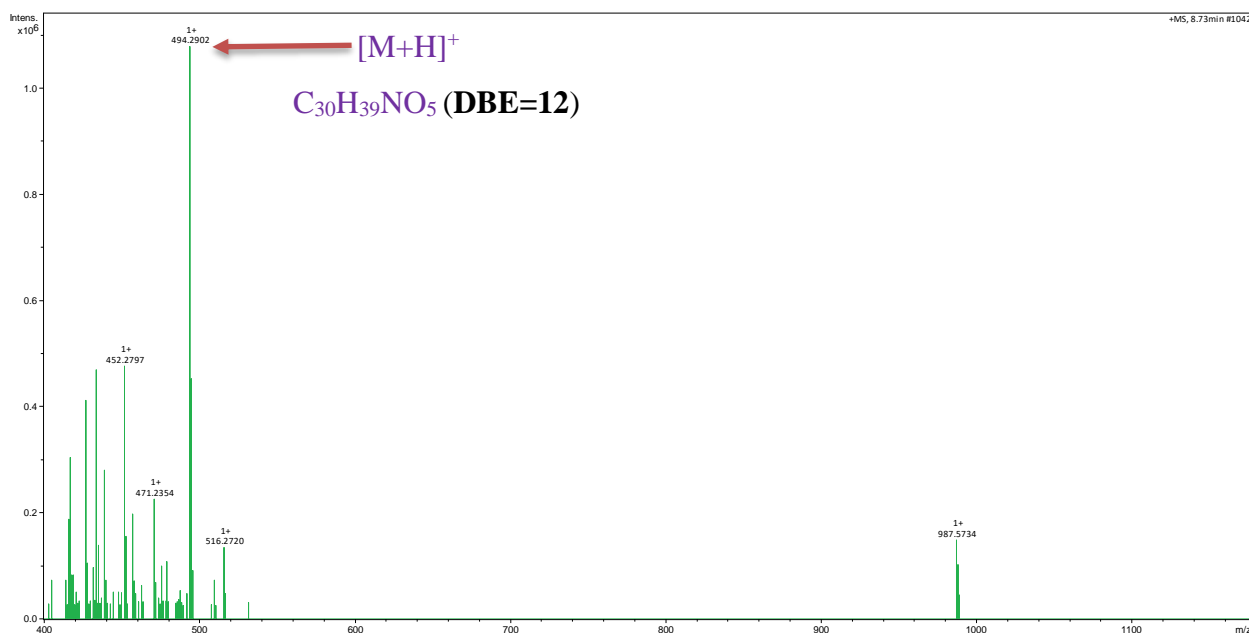


**Figure 70.** (+)-HR-ESI-MS of compound **DRT-G7**.

The  $^1H$  NMR spectrum (Fig.71) of compound **DRT-G7** gave almost the same general appearance of that of cytochalasin H except the additional methyl signal at  $\delta_H$  1.23 (3H, s, H-6) and the absence of the terminal double bond signals at  $\delta_H$  5.20 (1H, brs) and 4.98 (1H, brs). Moreover, comparison of its  $^1H$  NMR data with those of cytochalasin H, revealed that the carbon signals associated to the double bond C6-C12 were absent. This information together with the presence of additional oxygen suggested that the C6-C12 double bond was now epoxidized.

Comparison of the  $^1\text{H}$  and  $^{13}\text{C}$  NMR data of **DRT-G7** with those described in the literature confirmed that the structure of **DRT-G7** was epoxychochalsin H (**196**), a cytochalasin compound which has been previously reported to be isolated from the endophytic fungus *Phomopsis* sp. 68-GO-164 (Izawa *et al.*, 1989; Cole *et al.*, 1982).

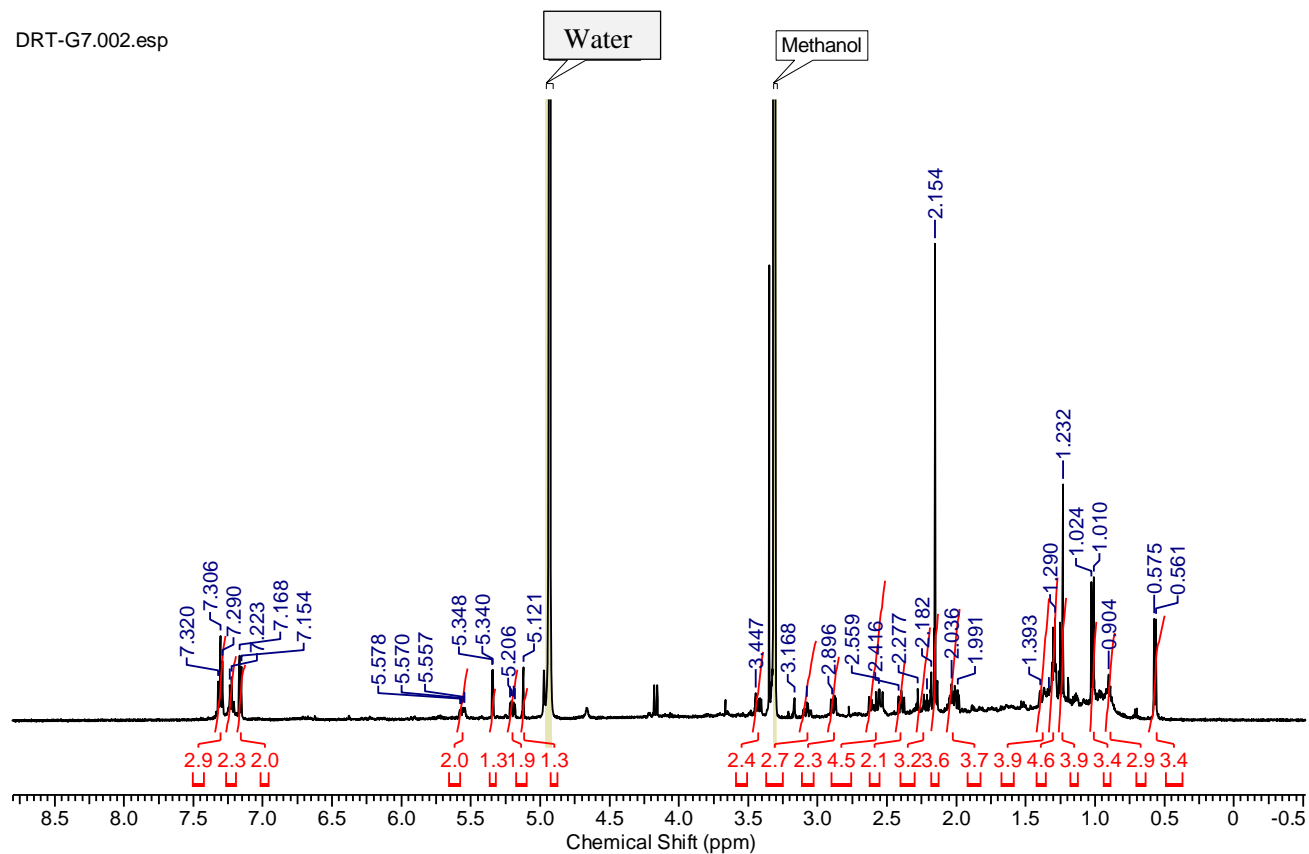
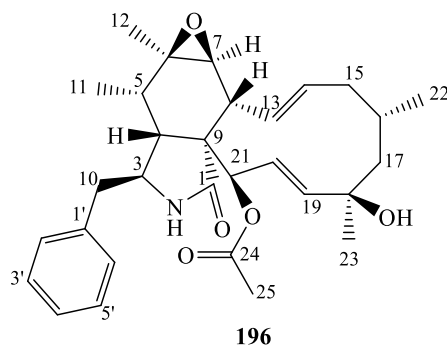


**Figure 71.**  $^1\text{H}$  NMR spectrum ( $\text{CD}_3\text{OD}$ , 500 MHz) of compound **DRT-G7**.



The complete assignments of  $^1\text{H}$  and  $^{13}\text{C}$  NMR for compound **DRT-G7** are given in Table 13.

**Table 13.**  $^1\text{H}$  and  $^{13}\text{C}$  NMR data ( $\text{CD}_3\text{OD}$ ) of compound **DRT-G7**.

Position	Compound DRT-G7	
	$\delta_{\text{H}}$ (nH, <i>mult.</i> , <i>J</i> in Hz)	$\delta_{\text{C}}$
1	-	174.6
2	-	-
3	3.44 (1H, <i>m</i> )	53.9
4	2.03 (1H, <i>m</i> )	49.6
5	1.29 (1H, <i>m</i> )	33.4
6	-	57.6
7	3.16 (1H, <i>brs</i> )	62.5
8	2.41 (1H, <i>m</i> )	47.9
9	-	52.4
10a	2.89 (1H, <i>m</i> )	45.5
10b	2.55 (1H, <i>m</i> )	
11	0.57 (3H, <i>d</i> , 6.5)	13.4
12	1.02 (1H, <i>brs</i> )	19.8
13	5.57 (1H, <i>m</i> )	127.8
14	5.12 (1H, <i>m</i> )	134.5
15a	2.27 (1H, <i>dd</i> , 11.5, 4.7)	43.5
15b	1.99 (1H, <i>m</i> )	
16	1.29 (1H, <i>m</i> )	27.1
17a	1.39 (1H, <i>dd</i> , 14.4, 3.3)	55.2
17b	1.23 (1H, <i>dd</i> , 14.3, 3.1)	
18	-	72.5
19	5.54 (1H, <i>m</i> )	138.3
20	5.20 (1H, <i>m</i> )	127.4
21	5.34 (1H, <i>s</i> )	77.4
22	0.90 (3H, <i>d</i> , 6.5)	26.3
23	1.29 (3H, <i>s</i> )	30.7
24	-	172.3
25	2.15 (3H, <i>s</i> )	20.5
1'		137.3
2' = 6'	7.16 (2H, <i>t</i> , 8.0)	129.6
3' = 5'	7.30 (2H, <i>brd</i> , 7.5)	130.0
4'	7.22 (1H, <i>brd</i> , 2.5)	127.6

\*The estimated chemical shifts for  $^{13}\text{C}$  were read in the HSQC-DEPT spectrum as the  $^{13}\text{C}$  NMR spectrum of the compound was not recorded; *mult.* = multiplicity.

#### II.4.2.3.4. Identification of compound DRT-G8

Compound **DRT-G8** was obtained as a white oil at the retention time 85 min. Its molecular formula was determined as  $C_{28}H_{35}NO_3$  on the basis of the pseudo molecular ion peak  $[M+H]^+$  at  $m/z$  434.2701 (calcd for  $C_{28}H_{35}NO_3$  434.2711).

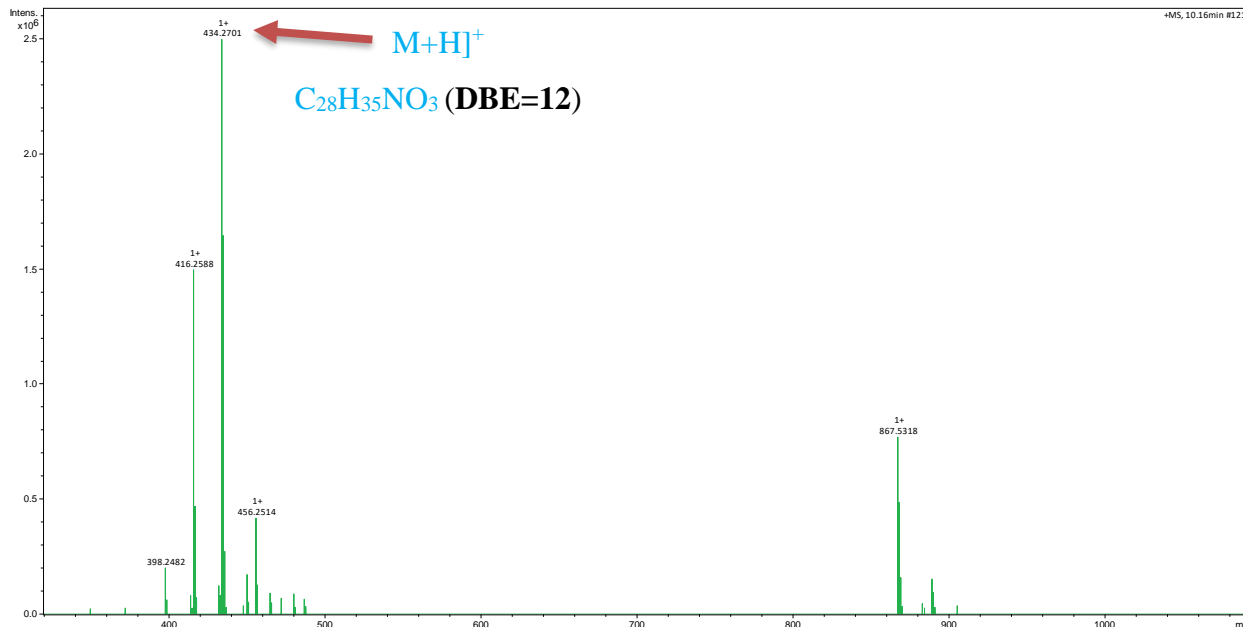


**Figure 72.** (+)-HR-ESI-MS of compound **DRT-G8**.

The  $^1H$  NMR spectrum of **DRT-G8** revealed the signals of a mono-substituted aromatic ring at  $\delta_H$  7.22 (1H, *m*, H-4') .7.23 (2H, *m*, H-2', 4'), and 7.32 (2H, *m*, H-3', 5'), four double bonds at  $\delta_H$  5.83 (1H, *m*, H-13), 5.58 (1H, *m*, H-14), 6.87 (1H, *m*, H-19), 5.52 (1H, *m*, H-20 and 5.18 (1H, *d*, 5.2) including one terminal double bond at  $\delta_H$  5.15 (1H, *brs*, H-12a) and 4.99 (1H, *brs*, H-12b), as well as three methyl groups at  $\delta_H$  1.79 (3H, *s*, H-23), 1.01 (3H, *d*, 6.5, H-22) and 0.78 (3H, *d*, 6.5, H-11). These data were in agreement with those of cytochalasin J, apart from the absence of an additional hydroxyl group at C-18, which was replaced by the double born group for 18 amu difference in molecular weight observed between both compounds. This was further corroborated by the fragment ion peak formed by the loss of 60 mass units in the ESI-MS spectrum. Thus, the absolute configuration was deduced from the reported compound and **DRT-G8** was identified as cytochalasin J2 (**197**) which was previously isolated from an Australian marine sediment-derived *Phomopsis* sp. (Shang *et al.*, 2017).

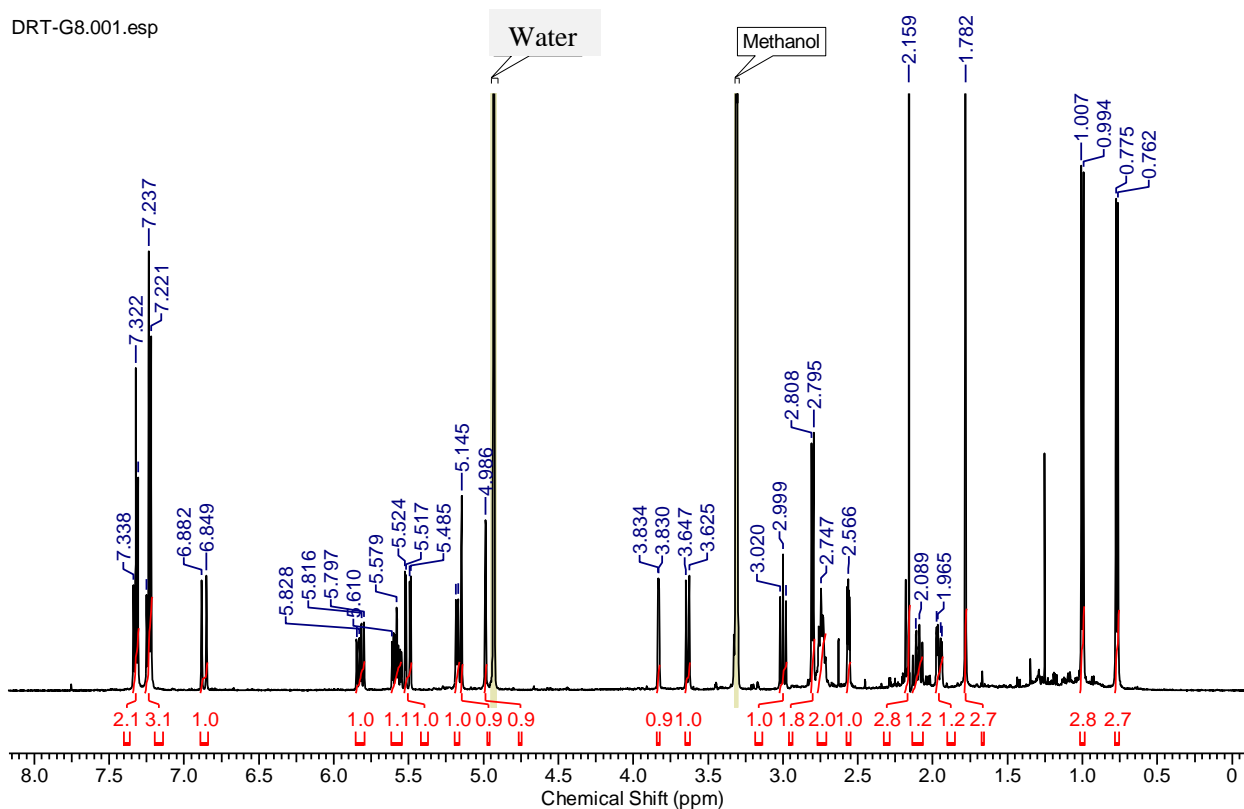


**Figure 73.**  $^1\text{H}$  NMR Spectrum ( $\text{CD}_3\text{OD}$ , 500MHz) of compound **DRT-G8**.

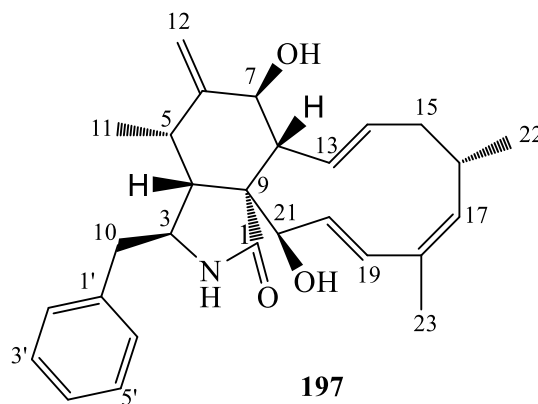


**Table 14** presents the complete assignments of  $^1\text{H}$  and  $^{13}\text{C}$  NMR for compound **DRT-G8**.

**Table 14.**  $^1\text{H}$  and  $^{13}\text{C}$  NMR data ( $\text{CD}_3\text{OD}$ ) of compound **DRT-G8**.

Position	Compound DRT-G8	
	$\delta_{\text{H}}$ (nH, <i>mult.</i> , <i>J</i> in Hz)	* $\delta_{\text{C}}$
1	-	178.5
2	-	-
3	3.31 (1H, <i>m</i> )	54.7
4	2.57 (1H, <i>dd</i> , 5.4, 3.2)	49.9
5	2.75 (1H, <i>m</i> )	33.3
6	-	147.2
7	3.64 (1H, <i>d</i> , 10.2)	72.2
8	3.02 (1H, <i>t</i> , 10.3)	47.1
9	-	52.4
10a	2.80 (1H, <i>t</i> , 5.1)	45.5
10b	2.65 (1H, <i>t</i> , 5.1)	
11	0.78 (3H, <i>d</i> , 6.5)	13.2
12a	5.15 (1H, <i>s</i> )	113.1
12b	4.99 (1H, <i>s</i> )	
13	5.83 (1H, <i>m</i> )	127.4
14	5.58 (1H, <i>m</i> )	137.7
15a	2.01 (1H, <i>m</i> )	44.8
15b	1.97 (1H, <i>m</i> )	
16	1.73 (1H, <i>m</i> )	32.5
17	5.18 (1H, <i>d</i> , 5.2)	135.8
18	-	136.0
19	6.87 (1H, <i>m</i> )	136.0
20	5.52 (1H, <i>m</i> )	126.6
21	3.83 (1H, <i>s</i> )	76.8
22	1.01 (3H, <i>d</i> , 6.5)	24.6
23	1.78 (3H, <i>s</i> )	21.2
1'		139.8
2' = 6'	7.23 (2H, <i>m</i> )	130.8
3' = 5'	7.32 (2H, <i>m</i> )	129.3
4'	7.22 (1H, <i>m</i> )	127.7

\*The estimated chemical shifts for  $^{13}\text{C}$  were read in the HSQC-DEPT spectrum as the  $^{13}\text{C}$  NMR spectrum of the compound was not recorded; *mult.* = multiplicity.

#### II.4.2.3.5. Identification of compound DRT-G9

(+)-HR-ESI-MS analysis of **compound DRT-G9** isolated as a white oil afforded pseudo-molecular ion peaks  $[M+H]^+$  at  $m/z$  434.2689 (calcd. for  $C_{28}H_{35}NO_3$  434.2693) attributed to the molecular formula  $C_{28}H_{35}NO_3$  (12 doublet bonds equivalent)

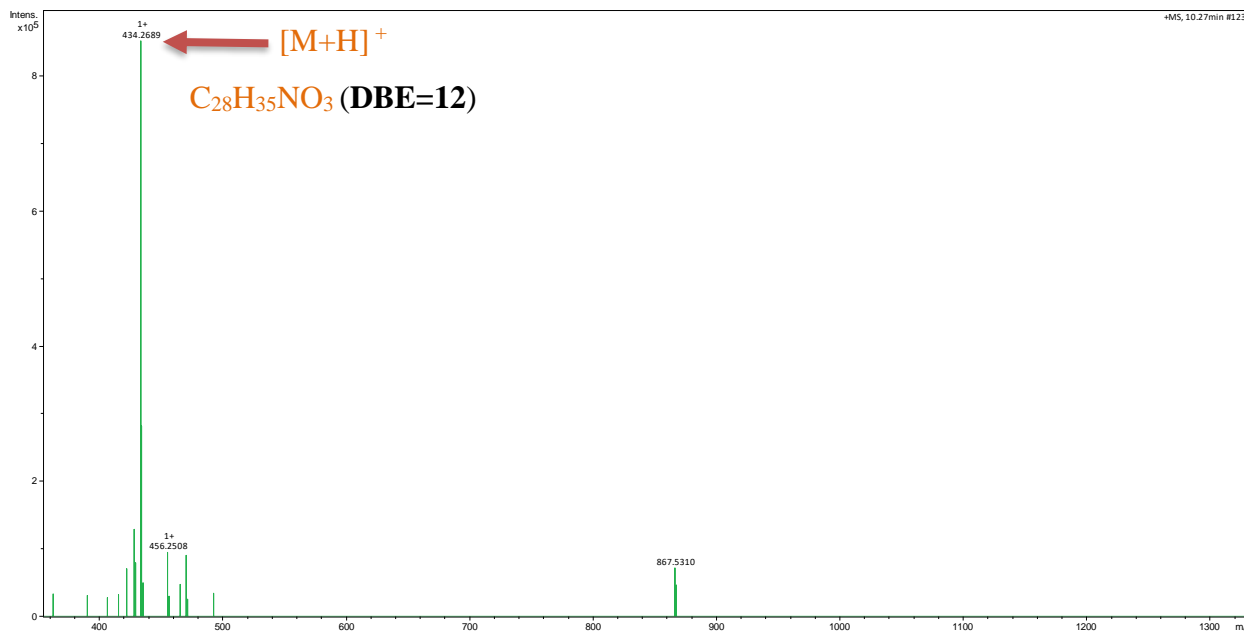


**Figure 74.** (+)-HR-ESI-MS of compound **DRT-G9**.

The analysis of its NMR spectroscopic data was closely resembled to those of **DRT-G8**, except for the presence of the aliphatic proton signals at  $\delta_H$  1.74 (1H, *m*, H-13), 3.63 (1H, *ddt*, 11.7, 9.0, 2.9, H-14), 2.35 (1H, *m*, H-19) and 2.39 (1H, *dd*, 13.0, 2.7-H-20a) in **DRT-G9** rather than olefinic protons signals in **DRT-G9**, suggested that they were substituted by different groups. This was further supported by the previous reported cytochalasin and due, the absolute configuration of **DRT-G9** was characteristic with analogs' data for cytochalasin J2 and identified as Cytochalasin J3 (**198**) previously isolated from the same Australian Marine Sediment-Derived fungus *Phomopsis* sp (Shang *et al.*, 2017).

DRT-G9.001.esp

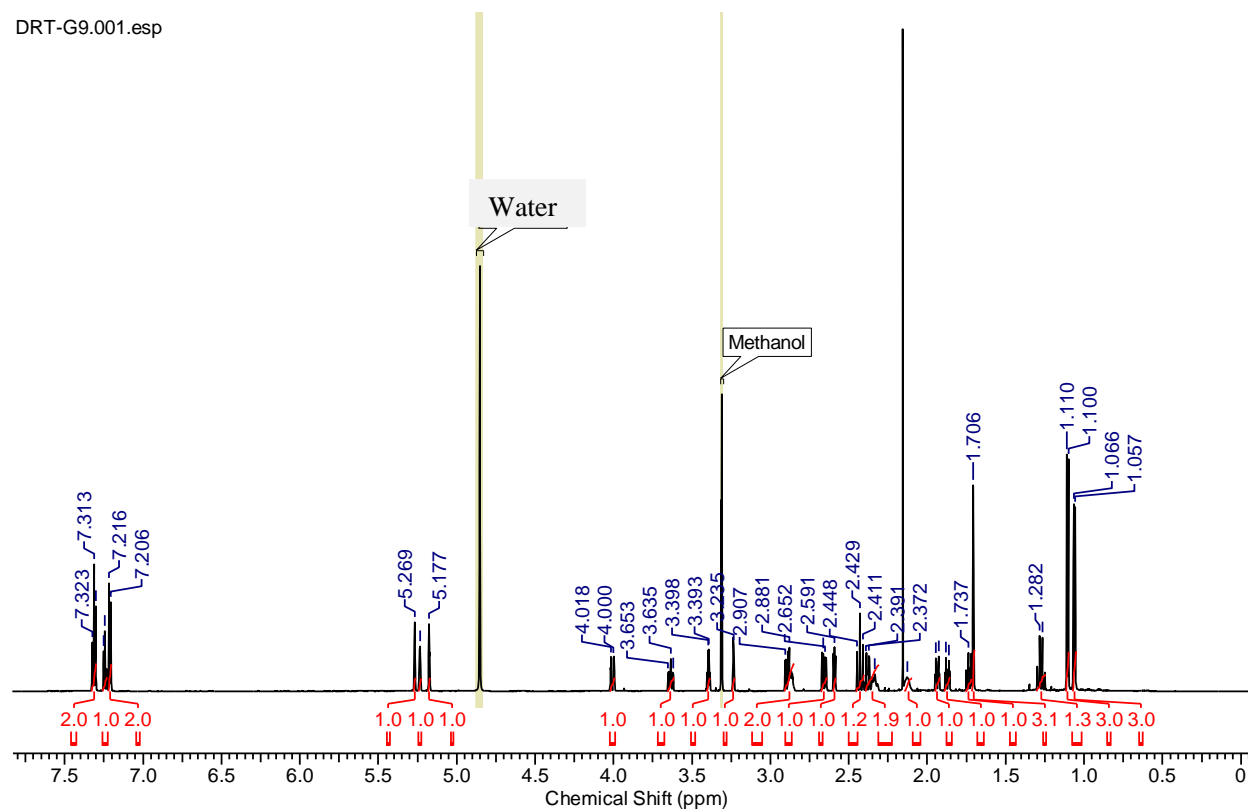
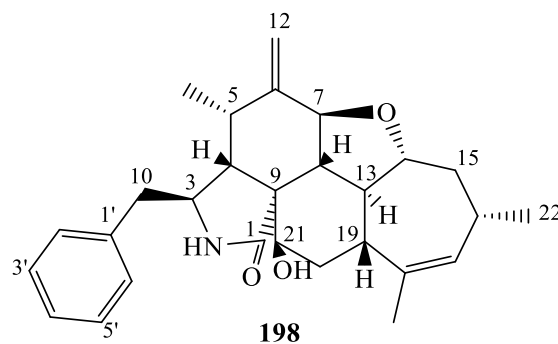


**Figure 75.**  $^1\text{H}$  NMR spectrum ( $\text{CD}_3\text{OD}$ , 500 MHz) of compound **DRT-G9**.



The complete assignments of  $^1\text{H}$  and  $^{13}\text{C}$  NMR for compound **DRT-G9** is presented in [Table 15](#).

Table 15.  $^1\text{H}$  and  $^{13}\text{C}$  NMR data ( $\text{CD}_3\text{OD}$ ) of compound **DRT-G9**.

Position	Compound DRT-G9	
	$\delta_{\text{H}}$ (nH, <i>mult.</i> , <i>J</i> in Hz)	$^*\delta_{\text{C}}$
1	-	178.2
2	-	-
3	3.39 (1H, <i>m</i> )	54.4
4	2.59 (1H, <i>m</i> )	46.4
5	2.87 (1H, <i>m</i> )	37.5
6	-	150.5
7	4.02 (1H, <i>dd</i> , 13.4, 2.0)	78.7
8	2.42 (1H, <i>dd</i> , 13.2, 12.6)	44.9
9	-	49.8
10a	2.89 (1H, <i>dd</i> , 13.8, 3.2)	44.6
10b	2.64 (1H, <i>dd</i> , 13.6, 9.3)	
11	1.06 (3H, <i>d</i> , 5.0)	15.0
12a	5.27 (1H, <i>brs</i> )	113.8
12b	5.17 (1H, <i>brs</i> )	
13	1.74 (1H, <i>m</i> )	46.5
14	3.63 (1H, <i>ddt</i> , 11.7, 9.0, 2.9)	89.5
15a	1.92 (1H, <i>ddd</i> , 11.8, 3.5, 2.5)	41.3
15b	1.26 (1H, <i>m</i> )	
16	2.13 (1H, <i>m</i> )	31.0
17	5.23 (1H, <i>brs</i> )	134.0
18	-	140.3
19	2.35 (1H, <i>m</i> )	36.3
20a	2.39 (1H, <i>dd</i> , 13.0, 2.7)	34.9
20b	1.88 (1H, <i>ddd</i> , 14.5, 3.9, 2.29)	
21	3.23 (1H, <i>brs</i> )	70.9
22	1.09 (3H, <i>d</i> , 7.3)	25.1
23	1.71 (3H, <i>s</i> )	23.6
1'		137.6
2'=6'	7.20 (2H, <i>d</i> , 8.0)	131.3
3'=5'	7.31 (2H, <i>dd</i> , 7.5)	129.2
4'	7.21 (1H, <i>brd</i> , 2.5)	127.6

\*The estimated chemical shifts for  $^{13}\text{C}$  were read in the HSQC-DEPT spectrum as the  $^{13}\text{C}$  NMR spectrum of the compound was not recorded; *mult.* = multiplicity.

#### II.4.2.3.6. Identification of compound DRT-G10

Compound **DRT-G10**, identified as cytochalasin J was obtained as white oil at a retention time of 8.21 min. Its UV spectrum revealed two maxima absorption bands at  $\lambda_{\max}$  195 and 217 nm. Its molecular formula was established by (+) HR-ESI-MS as  $C_{28}H_{37}NO_4$ ,  $m/z$  452.2796  $[M + H]^+$  (calcd, for  $C_{28}H_{37}NO_4$  452.2798.2957) which consistent with eleven double bond equivalents (Fig. 76).

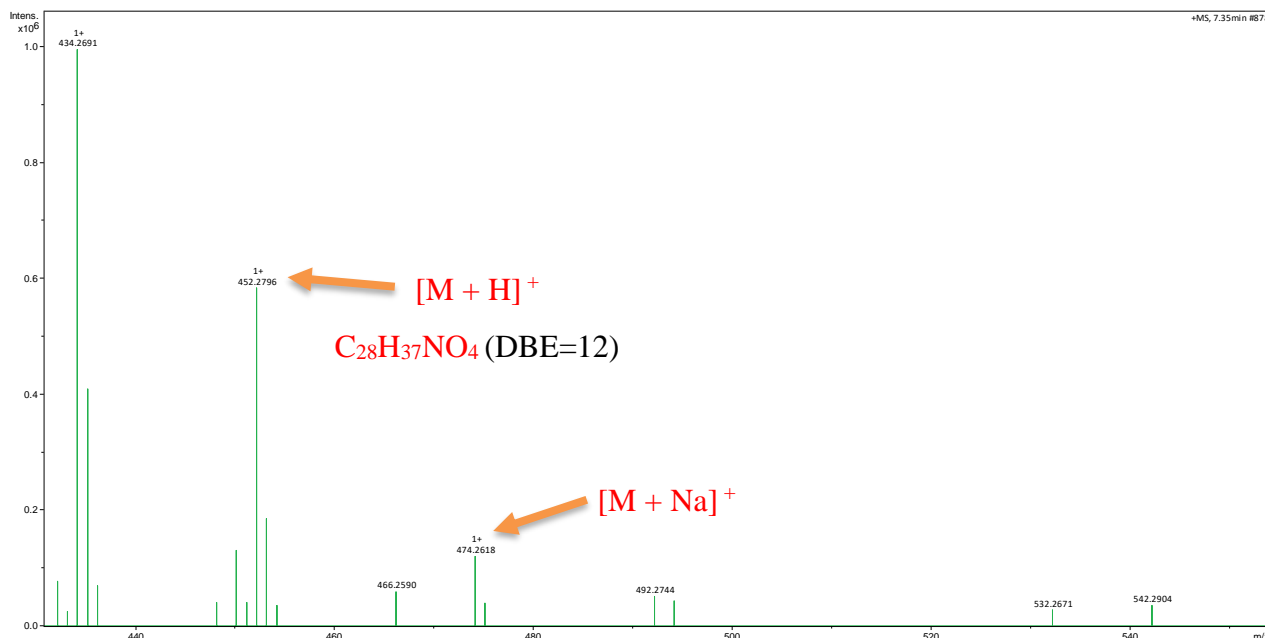


**Figure 76.** (+)-HR-ESI-MS of compound **DRT-G10**

The  $^1H$  NMR spectrum revealed one mono-substituted aromatic ring with the signals at  $\delta_H$  7.30 (2H, *brd*, 7.5, H-3', 5'), 7.21 (1H, *brd*, 7.5, H-4'), and 7.21 (2H, *t*, 8.0, H-2', 6'), three double bonds at  $\delta_H$  5.72 (1H, *m*, H-13) and 5.33 (1H, *m*, H-14); 5.75 (1H, *m*, H-19) and 5.84 (1H, *m*, H-20) including one terminal one at  $\delta_H$  5.21 (1H, *brs*, H-12a) and 5.01 (1H, *brs*, H-12b). Three methyl signals were also observed at  $\delta_H$  1.26 (3H, *s*, H-23), 1.00 (3H, *d*, 6.5, H-22) and 0.82 (3H, *d*, 6.5, H-11). In the addition, seven methines at  $\delta_H$  3.77 (1H, *brs*, H-7), 3.70 (1H, *brs*, H-21), 3.33 (1H, *m*, H-3), 2.80 (1H, *m*, H-5), 2.75 (1H, *m*, H-8), 2.60 (1H, *m*, H-4) and 1.79 (1H, *m*, H-16), three methylene groups at  $\delta_H$  2.75 (1H, *m*, H-10b) and 2.96 (1H, *m*, H-10a), 1.99 (1H, *dd*, 11.5, 4.7, H-15a) and 1.79 (1H, *m*, H-15b), 1.95 (1H, *dd*, 14.4, 3.3, H-17a) and 1.51 (1H, *dd*, 14.3, 3.1, H-17b) were observed. These  $^1H$  NMR data were also characteristics of cytochalasin derivative.



Table 16.  $^1\text{H}$  and  $^{13}\text{C}$  NMR data ( $\text{CD}_3\text{OD}$ ) of compound **DRT-G10**.

Position	Compound DRT-G10	
	$\delta_{\text{H}}$ (nH, mult., $J$ in Hz)	$^*\delta_{\text{C}}$
1	-	178.6
2	-	-
3	3.33 (1H, <i>m</i> )	54.9
4	2.60 (1H, <i>m</i> )	49.9
5	2.75 (1H, <i>m</i> )	33.4
6	-	150.2
7	3.76 (1H, <i>brs</i> )	72.3
8	2.75 (1H, <i>m</i> )	45.7
9	-	51.5
10a	2.96 (1H, <i>m</i> )	46.8
10b	2.75 (1H, <i>m</i> )	
11	0.82 (3H, <i>d</i> , 6.5)	13.5
12a	5.21 (1H, <i>brs</i> )	113.2
12b	5.00 (1H, <i>brs</i> )	
13	5.72 (1H, <i>m</i> )	127.7
14	5.33 (1H, <i>m</i> )	138.3
15a	1.99 (1H, <i>dd</i> , 11.5, 4.7)	44.5
15b	1.79 (1H, <i>m</i> )	
16	1.79 (1H, <i>m</i> )	29.5
17a	1.95 (1H, <i>dd</i> , 14.4, 3.3)	55.2
17b	1.51 (1H, <i>dd</i> , 14.3, 3.1)	
18	-	74.2
19	5.75 (1H, <i>m</i> )	138.1
20	5.84 (1H, <i>m</i> )	129.6
21	3.70 (1H, <i>s</i> )	76.7
22	1.00 (3H, <i>d</i> , 6.5)	26.4
23	1.26 (3H, <i>s</i> )	31.0
1'		137.3
2'=6'	7.22 (2H, <i>t</i> , 8.0)	129.6
3'=5'	7.30 (2H, <i>brd</i> , 7.5)	129.5
4'	7.21 (1H, <i>brd</i> , 7.3)	127.5

\*The estimated chemical shifts for  $^{13}\text{C}$  were read in the HSQC-DEPT spectrum as the  $^{13}\text{C}$  NMR spectrum of the compound was not recorded; mult. = multiplicity.

#### II.4.2.3.7. Identification of compound DRT-G11

Compound **DRT-G11** was obtained as a white oil at the retention time 8.21 min. Its molecular formula was determined to be  $C_{30}H_{39}NO_4$  by HRESIMS  $m/z$  478.2951  $[M + H]^+$ , (calcd for  $C_{30}H_{39}NO_4$  478.2956), indicating 12 double bond equivalents (Fig. 78).

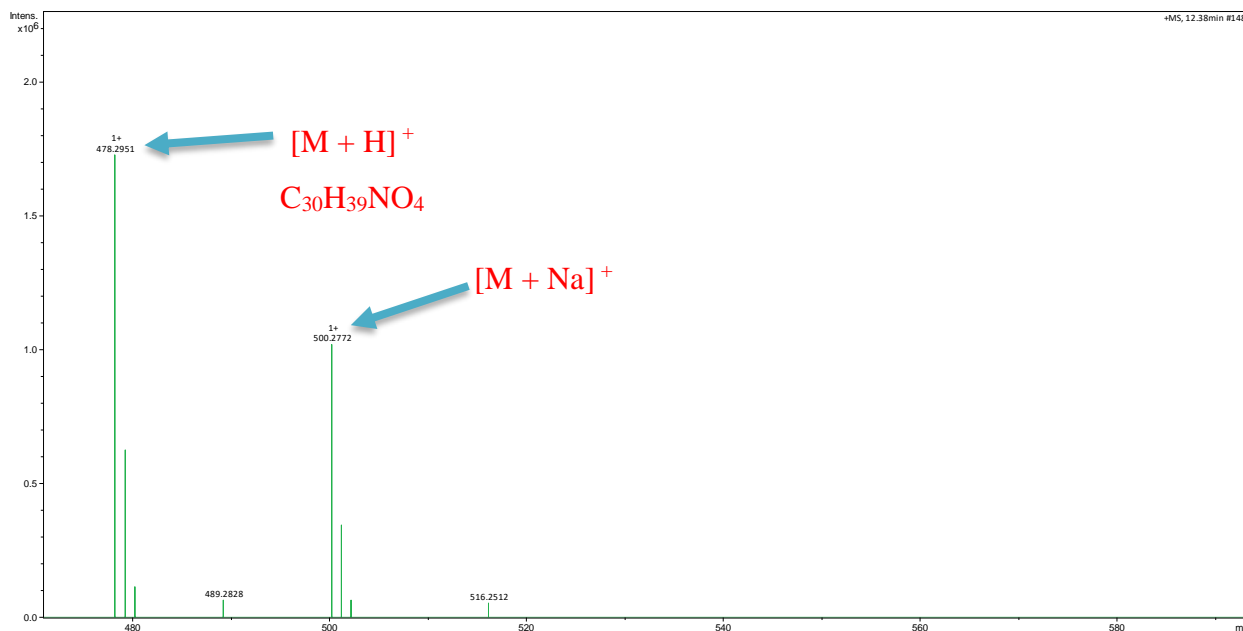


**Figure 78.** (+)-HR-ESI-MS of compound **DRT-G11**

The  $^1H$ -NMR spectrum of compound **DRT-G11** showed the monosubstituted benzene ring protons at  $\delta_H$  7.19 (2H, *d*, 7.0, H-2'/H-6'); 7.30 (2H, *d*, 7.6, H-3'/H-5'); and  $\delta_H$  7.22 (1H, *t*, 7.6, H-4'), five olefinic protons at  $\delta_H$  5.29 (1H, *m*, H-7); 5.75 (1H, *m*, H-13); 5.20 (1H, *m*, H-14); 5.50 (1H, *dd*, 2.1, 16.5, H-19); and  $\delta_H$  5.75 (1H, *dd*, 2.8, 16.5, H-20), five methyl groups at  $\delta_H$  0.83 (3H, *dd*, 2.1, 16.5, H-19); and  $\delta_H$  5.75 (1H, *dd*, 2.8, 16.5, H-20), five methyl groups at  $\delta_H$  0.83 (3H, *d*, 7.4, H-11); 1.70 (3H, *s*, H-12); 1.00 (3H, *d*, 6.4, H-22); 1.26 (3H, *s*, H-23); and  $\delta_H$  2.20 (3H, *s*, H-25) and several methine and methylene groups suggested the cytochalasin skeleton analogue of **DRT-G7**.

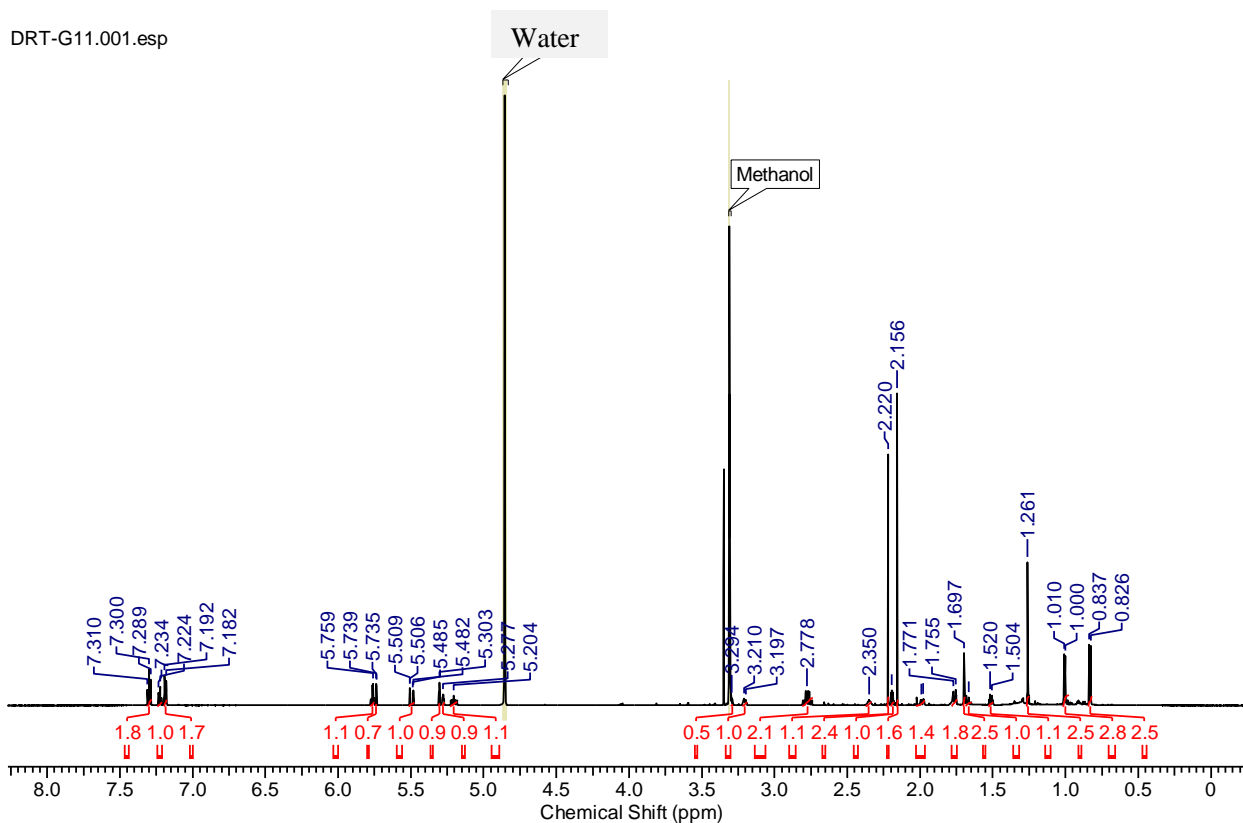
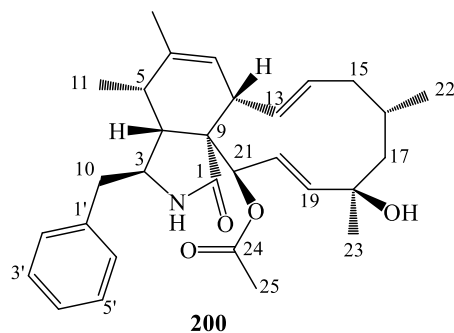


**Figure 79.**  $^1\text{H}$  NMR spectrum ( $\text{CD}_3\text{OD}$ , 500 MHz) of compound **DRT-G11**

The comparison of the  $^1\text{H}$  NMR data for **DRT-G11** ( $\text{CD}_3\text{OD}$ ) with those for cytochalasin N revealed that both compounds are closely related. This was confirmed on the  $^1\text{H}$  NMR spectrum - (Fig. 79) of compound **DRT-G11** by the absence of the heteromethine group H-7 as visible on the  $^1\text{H}$  NMR data recorded for cytochalasin N.

Based on the above investigation, compound **DRT-G11** was determined to be cytochalasin RKS-1778 (**200**), a known compound which has been previously reported from a soil fungus *Phoma* sp. SNF-1778 (Takeya *et al.*, 1997).



The complete assignments of  $^1\text{H}$  and  $^{13}\text{C}$  NMR for compound **DRT-G11** are presented in Table 17.

Table 17.  $^1\text{H}$  and  $^{13}\text{C}$  NMR data ( $\text{CD}_3\text{OD}$ ) of compound **DRT-G11**.

Position	Compound DRT-G11	
	$\delta_{\text{H}}$ (nH, <i>mult.</i> , <i>J</i> in Hz)	* $\delta_{\text{C}}$
1	-	177.5
2	-	-
3	3.29 (1H, <i>m</i> )	56.5
4	2.19 (1H, <i>m</i> )	52.9
5	2.35 (1H, <i>m</i> )	36.7
6	-	138.1
7	5.28 (1H, <i>brs</i> )	128.5
8	3.21 (1H, <i>m</i> )	43.8
9	-	56.4
10a	2.79 (1H, <i>m</i> )	45.2
10b	2.74 (1H, <i>m</i> )	
11	0.83 (3H, <i>d</i> , 6.5)	13.4
12	1.70 (1H, <i>brs</i> )	19.2
13	5.78 (1H, <i>m</i> )	130.6
14	5.20 (1H, <i>m</i> )	135.9
15a	1.98 (1H, <i>dd</i> , 11.5, 4.7)	43.9
15b	1.66 (1H, <i>m</i> )	
16	1.76 (1H, <i>m</i> )	29.5
17a	1.75 (1H, <i>dd</i> , 14.4, 3.3)	54.6
17b	1.51 (1H, <i>dd</i> , 14.3, 3.1)	
18	-	73.5
19	5.50 (1H, <i>m</i> )	138.3
20	5.20 (1H, <i>m</i> )	127.2
21	5.29 (1H, <i>s</i> )	78.0
22	1.00 (3H, <i>d</i> , 6.5)	26.1
23	1.25 (3H, <i>s</i> )	30.9
24	-	171.5
25	2.20 (3H, <i>s</i> )	20.4
1'		137.7
2' = 6'	7.30 (2H, <i>t</i> , 8.0)	130.7
3' = 5'	7.19 (2H, <i>brd</i> , 7.5)	129.5
4'	7.23 (1H, <i>brd</i> , 2.5)	127.5

\*The estimated chemical shifts for  $^{13}\text{C}$  were read in the HSQC-DEPT spectrum as the  $^{13}\text{C}$  NMR spectrum of the compound was not recorded; *mult.* = multiplicity.

#### II.4.2.4. Other classes of compounds isolated from *Diaporthe* sp.2.nov

##### II.4.2.4.1. Identification of Compound DRT-G12

(+)-HR-ESI-MS analysis of compound **DRT-G12** isolated as a white oil afforded pseudo-molecular ion peaks  $[M+H]^+$  at  $m/z$  247.0965 attributed to the molecular formula  $C_{14}H_{15}O_4$  consistent with eight double bond equivalents (Fig 80). Its UV spectrum revealed three maxima absorption bands at  $\lambda_{max}$  222, 257 and 340 nm.

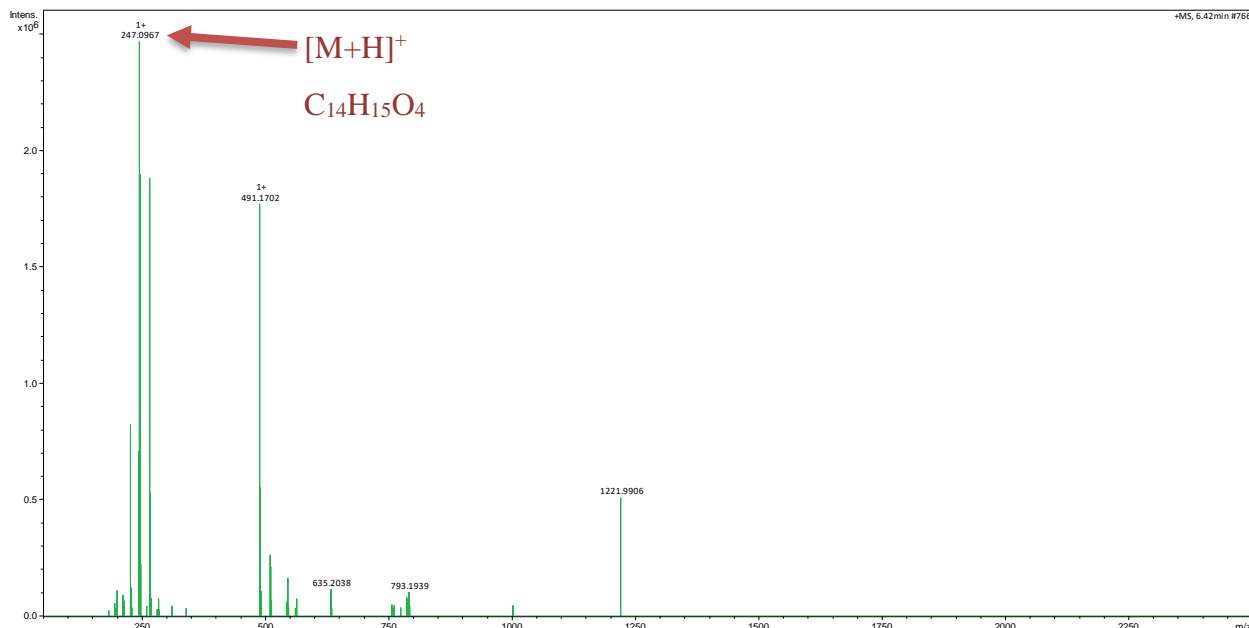


**Figure 80.** (+)-HR-ESI-MS of compound **DRT-G12**.

The  $^1H$  NMR spectrum of **compound DRT-G12** displayed nine protons signals among which one methoxyl proton  $\delta_H$  3.70 (1H, *s*), two phenolic hydroxyl protons at  $\delta_H$  8.84 (1H, *s*), 9.48 (1H, *s*), one methyl proton at  $\delta_H$  2.04 (3H, *s*). The  $^1H$  NMR spectrum also displayed five aromatic signals at  $\delta_H$  6.19 (1H, *brs*),  $\delta_H$  6.21 (1H, *brs*),  $\delta_H$  6.24 (1H, *t*, 2.0),  $\delta_H$  6.54 (1H, *s*), and  $\delta_H$  6.59 (1H, *s*) indicating that, compound **DRT-G12** has two different aromatic benzene rings.

DRT-12.001.esp

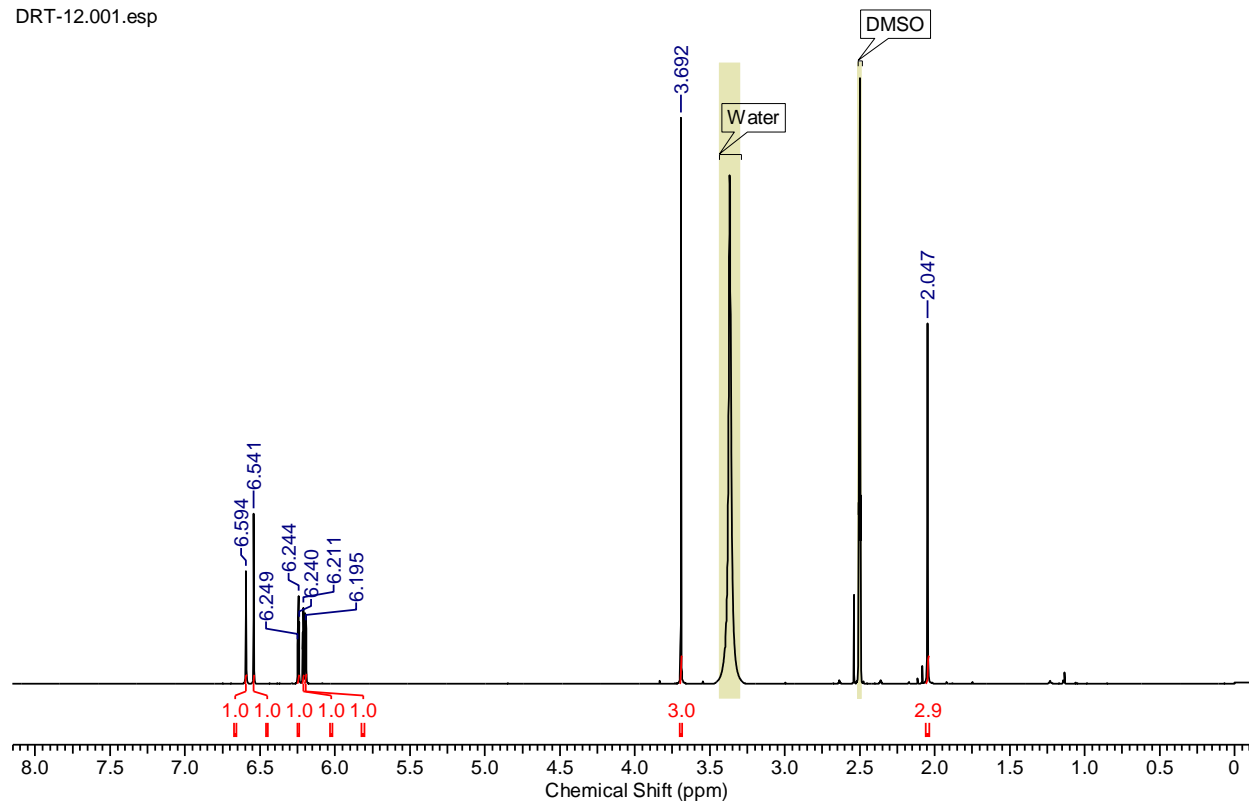


**Figure 81.**  $^1\text{H}$  NMR spectrum ( $\text{DMSO-}d_6$ , 500 MHz) of compound **DRT-G12**.

Based on the above investigation, the structure of **DRT-G12** was deduced to be, 5'-methoxy-6-methyl-biphenyl-3,4,3'-triol (**201**), a known compound which has been previously reported to be isolated from the endophytic fungus *Ulocladium* sp (Wang *et al.*, 2012).

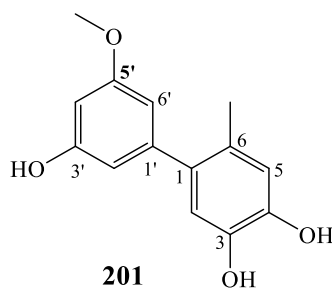


**Table 18** presents the complete assignments of  $^1\text{H}$  and  $^{13}\text{C}$  NMR for compound **DRT-G12**.

**Table 18.**  $^1\text{H}$  and  $^{13}\text{C}$  NMR data (DMSO- $d_6$ ) of compound **DRT-G12**.

Compound DRT-G12		
Position	$\delta_{\text{H}}$ (nH, <i>mult.</i> , <i>J</i> in Hz)	$^*\delta_{\text{C}}$
1	-	131.9
2	6.54 (1H, <i>s</i> )	116.2
3	-	144.0
4	-	142.7
5	6.59 (1H, <i>s</i> )	117.5
6	-	124.3
1'	-	144.5
2'	6.21 (1H, <i>brs</i> )	108.3
3'	-	157.0
4'	6.24 (1H, <i>t</i> , 2.0)	99.0
5'	-	159.3
6'	6.19 (1H, <i>brs</i> )	105.2
6-CH <sub>3</sub>	2.05 (3H, <i>s</i> )	19.5
3-OH	-	-
4-OH	8.80 (1H, <i>s</i> )	-
3'-OH	9.48 (1H, <i>s</i> )	-
5'-OCH <sub>3</sub>	3.69 (3H, <i>s</i> )	54.6

\*The estimated chemical shifts for  $^{13}\text{C}$  were read in the HSQC-DEPT spectrum as the  $^{13}\text{C}$  NMR spectrum of the compound was not recorded; *mult* = multiplicity.

#### II.4.2.4.2. Identification of Compound DRT-G13

Compound **DRT-G13** was isolated as a white solid with a retention time of 4.86 min. Its UV spectrum revealed three maxima absorption bands at  $\lambda_{\text{max}}$  230, 250 and 293 nm. Its molecular formula was established as C<sub>11</sub>H<sub>10</sub>O<sub>3</sub> from the pseudo molecular ion peak [M+H]<sup>+</sup> at  $m/z$  191.0692 (calcd for C<sub>11</sub>H<sub>10</sub>O<sub>3</sub>: 191.0694) and consistent with seven double bond equivalents (Fig. 82).

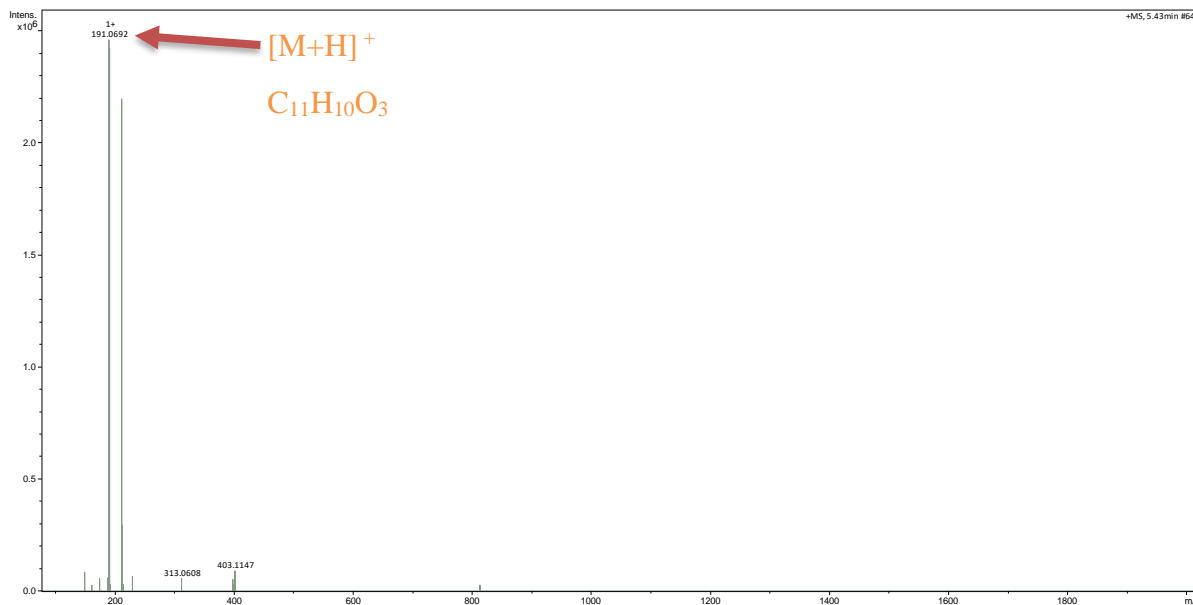


**Figure 82.** (+)-HR-ESI-MS of compound **DRT-G13**.

The <sup>1</sup>H NMR spectrum (Fig. 83) of compound **DRT-G13** displayed two the meta-coupled aromatic protons signals at  $\delta_{\text{H}}$  6.64 and  $\delta_{\text{H}}$  6.63 (1H each, *d*, 2.1), an olefinic proton singlet at  $\delta_{\text{H}}$  6.01 (1H, *d*, 0.8) together with two methyl singlet signals at  $\delta_{\text{H}}$  2.72 (3H, *brs*) and 2.32 (3H, *d*, 2.6), indicating that compound **DRT-G13** has two different benzene ring systems.

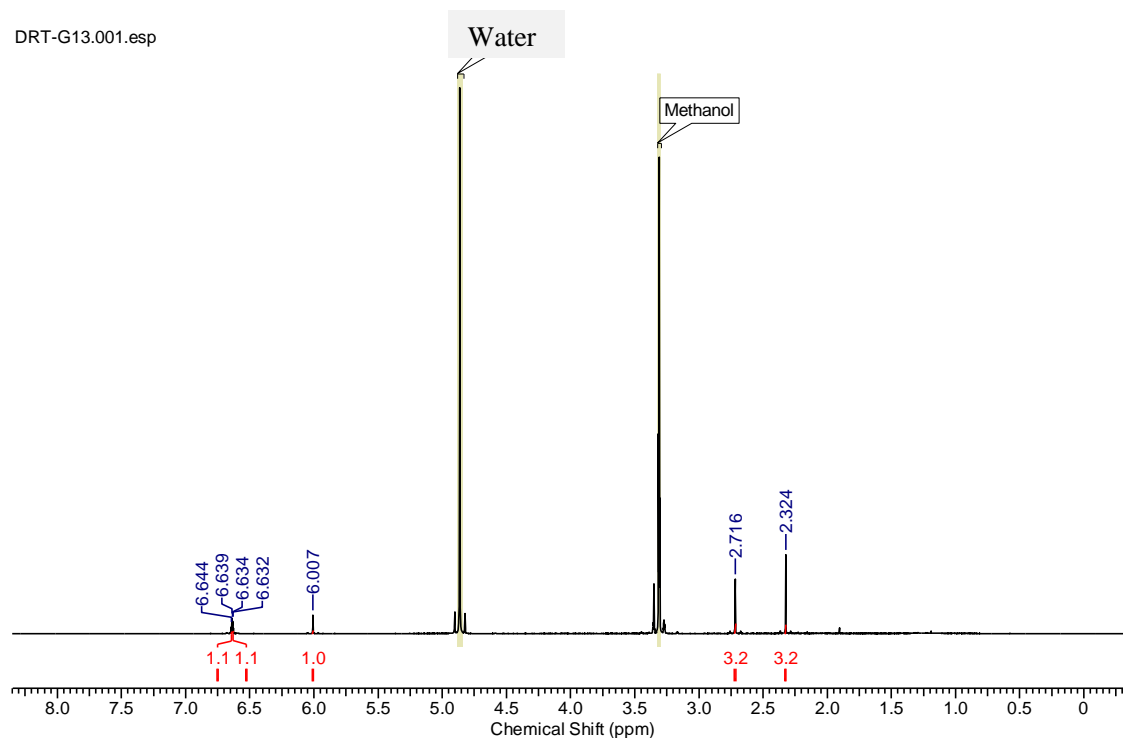
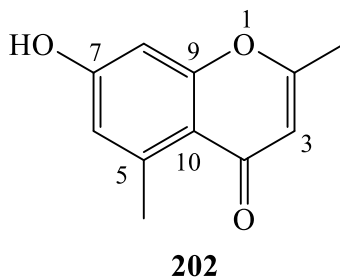


**Figure 83.** <sup>1</sup>H NMR spectrum (CD<sub>3</sub>OD, 500 MHz) of compound **DRT-G13**.

These observations were consistent with 2,5-dimethyl-7-hydroxychromone (**202**), a known compound previously reported from the Japanese rhubarb (*Rhei Rhizoma*) (Kashiwada, *et al.*, 1984), which was assigned to compound **DRT-G13**.



The complete assignment of  $^1\text{H}$  and  $^{13}\text{C}$  NMR in compound **DRT-G13** are given in table 19.

**Table 19.**  $^1\text{H}$  and  $^{13}\text{C}$  NMR data ( $\text{CD}_3\text{OD}$ ) of compound **DRT-G13**.

Compound <b>DRT-G13</b>		
Position	$\delta_{\text{H}}$ (nH, <i>mult.</i> , <i>J</i> in Hz)	* $\delta_{\text{C}}$
1	-	-
2	-	166.8
3	6.01 (1H, <i>d</i> , 0.5)	111.6
4	-	182.6
5	-	143.5
6	6.63 (1H, <i>brd</i> , 2.0)	118.2
7	-	164.6
8	6.64 (1H, <i>brd</i> , 2.0)	101.7
9	-	161.6
10	-	115.2
2- $\text{CH}_3$	2.72 (3H, <i>brs</i> )	19.6
5- $\text{CH}_3$	2.32 (3H, <i>d</i> , 0.5)	23.0

\*The estimated chemical shifts for  $^{13}\text{C}$  were read in the HSQC-DEPT spectrum as the  $^{13}\text{C}$  NMR spectrum of the compound was not recorded; *mult* = multiplicity.

#### II.4.2.4.3. Identification of compound **DRT-G14**

(+)-HR-ESI-MS analysis (Fig. 84.) of compound **DRT-G14** isolated as a white oil afforded pseudo-molecular ion peaks  $[\text{M}+\text{H}]^+$  at  $m/z$  279.1589 (calcd for  $\text{C}_{16}\text{H}_{22}\text{O}_4$  279.1592) attributed to the molecular formula  $\text{C}_{16}\text{H}_{22}\text{O}_4$  (six double bond equivalents). While, its UV-vis analysis provided the maxima absorption bands at  $\lambda_{\text{max}}$  204, 280 nm.

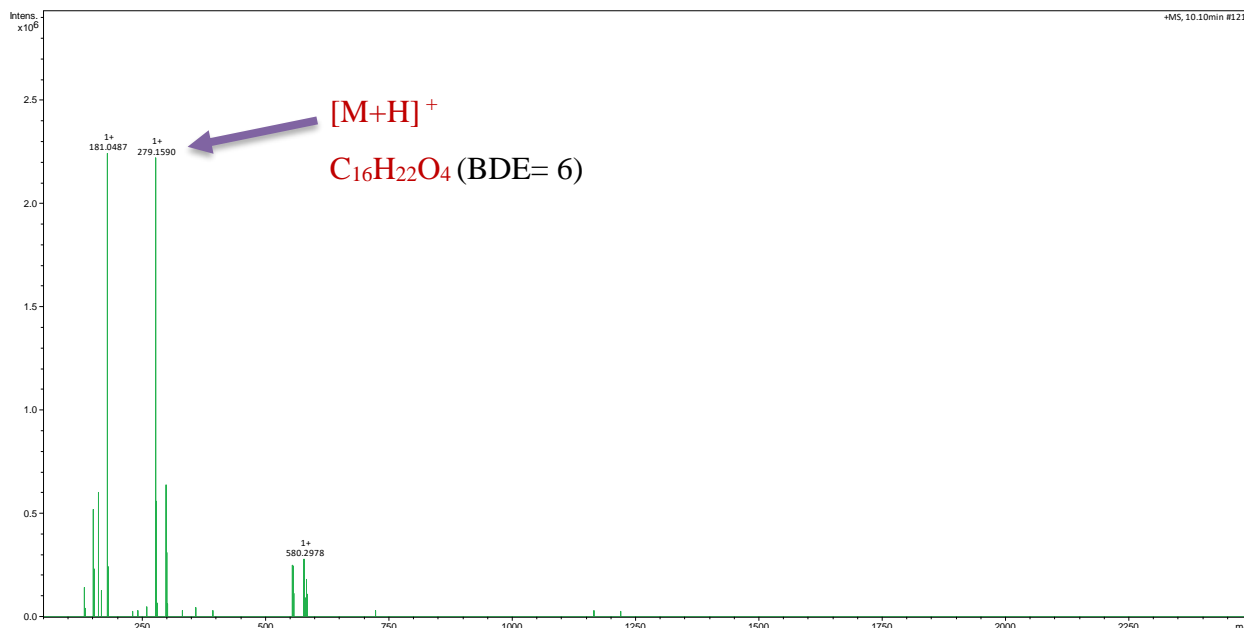


**Figure 84.** (+) -HR-ESI-MS of compound **DRT-G14**.

The  $^1H$  NMR spectrum of **DRT-G14** (Fig. 85) showed the presence of one meta-coupled aromatic protons of two methines at  $\delta_H$  6.13 and 6.22 (1H, *d*, 2.0 each, H-4, H-6), and  $\delta_H$  6.22 (1H, *d*, 0.6, H-6). Moreover, two geminal protons of a methylene were observed at  $\delta_H$  3.80 (1H, *d*, 19.1, H-2), 3.50 (1H, *d*, 19.1, H-2); situated between a phenyl ring and the carbonyl group of a six-membered lactone ring. In addition, the signal of an oxygenated methine at  $\delta_H$  5.60 (1H, *dd*, 8.5, 5.1, H-9), the signals of a six membered alkyl chain from 1.26-1.40 ppm (H-10 to H-15) and a signal of a terminal methyl proton at  $\delta_H$  0.90 (3H, *t*, 6.5, 7.5, H-16).

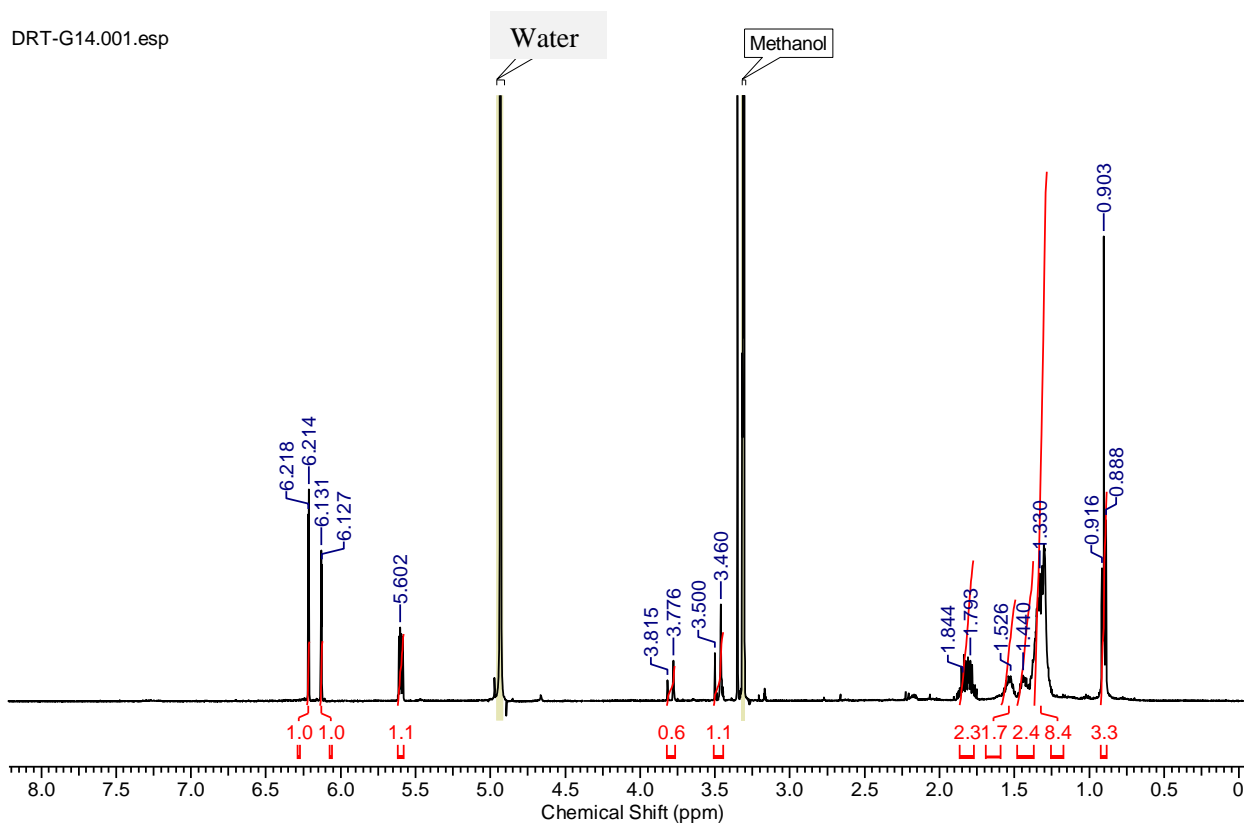
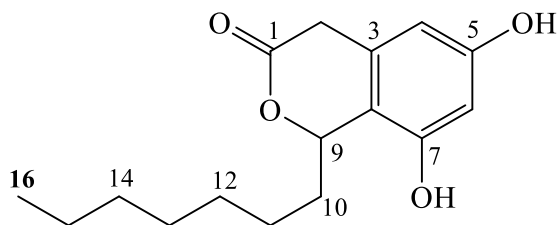


**Figure 85.**  $^1\text{H}$  NMR spectrum ( $\text{CD}_3\text{OD}$ , 500 MHz) of compound **DRT-G14**.

On the basis of previous reports and evidence, the structure of DRT-G14 was deduced as cytosporone C (**203**), a known compound which has been previously reported to be isolated from from the endophytic fungus *phomopsis* sp (Tan *et al.*, 2017).



**203**

The complete assignments of  $^1\text{H}$  and  $^{13}\text{C}$  NMR for compound DRT-G14 are presented in [Table 20](#).

**Table 20.**  $^1\text{H}$  and  $^{13}\text{C}$  NMR data ( $\text{CD}_3\text{OD}$ ) of compound **DRT-G14**.

Position	Compound DRT-G14	
	$\delta_{\text{H}}$ (nH, <i>mult.</i> , <i>J</i> in Hz)	* $\delta_{\text{C}}$
1	-	174.8
2a	3.80 (1H, <i>d</i> , 19.5)	35.0
2b	3.50 (1H, <i>d</i> , 19.5)	
3	-	132.5
4	6.22 (1H, <i>d</i> , 2.0)	101.8
5	-	159.4
6	6.13 (1H, <i>d</i> , 2.0)	105.8
7	-	155.0
8	-	114.0
9	5.60 (2H, <i>dd</i> , 5.5, 5.5)	79.8
10	1.84 (2H, <i>m</i> )	36.6
	1.79	
11	1.51 (2H, <i>m</i> )	26.4
	1.44	
12	1.26-1.40 (2H, overlapped)	29.9
13	1.26-1.40 (2H, overlapped)	29.9
14	1.26-1.40 (2H, overlapped)	32.5
15	1.26-1.40 (2H, overlapped)	23.3
16	0.90 (3H, <i>t</i> , 6.5, 7.5)	14.2

\*The estimated chemical shifts for  $^{13}\text{C}$  were read in the HSQC-DEPT spectrum as the  $^{13}\text{C}$  NMR spectrum of the compound was not recorded; *mult* = multiplicity

#### II.4.2.4.4. Identification of DRT-G15

Compound **DRT-G15** was obtained as a white amorphous solid. The molecular formula was established as  $\text{C}_{15}\text{H}_{20}\text{O}_5$  on the basis of the pseudo-molecular ion peaks  $[\text{M}+\text{H}]^+$  at  $m/z$  281.1687 observed in the (+)-HR-ESI-MS, indicating six double bond equivalent.

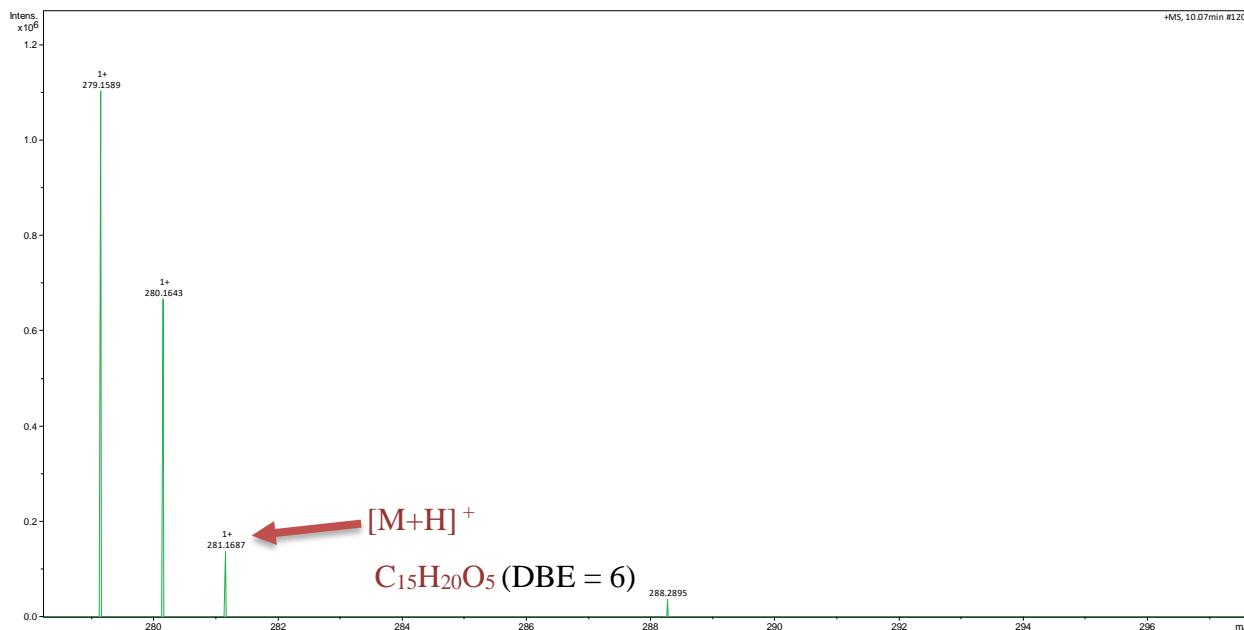


**Figure 86.** (+)-HR-ESI-MS of compound **DRT-G15**.

The <sup>1</sup>H NMR spectrum (Fig. 87) exhibited a signal of one aromatic proton at  $\delta_{\text{H}}$  6.78 (1H, *s*, H-3), an oxygenated methine at  $\delta_{\text{H}}$  5.46 (1H, *dd*, 8.7, 5.1, H-9), the signals of a six-membered alkyl chain from 1.25-2.24 ppm (H-9 to H-14) and a terminal proton signal at  $\delta_{\text{H}}$  0.89 (3H, *t*, 4.5, 5.5, H-3). These <sup>1</sup>H NMR data (Fig. 87) were closed to those of cytosporone C. The difference was the absence of the couple of germinal protons at  $\delta_{\text{H}}$  3.80 and 3.50 ppm. On the basis of foregoing evidence, the signals of all protons and carbons in the molecule were unambiguously assigned and compound **DRT-G15** was identified as cytosporone E (**205**), a known compound previously isolated from an endophytic fungus *Cytospora* sp. (Brady *et al.*, 2000).

DRT-G15.1H.esp

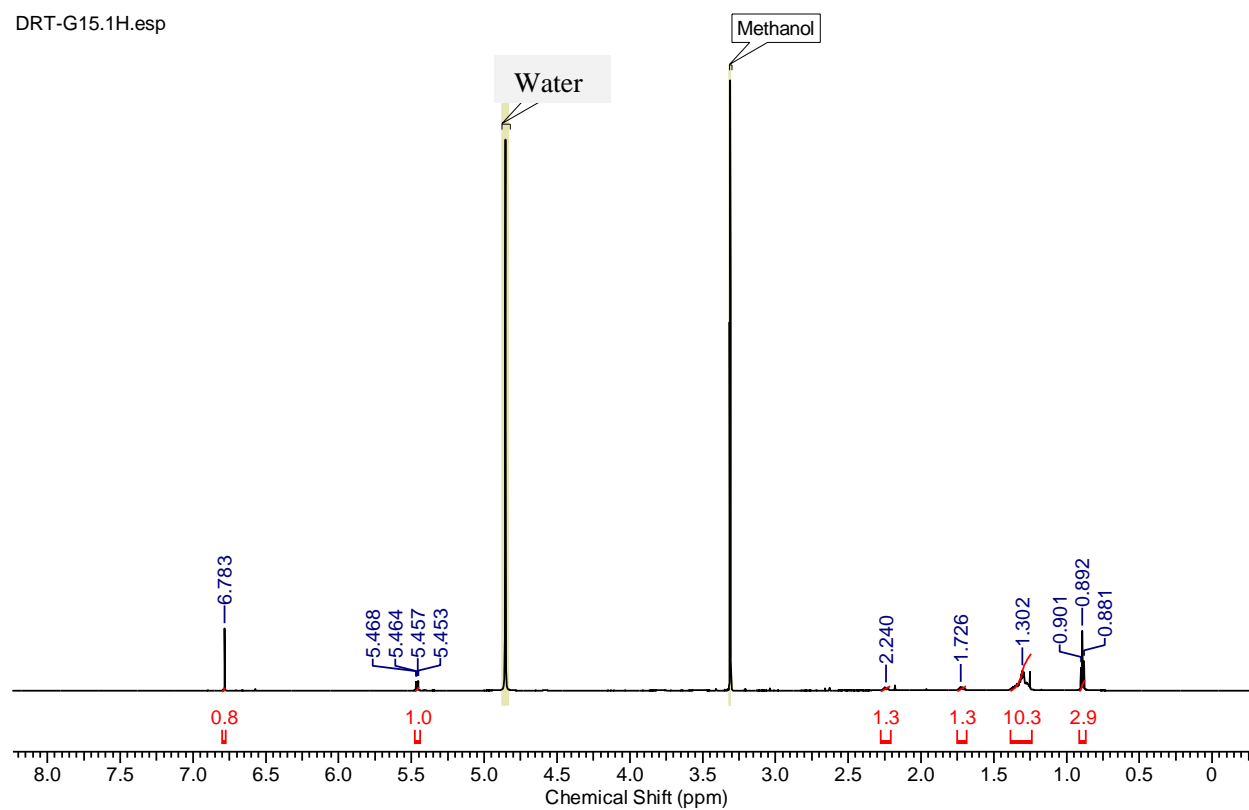
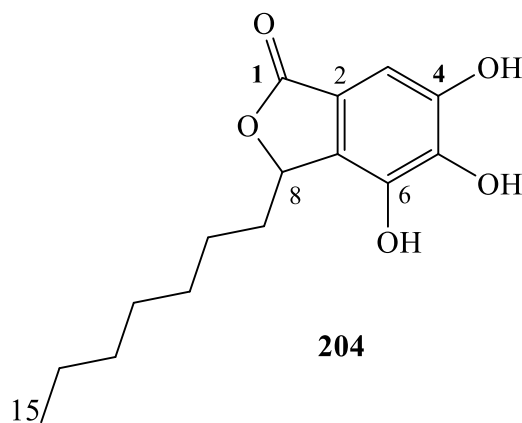


**Figure 87.**  $^1\text{H}$  NMR spectrum ( $\text{CD}_3\text{OD}$ , 500 MHz) of compound **DRT-G15**.



The complete assignments of  $^1\text{H}$  and  $^{13}\text{C}$  NMR for compound DRT-G15 are given in Table 21.

**Table 21.**  $^1\text{H}$  and  $^{13}\text{C}$  NMR data ( $\text{CD}_3\text{OD}$ ) of compound **DRT-G15**.

Position	Compound DRT-G15	
	$\delta_{\text{H}}$ (nH, <i>mult.</i> , <i>J</i> in Hz)	* $\delta_{\text{C}}$
1	-	174.5
2	-	131.4
3	6.78 (1H, <i>s</i> )	102.6
4	-	146.2
5	-	141.2
6	-	148.6
7	-	117.2
8	5.46 (1H, <i>dd</i> , 2.0, 2.0)	81.7
9a	2.24 (1H, <i>m</i> )	33.5
9b	1.72 (1H, <i>m</i> )	
10	1.25-1.38 (2H, overlapped)	25.3
11	1.25-1.38 (2H, overlapped)	30.0
12	1.25-1.38 (2H, overlapped)	29.9
13	1.25-1.38 (2H, overlapped)	32.3
14	1.25-1.38 (2H, overlapped)	23.5
15	0.89 (3H, <i>t</i> , 4.5, 5.5)	14.2

\*The estimated chemical shifts for  $^{13}\text{C}$  were read in the HSQC-DEPT spectrum as the  $^{13}\text{C}$  NMR spectrum of the compound was not recorded; *mult.* = multiplicity.

### II.4.3. Secondary metabolites from *Diaporthe* sp.1.nov

Three known compounds were fully characterized from *Diaporthe* sp.1.nov. Their structures were elucidated on the basis of 1D and 2D-NMR spectra, coupling constants, HRESIMS data, by comparison to the reported data and finally confirmed by LC-MS/MS.

#### II.4.3.1. Identification of compound DLT-G1

Compound **DLT-G1** was obtained as white solid in the mixture of DCM/MeOH (70: 30;), m.p 182-183 °C. Its molecular formula was established as  $\text{C}_{17}\text{H}_{24}\text{O}_4$  from the pseudo molecular ion peak  $[\text{M}+\text{H}]^+$  at  $m/z$  293.1744 (calcd for  $\text{C}_{17}\text{H}_{24}\text{O}_4$ : 293.1755) and consistent with six bond equivalents.

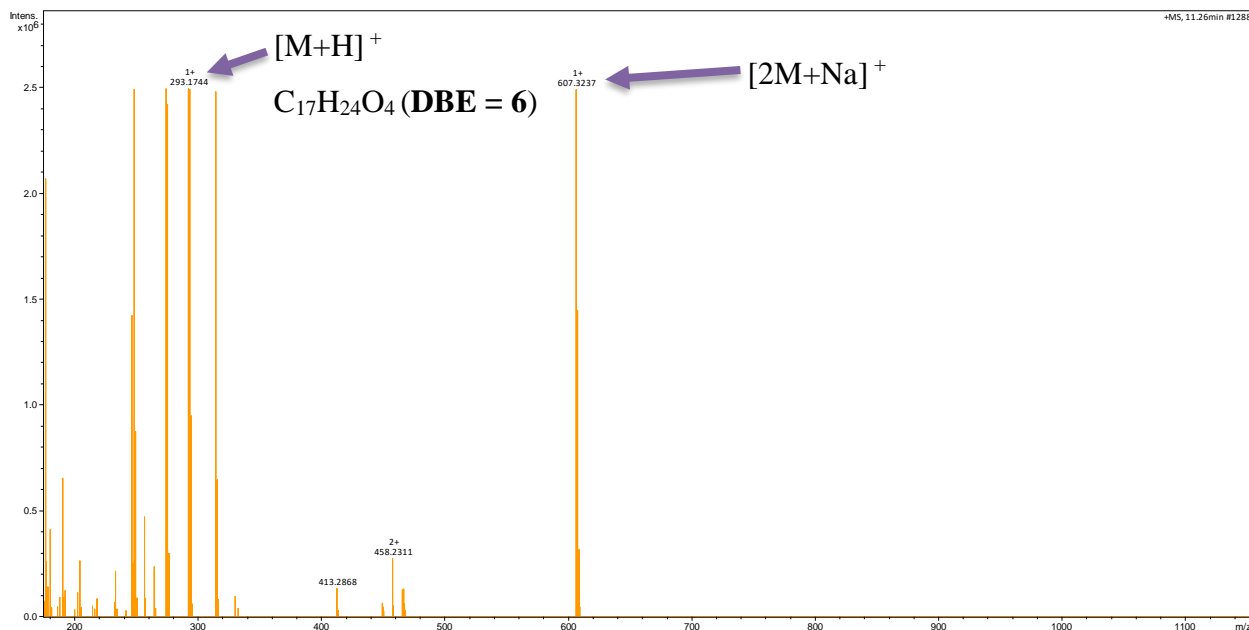


**Figure 88** (+)-HR-ESI-MS of compound **DLT-G1**.

The  $^1H$  NMR spectrum (Fig. 89) of compound **DLT-G1** displayed two meta-couple aromatic signals at  $\delta_c$  6.27 (1H, *d*, 1.5, H-2) and  $\delta_c$  6.21 (1H, *d*, 1.5, H-4) suggesting their meta- disposition. Furthermore, the  $^1H$  NMR spectrum also displayed an oxymethine proton at  $\delta_H$  5.07 (1H, *m*, H-8); one methoxymethyl signals at  $\delta_H$  3.33; seven methylene proton signals in the range  $\delta_H$  2.41-1.35 ppm. The signals for the remaining close methylene protons were observed between  $\delta_H$  1.24- 1.18 (H-12; H-11; H-10), one methyl signal at  $\delta_H$  1.21 (3H, *m*, 6.45, H-13) and an aromatic hydroxyl signal at  $\delta_H$  9.67 (1H, *s*).

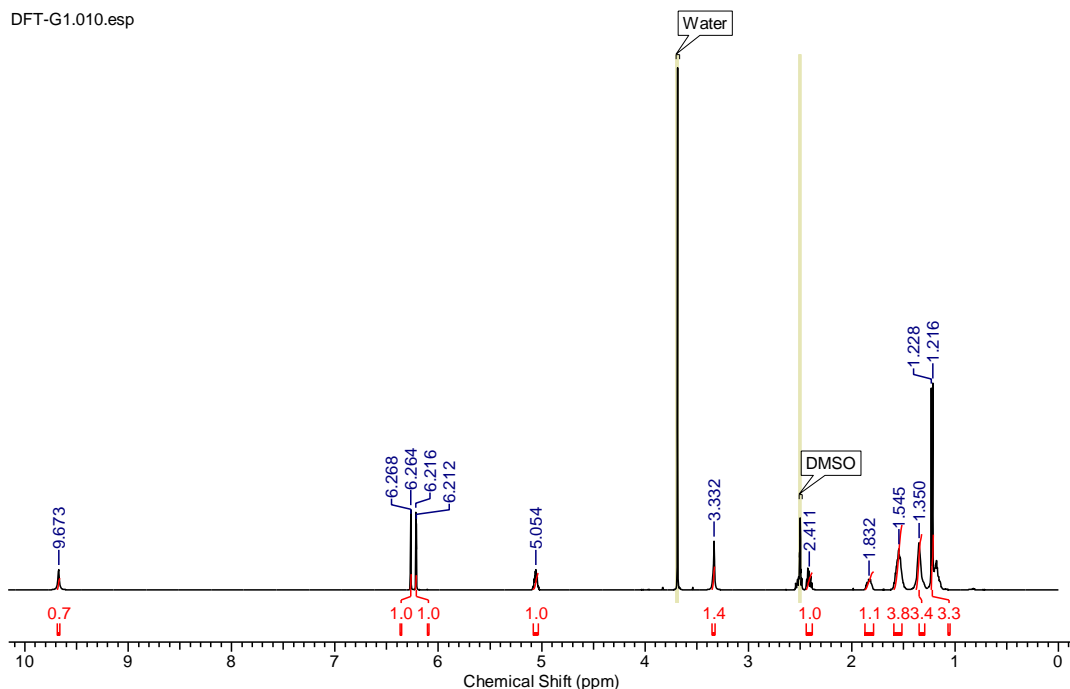


**Figure 89.**  $^1\text{H}$  NMR Spectrum (DMSO- $d_6$ , 500 MHz) of compound **DLT-G1**.

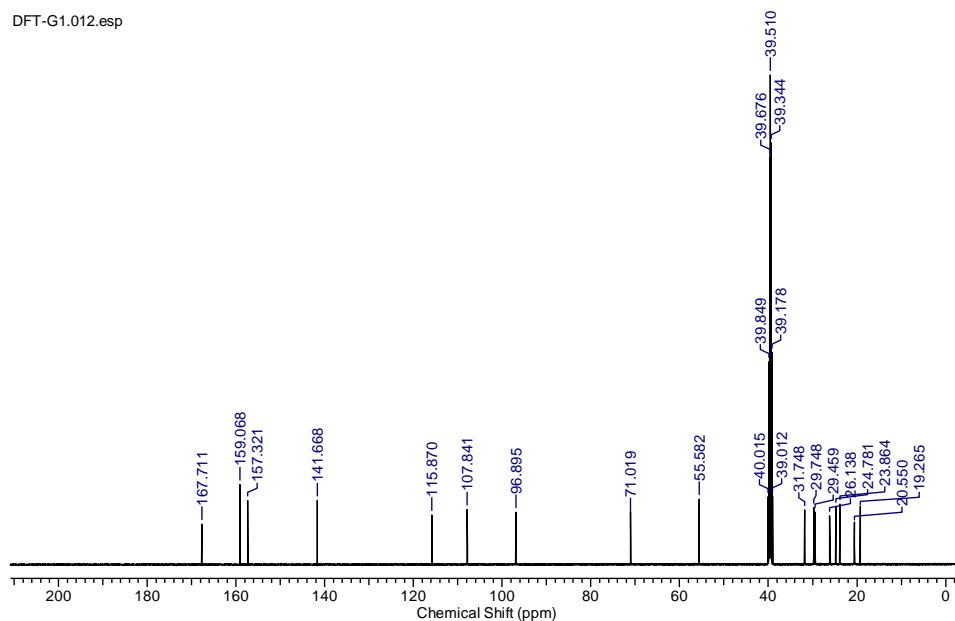
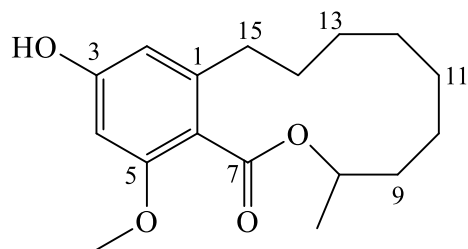


**Figure 90.**  $^{13}\text{C}$  NMR (DMSO- $d_6$ , 125 MHz) spectrum of compound **DLT-G1**.

Comparison of the  $^1\text{H}$  and  $^{13}\text{C}$  NMR data of **DFT-G1** with those described in the literature confirmed that the structure of **DFT-G1** was lasiodiplodin (**205**), a macrolide compound which has been previously reported to be isolated from the endophytic fungal *Lasiodiplodia* sp. 318 (Huang *et al.*, 2016).



205

The complete assignment of  $^{13}\text{C}$  and  $^1\text{H}$  NMR for compound **DLT-G1** is given in [Table 22](#) below.

**Table 22.**  $^1\text{H}$  and  $^{13}\text{C}$  NMR data (DMSO- $d_6$ ) of compound DLT-G1.

Position	Compound DLT-G1	
	$\delta_{\text{H}}$ (nH, mult., J in Hz)	* $\delta_{\text{C}}$
1	-	141.7
2	6.21 (1H, <i>d</i> , 1.5)	107.8
3	-	159.0
4	6.27 (1H, <i>d</i> , 1.5)	96.9
5	-	157.3
6	-	115.8
7	-	167.7
8	5.07 (1H, <i>m</i> )	71.0
9	1.83 (1H, <i>m</i> )	31.7
	1.54 (1H, <i>m</i> )	
10	1.18 (1H, <i>m</i> )	20.5
	1.34 (1H, <i>m</i> )	
11	1.21 (1H, <i>m</i> )	23.9
	1.22 (1H, <i>m</i> )	
12	1.23 (2H, <i>m</i> )	24.8
13	1.23 (2H, <i>m</i> )	26.1
14	1.54 (2H, <i>m</i> )	29.4
15	2.41 (2H, <i>m</i> )	29.7
16	3.66 (3H, <i>s</i> )	55.5
17	1.21 (3H, <i>d</i> , 6.5)	19.3
3-OH	9.67 (1H, <i>s</i> )	-

#### II.4.3.2. Identification of compound DLT-G2

Compound **DLT-G2**, m.p 95-96 °C was obtained as white solid in the mixture of DCM/MeOH (65:35;). Its molecular formula was established as  $\text{C}_6\text{H}_{14}\text{O}_6$  from the pseudo molecular ion peak  $[\text{M}+\text{H}]^+$  at  $m/z$  183.0864 (calcd for  $\text{C}_6\text{H}_{14}\text{O}_6$ : 183.0867) and consistent with zero double bond equivalent ([Fig. 91](#)).

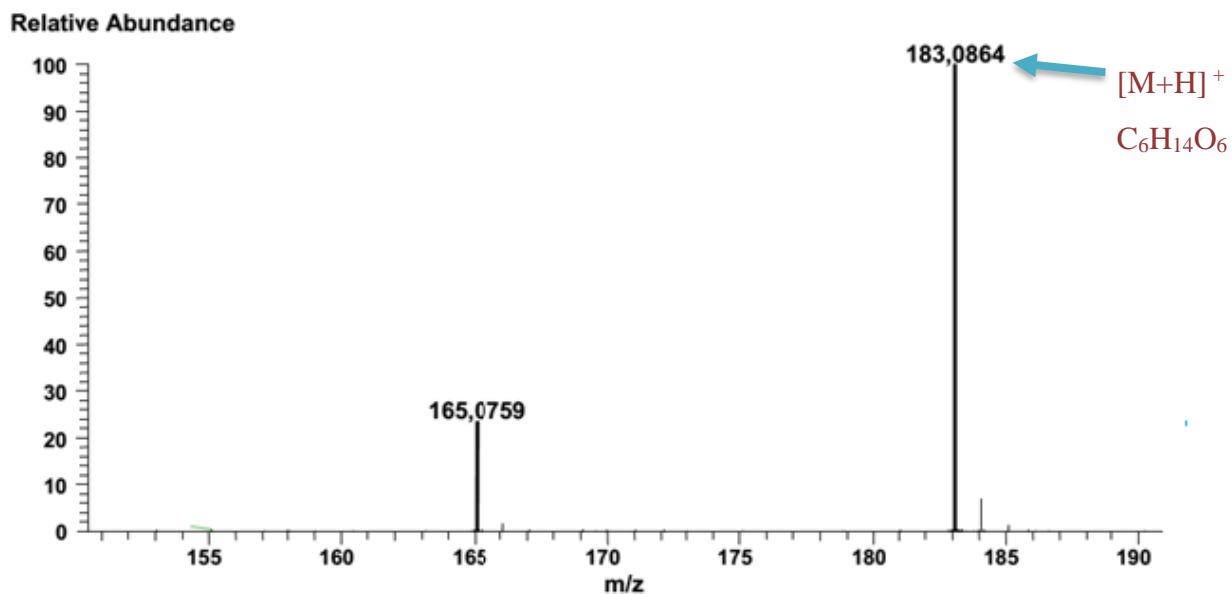


**Figure 91.** (+)-HR-ESI-MS of compound **DLT-G2**.

The  $^1\text{H}$  NMR spectrum of **DLT-G2** (Fig. 92) exhibited the presence of four methines protons at  $\delta_{\text{H}}$  3.60 (1H, m), 3.55 (1H, *t*, 8.0, 1.5), 3.46 (1H, *m*) and 3.38 (1H, m). The  $^1\text{H}$  NMR spectrum also displayed signals of four hydroxyl group at  $\delta_{\text{H}}$  4.40 (1H, *d*, 5.5), 4.32 (1H, *t*, 1.5; 8.0), 4.12 (1H, *d*; 1.5), and hydroxyl group.

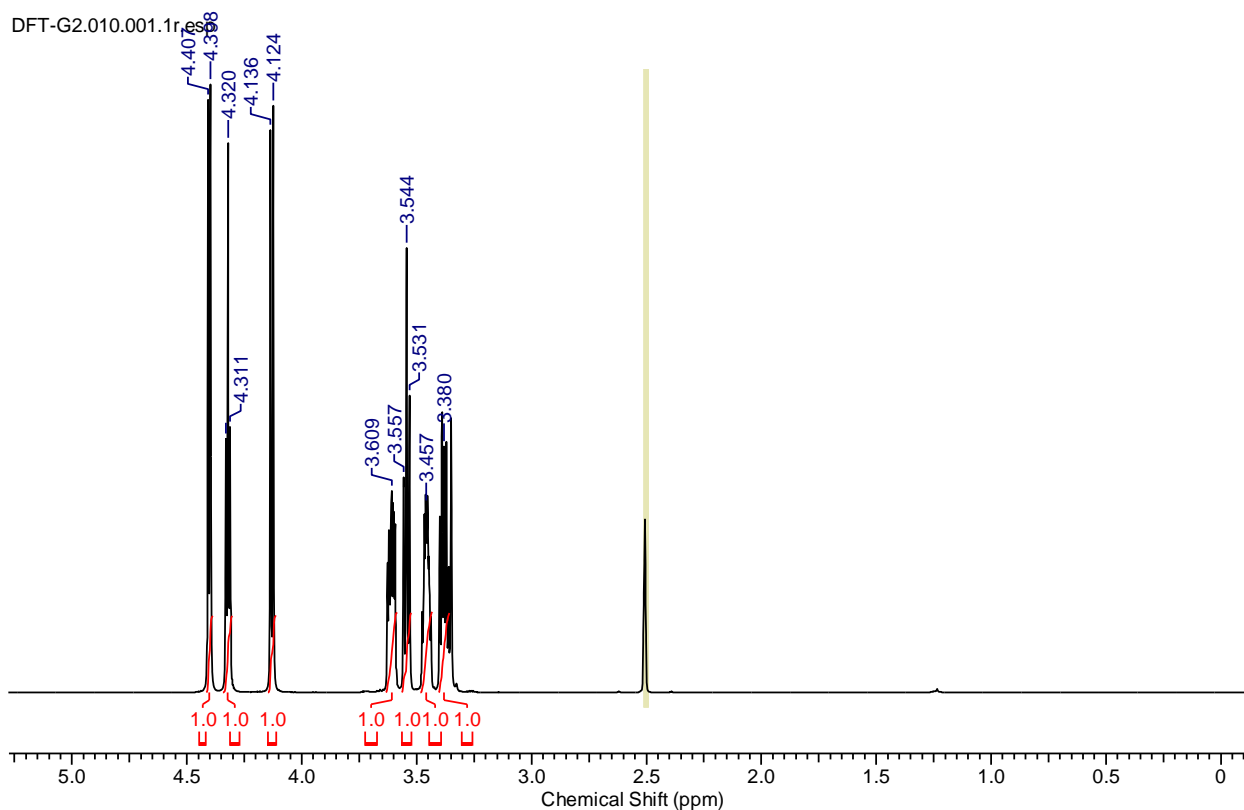


**Figure 92.**  $^1\text{H}$  NMR spectrum ( $\text{DMSO-}d_6$ , 500 MHz) of compound **DLT-G2**.

Moreover, the  $^{13}\text{C}$  NMR spectrum (**Fig. 93**) displayed a total of three carbons among which two oxymethines at  $\delta_c$  71.7 and 70.1 and one oxymethylene carbon at  $\delta_c$  64.3 (quaternary  $\text{sp}^2$ ).  $^1\text{H}$  NMR and  $^{13}\text{C}$  NMR spectra let to establish the molecular formula  $\text{C}_3\text{H}_7\text{O}_3$  corresponding to  $M:95\text{g/mol}$ . This let to confirm the presence of the symmetry in compound **DLT-G2**

DFT-G2.010.001.1r.esp

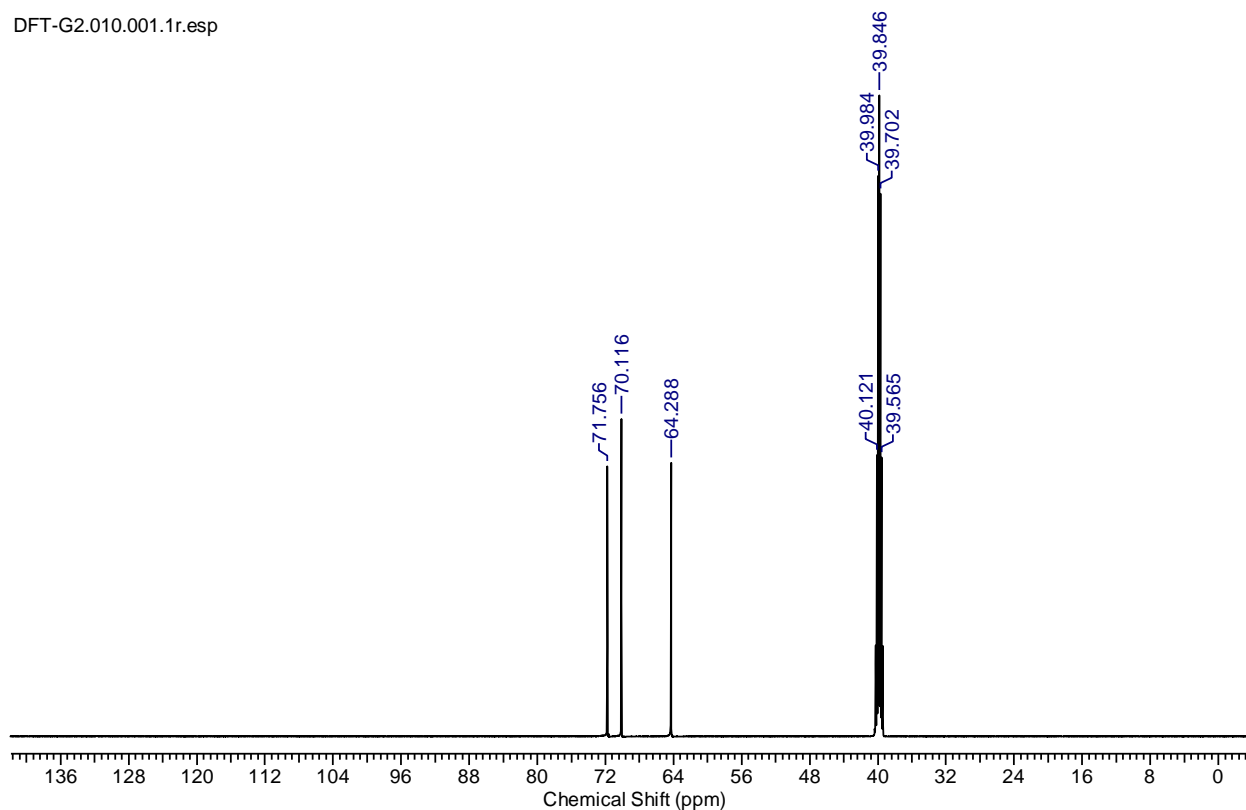
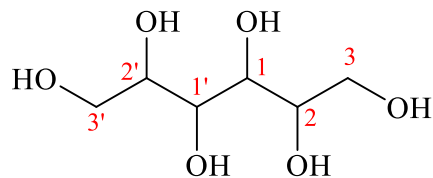


**Figure 93.**  $^{13}\text{C}$  NMR spectrum (DMSO- $d_6$ , 125 MHz) of compound **DLT-G2**.

The  $^1\text{H}$  and  $^{13}\text{C}$ -NMR spectral data were found to be identical to published data of sorbitol and thus proved the structure of compound **DLT-G2** was identified as sorbitol (**207**), a known sugar alcohol previously isolated from the endophytic fungal *puccinia graminis tritici* (Macleand et scott, 1976).



**206**

The complete assignment of  $^{13}\text{C}$  and  $^1\text{H}$  NMR for compound **DLT-G2** is given in Table **23** below.

**Table 23.**  $^1\text{H}$  and  $^{13}\text{C}$ -NMR (DMSO- $d_6$ ).data of compound **DLT-G2**.

Compound DLT-G2		
Position	$\delta_{\text{H}}$ (nH, <i>mult.</i> , <i>J</i> in Hz)	$\delta_{\text{C}}$
1	3.46 (1H, <i>m</i> )	70.5
2	3.55 (1H, <i>d</i> , 1.5, 2.5)	72.2
3	3.61 (1H, <i>m</i> )	64.8
	4.12 (1H, <i>d</i> , 1.5)	
1'	3.46 (1H, <i>d</i> , 1.5)	70.5
2'	3.55 (1H, <i>d</i> , 1.5, 2.5)	72.2
3'	3.61 (1H, <i>m</i> )	64.8
	4.12 (1H, <i>d</i> , 1.5)	
1-OH	4.40 (1H, <i>brs</i> )	-
2-OH	4.32 (1H, <i>m</i> )	-
3-OH	4.12 (1H, <i>m</i> )	-
1'-OH	4.40 (1H, <i>brs</i> )	-
2'-OH	4.32 (1H, <i>m</i> )	-
3'-OH	4.12 (1H, <i>m</i> )	-

#### II.4.3.3. Identification of compound DLT-G3

Compound **DLT-G3** was obtained as a white amorphous powder in the mixture of DCM/MeOH (7.5:2.5). Its HR-MS-ESI data (Fig. 94) indicated the molecular formula  $\text{C}_{14}\text{H}_{10}\text{O}_6$  from the pseudo molecular ion peak  $[\text{M}+\text{H}]^+$  at  $m/z$  275.0550 (calcd for  $\text{C}_{14}\text{H}_{10}\text{O}_6$ : 275.0554) consist of ten double bond equivalent.

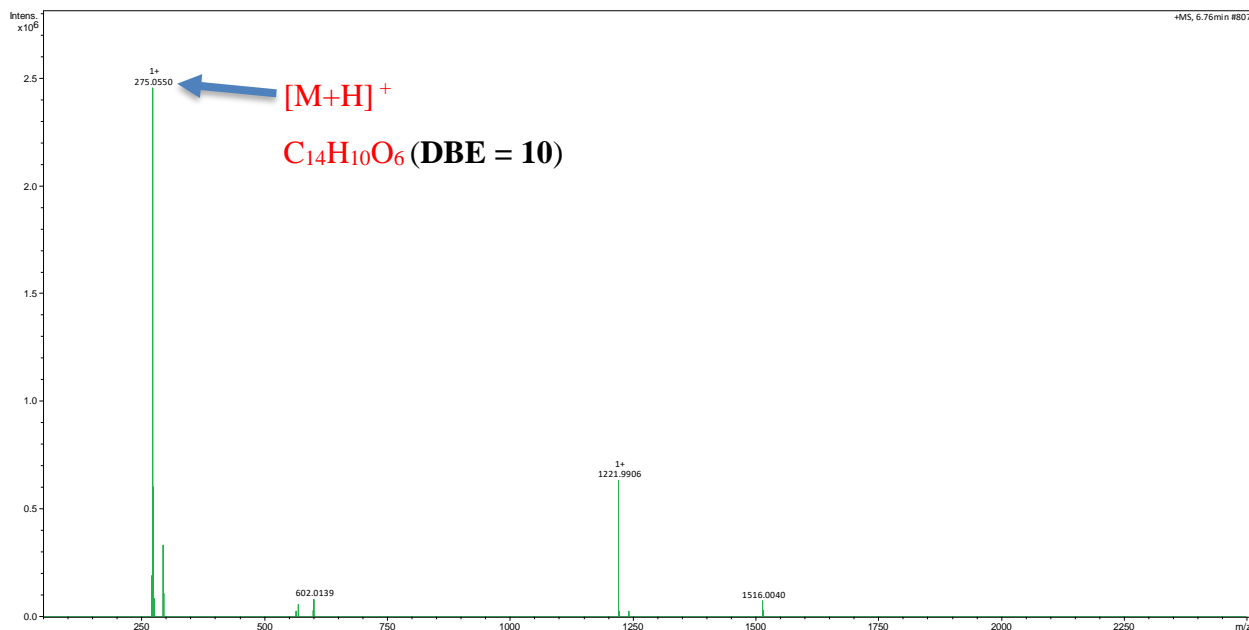


**Figure 94.** (+)-HR-ESI-MS of compound DLT-G3.

The <sup>1</sup>H NMR (Fig. 95) spectrum indicated the presence of two meta-coupled aromatic proton signals at  $\delta_{\text{H}}$  6.35 (1H, *d*, 1.98, H-8) and at  $\delta_{\text{H}}$  7.30 (1H, *d*, 1.83, H-10) and the aromatic methyl proton signal at  $\delta_{\text{H}}$  2.67 (1H, *s*). Additionally, it was observed the single aromatic proton signal at  $\delta_{\text{H}}$  6.68 (1H, *s*, H-4) suggesting that the second aromatic ring system was pentasubstituted.

DFT-G3.1H.esp

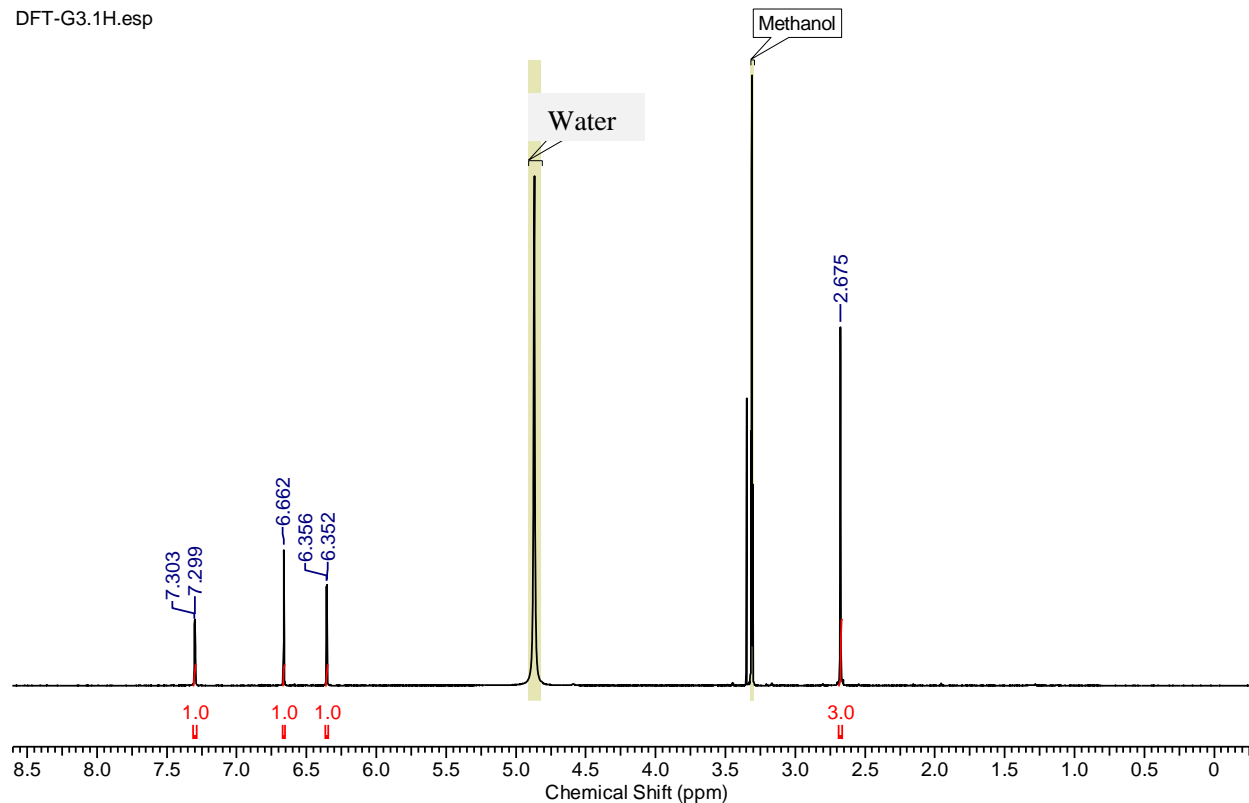


**Figure 95**  $^1\text{H}$  NMR Spectrum ( $\text{CD}_3\text{OD}$ , 500 MHz) of compound **DLT-G3**.

Based on the above investigation, compound DLT-G3 was determined to be 2-hydroxyalternariol (**207**) (Chapla *et al.*, 2014), a known compound which has been previously reported to be isolated from *Phomopsis* sp.

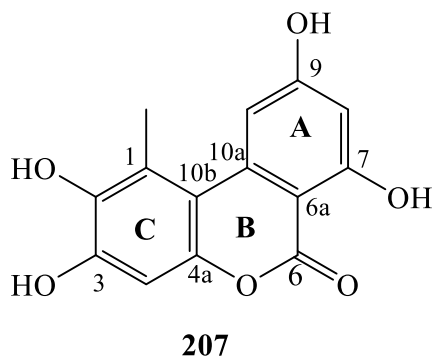


Table **24** shows the complete assignments of  $^{13}\text{C}$  and  $^1\text{H}$  NMR for compound **DLT-G3**.

**Table 24.**  $^1\text{H}$  and  $^{13}\text{C}$  NMR ( $\text{CD}_3\text{OD}$ ).data of compound **DLT-G3**.

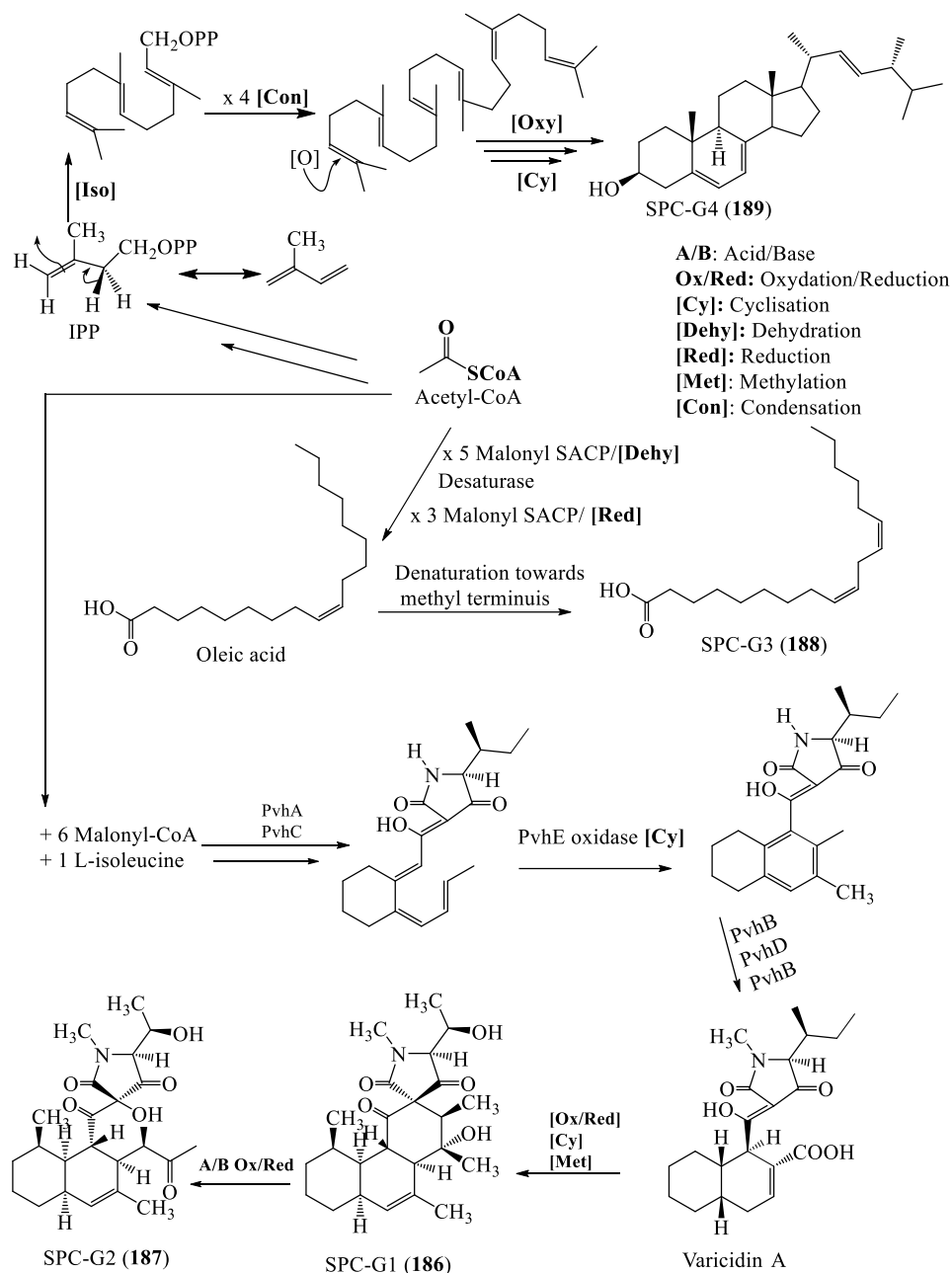
Compound DLT-G3		
Position	$\delta_{\text{H}}$ (nH, <i>mult.</i> , <i>J</i> in Hz)	* $\delta_{\text{C}}$
1	-	122.9
2	-	142.9
3	-	148.3
4	6.66 (1H, <i>s</i> )	101.6
4a	-	146.8
6	-	167.6
6a	-	99.3
7	-	166.3
8	7.30 (1H, <i>d</i> , 2.0)	101.6
9	-	166.5
10	6.35 (1H, <i>d</i> , 2.0)	105.3
10a	-	140.5
10b	-	110.9
1-CH <sub>3</sub>	2.67 (1H, <i>s</i> )	16.0

\*The estimated chemical shifts for  $^{13}\text{C}$  were read in the HSQC-DEPT spectrum as the  $^{13}\text{C}$  NMR spectrum of the compound was not recorded; *mult* = multiplicity.

## II.5. Biogenesis relationship of isolated compounds

### II.5.1. The hypothesis of the biogenetic relationship between the isolated compounds from *Simplicillium subtropicum*

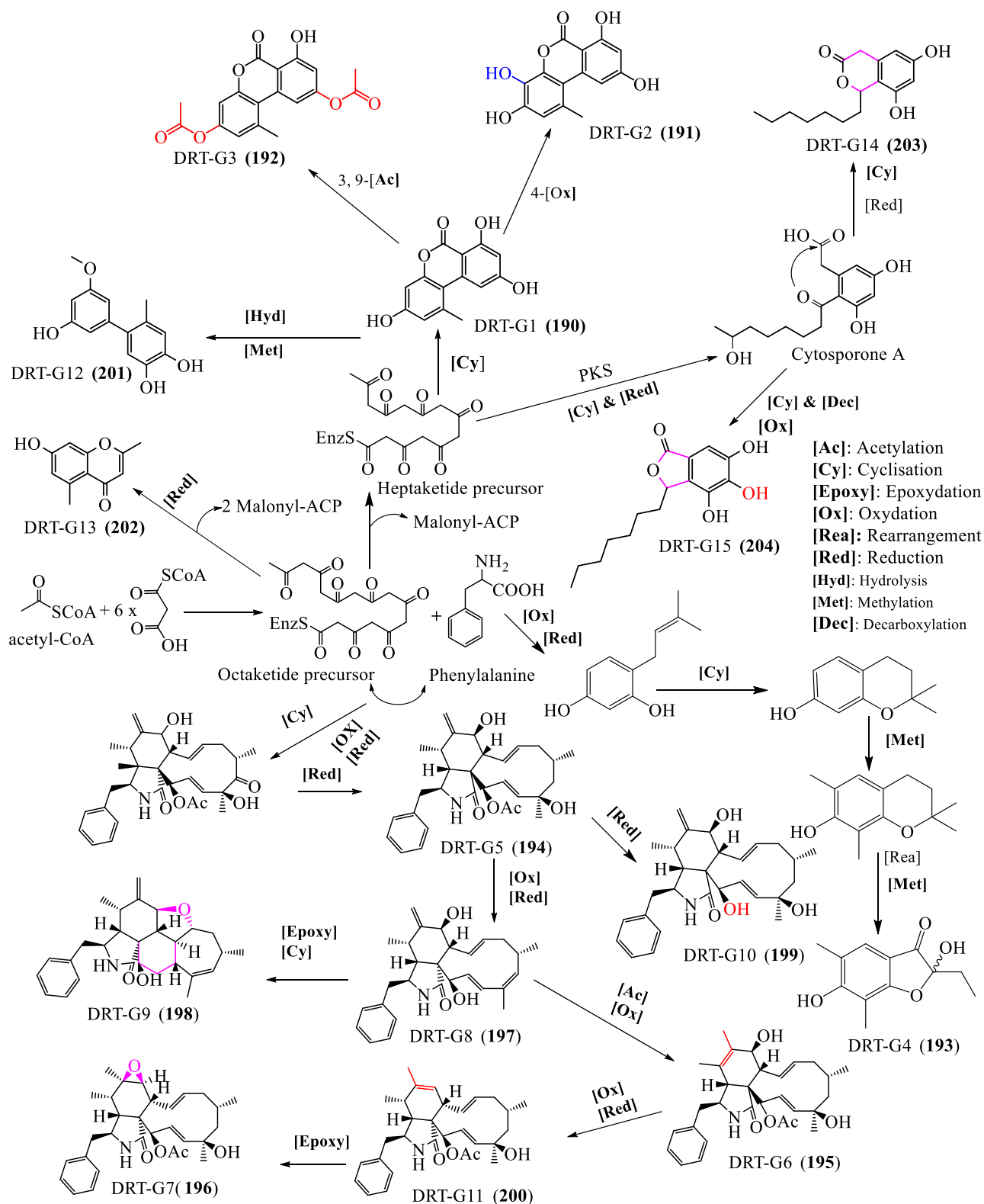
The structural determination of secondary metabolites isolated from *Simplicillium subtropicum* shows that these compounds mainly belong to Acetyl-CoA unit. [Scheme 9](#) displays a hypothesis of possible biosynthetic pathway of the isolated compounds.



**Scheme 9.** Proposed biogenetic relationship of the isolated from *Simplicillium subtropicum*.

### II.5.2. The hypothesis of the biogenesis of the isolated compounds from *Diaporthe* sp.2.nov

The structural determination of secondary metabolites isolated from *Diaporthe* sp.2.nov shows that these compounds mainly belong to the polyketide unit. [Scheme 10](#) displays a hypothesis of possible biosynthetic pathway of the major isolated ones.

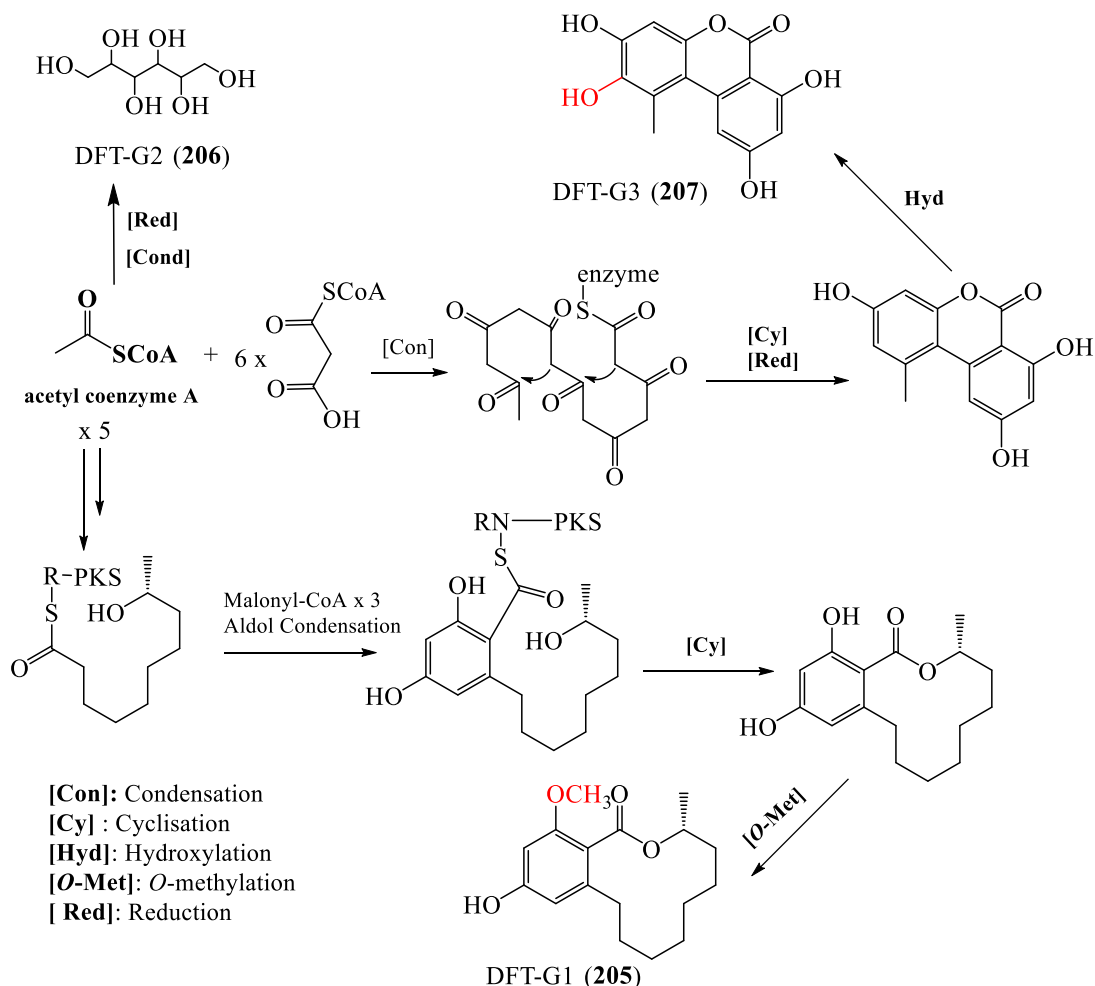


**Scheme 10.** Proposed biogenetic relationship of the isolated Compounds from *Diaporthe* sp.2.nov.

### II.5.3. The hypothesis of the biogenetic relationship between the isolated compounds from *Diaporthe* sp.1.nov

The structural determination of compounds isolated from the two *Diaporthe* shows that these compounds mainly belong Acetyl-CoA unit.

The hypothesis of possible biosynthetic pathway of the major isolated ones is shown in Scheme 11.



**Scheme 11.** Proposed biogenetic relationship of the isolated compounds from *Diaporthe* sp.1.nov.

## II.6. Biological activity of isolated compounds

### II.6.1. Antimicrobial activities of selected isolated compounds

The *in vitro* antibacterial and antifungal activities of the isolated polyketides simplicilone A (186) and B(187) were determined in a standard microdilution assay using the Gram-positive

bacteria *Bacillus subtilis* DSM10, *Staphylococcus aureus* DSM 346, *Micrococcus luteus* DSM 1790, *Mycobacterium smegmatis* ATCC 700084; the Gram-negative bacteria *Chromobacterium violaceum* DSM 30191, *Escherichia coli* DSM 1116, *Pseudomonas aeruginosa* PA14 and the fungi *Candida albicans* DSM 1665, *Schizosaccharomyces pombe* DSM70572, *Mucor hiemalis* DSM 2656, *Pichia anomala* DSM 6766, *Rhodotorula glutinis* DSM 10134 as test organisms as previously described by [Becker et al., 2020b](#) The broad-spectrum antibiotic ciprofloxacin and antifungal cycloheximide at 1.5 mg/mL. However, both compounds did not show any antibacterial and antifungal activities against the above organisms up to 67 µg/mL.

Some compounds and the crude extracts from the solid medium of *Diaporthe* sp.1.nov (**F18**) and *Diaporthe* sp.2.nov (**R38**) were tested for their antibacterial activities using the broth microdilution method by determining the MIC values against *Escherichia coli* ATCC 95922 (**EC**) ; *Shigella flexneri* NR518(**SF**); *Salmonella typhi* ATCC 19430 (**ST**); *Shigella dysenteriae* (**SHD**); *Salmonella enterica muenchen* (**SE**); *Staphylococcus aureus* ATCC 25923 (**SAt**), *Staphylococcus aureus* (**SA**); *Klebsiella pneumoniae* (**KP**); *Enterobacter aerogenes* (**EA**); *Enterobacter cloacae* (**ECI**).

Let's recall that activity is considered to be significant if MIC values are below 10 µg/mL for pure compounds, moderate when  $10 < \text{MIC} < 125$  µg/mL, and inactive when  $\text{MIC} > 125$  µg/mL ([Ambadiang et al., 2020](#)). However, for extracts and fractions, the activity is considered significant if these MIC values are below 100 µg/mL, moderately active when  $100 \leq \text{MIC} \leq 625$  µg/mL and poorly active when  $\text{MIC} > 625$  µg/mL. Results are provided in [Table 25](#).

**Table 25.** Antibacterial activities of extracts and selected isolated compounds.

Extracts & compounds	<i>EC</i>	<i>SF S.</i>	<i>ST</i>	<i>SHD</i>	<i>SE</i>	<i>S At</i>	<i>SA</i>	<i>K P</i>	<i>EA</i>	<i>ECl</i>
	<b>MIC (<math>\mu\text{g/mL}</math>)</b>									
Extract of <b>R<sub>38</sub></b>	<b>250</b>	-	-	<b>250</b>	-	-	-	-	-	-
Extract of <b>F<sub>18</sub></b>	<b>15.6</b>	-	-	-	<b>125</b>	-	-	-	-	<b>250</b>
Sorbitol ( <b>206</b> )	-	-	-	-	-	-	-	-	-	-
Lasiodiplodin ( <b>205</b> )	<b>62.5</b>	-	-	-	-	-	-	-	-	<b>62.5</b>
2-hydroxyalternariol ( <b>207</b> )	<b>62.5</b>	-	-	-	-	-	-	-	-	-
Ciprofloxacin*	0.078	0.321	0.156	0.078	0.321	0.078	0.321	0.078	0.321	0.078
Gentamicin*	0.039	0.039	0.039	0.078	0.15	0.039	0.039	0.078	0.039	0.039

MIC: Minimum inhibitory concentration in  $\mu\text{g/mL}$ ; -: not active (at 500  $\mu\text{g/mL}$  for extract, and 125  $\mu\text{g/mL}$  for compounds, \* Positive control in  $\mu\text{g/mL}$ .

*Escherichia coli* ATCC 95922 (**EC**); *Shigella flexneri* NR518(**SF**); *Salmonella typhi* ATCC 19430 (**ST**); *Shigella dysenteriae* (**SHD**); *Salmonella enterica muenchen* (**SE**); *Staphylococcus aureus* ATCC 25923 (**SAt**), *Staphylococcus aureus* (**SA**); *Klebsiella pneumoniae* (**KP**); *Enterobacter aerogenes* (**EA**); *Enterobacter cloacae* (**ECl**)

Therefore Table 25 shows that, compounds **205** and **207** showed moderate antibacterial activity against *Escherichia coli* ATCC 95922 with MIC value of 62.5  $\mu\text{g/mL}$  while compound **205** moderately inhibited the bacterial strain *Enterobacter cloacae* (MIC = 62.5  $\mu\text{g/mL}$ ). However, the crude extract of *Diaporthe* sp.1.nov (**F<sub>18</sub>**) displayed good antibacterial activity against *Escherichia coli* ATCC 95922 with MIC value of 15.6  $\mu\text{g/mL}$  and moderate activity against *Salmonella enterica muenchen* and *Enterobacter cloacae* with MIC values of 125  $\mu\text{g/mL}$  and 250  $\mu\text{g/mL}$  respectively. The crude extract of **R<sub>38</sub>** showed moderate antibacterial activity against *Escherichia coli* ATCC 95922 and *Shigella dysenteriae* with MIC value of 250  $\mu\text{g/mL}$  and 250  $\mu\text{g/mL}$ .

These results were in good agreement with secondary metabolites published in the literature on previously isolated *Diaporthe* and its asexual state *phomopsis* genus (Xu et al., 2021).

### II.6.2. Cytotoxicity activity

The *in vitro* cytotoxicity (IC<sub>50</sub>) of compounds 186 and 187 was investigated against the established cancers mouse fibroblast cell line L929 (DSMZ no. ACC 2) and KB3.1 using the 3-(4,5-dimethylthiazol-2-yl)-2,5-diphenyltetrazolium bromide (MTT) method in 96-well

microplates for tissue cultures. Epothilone B was used as reference. Table 26 below presented the results.

**Table 26.** Cytotoxic activities of 186 and 187 (IC<sub>50</sub> in µg/mL).

Cell line	<b>186</b>	<b>187</b>	Reference (IC <sub>50</sub> )
L929 (IC <sub>50</sub> )	-	-	Epothilone B (6.2x10 <sup>-4</sup> )
KB3.1 (IC <sub>50</sub> )	25	29	Epothilone B (3x10 <sup>-5</sup> )

According to Table 26 above, compounds **186** and **187** displayed cytotoxicity with in vitro cytotoxicity (IC<sub>50</sub>) values of 25 and 29 µg/mL, respectively, against the cervix carcinoma cell line KB3.1, but were inactive against the murine fibroblast cell line L929.

## GENERAL CONCLUSION AND OUTLOOK

The present work dealt with the isolation and chemical investigation of endophytic fungi harboured in *Duguetia* and *Trema* species. For this purpose, we have chosen *Duguetia staudtii* and *Trema guineensis*, the choice was motivated by their bioactive compounds previously reported with a high level of chemical diversity. Moreover, no work was previously reported on the endophytic fungi associated with the two plants. Our objective was to search for antibacterial and cytotoxic secondary metabolites from selected endophytic fungi associated with *Duguetia Staudtii* and *Trema guineensis*. Our studies led to the isolation of twenty-four endophytes fungi from stem bark, leaves and roots of these plants. Three of them, labelled SPC3, F<sub>18</sub> and R<sub>38</sub> were chosen for further studies on the basis of the LC-MS and/or antibacterial screening of their crude extracts from the small-scale culture. These endophytes were identified to be *Simplicillium subtropicum*. (SPC3) and two undescribed *Diaporthe* species: *Diaporthe* sp.1.nov (F<sub>18</sub>) and *Diaporthe* sp.2.nov (R<sub>38</sub>). The chemical investigation of their crude extracts afforded twenty-two compounds using different chromatographic techniques (LC-MS, CC, TLC, preparative HPLC). The structures of these compounds were fully elucidated by means of usual spectroscopic methods namely UV, IR, MS, 1D and 2D NMR; while others were confirmed by comparison of their spectral data with those previously reported in the literature. All were entirely characterized and found to belong to different class of compounds. Among the isolated compounds, four were found to be new derivatives viz. simplicilones A and B, 3, 9- diacetylalternariol and diapobenzofuranone while eighteen which have been previously reported were identified as: alternariol; 2-hydroxyalternariol; 4-hydroxyalternariol; cytochalasins, H, N, J, J<sub>2</sub>, J<sub>3</sub>; epoxycytochalasin H, cytochalasin RKS-1778, ergosterol; linoleic acid, 5'-methoxy-6-methyl-biphenyl-3,4,3'-triol, 2,5-dimethyl-7-hydroxychromone, cytosporone C and E; lasiodiplodin and sorbitol.

The selected isolated compounds were tested for their antimicrobial and cytotoxic activities. It emerges that some compounds showed moderate antibacterial activity with an MIC value of 62.5 µg/mL while the new isolated polyketides displayed cytotoxicity with *in vitro* cytotoxicity (IC<sub>50</sub>) values of 25 and 29 µg/mL respectively, against the cervix carcinoma cell line KB3.1. The studied *Diaporthe* strains have been found to be riche niche of biphenylpyrones and cytochalasins which can be the chemotaxonomic markers of these strains. Our outlook at the end of this research works consists into four (3) major points:

- Optimize the production of biphenylpyranones and cytochalasins found in the isolated *Diaporthe* strains and give hints in regards to their structure-activity relationship (SAR)
- Carry out a in vivo cytotoxicity of simplicilones A and B
- Carry out the bioassays of markers using others organisms and cells lines

---

# **CHAPTER III: EXPERIMENTAL PART**

### III. 1. GENERAL EXPERIMENTAL PROCEDURES

Silica gel 60 (230–400 mesh) were used as adsorbents for flash and column chromatography, respectively. The semi-pure compounds were finally purified successively over Sephadex LH-20 (bead size 25–100  $\mu\text{m}$ , Sigma-Aldrich) with  $\text{CH}_2\text{Cl}_2/\text{MeOH}$  (1:1, v/v), semi-preparative and preparative HPLC systems on reverse and normal phases (Büchi, Pure C-850, 2020, Switzerland). VP Nucleodur 100-5 C18ec column (250  $\times$  21 mm, 5  $\mu\text{m}$ : Machery-Nagel, Düren, Germany).

Merck TLC plates (silica gel 60 F254) were used for the detection of the purity of compounds. Melting points were determined with Gallekamp apparatus. UV spectra were recorded using a PerkinElmer Lambda 25 UV/Vis spectrometer

The LC-MS chromatograms of all fractions were obtained from an UltiMate 3000 Series UHPLC (Thermo Fischer Scientific, Waltman, MA, USA) utilizing a C18 Acquity UPLC BEH column (1.7  $\mu\text{m}$ , 2.1 $\times$ 50 mm; Waters, Milford, CT, USA) connected to an Amazon speed ESI-Iontrap-MS (Bruker, Billerica, MA, USA). High-resolution electrospray ionization mass spectrometry (HR ESIMS) spectra were recorded with an Agilent 1200 Infinity Series HPLC–UV system (Agilent Technologies, Santa Clara, USA) (column 2.1  $\times$  50 mm, 1.7  $\mu\text{m}$ , C18 Acquity UPLC BEH (waters)).

Optical rotations were recorded in methanol (Uvasol, Merck, Darmstadt, Germany) by using an Anton Paar MCP-150 polarimeter (Seelze, Germany) at 20  $^\circ\text{C}$ . UV/Vis spectra were recorded using methanol (Uvasol, Merck, Darmstadt, Germany) with a Shimadzu UV/Vis 2450 spectrophotometer (Kyoto, Japan).

The NMR experiments of pure compounds were recorded at a temperature 298 K with an Avance III 500 spectrometer (Bruker, Billerica, MA/USA,  $^1\text{H}$ -NMR: 500 MHz and  $^{13}\text{C}$ -NMR: 125 MHz) and an Ascend 700 spectrometer with 5 mm TCI cryoprobe (Bruker, Billerica, MA/USA,  $^1\text{H}$ -NMR: 700 MHz and  $^{13}\text{C}$ -NMR: 175 MHz). Coupling constants are given in hertz (Hz), chemical shifts in parts per million (ppm) were referenced to the solvent signals chloroform-*d* ( $^1\text{H}$ ,  $\delta_{\text{H}} = 7.27$  ppm;  $^{13}\text{C}$ ,  $\delta_{\text{C}} = 77.00$  ppm) and DMSO ( $^1\text{H}$ ,  $\delta_{\text{H}} = 2.50$  ppm;  $^{13}\text{C}$ ,  $\delta_{\text{C}} = 39.51$  ppm) and  $\text{CD}_3\text{OD}$  ( $^1\text{H}$ ,  $\delta_{\text{H}} = 4.78$  & 3.31 ppm;  $^{13}\text{C}$ ,  $\delta_{\text{C}} = 49.15$  ppm).

### III.1.1. Plant material

Different parts of *Duguetia staudtii* (Engl. and Diels) Chatrou were collected in July 2017, at the Dja rain forest in the locality of Lomié-Bertoua, East Region of Cameroon. The plant material was identified by Mr. Victor Nana, a botanist at the National Herbarium of Cameroon where a voucher specimen was deposited under the number 52711HNC. The different parts (leaves, bark and roots) of *Trema guineensis* (Schumach & Thonn) were collected in January 2019, at the mount Kala, Centre region of Cameroon and the plant material was identified under voucher number 42166HNC.

### III.1.2. Fungal material

The endophytic fungi *Simplicillium subtropicum*; *Diaporthe* sp.1.nov, F<sub>1</sub>.8, *Diaporthe* sp. 2.nov, R<sub>3</sub>.8 isolated from two Cameroonian medicinal plants *Duguetia Staudtii* and *Trema guineensis* were investigated in this study.

#### III.1.2.1. Isolation and purification of endophytic fungi

Fungal endophytes were isolated the same day, in most cases only two days after plant materials were collected. The isolation and purification of all the endophytes from the healthy fresh Leaves, barks, roots of plants were done according to the method previously reported (Talontsi et al., 2014; Petrini et al., 1987) with some modification. These steps were done at EPlaNProLab, HTTC, Yaounde. Briefly, Plant samples were washed under running tap water and obvious dirt, epiphytic mosses and algae cautiously removed. Pieces of approximately 3 cm of shoot and 1 cm<sup>2</sup> of leaves stem bark and roots including the midrib were prepared for surface sterilization. Samples were surface sterilized by immersion in 70 % ethanol for 1 minute, followed by 5 minutes in 3 % NaOCl solution and again 70 % ethanol for one minute to remove excess hypochlorite solution. These Leaves, barks, roots were then rinsed three times in sterile distilled water and dried on sterile tissue paper under a laminar flow hood. Samples were subsequently placed on the sterilized tissue to evaporate the remaining water. To check for successful surface sterilization, leaves, bark and roots were rolled over and both sides of the leaf cuttings were imprinted on petri dishes containing the culture medium PDA, respectively. Petri dishes with imprints were sealed, incubated at room 28°C and checked daily for fungal growth. If no fungal colonies developed, surface sterilization was considered successful. For each collected plant organ several pieces were used for isolation and small segments of the parts of each plant were transferred to Petri dishes containing potato dextrose agar (PDA) supplemented with 100 mg/mL penicillin

---

or/.and ampicillin and incubated at 28 °C. Fungal growth was controlled and documented daily as well as all isolates linked to a positive imprint test disposed After several days hyphae growing from the plants material were transferred to fresh plates with the same medium, incubated again and periodically checked for culture purity. The general procedure used in this study is summarized below (Fig. 96).

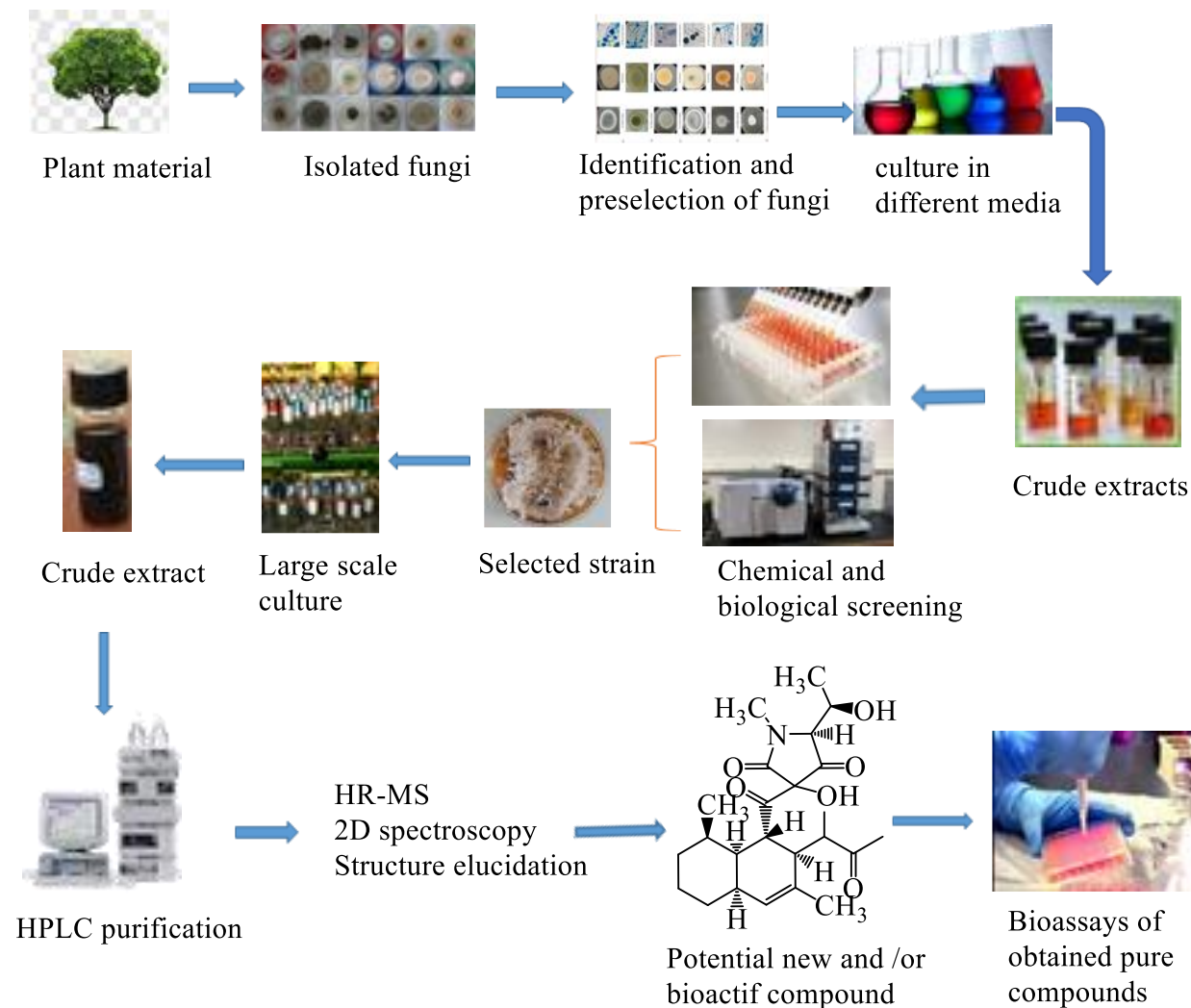


**Figure 96.** General workflow used during this work

#### III.1.2.1.1. Isolation of *Simplicillium subtropicum*. SPC3

The fungus was isolated from the stem bark of *Duguetia staudtii* (Engl. and Diels) Chatrou. *Simplicillium subtropicum*.SPC3 was isolated with five others isolates as follow (Fig. 97):

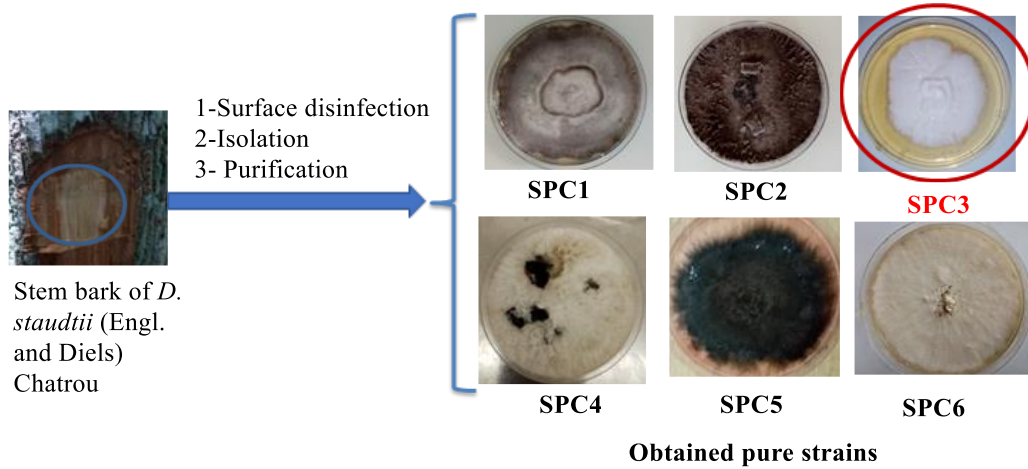


**Figure 97.** *Simplicillium subtropicum*. (SPC3= pure strain).

### III.1.2.1.2. Isolation of *Diaporthe* sp. 1.nov

*Diaporthe* sp.1. nov was isolated from the fresh leaves of the apparently healthy plant of *Trema guineensis* (Schumach & Thonn). It was isolated together with eleven others isolate as follow (Fig. 98):

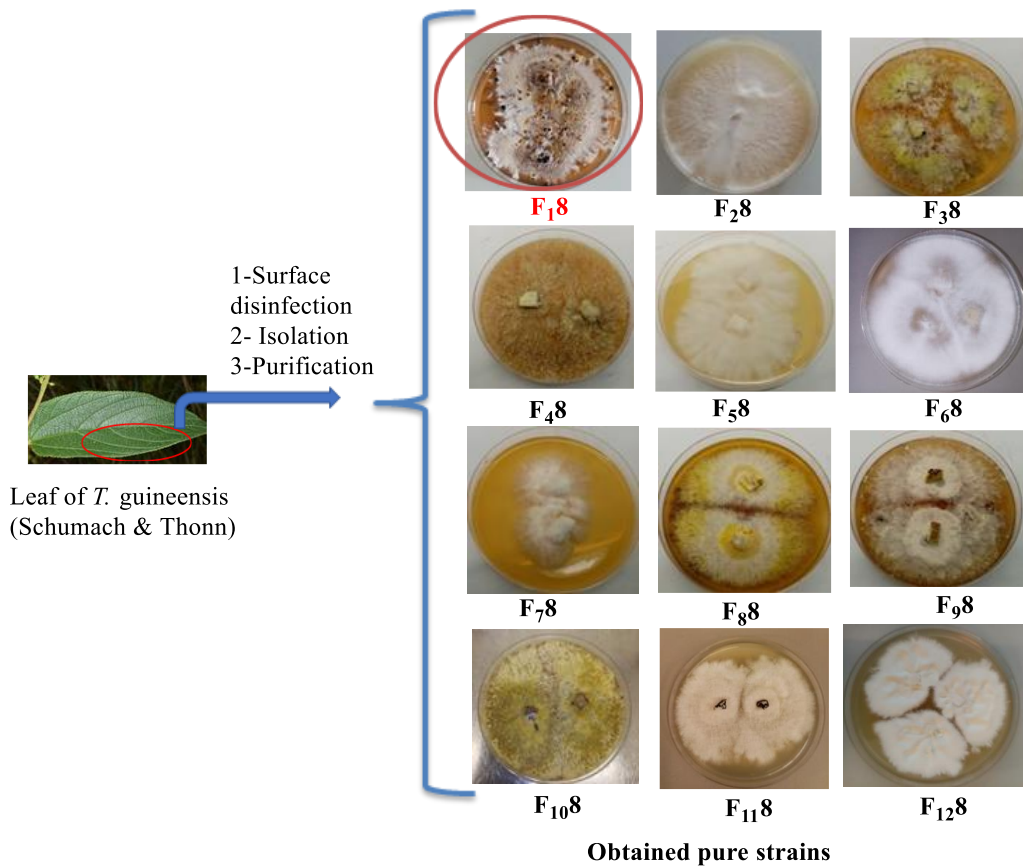


**Figure 98.** *Diaporthe* sp.1 nov (F18 = pure strain).

### III.1.2.1.3. Isolation of *Diaporthe* sp. 2.nov

*Diaporthe* sp. 2. nov was isolated from the fresh roots of the apparently healthy plant of *Trema guineensis* (Schumach & Thonn). It was isolated together with five others isolates as follow:

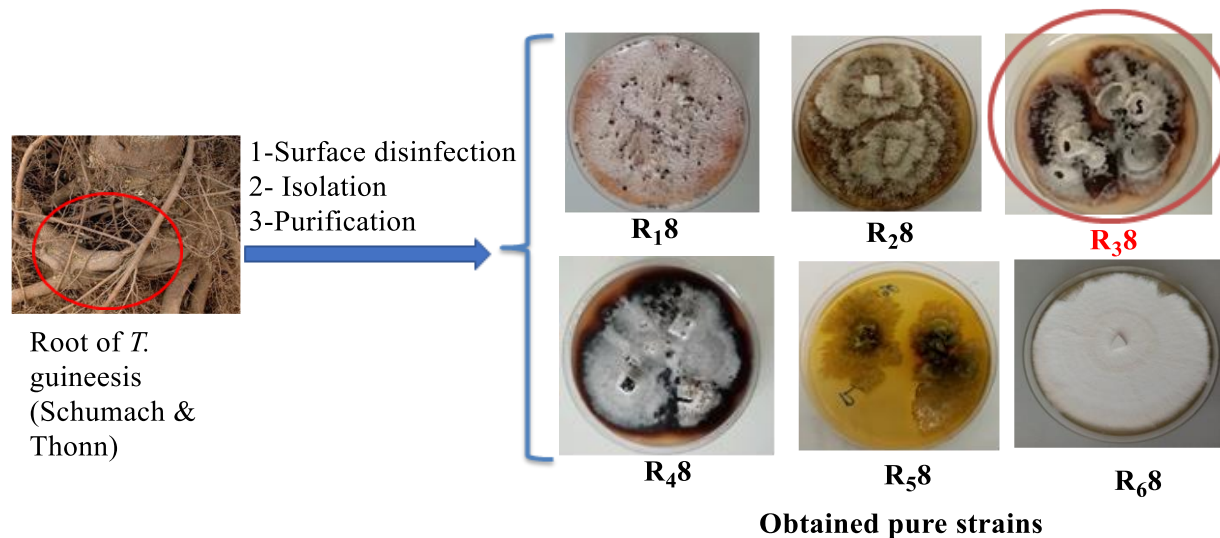


**Figure 99.** *Diaporthe* sp.2.nov (R<sub>38</sub> = pure strain).

### III.1.2.2. Identification of fungal strains: molecular analysis, sequencing and phylogenetic analysis

The endophytic fungi studied were identified by combination of morphological and molecular phylogenetic methods at the Department of Microbial Drugs (MWIS) at the Helmholtz Centre for Infection Research (HZI) in Germany.

#### III.1.2.2.1. Identification of *Simplicillium subtropicum*. SPC3

Genomic DNA was extracted from fungal colonies growing on YMG using the EZ-10 Spin Column Genomic DNA Miniprep kit (Bio Basic Canada Inc., Markham, ON, Canada) following the manufacturer's protocol. Molecular analysis was carried out using sequence data of internal transcribed spacer (ITS) regions. Amplification was performed using an ITS1F/ITS4 primer pair in a total reaction volume of 25  $\mu$ L, which was composed of 10–15 ng genomic DNA, 1 $\times$  PCR buffer, 200  $\mu$ M of each dNTP, 1.5 mM MgCl<sub>2</sub>, 0.4 pM of each primer and 0.5 U Taq polymerase (White *et al.*, 1990). The reaction was performed using an Eppendorf PCR System with cycling conditions consisting of 5 min at 96°C for primary denaturation, followed by 35 cycles of denaturation at 94°C for 40 s, annealing at 52°C for 30 s, extension at 72°C for 60 s, with a final extension at 72°C for 7 min.

The amplicons were Sanger sequenced in both directions using BigDye v3.1. The resulting consensus sequence files were edited using SeqMan software in the Lasergene package (DNASTAR Inc., Madison, WI, USA) and consensus sequence was compared with sequences in the GenBank using the Basic local alignment search tool (BLAST). The ITS-rDNA sequence was deposited in GenBank with the accession number MW074157.

Reference ITS-rDNA sequence data of related/representative *Simplicillium* species were obtained from GenBank. Bayesian analyses were performed in PAUP v.4.0b10 and MrBayes v3.2.2 (Ronquist *et al.*, 2012). The most suitable model of evolution was estimated by using Mrmodeltest v.2.2 (Nylander *et al.*, 2004).

### III.1.2.2.2. Phenotypic and Phylogenetic study of *Diaporthe* sp. 1. Nov and *Diaporthe* sp.2.nov

Their characterization was done at the Department of Microbial Drugs (MWIS) at the Helmholtz Centre for Infection Research (HZI) in Germany. For cultural characterization, the isolates were grown for 15 days on malt extract agar (MEA; HiMedia, Mumbai, India), oatmeal agar (OA; Sigma-Aldrich, St. Louis, Missouri, USA), and PDA at 21 °C in darkness (Guarnaccia *et al.*, 2018). Color notations in parentheses are taken from the color chart of The Royal Horticultural Society London (1966). The fungi were grown in 2 % tap water agar supplemented with sterile pine needles (PNA; Smith *et al.*, 1996) to induce sporulation.

For the molecular study, DNA of the fungi were extracted and purified directly from colony growing in yeast malt agar (YM agar; malt extract 10 g/L, yeast extract 4 g/L, D-glucose 4 g/L, agar 20 g/L, pH 6.3 before autoclaving), following the Fungal gDNA Miniprep Kit EZ-10 Spin Column protocol (NBS Biologicals, Cambridgeshire, UK). The amplification of the ITS, *cal*, *his3*, *tef1* and *tub2* loci were performed according to White *et al.*, 1990 (ITS), Carbone and Kohn (1999) (*cal* and *tef1*), Glass and Donaldson 1995 (*his3* and *tub2*) and Crous *et al.*, 2004 (*his3*). PCR products were purified and sequenced using Sanger Cycle Sequencing method at Microsynth Seqlab GmbH (Göttingen, Germany), and the consensus sequences obtained employing the de-novo assembly feature of the Geneious® 7.1.9 (<http://www.geneious.com>, (Kearse *et al.*, 2012) program package using a forward and reverse read.

In order to restrict the phylogenetic inference to the relevant species to compare with, a first phylogenetic analysis was carried out based on the combination of the five loci sequences (ITS, *cal*, *his3*, *tef1*, *tub2*) of our isolate and a selection of sequence data derived from type material or reference strains from all *Diaporthe* sp. available in NCBI. Each locus was aligned separately

using MAFFT v. 7.017 (algorithm G-INS-I, gap open penalty set to 1.53, offset value 0.123 with options set for automatically determining sequence direction automatically and more accurately) as available as a Geneious ® 7.1.9 plugin (Kato and Standley 2013) and manually adjusted in MEGA v. 10.2.4 (Kumar *et al.*, 2018). Alignment errors were minimized by using gblocks (Talavera and Castresana 2007); with options set for allowed block positions ‘with half’, minimum length of a block set to 5 and a maximum of 10 contiguous nonconserved positions) and concatenated by employing the phylosuite v 1.2.2 program package (Zhang *et al.*, 2020). Maximum-Likelihood tree inference followed using IQTree V2.1.3 (Minh *et al.*, 2020) preceded by calculation and automatic selection of the appropriate nucleotide exchange model using ModelFinder (Kalyanamoorthy *et al.*, 2017) based on Bayesian inference criterion. Bootstrap support was calculated by parallelizing 10 independent maximum-likelihood (ML) tree searches with 100 bootstrap replicates each to minimize computational burden. The total 1000 bootstrap replicates were consequently mapped onto the ML tree with the best (highest) ML score. After selection of the core group related to the sequences derived from *Diaporthe sp.1.nov* and *Diaporthe sp.2.nov.*, a second phylogenetic analysis was performed including all five sequenced loci, using *D. amygdali* CBS 126679<sup>T</sup> and *D. eres* CBS 138594<sup>T</sup> as outgroups. Sequence alignment and curation steps were identical, with exemption of a manual curation instead of employing automatic filtering for misaligned alignment sections using gblocks. A ML tree was inferred using IQTree 2.1.3 and ModelFinder to determine optimal substitution models for each partition, using 1000 bootstrap replicates to assign statistical support. Concurrently, a second tree was inferred following a Bayesian approach using MrBayes 3.2.7a (Ronquist *et al.*, 2012) with nucleotide substitution models previously determined using PartitionFinder2 (Lanfear *et al.*, 2016), options set for unlinked partitions, BIC, restricting models for Bayesian inference) and concatenated in Phylosuite V.1.2.2. Bayesian inference was done in Mr. Bayes v. 3.2.7 (Ronquist *et al.*, 2012), using four Markov Chain Monte Carlo (MCMC) with four incrementally heated chains (temperature parameter set to 0.15), starting from a random tree topology. Generations were set to 100.000.000 with convergence controlled by average standard deviation of split frequencies arriving below 0.01. Trees were sampled every 1000 generations with the first 25% of saved trees treated as “burn-in” phase. Posterior probabilities were mapped using the remaining trees. Bootstrap support (bs)  $\geq 70$  and posterior probability values (pp)  $\geq 0.95$  were considered

significant (Alfaro *et al.*, 2003). The sequences generated in this study are going to be deposited in GenBank and the alignments used in the phylogenetic analysis are under established.

### III.1.2. Prescreening of the isolated fungi

All the isolated were cultured in small scale in different culture media and extracted. HPLC and LC-MS were very useful to have the compounds profile and identified similar compounds. The obtain LC-MS and HPLC profiles were used to choose best culture medium, to detect compounds belonging to the same family, the ones possess the same chromophore group and the skeleton not yet isolated from the genus. These technics were used to screen the twenty-four pure culture isolates. The combination of LC-MS analysis, the identification of fungal strains and the antibacterial assays let to the selection of strains SPC, F<sub>18</sub> and R<sub>38</sub>.

### III.1.3. Fungal culture and extraction

*S. subtropicum* SPC3 well-grown agar culture was inoculated in a 500 mL-Erlenmeyer flask containing 200 mL of YMG medium consisting of 1.0% malt extract, 0.4% glucose, and 0.4% yeast extract, pH 6.3 and incubated at 23 °C. After 6 days, the cultures were harvested. The supernatant was filtrated from fungal mycelia and the latter were further extracted with acetone and the combined acetone solution was concentrated under reduced pressure to yield 2.0 g of crude extract.

*Diaporthe* sp. 1.nov. well-grown agar plate isolate was cultured in 500 mL x 30 Erlenmeyer flask containing 80 g of rice and 100 mL distilled water and incubated at 23 °C. After 30 days, the cultures were harvested. The fungal mycelia were then extracted with acetyl acetate and the solution was concentrated under reduced pressure to yield 15.6 g of crude extract.

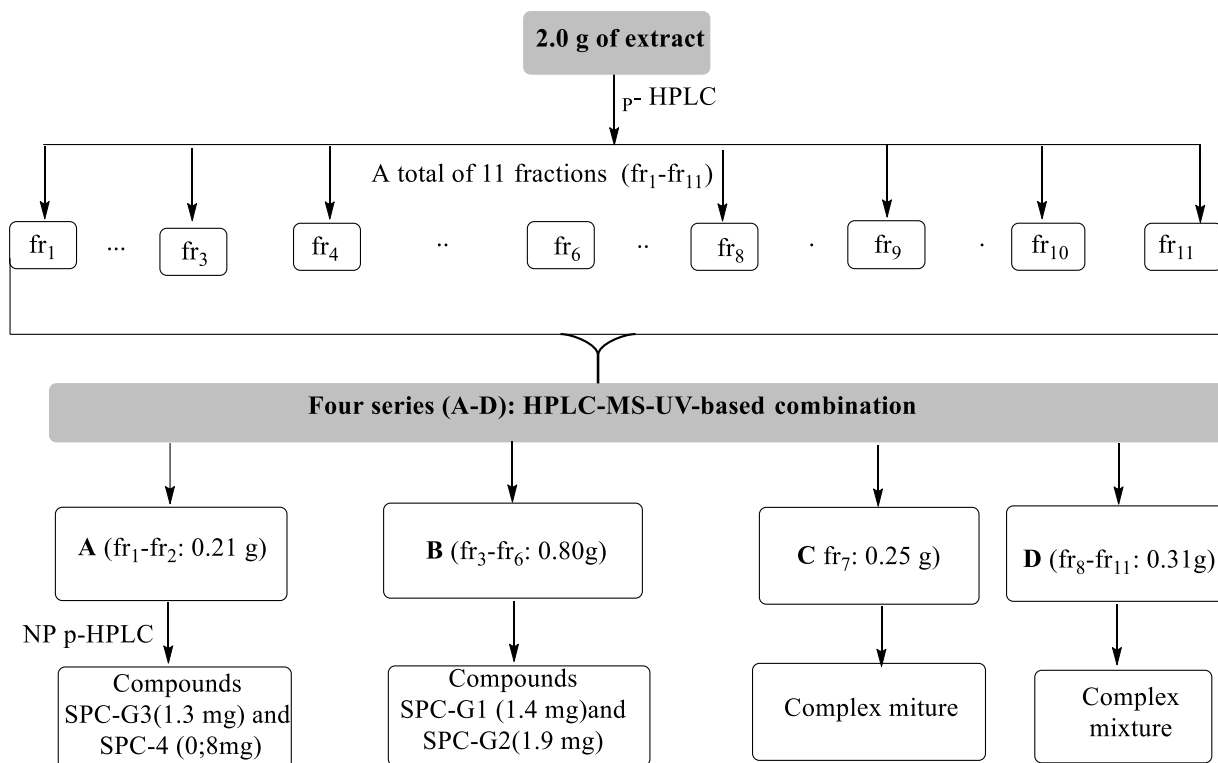
*Diaporthe* sp. 2.nov. well-grown agar plate culture was inoculated in a 500 mL x 45 Erlenmeyer flask containing 80 g of rice and 100 mL distilled water and incubated at 25 °C. After 28 days, the cultures were harvested. The fungal mycelia were then extracted with acetyl acetate and the solution was concentrated under reduced pressure to yield 12.0 g of crude extract

### III.1.4. Isolation and purification of secondary metabolites

#### III.1.4.1. Chemical investigation of *Simplicillium subtropicum*. SPC3 isolated from *Duguetia staudtii*

The acetone crude extract (2.0 g) was fractionated separately using preparative reverse phase HPLC (Büchi, Pure C-850, 2020, Switzerland). VP Nucleodur 100-5 C18ec column

(150×40 mm, 7 μm: Machery-Nagel, Düren, Germany) was used as stationary phase. Deionized water (Milli-Q, Millipore, Schwalbach, Germany) supplemented with 0.1 % formic acid (FA) (solvent A) and acetonitrile (ACN) with 0.1% FA (solvent B) were used as the mobile phase. The elution gradient used for fractionation was 0–15% solvent B for 3 min, 15–100% B for 20 min, and 1.0% B for 10 min. The flow rate was set to 30 mL/min and UV detection was carried out at 210, 320 and 350 nm. For this extract, 11 fractions (fr<sub>1</sub>-fr<sub>11</sub>) were combined in four sub-fractions (A-D) according to the observed peaks, and further analysis of the fractions using HPLC-MS-UV (DAD) revealed that fraction B constituted pure compounds, SPC-G1 (1.4 mg; RT = 9.1 min) and SPC-G2 (1.9 mg; RT = 12.0 min). Further purification of fraction A by preparative HPLC using the same gradient led to the isolation of two other compounds: SPC-G3 (1.3 mg; RT = 7.1 min) and SPC-G4 (0.8 mg; RT = 10.5 min) (Scheme 12).

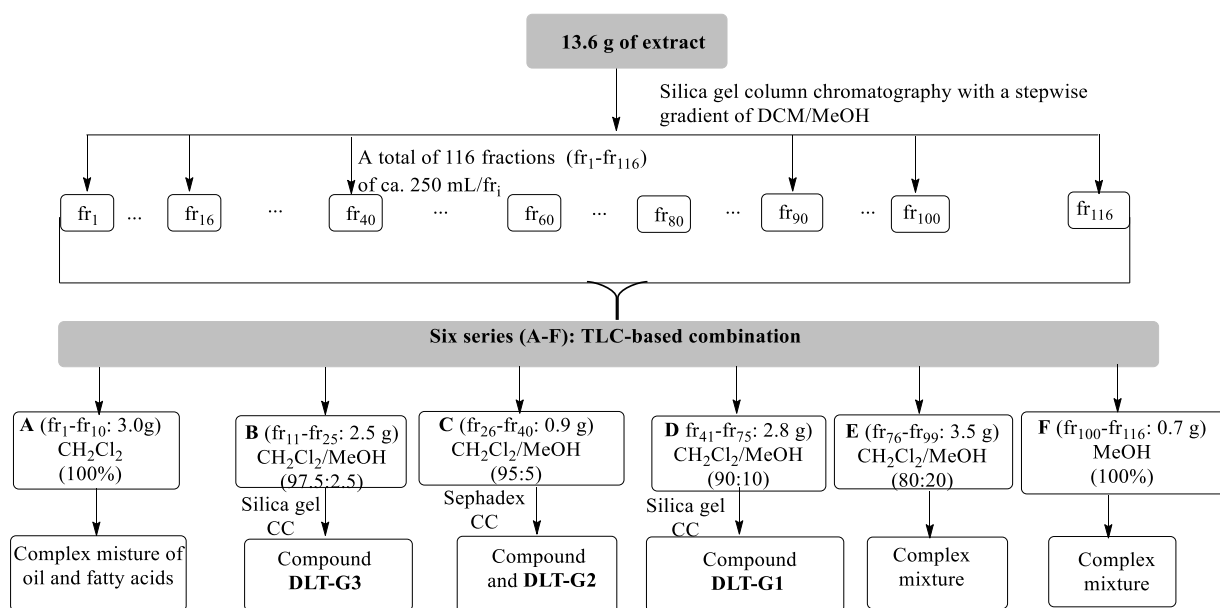


**Scheme 12.** Secondary metabolites from fermentation of *Simplicillium subtropicum* SPC3.

#### III.1.4.2. Chemical investigation of *Diaporthe* sp. 1.nov

The 13,6 g of the EtOAc extract (15.6) was subjected to CC (silica gel 200– 300 mesh) and eluted with gradients of CH<sub>2</sub>Cl<sub>2</sub>, CH<sub>2</sub>Cl<sub>2</sub>/MeOH (100 :0, 20 :80) and MeOH to yield 116 fractions (fr<sub>1</sub>-fr<sub>116</sub>) which were combined on the basis of TLC analysis as shown six main sub-fractions (A-

F, respectively). After monitoring with LC-HR-MS. Sub-fraction B (2.5 g) from the gradient  $\text{CH}_2\text{Cl}_2/\text{MeOH}$  (97.5:2.5) was subjected to silica gel column chromatography and eluted with an isocratic system of *n*-Hex/EtOAc (75: 25) to afford **GLT-G3** (12 mg, yellow solid). Sub-fraction C was subjected to further chromatographic separations over sephadex LH-20 using  $\text{CH}_2\text{Cl}_2/\text{MeOH}$  (1:1) as eluent to afford **GLT-G2** (2mg, white solid). Sub-fraction D (2.8 g) was subjected to silica gel column chromatography and eluted with an isocratic system of  $\text{CH}_2\text{Cl}_2/\text{MeOH}$  (95:5) to afford **GLT-G1** (2mg, white solid) (Scheme 13).



**Scheme 13.** Secondary metabolites from solid medium of *Diaporthe* sp.1.nov.

### III.1.4.3. Chemical investigation of *Diaporthe* sp.2. nov

The 12 g of fungal crude extract from *Diaporthe* sp.2.nov was subjected to a silica gel (230–400 mesh) column chromatography using a stepwise gradient of  $\text{CH}_2\text{Cl}_2/\text{MeOH}$  (ranging from 0 to 100% of MeOH), to afford a total of 98 fractions (fr<sub>1</sub>-fr<sub>98</sub>) of ca. 200 mL per fraction (Scheme 10). All these fractions were combined into 8 main sub-fractions (A–H) on the basis of their TLC analyses (Scheme 14).

Sub-fraction B (fr<sub>6</sub>-fr<sub>7</sub>: 462 g) obtained with  $\text{CH}_2\text{Cl}_2/\text{MeOH}$  (97.5:2.5) was subjected to a flash chromatography system (PLC 2020, Gilson, Wisconsin-USA) equipped with a VP Nucleodur C18 HTec column (10  $\mu\text{m}$ , 250×40 mm, Macherey-Nagel, Germany) maintained at room temperature. The chromatographic separation was performed by using a constant flow rate of 10 mL/min with the mobile phases made with solvent A: Deionized water  $\text{H}_2\text{O}$  (Milli-Q, Millipore,

Schwalbach, Germany) + 0.1% formic acid (FA) and solvent B: acetonitrile (ACN) + 0.1% formic acid. The binary gradient was: linear of 5% B for 5 min, automatic stepwise gradient from 5 to 100% B for 5–105 min, followed by 100% B for 10 min wash and finally by 80% ACN + 20% H<sub>2</sub>O for 10 min re-equilibration time and column storage. Peaks were detected using wavelengths of 210–600 nm and were automatically collected by time into glass tubes. Out of the hundred and twenty-seven tubes, twenty (20) tubes were selected according to the observed peaks, and further analysis of the fractions using HPLC-MS revealed that four of the obtained fractions constituted pure compounds **DRT-G5** (1.18 mg; RT = 52 min), **DRT-G8** (2.10 mg; RT = 85 min), **DRT-G9** (2.80 mg; RT = 92 min) and **DRT-G10** (3.20 mg; RT = 104 min). The LC-MS analysis of other fractions suggested the presence of very low amount of compounds and these fractions were not further investigated.

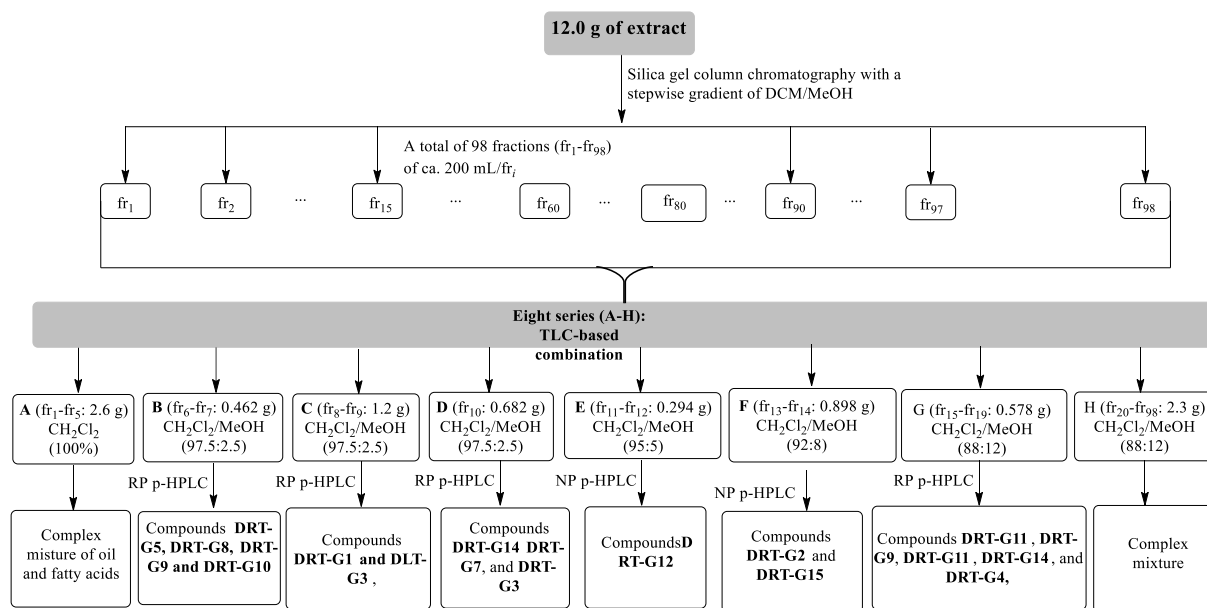
Sub-fraction C (fr<sub>6</sub>–fr<sub>7</sub>: 1.2 g) eluted with CH<sub>2</sub>Cl<sub>2</sub>/MeOH (97.5:2.5) was divided into three portions of 400 mg each. After dissolving every portion in 4 mL-vials, the injections were performed on a flash liquid chromatography with UV/ELSD detector, UV-Vis/UV scanning (Flash and prep HPLC, C-850, Büchi, New Castle, DE 19720, USA) equipped with a Gemini C18 (10µm, 250×50 mm, Phenomenex, California, USA) maintained at room temperature. Equivalent fractions from the three repeated runs were combined to give compounds **DRT-G1** (1.19 mg, white solid, *t<sub>R</sub>*: 4.86 min), and two other sub-fractions (C<sub>1</sub>–C<sub>2</sub>).

Sub-fraction D (fr<sub>10</sub>: 682 mg) eluted from an opened column chromatography with CH<sub>2</sub>Cl<sub>2</sub>/MeOH (95:5) was divided into two portions of 341 mg each. After dissolving every portion in 4 mL-vials, the injections were also achieved on a flash and prep HPLC system. Equivalent fractions from the three repeated runs were combined to give three sub-fractions (D<sub>1</sub>–D<sub>3</sub>). All these sub-fractions D<sub>1</sub> (12 mg), D<sub>1</sub> (8 mg) and D<sub>3</sub> (15.8 mg) were further purified separately over normal phase preparative HPLC with DAD detector (Agilent 1100 Series) with a Nucleosil 120 OH Diol column (7 µm, 250×21 mm) used as the stationary phase and the solvent mixture CH<sub>2</sub>CH<sub>2</sub>/MeOH (92:8) as the mobile phase. The elution was performed for 25 min each with a flow rate of 2 mL/min, an automatic pressure in the range of 1-10 bar and the UV absorptions were set at 210, 254 and 366 nm to yield compounds **DRT-G14** (3.21 mg, yellow oil, RT: 8 min), **DRT-G7** (1.24 mg, yellow oil, RT: 14 min), **DRT-G3** (9.2 mg, white neat solid, RT: 22 min), respectively.

Sub-fraction E (fr<sub>11</sub>–fr<sub>12</sub>: 294 mg) was further purified to yield **DRT-G12** (1.45 mg, yellow neat solid, RT: 15.00 min).

The purification of series F (fr<sub>13</sub>–fr<sub>14</sub>: 898 mg) yielded compounds **DRT-G2** (3.45 mg, white amorphous powder, RT: 16.17 min), **DRT-G15** (1.31 mg, yellow neat solid, RT: 30.22 min).

Sub-fraction G (fr<sub>15</sub>–fr<sub>19</sub>: 578 mg) obtained with CH<sub>2</sub>Cl<sub>2</sub>/MeOH (88:12) was also purified to give compounds **DRT-G11** (5.93 mg, white oil, RT: 35.20 min), **DRT-G9** (8.33 mg, white oil, RT: 38.17 min); **DRT-G4** (0.79 mg, yellow oil, *t<sub>R</sub>*: 22 min); **DRT-G11** (1.60 mg, yellow oil, RT: 45.12 min) and **DRT-G14** (1.23 mg, white oil).



**Scheme 14.** Secondary metabolites from solid medium of *Diaporthe* sp.2.nov.

### III.1.5. Determination of absolute stereochemistry by Mosher reaction

The reaction was performed based on a modified Mosher ester procedure described by Hoye *et al.* (2007). Preparation of each of the diastereomeric *S*- and *R*-MTPA esters and then, comparative ( $\Delta\delta^{\text{SR}}$ ) analysis of the <sup>1</sup>H NMR spectral data of these two esters. By analyzing the sign of the difference in chemical shifts for a number of analogous pairs of protons (the set of  $\Delta\delta^{\text{SR}}$  values) in the diastereomeric esters (or amides), the absolute configuration of the original carbinol (or amino) stereocenter was reliably deduced. A typical Mosher ester analysis requires approximately 4–6 h of active effort over a 1- to 2-d period. Reaction with (*R*)-(-)- $\alpha$ -(trifluoromethyl) phenylacetyl chloride. The compounds (1 mg of each) were transferred into NMR tubes and were dried under vacuum. Deuterated pyridine (0.5 mL) and (*R*)-MTPA chloride

were added immediately under a N<sub>2</sub> gas stream. The reagent was added in the ratio of 0.14 mM reagent to 0.10 mM of the compound (Dale and Mosher, 1973). The NMR tubes were shaken carefully to mix the samples and MTPA chloride evenly. The reaction NMR tubes were permitted to stand at room temperature and monitored by <sup>1</sup>H-NMR until the reaction was completed. <sup>1</sup>H-<sup>1</sup>H COSY was measured to confirm the assignment of the signals. Reaction with (*S*)-(-)- α-(trifluoromethyl) phenylacetyl chloride. Another portion of each compound (1 mg) was transferred into NMR tube. The reaction was performed in the same manner as described before to yield the (*S*)-MTPA ester.

## III.2. Physico-Chemical properties of isolated compounds

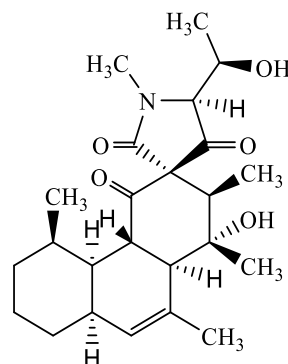
### III.2.1. Compounds isolated from *Simplicillium subtropicum*. SPC3

#### ➤ **Simplicilone A**

Physical aspect: colourless oil

HRESIMS *m/z* 418.2589 [M+H]<sup>+</sup> (calcd. For C<sub>24</sub>H<sub>35</sub>NO<sub>5</sub>, 418.2593)

<sup>1</sup>H and <sup>13</sup>C NMR data (500/125 MHz, CDCl<sub>3</sub>), see Table 3



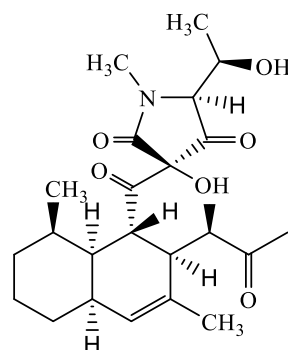
#### ➤ **Simplicilone B**

Physical aspect: colourless oil

[α]<sub>D</sub><sup>25</sup> 0° (c 0.27, MeOH); UV (MeOH):

HRESIMS *m/z* 434.2542 [M+H]<sup>+</sup> (calcd for C<sub>24</sub>H<sub>35</sub>NO<sub>6</sub>, 434.2542)

<sup>1</sup>H and <sup>13</sup>C NMR data (500/125 MHz, CDCl<sub>3</sub>), see Table 4

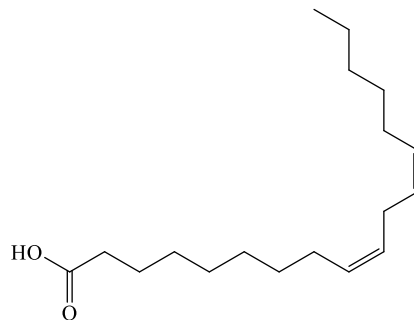


➤ **Linoleic acid**

Physical aspect: white oil

(-)-ESI-MS  $m/z$  279.12  $[M-H]^+$ , for  $C_{18}H_{32}O_2$

$^1H$  and  $^{13}C$  NMR data (500/125 MHz,  $CDCl_3$ , see Table 5



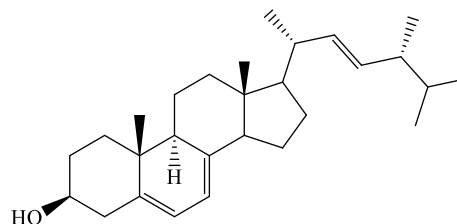
➤ **Ergosterol**

Physical aspect: white solid

Reacted positively to Liebermann-Burchard reagent

HRESIMS  $m/z$  397.2542  $[M+H]^+$  (calculated for  $C_{28}H_{44}O$ , 397.2542)

$^1H$  and  $^{13}C$  NMR data (500/125 MHz,  $CDCl_3$ ) see Table 6



### III.2.2. Compounds isolated from *Diaporthe* sp.2.nov

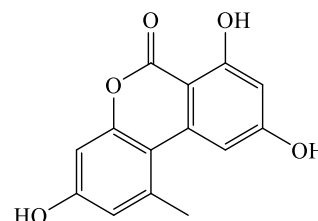
➤ **Alternariol**

Physical aspect : white solid

UV (MeOH) –  $\lambda_{max}$  nm (PDA): 222, 257 and 340 nm

HRESIMS  $m/z$  259.0598  $[M+H]^+$  (calcd for  $C_{14}H_{11}O_5$ , 259.0562)

$^1H$  and  $^{13}C$  NMR data (500/125 MHz,  $DMSO-d_6$ ) see Table 7



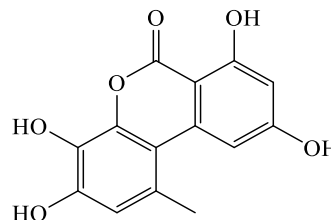
➤ **4-hydroxyalternariol**

Physical aspect : colourless oil

UV (MeOH) –  $\lambda_{max}$  nm (PDA): 218, 256 and 344 nm

HRESIMS at  $m/z$  275.0547  $[M+H]^+$  (calcd for  $C_{14}H_{11}O_5$ , 275.0511)

$^1H$  and  $^{13}C$  NMR data (500/125 MHz,  $DMSO-d_6$ ) see Table 8



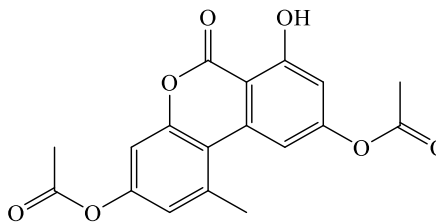
➤ **3, 9-diacetylalternariol**

Physical aspect: colourless oil

UV (MeOH) –  $\lambda_{\max}$  nm (PDA): 222, 257 and 330 nm

HRESIMS at  $m/z$  343.0810  $[M+H]^+$  (calcd. for  $C_{18}H_{14}O_7$ , 343.0812)

$^1H$  and  $^{13}C$  NMR data (500/125 MHz, DMSO- $d_6$ ) see Table 9

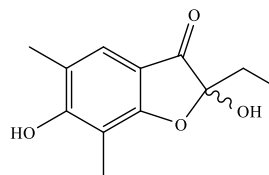


➤ **Diapobenzofuranone**

Physical aspect: yellow oil

$[\alpha]_D^{25} 0^\circ$  ( $c$  0.27, MeOH); UV (MeOH):  $\lambda_{\max}$  (PDA): 218, 290, 342 nm. HRESIMS at  $m/z$  223.0961  $[M+H]^+$  (calcd. for  $C_{12}H_{15}O_4$ , 223.0965).

$^1H$  and  $^{13}C$  NMR data (500/125 MHz, DMSO- $d_6$ ) see Table 10



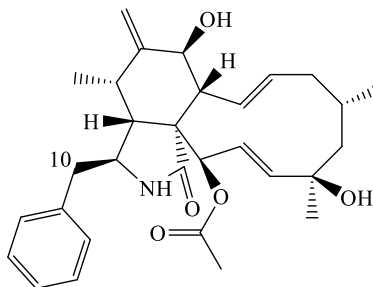
➤ **Cytochalasin H**

Physical aspect: white crystal

UV (MeOH) –  $\lambda_{\max}$  nm (PDA): 201 and 218 nm

HRESIMS  $m/z$  494.2895,  $[M+H]^+$  (calcd, for  $C_{30}H_{39}NO_5$ , 494.2897)

$^1H$  and  $^{13}C$  NMR data (500/125 MHz,  $CD_3OD$ ) see Table 11



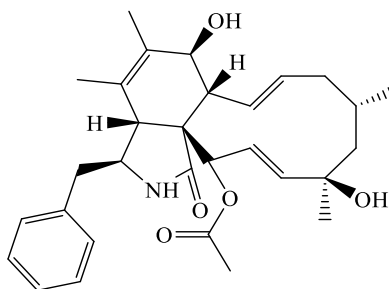
➤ **Cytochalasin N**

Physical aspect: yellow oil

UV (MeOH) –  $\lambda_{\max}$  nm (PDA): 200 and 217 nm

HRESIMS  $m/z$  494.2899  $[M+H]^+$  (calcd, for  $C_{30}H_{39}NO_5$ , 494.2897)

$^1H$  and  $^{13}C$  NMR data (500/125 MHz,  $CD_3OD$ ) see Table 12



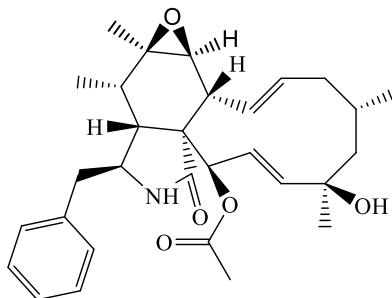
➤ **Epoxychochalasin H**

Physical aspect: white oil

UV (MeOH) –  $\lambda_{\max}$  nm (PDA): 195 and 217 nm

HRESIMS  $m/z$  494.2902  $[M+H]^+$  (calcd, for  $C_{30}H_{39}NO_5$ , 494.2905)

$^1H$  and  $^{13}C$  NMR data (500/125 MHz,  $CD_3OD$ ) see Table 13

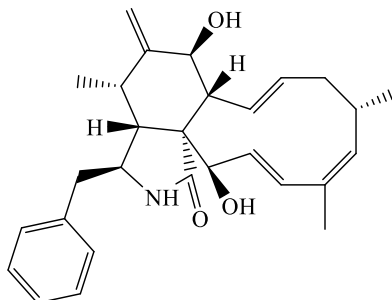


➤ **Cytochalasin J2**

Physical aspect: white oil

HRESIMS  $m/z$  434.2701  $[M+H]^+$  (calcd. for  $C_{28}H_{35}NO_3$ , 434.2650)

$^1H$  and  $^{13}C$  NMR data (500/125 MHz,  $CD_3OD$ ) see Table 14

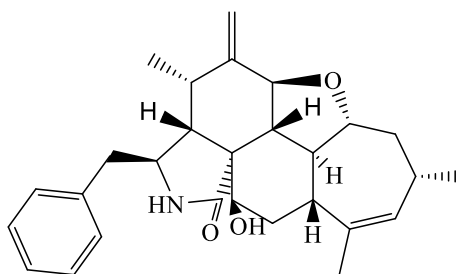


➤ **Cytochalasin J3**

Physical aspect: white oil

HRESIMS  $m/z$  434.2689  $[M+H]^+$  (calcd. for  $C_{28}H_{35}NO_3$ , 434.2650)

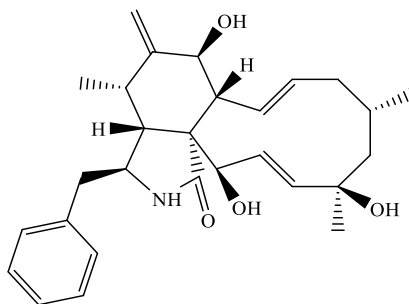
$^1H$  and  $^{13}C$  NMR data (500/125 MHz,  $CD_3OD$ ) see Table 15



➤ **Cytochalasin J**

Physical aspect: white oil

HRESIMS as  $C_{28}H_{37}NO_4$ ,  $m/z$  452.2796  $[M+H]^+$  (calcd, for  $C_{28}H_{37}NO_4$ , 452.2798.2957)  $^1H$  and  $^{13}C$  NMR data (500/125 MHz,  $CD_3OD$ ) see Table 16

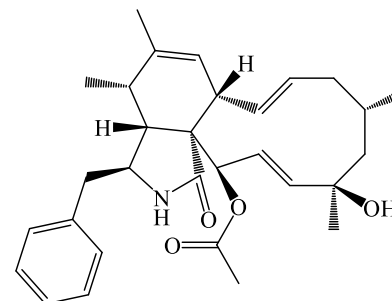


➤ **Cytochalasin RKS-1778**

Physical aspect: white oil

HRESIMS  $m/z$  478.2951  $[M+H]^+$  (calcd for  $C_{30}H_{39}NO_4$ , 478.2956)

$^1H$  and  $^{13}C$  NMR data (500/125 MHz,  $CD_3OD$ ) see Table 17



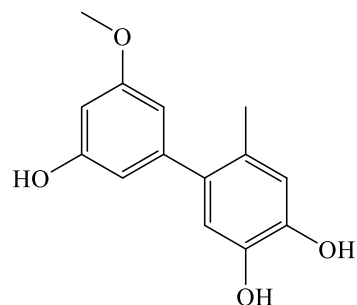
➤ **5'-methoxy-6-methyl-biphenyl-3,4,3'-triol**

Physical aspect: white oil

UV (MeOH) –  $\lambda_{\text{max}}$  nm (PDA): 222, 257 and 340 nm

HRESIMS  $m/z$  247.0965  $[M + H]^+$  (calcd for  $C_{14}H_{15}O_4$ : 247.0965)

$^1\text{H}$  and  $^{13}\text{C}$  NMR data (500/125 MHz,  $\text{CD}_3\text{OD}$ ) see Table 18



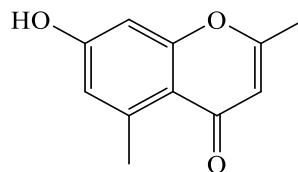
➤ **2,5-dimethyl-7-hydroxychromone**

Physical aspect: white solid

UV (MeOH) –  $\lambda_{\text{max}}$  nm (PDA): 230, 250 and 293 nm

HRESIMS  $m/z$  191.0692  $[M + H]^+$  (calcd for  $C_{11}H_{10}O_3$ : 191.0694)

$^1\text{H}$  and  $^{13}\text{C}$  NMR data (500/125 MHz,  $\text{CD}_3\text{OD}$ ) see Table 19



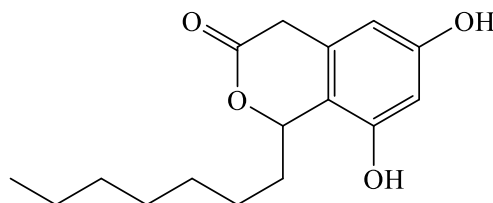
➤ **Cytosporone C**

Physical aspect: white oil

UV (MeOH) –  $\lambda_{\text{max}}$  nm (PDA): 204, 280 nm

HRESIMS  $m/z$  279.1589  $[M+H]$  (calcd for  $C_{16}H_{22}O_4$ , 279.1591)

$^1\text{H}$  and  $^{13}\text{C}$  NMR data (500/125 MHz,  $\text{CD}_3\text{OD}$ ) see Table 20

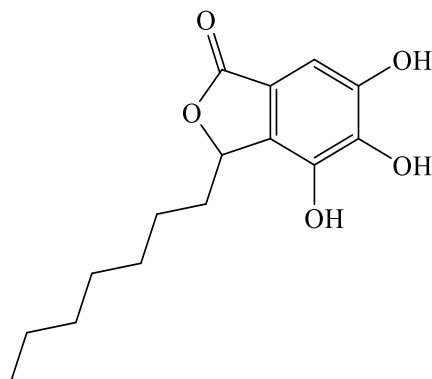


➤ **Cytosporone E**

Physical aspect: white solid

HRESIMS  $m/z$  281.1687  $[M+H]^+$  (calcd for  $C_{15}H_{20}O_5$ , 295.1540)

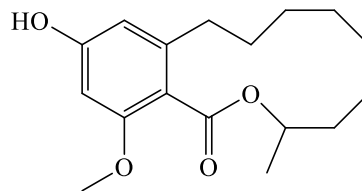
$^1\text{H}$  and  $^{13}\text{C}$  NMR data (500/125 MHz,  $\text{CD}_3\text{OD}$ ) see Table 21



**III.2.3. Compounds isolated from *Diaporthe* sp. 1.nov**➤ **Lasiodiplodin**

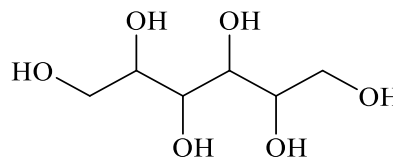
Physical aspect : white solid

m.p 182-183 °C

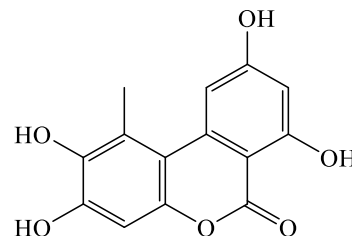
[ $\alpha$ ]<sub>D</sub><sup>25</sup>+17.2° (c 0.15), CHCl<sub>3</sub>)HRESIMS  $m/z$  293.1753 [M+H]<sup>+</sup> (calcd for C<sub>17</sub>H<sub>24</sub>O<sub>4</sub>: 293.1755)<sup>1</sup>H and <sup>13</sup>C NMR data (500/125 MHz, DMSO-*d*<sub>6</sub>)  
see Table 22➤ **Sorbitol**

Physical aspect : white solid

m.p 95-96 °C

HRESIMS at  $m/z$  183.0864 [M+H]<sup>+</sup> (calcd for C<sub>6</sub>H<sub>14</sub>O<sub>6</sub>: 183.0860)<sup>1</sup>H and <sup>13</sup>C-NMR data (500/125 MHz, DMSO-*d*<sub>6</sub>)  
see Table 23➤ **2-hydroxyalternariol**

Physical aspect: white oil

HRESIMS  $m/z$  275.0550 [M+H]<sup>+</sup> (calcd for C<sub>14</sub>H<sub>10</sub>O<sub>6</sub>: 275.0554)<sup>1</sup>H and <sup>13</sup>C NMR data (500/125 MHz, CD<sub>3</sub>OD)  
see Table 24**III.3. Biological materials and methods****III.3.1. Antimicrobial assays**

The antifungal and antibacterial activities (Minimum Inhibition Concentration, MIC) of compounds 186 and 187 were determined in serial dilution assays as described previously (Becker *et al.*, 2020b). The Compounds 186 and 187 were previously dissolved in MeOH (1 mg/mL) for the antimicrobial activity assay.

Minimum inhibitory concentrations (MICs) of 186 and 187 were determined in a standard microdilution assay using *Bacillus subtilis* DSM10, *Staphylococcus aureus* DSM 346, *Micrococcus luteus* DSM 1790, *Mycolicibacterium smegmatis* ATCC 700084, *Chromobacterium*

*violaceum* DSM 30191, *Escherichia coli* DSM 1116, *Pseudomonas aeruginosa* PA14, *Candida albicans* DSM 1665, *Schizosaccharomyces pombe* DSM70572, *Mucor hiemalis* DSM 2656, *Pichia anomala* DSM 6766, *Rhodotorula glutinis* DSM 10134 as test organisms for evaluating antibacterial and antifungal activities. The assay was carried out in 96-well microtiter plates with U-base (TPP Techno Plastic Products AG, Trasadingen, Switzerland) providing embryoid bodies (EBS) medium (0.5% casein peptone, 0.5% glucose, 0.1% meat extract, 0.1% yeast extract, 50 mM HEPES (11.9 g/L), Ph 7.0) for bacteria and YMG medium (1.0% malt extract, 0.4% glucose, 0.4% yeast extract, Ph 6.3) for yeasts and filamentous fungi. First, a stock culture of each bacterium and yeast was transferred to Erlenmeyer flasks (100 mL) filled with 30 mL of the respective growth medium. Suspensions of *B. subtilis* and *C. albicans* were incubated on a rotary shaker at 30 °C for 18–24 h, while *E. coli* was grown at 37 °C. Subsequently, the cultures were adjusted to cell densities of  $6.7 \times 10^5$  cells/mL using a hemocytometer. The spore suspension of *M. hiemalis* was prepared at a concentration of  $6.7 \times 10^5$  conidia/mL using YMG medium. For the test, 20  $\mu$ L aliquots of each compound at 1.5 mg/mL in MeOH and 20  $\mu$ L of the appropriate reference drug (broad spectrum antibiotic ciprofloxacin and antifungal cycloheximide at 1.5 mg/mL) were pipetted into the first row (A) of the 96-well microtiter plate. MeOH (20  $\mu$ L) served as a negative control. Using a multichannel pipette, 150  $\mu$ L of the prepared inoculum comprising the test pathogen in the respective culture medium was aliquoted in all the rows. To the first row, an additional 130  $\mu$ L of the pathogen–medium mixture was added and mixed by up-down pipetting, before transferring 150  $\mu$ L of this mixture to the second row. A 1 : 1 serial dilution was conducted in the subsequent rows to generate final compound concentrations ranging from 100 to 0.78  $\mu$ g/mL. A volume of 150  $\mu$ L was discarded after the last row (H). Plates were incubated at 30 °C on a microplate vibrating shaker (Heidolph Titramax 1000, Schwabach, Germany) at 600 rpm for 24–48 h. The lowest concentration of the compounds preventing visible growth of the test organism was recorded as the MIC. Antibacterial activities (Minimum Inhibition Concentration, MIC of compounds 205, 206 and 207 were performed in serial dilution assays as described previously ([Ambadiang et al., 2020](#)).

### III.3.3. Cytotoxicity assays

Compounds **186** & **187** were dissolved as described in the previous section. In vitro cytotoxicity (IC<sub>50</sub>) was investigated against the established mouse fibroblast cell line L929 (DSMZ no. ACC 2) and KB3.1 (human papillomavirus-related endocervical adenocarcinoma)

using the 3-(4,5-dimethylthiazol-2-yl) 2,5-diphenyltetrazolium bromide (MTT) method in 96-well microplates for tissue cultures. The cell line L929 was cultured in Dulbecco's Modified Eagle's Medium (DMEM; Lonza, Basel, Switzerland), supplemented with 10% foetal bovine serum (FBS; Thermo Fisher Scientific, Waltham, MA, USA) and incubated under 10% CO<sub>2</sub> at 37 °C for 5 days. The assay was conducted following the procedure described previously by [Surup \*et al.\*, 2018](#).

---

# REFERENCES

- Adeleke, B.S., Babalola, O.O. (2021) Pharmacological Potential of Fungal Endophytes Associated with Medicinal Plants: A Review. *J. Fungi*, **7**, 147.
- Adelin, E., Martin, M-T., Bricot, M-F., Cortial, S., Retailleau, P., Ouazzani, J. (2012) Biotransformation of natural compounds: Unexpected thio conjugation of Sch-642305 with 3 mercaptolactate catalyzed by *Aspergillus niger* ATCC 16404 cells. *Phytochemistry* **84**, 135-140.
- Alfaro, M.E., Zoller, S., Lutzoni, F. (2003) Bayes or bootstrap. A simulation study comparing the performance of Bayesian Markov chain Monte Carlo sampling and bootstrapping in assessing phylogenetic confidence. *Mol. Biol. Evol.* **20**, 255–266.
- Aly, A. H., Debbab, A., and Proksch, P. (2011). Fungal endophytes: unique plant inhabitants with great promise. *Appl. Microbiol. Biotechnol.* **90**, 1829-1845.
- Aly, A.H., Debbab, A., Kjer, J., Proksch, P. (2010) Fungal endophytes from higher plants: a prolific source of phytochemicals and other bioactive natural products. *Fungal Divers* **41**, 1–16.
- Ambadiang, M.M.M., Atontsa, B.C.K., Tankeo, S.B., Nayim, P., Wamba, B.E.N., Gabin T. M. Bitchagno, G.T.M., James D. S. Mpetga, J.D.S., Penlap, V.B., Kuete, V. (2020) Bark extract of *Cassia sieberiana* DC. (Caesalpiniaceae) displayed good antibacterial activity against MDR gramnegative phenotypes in the presence of phenylalanine-arginine  $\beta$ -naphthylamide. *Complementary Medicine and Therapies.* **20** :342.
- Andolfi, A., Boari, A., Evidente, M., Cimmino, A., Vurro, M., Ash, G., Evidente, A. (2015) Gulpyrones A and B and phomentrioxins B and C Produced by *Diaporthe gulyae*, a potential mycoherbicide for saffron thistle (*Carthamus lanatus*). *J. Nat. Prod.* **78**, 623–629.
- Aoki, H., Okuhara M. (1980) Natural  $\beta$ -lactam antibiotics. *Ann. Rev. Microbiol* **34**, 159-181.
- Arnold, A. E., Lutzoni, F. (2007) Diversity and host range of foliar endophytes: Are tropical leaves biodiversity hotspots? *Ecology* **88**, 541-549.
- Bacon, C.W., White, J.F. (2000) Microbial Endophytes. Marcel Deker, New York, USA.
- Bartett, D.W., Clough, J.M., Godfrey, C.R.A., Godwin, J.R., Hall, A.A., Heaney, S.P., Maund, S.J. (2001) Understanding the strobilurin fungicides. *Pestic Outlook* **12**, 143–148.

- Becker, K., Wessel, A.C., Luangsa-Ard, J.J., Stadler, M. (2020b) Viridistratins A–C, antimicrobial and cytotoxic benzo[*j*]fluoranthenes from stromata of *Annulohyphoxylon viridistratum* (Hyphoxylaceae, Ascomycota). *Biomolecules* **10**, 805.
- Beiler, K.J., Durall, D.M., Simard, S.W., Maxwell, S.A., Kretzer, A.M. (2010) Architecture of the wood-wide web: *Rhizopogon* spp. genets link multiple Douglas-fir cohorts. *New Phytol.* **185**, 543–553.
- Beno, M. A., Cox, R. H., Wells, J. M., Cole, R. J., Kirksey, J. W., Christoph, G. G. J. (1977) Structure of a new [11] cytochalasin, cytochalasin H or kodo-cytochalasin-1. *J. Am. Chem. SOC.* **99**, 4123.
- Berova, N., Di Bari, L., Pescitelli, G. (2007) Application of electronic circular dichroism in configurational and conformational analysis of organic compounds *Chem. Soc. Rev.* **36**, 914-931.
- Bills, G. F., Gloer, J. B. (2016) Biologically active secondary metabolites from the fungi. *Microbiol. Spectr.* **4**, 1087–1119.
- Binder, M., and Tamm, C. (1973) The Cytochalasans : A New Class of Biologically Active Microbial Metabolites. *Angew. Chem. Internat. Edit.* **12** :1- 5.
- Borchardt, J. K. (2002) The beginnings of drug therapy: Ancient mesopotamian medicine. *Drug News Perspect.* **15**, 187-192.
- Botella, L., Diez, J.J. (2011) Phylogenetic diversity of fungal endophytes in Spanish stands of *Pinus halepensis*. *Fungal Divers* **47**, 9 18.
- Brady, S.F., Wagenaar, M.M., Singh, M.P., Janso, J.E., Clardy, J. (2000) The cytosporones, new octaketide antibiotics isolated from an endophytic fungus. *Org. Lett.* **2**, 4043–4046.
- Brissow, E.R., da Silva, I.P., de Siqueira, K.A., Senabio, J.A., Pimenta, L.P., Januario, A.H., Magalhaes, L.G., Furtado, R.A., Tavares, D.C., Sales Junior, P.A., et al. (2017) 18-Des-hydroxy cytochalasin: An antiparasitic compound of *Diaporthe phaseolorum* 92C, an endophytic fungus isolated from *Combretum lanceolatum* Pohl ex Eichler. *Parasitol. Res.* **116**, 1823–1830.
- Butler MS. (2004) The Role of Natural Product Chemistry in Drug Discovery. *J. Nat. Prod.* **67**, 2141-53.
- Cantrell, D. A. and Smith, K. A. (1984) The interleukin-2 T-cell system: a new cell growth model. *Science* **224**, 1312-1316.

- Chain, E., Florey, H.W., Gardner, N.G., Heatley, N.G., Jennings, M.A., Orr-Ewing, J., et al. (1940) Penicillin as a chemotherapeutic agent. *Lancet*. **236**, 226–228.
- Chambers, H.F. (2001) The changing epidemiology of *Staphylococcus aureus* ? *Emerg. Infect. Dis.*, **7**, 178–182.
- Chapla, V. M., Zeraik, M. L., Leptokarydis, I. H., Silva, G. H., Bolzani, V. S., Young, M. C., et al. (2014) Antifungal compounds produced by *Colletotrichum gloeosporioides*, an endophytic fungus from *Michelia champaca*. *Molecules* **19**, 19243–19252.
- Chen, C.J., Liu, X.X., Zhang, W.J., Zang, L.Y., Wang, G., Ng, S.W., Tan, R.X., Ge, H.M. (2015) Sesquiterpenoids isolated from an endophyte fungus *Diaporthe* sp. *RSC Adv.* **5**, 17559–17565.
- Chepkirui, C.; Stadler, M. (2017) The genus *Diaporthe*: a rich source of diverse and bioactive metabolites. *Mycol. Prog.* **16**, 477–494.
- Chin, Y. W., Balunas, M. J., Chai, H. B., Kinghorn, A. D. (2006) Drug discovery from natural sources. *The AAPS journal* **8**, E239-E253.
- Cole, R. J., Wilson, D. M., Harper, J. L., Cox, R. H., Cochran, T. W., Cutler, H. G., Bell, D. K. (1982) *J. Agric. Food Chem.* **30**, 301–304.
- Cole, R.J., Schweikert, M.A. (2003) Handbook of secondary fungal metabolites. *Academic Press*, New York. Vol. 1.
- Crous, P.W., Groenewald, J.Z., Risede, J.M., Simoneau, P., Hyde, K.D. (2004) *Calonectria* species and their *Cylindrocladium* anamorphs: species with *sphaeropedunculate vesicles*. *Studies in Mycology* **50**, 415–430.
- Cui, H., Ding, M., Huang, D., Zhang, Z., Liu, H., Huang, H., She, Z. (2017) Chroman-4-one and pyrano[4,3-b] chromenone derivatives from the mangrove endophytic fungus *Diaporthe phaseolorum* SKS019. *RSC Adv.* **7**, 20128–20134.
- Cui, H., Lin, Y., Luo, M., Lu, Y., Huang, X., She, Z. (2017) Diaporisoindoles A-C: Three isoprenylisoindole alkaloid derivatives from the mangrove endophytic fungus *Diaporthe* sp. SYSU-HQ3. *Org. Lett.* **19**, 5621–5624.
- Cui, H., Liu, Y., Li, J., Huang, X., Yan, T., Cao, W., Liu, H., Long, Y., She, Z. (2018) Diaporindenones A-D: Four unusual 2,3-dihydro-1Hindene analogues with anti-inflammatory activities from the mangrove endophytic fungus *Diaporthe* sp. SYSU-HQ3. *J. Org. Chem.* **83**, 11804–11813.

- Dai, Y., Lin, Y., Pang, X., Luo, X., Salendra, L., Wang, J.F., Zhou, X.F., Lu, Y.J., Yang, B., Liu, Y. (2018) Peptides from the soft coral-associated fungus *Simplicillium* sp. SCSIO41209. *Phytochemistry* **154**, 56–62.
- Dang, L.Q., Shin, T.S., Park, M.S., Choi, Y.H., Choi, G.J., Jang, K.S., Kim, I.S., Kim, J.C. (2014) Antimicrobial Activities of Novel Mannosyl Lipids Isolated from the Biocontrol Fungus *Simplicillium lamellicola* BCP against Phytopathogenic Bacteria. *J. Agric. Food Chem.* **62**, 3363–3370.
- De Medeiros, A.G., Savi, D.C., Mitra, P., Shaaban, K.A., Jha, A.K., Thorson, J.S., Rohr, J., Glienke, C. (2018) Bioprospecting of *Diaporthe terebinthifolii* LGMF907 for antimicrobial compounds. *Folia Microbiol.* **63**, 499–505.
- Debbab, A., Aly, A. H., and Proksch, P. (2012) Endophytes and associated marine derived fungi—ecological and chemical perspectives. *Fungal Diversity* **57**, 45-83.
- Dong, Q.L., Dong, R.Z., Xing, X.Y., Li, Y.K. (2018) A new antibiotic produced by the cyanobacterium-symbiotic fungus *Simplicillium lanosoniveum*. *Nat. Prod. Res.* **32**, 1348–1352.
- Duan, Y.D., Jiang, Y.Y., Guo, F.X., Chen, L.X., Xu, L.L., Zhang, W., Liu, B. (2019) The antitumor activity of naturally occurring chromones: A review. *Fitoterapia*, **135**, 114–129.
- Ehrlich, J., Bartz, Q.R., Smith, R.M., Joslyn, D.A., Burkholder, P.R. (1947) Chloromycetin, a New Antibiotic from a Soil Actinomycete. *Science* **106**, 417.
- Endo, A. (1985) Compactin (ML-236B) and related compounds as potential cholesterol lowering agents that inhibit HMG-CoA reductase. *J. Med. Chem.* **28**, 401-405.
- Evidente, M., Boari, A., Vergura, S., Cimmino, A., Vurro, M., Ash, G., Superchi, S., Evidente, A. (2015) Structure and absolute configuration of kongiidiazadione, a new phytotoxic 3 substituted-5-diazenylcyclopentendione produced by *Diaporthe Kongii*. *Chirality* **27**, 557–562.
- Fleming, A. (1929) On the antibacterial action of cultures of a *Penicillium* with special reference to their use in the isolation of B. influenza. *British. J. Exp.Pathol.* **10**, 226–236.
- Fleming, A. (1945) Penicillin's finder assays its future. *N. Y. Times*, 26, 21.
- Fukuda, T., Sudoh, Y., Tsuchiya, Y., Okuda, T., Igarashi, Y. (2014) Isolation and biosynthesis of preussin B, a pyrrolidine alkaloid from *Simplicillium lanosoniveum*. *J. Nat. Prod.* **77**, 813–817.

- Glass, N.L., Donaldson, G.C. (1995) Development of primer sets designed for use with the PCR to amplify conserved genes from filamentous ascomycetes. *Appl. Environ. Microbiol.* **61**, 1323–1330.
- Golinska, P., Wypij, M., Agarkar, G., Rathod, D., Dahm, H., Rai, M. (2015) Endophytic actinobacteria of medicinal plants: diversity and bioactivity. *Antonie Van Leeuwenhoek* **108**, 267–289.
- Gomes, R.R., Glienke, C., Videira, S.I.R., Lombard, L., Groenewald, J., Crous, P.W. (2013) *Diaporthe*: a genus of endophytic, saprobic and plant pathogenic fungi. *Persoonia* **31**, 1–41.
- Guarnaccia, V., Groenewald, J.Z., Woodhall, J. et al. (2018) *Diaporthe* diversity and pathogenicity revealed from a broad survey of grapevine diseases in Europe. *Persoonia* **40**, 135–153.
- Guo, C.J., Knox, B.P., Chiang, Y.M., Lo, H.C., Sanchez, J.F., Lee, K.H., Oakley, B.R., Bruno, K.S., Wang, C.C.C. (2012) Molecular genetic characterization of a cluster in *A. terreus* for biosynthesis of the meroterpenoid terretonin. *Org. Lett.* **14**, 5684–5687.
- Hamilton-Miller, J.M.T., (2008) Development of the semi-synthetic penicillins and cephalosporins. *Int. J. Antimicrob. Agents* **31**, 189–192.
- Happi, M.G., Kouam, S.F., Talontsi, F.M., Nkenfou, C., Longo, F., Ngadjui, B.T., Spiteller, M. (2013) New Dimeric naphthopyrones with antimicrobial activity from *Aspergillus niger*, an Fungal Endophyte isolated from the Cameroonian Plant *Entandrophragma* sp. *Z. Naturforsch.* **70**, 625–630.
- Hermann. (1985) *Eléments de Microbiologie*. Editeur des sciences et des arts, Paris, France, 4 15.
- Hoye, T. R., Jeffrey, C. S., Shao, F. (2007) Mosher ester analysis for the determination of absolute configuration of stereogenic (chiral) carbinol carbons. *Nat. Protoc.* **2**, 2451–2458.
- Hu, Z.X., Wu, Y., Xie, S.S., Sun, W.G., Guo, Y., Li, X.N., Liu, J.J., Li, H., Wang, J.P., Luo, Z.W., et al. (2017) Phomopsterones A and B, two functionalized ergostane-type steroids from the endophytic fungus *Phomopsis* sp. TJ507A. *Org. Lett.* **19**, 258–261.
- Huang, D., Shao, Z.Z., Yu, Y., Cai, M.M., Zheng, L.Y., Li, G.Y., Yu, Z.N., Yi, X.F., Zhang, J.B., Hao, F.H. (2018) Identification, characteristics and mechanism of 1-deoxy-N acetylglucosamine from deep-sea *Virgibacillus dokdonensis* MCCC 1A00493. *Mar. Drugs* **16**, 52.
- Huang, R., Jiang, B.G., Li, X.N., Wang, Y.T., Liu, S.S., Zheng, K.X., He, J., Wu, S.H. (2018) Polyoxygenated cyclohexenoids with promising-glycosidase inhibitory activity produced by

- 
- Phomopsis* sp. YE3250, an endophytic fungus derived from *Paeonia delavayi*. *J. Agric. Food Chem.* **66**, 1140–1146.
- Huang, X., Zhou, D., Liang, Y., Liu, X., Cao, F., Qin, Y., Mo, T., Xu, Z., Li, J., Yang, R. (2019) Cytochalasins from endophytic *Diaporthe* sp. GDG-118. *Nat. Prod. Res.* **35**, 3396-3403.
- Huang, J., Xu, J., Wang, Z., Khan, D., Niaz, S.I., Zhu, Y., Lin, Y., Li, J., Liu, L. (2016) New lasiodiplodins from mangrove endophytic fungus *Lasiodiplodia* sp. 318. *Nat. Prod. Res.* **31**, 326-332.
- Hyde, K. D., Xu, J., Rapior, S., (...) Stadler, M. (2019) The amazing potential of fungi : 50 ways we can exploit fungi industrially. *Fungal Diversity* **97**, 1–136.
- Ishijima, H., Uchida, R., Ohtawa, M., Kondo, A., Nagai, K., Shima, K., Nonaka, K., Masuma, R., Iwamoto, S., Onodera, H., Nagamitsu, T., Tomoda, H. (2016) Simplifungin and valsafungins, antifungal antibiotics of fungal origin, *J. Org. Chem.* 2016, **81**, 7373–7383.
- Ishikawa, H. (1999) Mizoribine and mycophenolate mofetil. *Curr. Med. Chem.* **6**, 575-598.
- Ito, A., Maeda, H., Tonouchi, A., Hashimoto, M. (2015) Relative and absolute structure of phomolide C. *Biosci. Biotechnol. Biochem.* **79**, 1067–1069.
- Izawa, Y., Hirose, T., Shimizu, T., Koyama, K. (1989) Six new 10-5 pheynl- [11] cytochalasans, cytochalasins N-S from *Phomopsis* sp. *Tetrahedron* **45**, 2323-35.
- Izawa, Y., Hirose, T., Shimizu, T., Koyama, K., Natori, S. (1989) Six new 10- phenyl [11] cytochalasans, cytochalasins N-S from *Phomopsis* sp. *Tetrahedron* **45**, 2323-2335.
- Janos Berdy, J. (2005) Bioactive Microbial Metabolites. *J. Antibiot.* **58**, 1–26.
- Józwiak, M., Filipowska, A., Fiorino, F., Struga, M. (2020) Anticancer activities of fatty acids and their heterocyclic derivatives. *Eur. J. Pharmacol.* **871**, 172937.
- Kalyaanamoorthy, S., Minh, B.Q., Wong, T.K.F., von Haeseler, A., Jermini, L.S. (2017) Model Finder: fast model selection for accurate phylogenetic estimates. *Nat. Methods* **14**, 587–589.
- Kang, J., Wang, H., and Chen, R. (2003) Studies on the constituents of the mycelium produced by fermenting culture of *Flammulina velutipes* (W. Curt.:Fr.) Singer (Agaricomycetideae). *Int. J. Med. Mushrooms* **5**, 391–396.
- Kang, J., Wang, H., Chen, R. (2003) Studies on the constituents of the mycelium produced by fermenting culture of *Flammulina velutipes* (W. Curt. Fr.) Singer (Agaricomycetideae). *Int. J. Med. Mushrooms* **5**, 391–396.
-

- Kashiwada, Y., Nonaka, G-I., Nishioka I. (1984) Studies on Rhubarb (Rhei Rhizoma). V. Isolation and characterization of Chromone and chromanone derivatives. *Chem. Pharm Bull.* **32**, 3493- 3500.
- Katoh, K., Standley, D.M. (2013) MAFFT multiple sequence alignment software v. 7: improvements in performance and usability. *Mol. Biol. Evol.* **30**, 772–780.
- Kearse, M., Moir, R., Wilson, A., Stones-Havas, S., Cheung, M., Sturrock, S., Buxton, S., Cooper, A., Markowitz, S., Duran, C., Thierer, T., Ashton, B., Mentjies, P., Drummond, A. (2012) Geneious basic: an integrated and extendable desktop software platform for the organization and analysis of sequence data. *Bioinformatics* **28**, 1647–1649.
- Keatingeclay, AT. (2012) The structures of type I polyketide synthases. *Nat. Prod. Rep.* **29** :1050–73
- Kharwar, R. N., Mishra, A., Gond, S. K., Stierle, A., and Stierle, D. (2011) Anticancer compounds derived from fungal endophytes: their importance and futurs challenges. *Nat. Prod. Rep.* **28**, 1208-1228.
- Kogel, K. H., Franken, P., Hueckelhoveb, R. (2006) Endophyte or parasite-what decides? *Cutt. Opin. Plant. Biol.* **9**, 358-363.
- Koolen, H. H. F., Menezes, L.S. Souza, M.P., Silva, F. M. A., Almeida, F. G. O., de Souza, A. Q.L., Nepel, A., Barison, A., da Silva, F.H., Evangelista, D.E., Afonso D. L., de Souza, A. D.L. (2013) Talaroxanthone, a Novel Xanthone Dimer from the Endophytic Fungus *Talaromyces* sp. Associated with *Duguetia stelechantha* (Diels) R. E. Fries. *J. Braz. Chem. Soc.* **24**, 880-883.
- Koyama, N., Nagahiro, T., Yamaguchi, Y., Ohshiro, T., Masuma, R., Tomoda, H., Omura, S. (2005) Spyridone, a novel inhibitor of lipid droplet accumulation in mouse macrophages produced by *Phoma* sp. FKI-1840. *J. Antibiot.* **58**, 338–345.
- Kuete V. (2010) Potential of Cameroonian plants and derived products against microbial infections : A review. *Planta Med.***76** :1–13.
- Kumar, A., Patil, D., Rajamohanam, P. R., and Ahmad, A. (2013) Isolation, purification and characterization of vinblastine and vincristine from endophytic fungus *Fusarium oxysporum* isolated from *Catharanthus roseus*. *PLoS one* **8**, e71805.
- Kumar, S., Stecher, G., Li, M., Knyaz, C., Tamura, K. (2018) MEGA X: Molecular evolutionary Genetics analysis across computing platforms. *Mol. Biol. Evol.* **35**, 1547–1549.

- Kumara, P.M., Shweta, S., Vasanthakumari, M.M., Sachin, N., Manjunatha. B.L., Jadhav, S.S., Ravikanth, G., Ganeshaiyah, K.N., Shaanker, R.U. (2014) Endophytes and plant secondary metabolite synthesis: molecular and evolutionary perspective. In: Verma VC, Gange AC (eds) Advances in endophytic research. *Springer, New Delhi* p 177–190.
- Lanfear, R., Frandsen, P.B., Wright, A.M., Senfeld, T., Calcott, B. (2016) Partition Finder 2: New Methods for Selecting Partitioned Models of Evolution for Molecular and Morphological Phylogenetic Analyses. *Mol. Biol. Evol.* **34**, 772–773.
- Le Pogam, P., Boustie, J. (2016) Xanthones of lichen source: A 2016 update. *Molecules* **21**, 294.
- Lee KH, Hayashi N, Okano M, Hall IH, Wu RY, McPhail AT. 1982. Lasiodiplodin, a potent antileukemic macrolide from *Euphorbia splendens*. *Phytochemistry*. **21**, 1119–1121.
- Lee, J. C., Lobkovsky, E., Pliam, N. B., Strobel, G., and Clardy, J. (1995) Subglutinols A and B: immunosuppressive compounds from the endophytic fungus *Fusarium subglutinans*. *J. Org. Chem.*, **60**, 7076-7077.
- Lee, J., Yi, J.M., Kim, H., Lee, Y.J., Park JS, Bang OS, Kim NS. (2014) Cytochalasin H, an active anti-angiogenic constituent of the ethanol extract of *Gleditsia sinensis* Thorns. *Biol. Pharm. Bull.* **37**, 6-12.
- Lee, J.C., Lobkovsky, E., Pliam, N.B., Strobel, G., Clardy, J. (1995) Subglutinols A and B: immunosuppressive compounds from the endophytic fungus *Fusarium subglutinans*. *J. Org.Chem.* **60**, 7076–7077.
- Li, G., Kusari, S., Kusari, P., Kayser, O., Spiteller, M. (2015) Endophytic *Diaporthe* sp. LG23 produces a potent antibacterial tetracyclic triterpenoid. *J. Nat. Prod.* **78**, 2128–2132.
- Liang, X., Nong, X.H., Huang, Z.H., Qi, S.H. (2017) Antifungal and antiviral cyclic peptides from the deep-sea-derived fungus *Simplicillium obclavatum* EIODSF 020. *J. Agric. Food Chem.* **65**, 5114–5121.
- Liang, X., Zhang, X.Y., Nong, X.H., Wang, J., Huang, Z.H., Qi, S.H. (2016) Eight linear peptides from the deep-sea-derived fungus *Simplicillium obclavatum* EIODSF 020. *Tetrahedron* **72**, 3092–3097.
- Liu, F., Cai, L. (2012) Morphological and molecular characterization of a novel species of *Simplicillium* from China. *Cryptogamie, Mycologie* **33**, 137–144.
- Liu, Y., Hu, Z., Lin, X., Lu, C., Shen, Y. (2013) A new polyketide from *Diaporthe* sp. SXZ-19, an endophytic fungal strain of *Camptotheca acuminata*. *Nat. Prod. Res.* **27**, 2100–2104.

- Liu, Y., Ruan, Q., Jiang, S., Qu, Y., Chen, J., Zhao, M., Yang, B., Liu, Y., Zhao, Z., Cui, H. (2019) Cytochalasins and polyketides from the fungus *Diaporthe* sp. GZU-1021 and their anti-inflammatory activity. *Fitoterapia* **137**, 104187.
- Liu, Z., Zhao, J., Liang, X., Lv, X., Li, Y., Qu, J., Liu, Y. (2018) Dothiorelone derivatives from an endophyte *Diaporthe pseudomangiferaea* inhibit the activation of human lung fibroblasts MRC-5 cells. *Fitoterapia* **127**, 7–14.
- Luo, X., Lin, X., Tao, H., Wang, J., Li, J., Yang, B., Zhou, X., Liu, Y. (2018) Isochromophilones A-F, cytotoxic chloroazaphilones from the marine mangrove endophytic fungus *Diaporthe* sp. SCSIO 41011. *J. Nat. Prod.* **81**, 934–941.
- Luo, X., Yang, J., Chen, F., Lin, X., Chen, C., Zhou, X., Liu, S., Liu, Y. (2018) Structurally diverse polyketides from the mangrove-derived fungus *Diaporthe* sp. SCSIO 41011 with their anti-influenza A virus activities. *Front. Chem.* **6**, 282.
- Luo, Y.F., Zhang, M., Dai, J.G., Pedpradab, P., Wang, W.J., Wu, J. (2016) Cytochalasins from mangrove endophytic fungi *Phomopsis* spp. xy21 and xy22. *Phytochem. Lett.* **17**, 162–166.
- Luyen, V.T. (2017) Identification of the entomopathogenic fungi sample DL0069 by combination of morphological and molecular phylogenetic analyses. *Vietnam Journal of Science and Technology* **55**, 117–123.
- Maclean, D.J., Scott, K.J. (1976) Identification of Glucitol (Sorbitol) and Ribitol in a Rust Fungus, *Puccinia graminis* f. sp. *Tritici*. *Journal of General Microbiology* **97**, 83-89.
- Madigan, M., Martinko, J. (2006) Brock biology and microorganism. 11<sup>th</sup> ed., Pearson Prentice Hall, Upper Saddle River, NJ, p.5.
- Mandavid, H., Rodrigues, A.M.S., Espindola, L.S., Eparvier, V., Stien, D. (2015) Secondary metabolites isolated from the amazonian endophytic fungus *Diaporthe* sp. SNB-GSS10. *J. Nat. Prod.* **78**, 1735–1739.
- Meepagala, K.M., Briscoe, W.E., Techen, N., Johnson, R.D., Clausen, B.M., Duke, S.O. (2018) Isolation of a phytotoxic isocoumarin from *Diaporthe* eres-infected *Hedera helix* (English ivy) and synthesis of its phytotoxic analogs. *Pest Manag. Sci.* **74**, 37–45.
- Minh, B.Q., Schmidt, H.A., Chernomor, O., Schrempf, D., Woodhams, M.D., von Haeseler, A., Lanfear, R. (2020) IQ-TREE 2: New models and efficient methods for phylogenetic inference in the genomic era. *Mol. Biol. Evol.* 6–10.

- Mishra, V.K., Passari, A.K., Chandra, P., Leo, V.V., Kumar, B., Gupta, V.K., Singh, B.P. (2017a) Determination and production of antimicrobial compounds by *Aspergillus clavatonanicus* strain MJ31, an endophytic fungus from *Mirabilis jalapa* L. using UPLC-ESI MS/MS and TD GC-MS. *PLoS One* **12**, 1–24.
- Mishra, V.K., Singh, G., Passari, A.K., Yadav, M.K., Gupta, V.K., Singh, B.P. (2016) Distribution and antimicrobial potential of endophytic fungi associated with ethnomedicinal plant *Melastoma malabathricum* L. *J Environ Biol.* **37**, 229–237.
- Morris, M.I., Villmann, M. (2006a) Echinocandins in the management of invasive fungal infections, part 1. *Am J Health Syst Pharm* **63**, 1693–1703.
- Murali, T.S., Suryanarayanan, T.S., Geeta, R. (2006) Endophytic Phomopsis species: host range and implications for diversity estimates. *Can. J. Microbiol.* **52**, 673–680.
- Nakanishi, K. (1999) An historical perspective of natural products chemistry. *Comprehensive. Nat. Prod. Chem.* **8**, xxi-xxxviii.
- Nakashima, K.I., Tomida, J., Kamiya, T., Hirai, T., Morita, Y., Hara, H., Kawamura, Y., Adachi, T., Inoue, M. (2018) Diaporthols A and B: Bioactive diphenyl ether derivatives from an endophytic fungus *Diaporthe* sp. *Tetrahedron Lett.* **59**, 1212–1215.
- Newman, D. J., Cragg, G. M. (2016) Natural products as sources of new drugs from 1981 to 2014. *J. Nat. Prod.* **79**, 629–661.
- Newman, D. J., Cragg, G. M., Snader, K. M. (2003) Natural products as source of new drugs over the period 1981-2002. *J. Nat. Prod.* **66**, 1022-1037.
- Niu, Z., Chen, Y., Guo, H., Li, S.N., Li, H.H., Liu, H.X., Liu, Z., Zhang, W. (2019) Cytotoxic polyketides from a deep-sea sediment derived fungus *Diaporthe phaseolorum* FS431. *Molecules* **24**, 3062.
- Noriler, S.A., Savi, D.C., Ponomareva, L.V., Rodrigues, R., Rohr, J., Thorson, J.S., Glienke, C., Shaaban, K.A. (2019) Vochysiamides A and B: Two new bioactive carboxamides produced by the new species *Diaporthe vochysiae*. *Fitoterapia* **138**, 104273.
- Nylander, J.A.A. *MrModeltest v2*. (2004) *Program Distributed by the Author*; Evolutionary Biology Centre, Uppsala University: Uppsala, Sweden.
- Ola, A.R.B., Debbab, A., Kurtan, T., Broetz-Oesterhelt, H., Aly, A.H., Proksch, P. (2014) Dihydroanthracenone metabolites from the endophytic fungus *Diaporthe melonis* isolated from *Annona squamosa*. *Tetrahedron Lett.* **55**, 3147–3150.

- 
- Pes, M.P., Mazutti, M.A., Almeida, T.C., Curioletti, L.E., Melo, A.A., Guedes, J.V.C., Kuhn, R.C. (2016) Bioherbicide based on *Diaporthe* sp. Secondary metabolites in the control of three tough weeds. *Afr. J. Agric. Res.* **11**, 4242–4249.
- Petersen, A. B., Rønneest, M. H., Larsen, T. O., Clausen, M. H. (2014) The chemistry of griseofulvin. *Chem. Rev.* **114**, 12088–12107.
- Petrini, O. (1987) Endophytic fungi of alpine Ericaceae. The endophytes of *Loiseleuria procumbens*. in Laursen, G.A., Arnirati, J.F., and Red-head, S.A. (editors), Arctic and Alpine Mycology II. Environmental Science Research, Plenum Press, New York and London. **6**, 71-77.
- Piel J. (2015) Biosynthesis of polyketides by trans-AT polyketide synthases. *Nat. Prod. Rep.* **27** :996–1047.
- Piepenbring, M. (2015) Introduction to Mycology in the Tropics. The American phytopathological Society. *St Paul Minnesota, 55121*, U.S.A. P.32-48.
- Pirttilä, A.M., Laukkanen, H., Hohtola. A. (2002) Chitinase production in pine callus (*Pinus sylvestris* L.): a defense reaction against endophytes? *Planta* **214**, 848–852.
- Priti, V., Ramesla, B., Singh, S., Ravikanth, G., Ganeshaiyah, K., Suryanarayanan, T., Uma Shaanker, R. (2009) How promising are endophytic fungi as alternative sources of plant secondary metabolites? *Curr. Sci.* **97**, 477 -478.
- Rai, S., Kashyap, P.L., Kumar, S., Srivastava, A.K., Ramteke, P.W. (2016) Comparative analysis of microsatellites in five different antagonistic *Trichoderma* species for diversity assessment. *World J Microbiol Biotechnol.* **32** :8.
- Rai, S., Kashyap, P.L., Kumar, S., Srivastava, A.K., Ramteke, P.W. (2016) Comparative analysis of microsatellites in five different antagonistic *Trichoderma* species for diversity assessment. *World J Microbiol Biotechnol.* **32**,8.
- Raistrick, H., Stickings, C.E., Thomas, R. (1953) Studies in the biochemistry of micro-organisms. 90. Alternariol and alternariol monomethyl ether, metabolic products of *Alternaria tenuis*. *Biochem. J.*, **55**. 421–433.
- Ratnaweera, P.B., Jayasundara, J.M.N.M., Herath, H.H.M.S.D., Williams, D.E., Rajapaksha, S.U., Nishantha, K.M.D.W.P., de Silva, E.D., Andersen, R.J. (2020) Antifeedant, contact toxicity and oviposition deterrent effects of phyllostine acetate and phyllostine isolated from the
-

- endophytic fungus *Diaporthe miriciae* against *Plutella xylostella* larvae. *Pest Manag. Sci.* **76**, 1541–1548.
- Rice, L.B. (2008) Federal funding for the study of antimicrobial resistance in nosocomial pathogens: No ESKAPE. *J. Infect. Dis.*, 197, 1079.
- Riga, R., Happyana, N., Quentmeier, A., Zammarelli, C., Kayser, O., Hakim, E.H. (2019) Secondary metabolites from *Diaporthe lithocarpus* isolated from *Artocarpus heterophyllus*. *Nat. Prod. Res.* **35**, 2324–2328.
- Rishton, G. M. (2008) Natural products as a robust source of new drugs and drug leads: past successes and present day issues. *The American journal of cardiology* **101**, S43–S49.
- Rodriguez, R. J., White, J. F. Jr., Arnold, A. E., Redman, R. S. (2009) Fungal endophytes: diversity and functional roles. *New Phytol.* **182**, 314–330.
- Rodriguez, R.J., Redman, R.S., Henson, J.M. (2004) The role of fungal symbioses in the adaptation of plants to high stress environments. *Mitig Adapt Strat Global Change* **9**, 261–272.
- Ronquist, F., Teslenko, M., van der Mark, P., Ayres, D.L., Darling, A., Höhna, S., Larget, B., Liu, L., Suchard, M.A., Huelsenbeck, J.P. (2012) MrBayes 3.2: Efficient Bayesian Phylogenetic Inference and Model Choice Across a Large Model Space. *Syst. Biol.* **61**, 539–542.
- Rossmann, A.Y., Adams, G.C., Cannon, P.F., Castlebury, L.A., Crous, P.W., Gryzenhout, M., Jaklitsch, W.M., Mejia, L.C., Stoykov, D., Udayanga, D., Voglmayr, H. (2015) Recommendations of generic names in Diaporthales competing for protection or use. *IMA Fungus* **6**, 145–154.
- Roy, S., Dutta, T., Sarkar, T.S., Ghosh, S. (2013) Novel xylanases from *Simplicillium obclavatum* MTCC 9604: comparative analysis of production, purification and characterization of enzyme from submerged and solid-state fermentation. *SpringerPlus* **2**, 382.
- Rutledge, P. J., Challis, G. L. (2015) Discovery of microbial natural products by activation of silent biosynthetic gene clusters. *Nat. Rev. Microbiol.* **13**, 509–523.
- Santamaria, J., Bayman, P. (2005) Fungal epiphytes and endophytes of coffee leaves (*Coffea arabica*). *Microbial Ecology* **50**, 1–8.
- Schloss, S., Hackl, T., Herz, C., Lamy, E., Koch, M., Rohn, S., Maul, R. (2017) Detection of a toxic methylated derivative of phomopsis A produced by the legume-infesting fungus *Diaporthe toxica*. *J. Nat. Prod.* **80**, 1930–1934.

- Schulz, B., Boyle, C. (2005) The endophytic continuum. *Mycol Res* **109**, 661–686
- Sebastianes, F.L.S., Cabedo, N., El Aouad, N., Valente, A.M.M.P., Lacava, P.T., Azevedo, J.L., Pizzirani-Kleiner, A.A., Cortes, D. (2012) 3-Hydroxypropionic acid as an antibacterial agent from endophytic fungi *Diaporthe phaseolorum*. *Curr. Microbiol.* **65**, 622–632.
- Selosse, M.A., Faccio, G., Scappaticci, G., Bonfante, P. (2004) Chlorophyllous and achlorophyllous specimens of *Epipactis microphylla* (Neottieae, Orchidaceae) are associated with ectomycorrhizal septomycetes, including truffles. *Microb. Ecol.* **47**, 416–4260.
- Shang, Z., Raju, R., Salim, A.A., Khalil, Z.G., Robert J., Capon, R.J. (2017) Cytochalasins from an Australian Marine Sediment-Derived *Phomopsis* sp. (CMB-M0042F): Acid-Mediated Intramolecular Cycloadditions Enhance Chemical Diversity. *J. Org. Chem.* **82**, 9704-9709.
- Sharma, V., Singamaneni, V., Sharma, N., Kumar, A., Arora, D., Kushwaha, M., Bhushan, S., Jaglan, S., Gupta, P. (2018) Valproic acid induces three novel cytotoxic secondary metabolites in *Diaporthe* sp., an endophytic fungus from *Datura inoxia* Mill. *Bioorganic Med. Chem. Lett.* **28**, 2217–2221.
- Shi, Q., Meroueh, S. O., Fisher, J. F., Mobashery, S. (2011) A computational evaluation of the mechanism of penicillin-binding protein-catalyzed cross-linking of the bacterial cell wall. *J. Am. Chem. Soc.* **133**, 5274-5283.
- Shin, T.S., Yu, N.H., Lee, J., Choi, G.J, Kim JC, Shin CS (2017) Development of a biofungicide using a mycoparasitic fungus *Simplicillium lamellicola* BCP and its control efficacy against gray mold diseases of tomato and ginseng. *The Plant Pathology Journal* **33**, 337–344.
- Shweta, S., Shivanna, M.B., Gurumurthy, B.R., Uma Shaanker, R., Santhosh Kumar, T.R., Ravikanth, G. (2014) Inhibition of fungal endophytes by camptothecine produced by their host plant, *Nothapodytes nimmoniana* (Grahm) Mabb. (Icacinaceae). *Curr Sci.* **107** : 994-1000.
- Shweta, S., Shivanna, M.B., Gurumurthy, B.R., Uma Shaanker, R., Santhosh Kumar, T.R., Ravikanth, G. (2014) Inhibition of fungal endophytes by camptothecine produced by their host plant, *Nothapodytes nimmoniana* (Grahm) Mabb. (Icacinaceae). *Curr. Sci.* **107**, 994-1000.
- Smith, H., Wingfield, M.J., Crous, P.W., Coutinho, T.A. (1996) *Sphaeropsis sapinea* and *Botryosphaeria dothidea* endophytic in *Pinus* spp. and *Eucalyptus* spp. in South Africa. *S. Afr. J. Bot.* **62**, 86–88.

- 
- Sousa, J.P.B., Aguilar-Perez, M.M., Arnold, A.E., Rios, N., Coley, P.D., Kursar, T.A., Cubilla Rios, L. (2016) Chemical constituents and their antibacterial activity from the tropical endophytic fungus *Diaporthe* sp. F2934. *J. Appl. Microbiol.* **120**, 1501–1508.
- Souza, A.R.C., Baldoni, D.B., Lima, J., et al. (2015) Bioherbicide production by *Diaporthe* sp. isolated from the Brazilian Pampa biome. *Biocatal Agric Biotechnol.* **4**, 575–578.
- Souza, B.S., dos Santos, T.T. (2017) Endophytic fungi in economically important plants: ecological aspects, diversity and potential biotechnological applications. *J Bioenergy Food Sci* **4**, 113–126.
- Specian, V., Sarragiotto, M.H., Pamphile, J.A., Clemente, E. (2012) Chemical characterization of bioactive compounds from the endophytic fungus *Diaporthe helianthi* isolated from *Luehea divaricata*. *Braz. J. Microbiol.* **43**, 1174–1182.
- Stierle, A., Strobel, G., and Stierle, D. (1993) Taxol and taxane production by *Taxomyces andreanae*, an endophytic fungus of *Pacific yew*. *Science–New York then Washington* **260**, 214.
- Stierle, A., Strobel, G., Stierle, D. (1993) Taxol and taxane production by *Taxomyces andreanae*, an endophytic fungus of *Pacific yew*. *Science*, **260**, 214–216.
- Strack, D., Fester, T., Hause, B., Schliemann, W., Walter, M.H. (2003) Review Paper: Arbuscular Mycorrhiza: Biological, Chemical, and Molecular Aspects. *J. Chem. Ecol.* **29**, 1955–1979.
- Sun, J.Z., Liu, X.Z., McKenzie, E.H., Jeewon, R., Liu, K.J., Zhang, X.L., Zhao, Q., Hyde, K.D. (2019) Fungicolous fungi: terminology, diversity, distribution, evolution, and species checklist. *Fungal Diversity* **95**, 337–430.
- Sung, G.H., Spatafora, J.W., Zare, R., Hodge, K.T., Gams, W. (2001) A revision of *Verticillium* sect. *Prostrata*. II. Phylogenetic analyses of SSU and LSU nuclear rDNA sequences from anamorphs and teleomorphs of the Clavicipitaceae. *Nova Hedwigia* **72**, 311–328.
- Surup, F., Halecker, S., Nimtz, M., Rodrigo, S., Schulz, B., Steinert, M., Stadler, M. (2018) Hyfraxins A and B, cytotoxic ergostane-type steroid and lanostane triterpenoid glycosides from the invasive ash dieback ascomycete *Hymenoscyphus fraxineus*. *Steroids* **135**, 92–97.
- Sweet, R. M., Dahl, L. F. (1970) Molecular Architecture of the Cephalosporins. Insights into Biological Activity Based on Structural Investigations. *J. Am. Chem. Sco.* **92**, 5489–5507.
- Takata, K., Iwatsuki, M., Yamamoto, T., Shirahata, T., Nonaka, K., Masuma, R., Hayakawa, Y., Hanaki, H., Kobayashi, Y., Petersson, G.A., Omura, S., Shiomi, K. (2013) Aogacillins A
-

- and B produced by *Simplicillium* sp. FKI-5985: new circumventors of arbekacin resistance in MRSA. *Organic Letters* **15**, 4678–4681.
- Talavera, G., Castresana, J. (2007) Improvement of phylogenies after removing divergent and ambiguously aligned blocks from protein sequence alignments. *Syst. Biol.* **56**, 564–577.
- Talontsi, F.M., Lamshöft, M., Douanla-Meli, C., Kouam, S.F., Spiteller, M. (2014) Antiplasmodial and Cytotoxic Dibenzofurans from *Preussia* sp. harboured in *Enantia chlorantha* Oliv. *Fitoterapia* **93C**, 233–238.
- Tan, Q.W., Fang, P.H., Ni, J.C., Gao, F., Chen, Q.J. (2017) Metabolites Produced by an Endophytic *Phomopsis* sp. and Their Anti-TMV Activity. *Molecules* **22**, 2073.
- Tan, R. X., and Zou, W. X. (2001) Endophytes: a rich source of functional metabolites. *Nat. Pro. Rep.*, **18**, 448-459.
- Tan, R.X., Zou, W.X. (2001) Endophytes: A rich source of functional metabolites. *Nat. Prod. Rep.* **18**, 448-459.
- Tanahashi, T.; Kuroishi, M.; Kuwahara, A.; Nagakura, N.; Hamada, N. (1997) Four phenolics from the cultured lichen mycobiont of *Graphis scripta* var. *pulverulenta*. *Chem. Pharm. Bull.* **45**, 1183–1185
- Tanahashi, T.; Takenaka, Y.; Nagakura, N.; Hamada, N. (2003) 6*H*-Dibenzo[*b,d*]pyran-6-one derivatives from the cultured lichen mycobionts of *Graphis* spp. and their biosynthetic origin. *Phytochemistry*, **62**, 71
- Taniguchi, T., Monde, K., Nakanishi, K., and Berova, N. (2008) Chiral sulfinates studied by optical rotation, ECD and VCD: the absolute configuration of a *cruciferous phytoalexin* brassicanal C. *Org. Biomol. Chem.* **6**, 4399-4405.
- Tanney, J.B., McMullin, D.R., Green, B.D., Miller, J.D., Seifert, K.A. (2016) Production of antifungal and antiinsectan metabolites by the *Picea* endophyte *Diaporthe maritima* sp. nov. *Fungal Biol.* **120**, 1448–1457.
- Tian, W., Liao, Z., Zhou, M., Wang, G., Wu, Y., Gao, S., Qiu, D., Liu, X., Lin, T., Chen, H. (2018) Cytoskyrin C, an unusual asymmetric bisanthraquinone with cage-like skeleton from the endophytic fungus *Diaporthe* sp. *Fitoterapia*, **128**, 253–257.
- Uzma, F., Hashem, A., Murthy, N., Mohan, H.D., Kamath, P.V., Singh BP, Venkataramana, M., Gupta, V.K., Siddaiah, C.N., Chowdappa, S., Alqaeawi, A.A., Abdallah, E.F. (2018)

- Endophytic fungi—alternative sources of cytotoxic compounds: a review. *Front Pharmacol* **9**, 1–37.
- Vennila, R., Muthumary, J. (2011) Taxol from *Pestalotiopsis pauciseta* VM1, an endophytic fungus of *Tabebuia pentaphylla*. *Biomedicine & Preventive Nutrition* **1**, 103-108.
- Ventola, C. L. (2015) The antibiotic resistance crisis: part 1: causes and threats. *Pharmacy and therapeutics*, **40**, 277–283.
- Walsh, C. (2003) *Antibiotics: Actions, Origins, Resistance*. Washington D. C., USA, 3-155.
- Chepkirui, C., Stadler, M., (2017) The genus *Diaporthe*: a rich source of diverse and bioactive metabolites. *Mycol. Prog.* **16**, 477–494.
- Wang, Q.X.; Bao, L.; Yang, X.L.; Guo, H.; Yang, R.N.; Ren, B.; Zhang, L.X.; Dai, H.Q.; Guo, L.D.; Liu, H.W. (2012) Polyketides with antimicrobial from the solid culture of an endophytic fungus *Ulocladium* sp. *Fitoterapia* **83**, 209–214.
- White, T.J.; Bruns, T.; Lee, S.; Taylor, J. (1990) Amplification and direct sequencing of fungal ribosomal genes for phylogenetics. In: Gelfand M, Sninsky JI, White TJ (Eds) PCR protocols: a guide to methods and applications. *Academic, New York* 315–322.
- Wiemann, P., Keller, N. P. (2014) Strategies for mining fungal natural products. *J. Ind. Microbiol. Biotechnol.* **41**, 301–313.
- Williams, R. B., Henrikson, J. C., Hoover, A. R., Lee, A. E., Cichewicz, R. H. (2008) Epigenetic remodeling of the fungal secondary metabolome. *Org. Biomol. Chem.* **6**, 1895–1897.
- Wood, A. J., Rowinsky, E. K., and Donehower, R. C. (1995) Paclitaxel (taxol). *N. Engl. J. Med.* **332**, 1004-1014.
- Wright, D.P., Read, D.J., Scholes, J.D. (1998) Mycorrhizal sink strength influences whole plant carbon balance of *Trifolium repens* L. *Plant Cell Environ.*, **21**, 881-891.
- Wulansari, D., Julistiono, H., Nurkanto, A., Agusta, A. (2016) Antifungal activity of (+)-2,20 epicytoskyrin A and its membrane-disruptive action. *Makara J. Sci.* **20**, 160–166.
- Xu, T.C., Lu, Y.H., Wang, J.F., Song, Z.Q., Hou, Y.G., Liu, S.S., Liu, C.S., Wu, S.H. (2021) Bioactive Secondary Metabolites of the Genus *Diaporthe* and Anamorph *Phomopsis* from Terrestrial and Marine Habitats and Endophytes: 2010–2019. *Microorganisms* **9**, 217.
- Yan, B.F., Fang, S.T., Li, W.Z., Liu, S.J., Wang, J.H., Xia, C.H. (2015) A new minor diketopiperazine from the sponge-derived fungus *Simplicillium* sp. YZ-11. *Nat. Prod. Res.* **29**, 2013–2017.

- Yedukondalu, N., Arora, P., Wadhwa, B., Malik, F.A., Vishwakarma, R.A., Gupta, V.K., Riyaz-Ul-Hassan, S., Ali, A. (2017) Diapolic acid A-B from an endophytic fungus, *Diaporthe terebinthifolii* depicting antimicrobial and cytotoxic activity. *J. Antibiot.* **70**, 212–215.
- Yenn, T.W., Ring, L.C., Nee, T.W., Khairuddean, M., Zakaria, L., Ibrahim, D. (2017) Endophytic *Diaporthe* sp. ED2 produces a novel anti-candidal ketone derivative. *J. Microbiol. Biotechnol.* **27**, 1065–1070.
- Yu, D., Xu, F., Zeng, J., Zhan, J. (2012) Type III polyketide synthases in natural product biosynthesis. *Lubmb Life.* :**64** :285–95.
- Yuan, Z.L., Chen, Y.C., Yang, Y. (2009) Diverse non-mycorrhizal fungal endophytes inhabiting an epiphytic, medicinal orchid (*Dendrobium nobile*): estimation and characterization. *World J. Microbiol Biotechnol.* **25**, 295.
- Zare, R., Gams, W. (2001) A revision of *Verticillium* section Prostrata. IV. The genera *Lecanicillium* and *Simplicillium* gen. nov. *Nova Hedwigia* **71**, 1–50.
- Zare, R., Gams, W., Culham, A. (2000) A revision of *Verticillium* sect. *Prostrata*. I. Phylogenetic studies using ITS sequences. *Nova Hedwigia*, **71**, 465–480.
- Zhang, D., Gao, F., Jakovlić, I., Zou, H., Zhang, J., Li, W.X., Wang, G.T. (2020) PhyloSuite: An integrated and scalable desktop platform for streamlined molecular sequence data management and evolutionary phylogenetics studies. *Molecular Ecology Resources* **20**, 348–355.
- Zhang, H.W., Song, Y.C., Tan, R.X. (2006) Biology and chemistry of endophytes. *Nat. Prod. Rep.* **23**, 753–771.
- Zhang, M., Hou, X.F., Qi, L.H., Yin, Y., Li Q, Pan, H.X., Chen, X.Y., Tang, G.L. (2015) Biosynthesis of trioxacarcin revealing a different starter unit and complex tailoring steps for type II polyketide synthase. *Chem Sci.* **6** :3440–7.
- Zhao, C., Zhu, T., Zhu, W. (2013) New marine natural products of microbial origin from 2010 to 2013. *Chinese J. Org. Chem.* **33**, 1195–1234.
- Zheng, C.J., Shao, C.L., Chen, M., Niu, Z.G., Zhao, D.L., Wang, C.Y. (2015) Merosesquiterpenoids and ten-membered macrolides from a soft coral-derived *Lophiostoma* sp. fungus. *Chem. Biodivers.* **12**, 1407–1414.

# Appendix

## Publications related to the thesis

1. **Anoumedem, E.G.M.**, Mountessou, B.Y.G., Kouam, S.F., Narmani, A., Surup, F. (2020) Simplicilones A and B isolated from the endophytic fungus *Simplicillium subtropicum* SPC3, *J. Antibiot* **9**, 753.
2. Mountessou, B.Y.G., **Anoumedem, E.G.M.**, Kemkuignou, B.M., Marin-Felix, Y., Stadler, M. Kouam, S.F. Secondary metabolites of *Diaporthe* sp., isolated from the Cameroonian medicinal plant *Trema guineensis* (Schumach. & Thonn.) Ficalho (*Under revision in BJOC*).